DISCOVERY AND CHARACTERIZATION OF THE MTOR-P73 SIGNALING AXIS IN HUMAN CANCER

By

Jennifer Margaret Rosenbluth

Dissertation

Submitted to the Faculty of the

Graduate School of Vanderbilt University

in partial fulfillment of the requirements

for the degree of

DOCTOR OF PHILOSOPHY

in

Biochemistry

August, 2009

Nashville, Tennessee

Approved:

Professor Carlos Arteaga

Professor Bruce Carter

Professor David Cortez

Professor Scott Hiebert

Professor Jennifer Pietenpol

Professor Sandra Zinkel

To my parents,

and to San

ACKNOWLEDGEMENTS

I am grateful to all those who have supported my dissertation research through helpful discussions and advice over the past four years. First and foremost, I have innumerable thanks for my mentor, Jennifer Pietenpol. Without her renowned energy and commitment none of this would have been possible. I am thankful that such a brilliant scientist took the time to teach me both the details of data generation, and about finding the big picture in the fight against cancer.

Thanks also to all the members of the Pietenpol lab, past and present, who have made my training experience both fruitful and entertaining. I've enjoyed hanging out by the lab drawer, our 'office water cooler', and coffee machine in both its old and new incarnations. These were the shoulders I cried on, as my lab ornament went from second to last, to last place, to triaged year after year.

I'd particularly like to acknowledge Lucy Tang, who worked with me on many projects and always generated beautiful data – I was constantly encouraged and heartened by her dedication and expertise. Deb Mays taught me core techniques; these were the bedrock of this thesis. I thank her for all of her incredible help and for countless wonderful late-night discussions. Kimberly Johnson is our lab manager, lab 'mom', IHC expert, and dispenser of general wisdom. I have never seen any problem that she could not figure out, given enough time. (By the way, for future reference she also makes the best strawberry cake in the history of strawberry cakes.) I also thank Tracy Triplett for her infectious enthusiasm; during her time as a technician in our lab she helped me jump many hurdles.

Students and colleagues made Vanderbilt the place to be – they engendered a true spirit of learning. During my first years in the lab Carmen Perez was my fellow late-night denizen and I thank her for putting up with my barrages of questions with such equanimity. I'd also like to thank my current and former lab bench neighbors, Katy Eby and Kristy Schavolt, for their camaraderie in spite of the piles of papers that I tried, but sometimes failed, to keep at bay. Former lab members who have shared their expertise with me also include Jamie Hearnes, Chris Barbieri, Kim Brown, and Earle Burgess. I've also had the pleasure of working with two talented rotation students, Bianca Sirbu and Peter Knowlton, who impressed me with their diligence and enthusiasm. I would like to thank members of the Cortez and Zinkel laboratories for helpful discussions during lab meetings.

All of my projects have been collaborative endeavors, and in addition to those above I'd like to express my gratitude to the following people: Aixiang Jiang and Yu Shyr for helping me with some complicated biostatistics, Maria Pino, for her help during my exciting (and stressful!) first paper, and also Joshua Bauer, Bojana Jovanovic, Robert Carnahan and the VMAC, Violeta Sanchez, Melinda Sanders, Maria Olivares, Cheryl Coffin, Bo Lu, Sarah Knutson, Kathy Shelton, Mark Magnuson, and the Magnuson laboratory. I'd also like to thank Chris Barton for his insights and sense of humor, and both of our newer lab members Chris Pendleton and Brian Lehmann.

I would like to thank my thesis advisory committee members: Carlos Arteaga, Bruce Carter, David Cortez, Scott Hiebert, and Sandra Zinkel. I appreciate all of their advice and guidance; many of their ideas and practical suggestions were so good I've

seen them spread from my projects into others. I am grateful to them for sharing their time so generously with me, and for encouraging me to think about the big picture.

I thank Michael Waterman and the Department of Biochemistry, Terry Dermody and the Vanderbilt MSTP, the Vanderbilt-Ingram Cancer Center, the DOD, and the Keystone Symposia for supporting my training and travel. (My precise sources of funding for the work herein were: the National Institute of Health grants CA70856 and CA105436 (J. A. Pietenpol), ES00267 and CA68485 (core services), US Army Medical Research and Materiel Command Grant W81XWH-04-1-0304 (J.M. Rosenbluth), and GM07347 (MSTP training).) I would also like to thank Marlene Jayne for help with all and sundry issues related to Biochemistry graduate training, and Robert Dortch, Peggy Fisher, Melvin Fitzgerald, Brenda Bilbrey, Cindy Sullivan, and Jan Lotterer for administrative support.

Thank you to my parents and my sister for all their encouragement in my life. My mother and father supported me through all of my choices, and gave me confidence in those choices. My sister has been my closest friend, always available to lend an ear; she reminds me how quickly time passes and how precious it is. Finally, I need to thank Daniel Mordes, who has been by my side throughout these graduate years. He is an outstanding and exceptionally talented, almost cylon-like scientist, and he's always kept me focused. Thank you for being there during the worst of times ('my paper was rejected'), and helping me to celebrate the best of times ('my paper was accepted!'). His great support enabled me to do this work.

TABLE OF CONTENTS

LIST OF TABLES

LIST OF FIGURES

LIST OF ABBREVIATIONS

3T3	3-day transfer, inoculum 3 x 10^5 cells
4EBP1	eukaryotic translation initiation factor 4E binding protein 1
5AZA	5-azacytidine
AD1	activation domain 1
AD2	activation domain 2
AFP	alpha-fetoprotein
AMP	adenosine monophosphate
AMPK	5'-AMP-activated protein kinase
ARMS	alveolar rhabdomyosarcoma
ATCC	American Type Culture Collection
BAC	bacterial artificial chromosome
BAX	BCL2-associated X protein
CEAS	Cis-regulatory Element Annotation System
ChIP	chromatin immunoprecipitation
Chk1	checkpoint kinase 1
Chk2	checkpoint kinase 2
Crm1	required for chromosome region maintenance, exportin-1
C-terminal	carboxy-terminal
DAVID	database for annotation, visualization and integrated discovery
DBD	DNA-binding domain
DDR	DNA damage response

DMEM	Dulbecco's modified Eagle's medium
DRAM	damage-regulated autophagy modulator
dsDNA	double-stranded DNA
EGF	epidermal growth factor
ERMS	embryonal rhabdomyosarcoma
ES	embryonic stem
FKHR	forkhead in rhabdomyosarcoma
FOXO1	forkhead box O1
FRAP1	FK506 binding protein 12-rapamycin associated protein 1
GABARAP	GABA(A) receptor-associated protein
GADD45A	growth arrest and DNA-damage-inducible, alpha
GAP	GTPase activating protein
GAPDH	glyceraldehyde-3-phosphate dehydrogenase
GATE-16	golgi-associated ATPase enhancer 16
GβL	G protein beta subunit-like
GSK3β	glycogen synthase kinase 3 beta
HMEC	human mammary epithelial cell
HNSCC	head and neck squamous cell carcinoma
iASPP	inhibitor of apoptosis stimulating protein of p53
IGF1	insulin-like growth factor 1
IGF1R	insulin-like growth factor 1 receptor
JAG1	Jagged 1
JAG2	Jagged 2

KEGG	Kyoto Encyclopedia of Genes and Genomes
LC3	microtubule-associated protein 1 light chain 3
LDL	low density lipoprotein
LDLR	low density lipoprotein receptor
LIPC	lipase C, hepatic
LIPG	lipase G, endothelial
LOH	loss of heterozygosity
LTR	long terminal repeat
MAP1LC3	microtubule-associated protein 1 light chain 3
MDM2	mouse double minute 2 homolog
MEF	mouse embryo fibroblast
MEME	Multiple Em for Motif Elicitation
miRNA	microRNA
mLST8	mammalian lethal with sec-13
MMTV	mouse mammary tumor virus
MSC	mesenchymal stem cell
mTOR	mammalian target of rapamycin
mTORC1	mammalian target of rapamycin complex 1
mTORC2	mammalian target of rapamycin complex 2
ncRNA	non-coding RNA
NES	nuclear export signal
NLS	nuclear localization signal
NMR	nuclear magnetic resonance

NRSF	neuron restrictive silencer factor
N-terminal	amino-terminal
OD	oligomerization domain
p53	tumor protein p53
p63	tumor protein p73-like
p70S6K	ribosomal protein S6 kinase, 70kDa
p73	tumor protein p73
PARP	poly (ADP-ribose) polymerase
PAX3	paired box 3
PAX7	paired box 7
PBS	phosphate buffered saline
PCR	polymerase chain reaction
PDK1	3-phosphoinositide dependent protein kinase-1
PDK2	3-phosphoinositide dependent protein kinase-2
PET	paired-end ditags
PI3K	phosphoinositide-3 kinase
PML	promyelocytic leukemia
PP2A	protein phosphatase 2A
PPARγ	peroxisome proliferator activated receptor gamma
PRAS40	proline-rich Akt substrate, 40 kDa
PROTOR/PRR5	protein observed with Rictor-1 / proline rich protein 5
PTEN	phosphatase and tensin homolog
qRT-PCR	quantitative, real-time, polymerase chain reaction

REDD1	regulated in development and DNA damage responses 1
RHEB	ras homolog enriched in brain
RNAi	RNA interference
RPMI	Roswell Park Memorial Institute medium
SAM	sterile alpha motif
SELEX	systematic evolution of ligands by exponential enrichment
SGK1	serum / glucocorticoid-regulated kinase 1
shRNA	short hairpin RNA
SIN1	stress activated protein kinase-interacting protein 1
siRNA	small interfering RNA
STAT1	signal transducer and activator of transcription 1
TCM	tumor conditioned medium
TGFβ	transforming growth factor β
TK	thymidine kinase
TRIM32	tripartite motif-containing 32
TSC	tuberous sclerosis complex
TTBS	tris-tween buffered saline
ULK1	unc-51-like kinase 1
UV	ultraviolet radiation
UVRAG	UV radiation resistance associated gene
WWOX	WW domain containing oxidoreductase
YAP	Yes-associated protein

CHAPTER I

INTRODUCTION

This dissertation focuses on the discovery and analysis of the mTOR-p73 signaling axis and human cancer. In this chapter, the current knowledge of mammalian transcription factors and gene regulatory networks in the context of recent genomic advances will be presented, as well as the role of p73 signaling during development and tumorigenesis. Relevant anti-cancer strategies will be reviewed, including a discussion of mTOR inhibitors. The major focus of this dissertation research was to understand p73 biology through its essential function as a transcription factor, the gene expression that it regulates. The data generated and presented in subsequent chapters has implications both for transcription factor signaling at large, as well as anti-cancer strategies that use predefined cancer subgroups.

Mammalian Transcription Factors

Post-genomic revelations about transcription factors

There are over 2,000 transcription factors in the human genome (1,2). These factors, by definition, bind to specific sequences of DNA to control recruitment of RNA polymerase and thus gene expression. Structurally, they contain both a DNA-binding domain and an activation domain. These domains can be functionally uncoupled; many hybrid proteins engineered to contain the DNA-binding domain of one transcription

factor and the activation domain of another can activate the same genes as the first. Transcription factors can be classified by the structure of their DNA-binding domain; annotation of the human genome reveals that ~10% of all genes encode a basic-helix-loop-helix, basic-leucine zipper, winged helix, zinc finger, or other structure predicted to bind DNA (1,2).

DNA-binding is sequence specific, and usually occurs at regulatory sites in promoters, introns, and enhancers (see below). These sites are used by transcription factors to modulate transcript levels, but are not essential for gene expression per se. A preinitiation complex of proteins is sufficient to enable a basal level of transcription. The DNA-binding domain of a transcription factor binds a regulatory site, often regardless of its orientation relative to the transcriptional start site, and the activation domain interacts with the preinitiation complex or with RNA polymerase II. These interactions stabilize the binding of RNA polymerase to DNA and promote successful completion of transcription initiation; the stronger the interactions, the greater the frequency with which initiation is completed (3). Transcription factors can also recruit other proteins to these regions, for example proteins that modify the architecture of surrounding chromatin to be in a more open or closed conformation.

Technological advances have allowed researchers to study the complex, wide-ranging effects of transcription factors in greater detail. Not only is there local organization of transcription factors at the loci that they bind, but also 3-dimensional organization of factors within the nucleus. This has been demonstrated through chromosome conformation capture, which uses a ligand efficiency-based measure to determine how frequently two regions are in close enough proximity to be cross-

linked (4). Chromosome conformation capture in combination with fluorescence in situ hybridization has been used to demonstrate how two distant regions can be connected by transcription factors. In one scenario the factor binds to both a regulatory sequence and to transcriptional machinery at a distant transcriptional start site through bending of intervening chromatin (5). In another scenario, two genes may be transcribed by the same transcription 'factory' (region of nucleus containing a high concentration of transcriptional machinery) (6,7). Through such mechanisms, distant intra- and inter-chromosomal sequences can be adjacent to one another. Whole-genome technologies have demonstrated that this is a highly regulated process that allows areas of the nucleus to contain high concentrations of factors engaged in transcribing functionally related genes (5-7).

Surprisingly, despite this complexity of nuclear architecture, and the observations that binding events for any given transcription factor vary widely between species (8), the DNA sequence itself seems sufficient to recruit and activate transcriptional machinery. This has been demonstrated using a mouse model of Down syndrome, in which mice stably transmit the human chromosome 21 as an extra chromosome to the full complement of mouse chromosomes (9). Mice from this strain, maintained for generations in a laboratory, were analyzed to determine the effect on a human chromosome of incubation in the milieu of a mouse nucleus. Surprisingly, in the mice carrying the ectopic human chromosome, transcription factors were recruited onto the human chromosome in a human pattern, rather than in the patterns of binding they exhibited on orthologous mouse sequences (9). This resulted in a human pattern of gene expression from the chromosome. In addition, the mouse epigenetic machinery was

maintaining a human-like epigenetic pattern. These results suggested that it is the DNA sequence itself and not nuclear context or architecture that determines transcription factor binding and activity. Because extant bioinformatic tools are unable to predict transcription factor binding sites with great fidelity, it is clear that there is much we do not know about sequence-based regulation of transcription factor binding and activity.

A greater understanding of this activity would have broad implications. The import that even a single transcription factor can have is illustrated by experiments in human stem cells. Expression of just one to four transcription factors is sufficient to induce stem cell-like pluripotency in adult fibroblasts (10), or induce transdifferentiation of adipose cells into muscle cells (11). In fact, even a single transcription factor binding site can have a significant impact at both a cellular and whole-organism level. For example, changing a single enhancer in a transgenic mouse model recapitulated the classic Darwinian model of evolution that describes small differences between the human arm, bat wing, and whale flipper. By swapping an enhancer upstream of the *Prx1* gene promoter in mice with the orthologous bat enhancer, mice were created with only one key phenotype: longer forearms (12). That is the first of many evolutionary steps that would be needed to transition from running on a forearm (mouse) to flying with a forearm (bat). Experiments such as these demonstrate the impact of transcription factor binding sites. However, in situ experiments are intensive and can only be performed by altering one binding site at a time.

Using genomic technologies described below, researchers began mapping transcription factor binding sites in a comprehensive manner. Such studies revealed that distinct transcription factors can bind thousands of sites in the human genome. These

studies allow greater exploration of sequence-based determinants of transcription factor activity, and, when coupled with microarray analyses, gene expression resulting from this activity. By considering a collection of transcription factor binding sites as a profile, one can gain insight to the biologic import of these protein-DNA interactions.

Gene Regulatory Networks

High-throughput detection of protein-DNA complexes

Chromatin immunoprecipitation (ChIP)-based techniques allow detection of specific protein-DNA interactions. There are two basic principles in ChIP. First, cells are cross-linked using an agent that induces reactive bond formation such as formaldehyde in order to trap transcription factors at cognate binding sites. Second, chromatin is fragmented and antibodies are used to isolate proteins of interest along with any sequences of DNA to which they are bound. After the cross-links are reversed, associated DNA fragments can be detected using a variety of methods such as polymerase chain reaction (PCR), hybridization, or direct sequencing. A transcription factor will have varying affinity for different DNA sequences; thus a factor will spend different amounts of time occupying distinct binding sites. Based on this principle, quantitative information can be gained from some ChIP methods.

Thousands of protein-DNA interactions can be detected in a single experiment by traditional sequencing of tags (~40-50 bp in length) in the DNA fragments followed by alignment of these sequences to the genome. This method is cost-effective, and has been extensively validated. However, it is not comprehensive, may contain some bias due to

preferential sequencing, and is not quantitative (13). This method has been called ChIPSeq, although this should be distinguished from newer sequencing-based methods described below.

Whole-genome ChIP can also be performed by hybridizing a pool of ChIP-enriched DNA fragments to tiling oligonucleotide arrays. This is called ChIP-on-Chip and provides quantitative information based on the level of enrichment of DNA sequences after ChIP compared to input. ChIP-on-Chip has additional advantages: it has been extensively tested in large multi-institutional studies and has been proven reproducible (14). ChIP-on-Chip analyses were originally performed with limited arrays that only detected binding events in human promoters. Technologic advances lead to the development of comprehensive whole-genome tiling arrays which demonstrated that most transcription factor binding sites do not actually occur in promoters (15). Both ChIP-Seq and ChIP-on-Chip are described in additional detail in later sections.

Finally, ChIP coupled with massively parallel sequencing platforms enables sequencing of millions of fragments; saturation is obtained and quantitative binding information achieved (16). This technique is currently too expensive for routine use by most laboratories, and has not been tested in a multi-institutional study like ChIP-on-Chip, so reproducibility is unknown and sequencing bias is not yet fully understood (14). However, as the latter technology becomes more affordable it has the potential to replace ChIP-on-Chip as the technique of choice for mapping genomic binding sites.

Determinants of transcription factor activity

As a growing number of transcription factor binding profiles are analyzed using these high-throughput techniques, aspects of transcription factor biochemistry are being re-evaluated given an unexpected level of complexity. All told, a multi-layered model explains how cells both regulate transcription factor binding and establish the loci at which transcription factors are active.

DNA Response Elements: Transcription factors bind specific DNA motifs, or response elements. These sequences can be highly precise or degenerate. Through a combination of in vitro and in vivo techniques, hundreds of such motifs have been measured (17). Response elements were originally reported as consensus 'strings' that give the most frequent nucleotide at each position in the motif. An even greater amount of information can be conveyed through matrix representations, which give the complete nucleotide occurrence probability for each position in the motif. These motifs are tools that can be used to scan the genome to identify novel candidate transcription factor binding sites. However, such methods have a high rate of error. Transcription factors can bind regions without a classical motif, or with a highly degenerate motif. Conversely, perfect motifs may not be bound at all by the cognate transcription factor. Often transcription factors bind only a small fraction of potential binding sites at a given time.

Epigenetic milieu: Another layer of regulation occurs through epigenetic marks such as DNA methylation, histone methylation, and histone acetylation that modify chromatin in distinct and complex patterns. This provides a 'code' that can alter transcription factor binding and activity. Multiple whole-genome analyses support this

model, most notably ChIP-on-Chip experiments through the ENCODE Project Consortium, and ChIP-Seq experiments in a variety of human cells (18,19).

One key mark that distinguishes distal enhancer elements is monomethylated histone H3 lysine 4 (H3K4me1). This was confirmed by ChIP-Seq measurements of STAT1 binding in HeLa cells before and after stimulation with interferon-gamma (18). H3K4me1 marked sites in untreated cells to which STAT1 subsequently bound after interferon-gamma treatment (18). These data, in conjunction with other studies of transcription factor binding, suggest that H3K4me1 is a dominant indicator of distal regulatory regions.

How are such marks maintained? Much remains unknown, however it is likely that the cell's epigenetic machinery transitions regulatory sequences from a 'poised' status to an active or repressed status. For example, cells maintain a 'bivalent mark' of both H3K4me3 and H3K27me3 at regulatory regions of development-specific genes in stem cells (20). As cell fate decisions are made, lineage-specific regions may become either actively marked (H3K4me3) or repressively marked (H3K27me3 or no mark). Furthermore, regulatory regions such as enhancers usually contain multiple transcription factor binding sites. Thus many factors could be recruiting histone modifying proteins in an additive manner at any given location. Indeed, analysis of STAT1-bound loci identified nearby motifs that could be bound by other transcription factors and cofactors during cellular maintenance and homeostasis (18). Given the massive combinations of histone and DNA modifications that mark regulatory regions, active regions, closed regions, etc., there is the potential for exquisite regulation of transcription factor binding.

Association with co-factors: As mentioned above, multiple transcription factors often bind in the same regulatory locus. These factors modify surrounding chromatin, but also interact with one another. Such interactions can either mediate recruitment of additional factors, stabilize factor binding, or inhibit factor binding to fine-tune transcriptional responses. One of the most striking examples is the pioneer factor FoxA1, that is capable of binding to chromatin even if it is in the 'closed' conformation, unwinding chromatin and allowing for subsequent binding events (21). FoxA1 binds predominantly to distal enhancer regions and epigenetic marks such as H3K4me1 are the major determinant of its binding (21). In breast cancer cells, FoxA1 binds H3K4me1-marked regions and then recruits the estrogen receptor to the same loci. Interestingly, in prostate cancer cells FoxA1 binds a different set of loci, which are also marked with H3K4me1. In prostate, FoxA1 recruits the androgen receptor to these loci to regulate tissue-specific gene expression. Thus, specific transcriptional programs can depend on differential regulation of epigenetic machinery as well as distinct expression of collaborative transcription factors (21). We applied such principles to our analysis of the p53 homolog, p73, as described in Chapters IV and V.

p73 Signaling During Development and Tumorigenesis

The p53 family of transcription factors: p53, p63 and p73

The mammalian p53, p63, and p73 genes descended from an ancestral gene, and share a common domain architecture and significant sequence identity (22). However, their differences in vivo are striking. While p53 is mutated in over 50% of human

tumors, p63 and p73 are rarely mutated (23). Instead, the p63 locus is amplified in a small percentage of squamous carcinomas (24-26), and p73 is over-expressed in several tumor types (23). In addition, while p53 null mice have an increased frequency of spontaneous tumor formation, p63 and p73 null mice die tumor-free from developmental defects (27,28), as discussed further below. Although p63 and p73 can engage apoptotic pathways in vitro (29-34), it is clear that they are not classic Knudson-like tumor suppressors like p53.

One possibility is that p63 and p73 are tumor suppressors that are inactivated during tumorigenesis by a non-classical mechanism. Investigation of this possibility is complicated by the complexity of RNA isoforms expressed and the potential for tissue-specific expression. There are nine possible isoforms for p53, six for p63, and thirty-five for p73 that can arise through a combination of promoter usage and alternative splicing (35,36). For p63 and p73, two classes of isoforms exist that either contain (TA) or lack (ΔN) the N-terminal transactivation domain required for full activation of target genes (37) (Figure 1). All isoforms contain a DNA-binding domain, nuclear localization signal, and tetramerization domain (Table 1). At the C-terminus, p53 contains a basic domain, whereas p63 and p73 contain sterile alpha motifs that undergo extensive alternative splicing. These domains are described in greater detail below:

Transactivation Domain: The N-terminal domain of p53 contains two activation domains termed AD1 and AD2 (38). These domains interact with basal transcriptional machinery and are essential for p53 function. In addition, nuclear magnetic resonance spectroscopy demonstrated that these domains are unstructured, and likely remain so unless they are bound by a p53 regulatory protein (38). Proteins that interact with AD1

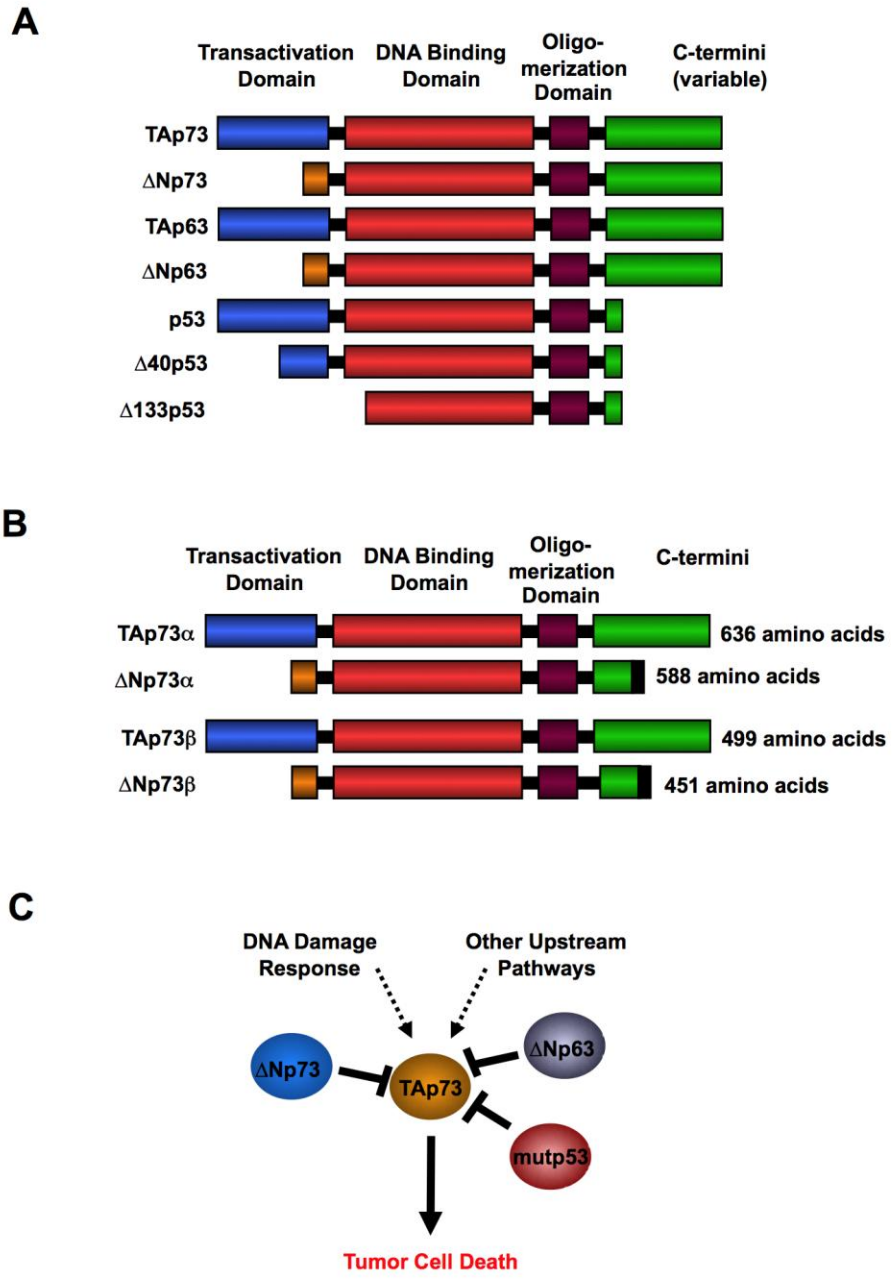

Figure 1: p53 family isoforms and model of p53 family function. A) Active isoforms of the p53 family contain a transactivation domain, whereas inhibitory isoforms lack a transactivation domain. B) Schematic depicting key N- and C-terminal p73 isoforms. C) Other family member isoforms may inhibit TAp73 in cells, thus preventing TAp73 from engaging in tumor suppressive functions and reducing selective pressure for mutation of p73 during tumorigenesis.

Table 1: Sequence identity between p53 family proteins by domain

Domain	p53/p73	p53/p63	p63/p73
Transactivation	30%	22%	30%
DNA-binding	63%	60%	87%
Oligomerization	42%	37%	65%
Sterile Alpha Motif			51%

and AD2 include the negative regulator mdm2 (an E3 ligase) and the positive regulator p300 (an acetyltransferase). Such interactions not only alter p53 activity, but also modify histone acetylation at p53-bound chromatin (39). Interestingly, recent evidence suggests that p53 can undergo alternative splicing to create a protein that lacks AD1 but retains AD2 (Figure 1A). This isoform is impaired in the ability to induce cell cycle arrest but retains potent apoptotic activity. Some of this effect is due to increased stability of p53 secondary to decreased interaction with mdm2 (36,40).

Full-length TAp63 and TAp73 have only one activation domain, AD1, that is 22% and 29% homologous to the AD1 of p53. The AD1s of p53, p63, and p73 share similar interacting proteins and functional effect. Cryptic promoter usage and alternative splicing can yield truncated ΔNp63 and ΔNp73 proteins that lack AD1 (41). These ΔN proteins contain 13 or 14 unique residues, which in conjunction with a proline-rich domain act as an AD2 (42). AD2 is weaker than AD1, thus ΔN isoforms act as dominant-negatives to TA isoforms, at least in some contexts. (This results from ΔN:TA hetero-dimerization and sequestration of TA proteins from binding sites.) There is evidence that TAp73 binds and regulates the ΔN promoter in some cell lines and tumor types (43). However, the determinants of cryptic promoter usage and particularly of alternative splicing are largely unknown.

DNA-Binding Domain: The DNA-binding domain is the most conserved domain between p53 family members and across species. Crystal structures of this region demonstrate that it is composed of a core antiparallel β-sheet that serves as a scaffold for both the protein loops that contact DNA and the zinc atom in this domain (41). Importantly, key residues that contact DNA are conserved in p53, p63, and p73; missense

mutations in these residues abolish binding of p53 to DNA (41). Although p63 and p73 are not mutated during tumorigenesis, missense germline mutations in p63 in some of the same residues lead to autosomal dominantly inherited syndromes that display features such as limb malformations, facial clefting, and ectodermal displasia (44).

Subtle differences in the DNA binding domain may result in sequence-specific binding differences between p53, p63, and p73. All family members can bind the canonical p53 response element that contains two half sites of RRRCWWGYYY, separated by a spacer of up to 13 bp (where R = purine, C = cytosine, W = adenine or thymidine, G = guanine, and Y = pyrimidine) (45,46). However, p63 and p73 contain some differences in the residues of the protein loops that contact DNA (39). And p63 preferentially recognizes the half-site RRRCGTGYYY, indicating that differences in sequence-specific binding may be the result of these subtle structural differences (47,48). Our analysis of p73 sequence-specific binding is presented in Chapter IV.

Nuclear targeting regions: p53 contains a bipartite nuclear localization signal (NLS) at residues 305-322 and nuclear export signal (NES) at residues 11-27 and 340-351. These sequences allow p53 to shuttle between the nucleus and cytoplasm, and are conserved in both p63 and p73 (38). For p53 and p73, these domains are sufficient for the nuclear import and export of reporter proteins (49,50). Interestingly, residues in these domains can be post-translationally modified in p53, leading to enhanced binding to response elements. The residues that are post-translationally modified in p53 are not conserved in p73, suggesting distinct activities for these two family members (38).

Oligomerization domain: Each p53 family member binds to DNA as a dimer of dimers, mediated by secondary structures within the oligomerization domain. Monomers

bind each other through antiparallel β-sheet and antiparallel helix interactions. Dimers bind each other through parallel helix-helix interactions (38). Tetramerization is required for many of the known functions of these family members, and may also be the mechanism by which ΔN isoforms act as dominant negatives against their full-length counterparts. Interestingly, p53 cannot hetero-tetramerize with either p63 or p73, but in vitro studies demonstrate that p63 and p73 can weakly interact with one another (51).

C-terminal domains: p53 family members contain intriguing differences in their C-terminal domains. p53 has a basic domain, which is a regulatory structure that undergoes extensive post-translational modification. p63 and p73 contain C-terminal sterile alpha motif (SAM) domains. The SAM domain is a conserved transcription factor motif implicated in protein-protein interactions. It was originally named 'Sterile' based on its presence in four proteins crucial for yeast sexual differentiation and 'Alpha' based on secondary-structure predictions of high α-helical content. Over 1300 proteins in all genomes contain SAM domains that are linked to diverse and wide-ranging functions (52). In p63, the SAM domain is mutated in developmental syndromes associated with ectodermal dysplasia and facial clefting (44). In p73, the SAM domain binds to both anionic and zwitterionic lipids (53), although the functional implications of these interactions are unknown. In both p63 and p73, the C-terminal domains can act as inhibitory domains, possibly by preventing association between transcriptional co-activators and the N-terminus (54). The SAM domains also undergo extensive alternative splicing, leading to three isoforms in p63 (α-γ) and at least seven in p73 (α-η). Select isoforms of p73 are depicted in Figure 1. Unlike the TA and ΔN N-terminal

isoforms, which are defined by the presence or absence of the transcriptional activation domain, the functions of the C-terminal isoforms are unknown.

p53 family isoforms in tumorigenesis

The various isoforms of p53 family members play differential and often opposing roles during tumorigenesis. The purported active isoform of p73, TAp73, is of particular interest because it is frequently expressed in human cancers (37) and can be inhibited by either ΔNp63 or ΔNp73 (37,55) (Figure 1C). In particular, ΔNp63:TAp73 complexes that inactivate TAp73 exist in head and neck squamous cell carcinoma (HNSCC) and 'basal-like' breast cancer cell lines, and evidence suggests these complexes occur in vivo in the corresponding tumor types (56-58). In addition, tumor-specific mutant forms of p53 have the ability to bind and inhibit p73 (59) (Figure 1A). Thus the ability of ΔNp63, ΔNp73, or mutant p53 to inhibit TAp73 may obviate the need for mutation of p73 during tumorigenesis. A single mutation in p53 might decrease both p53 and p73 activities. Similarly, an increase in ΔNp63 or ΔNp73 levels could be another means of inactivating TAp73, ultimately preventing TAp73 from engaging in tumor suppressive activities.

Even though recently discovered p53 isoforms can inhibit p53 transcriptional activity, p53 is mutated in cancers (36,40). The p53 locus can undergo alternative splicing and contains two promoters, thus creating two classes of isoforms that also either contain or lack an N-terminal transactivation domain. Those isoforms that lack the transactivation domain have been shown to inhibit full-length p53 in co-transfection experiments (36), and are over-expressed in tumors (36,60-62). Thus the p53, p63, and

p73 genes share similar organization and can each give rise to active and inhibitory isoforms.

Why might inhibitory isoforms have a differential effect on the need for mutation of p53 versus p73? Three possible answers are: 1) TAp73 is not a tumor suppressor, or is a much weaker tumor suppressor than p53. 2) Tissue-specific and context-dependent upstream signals and regulators control whether p53 and/ or p73 is active in tumor suppression. 3) ΔNp73 has oncogenic properties that are separate from its ability to inhibit p53 family members. Even the first of these possibilities, whether or not TAp73 is a tumor suppressor, was surprisingly difficult to demonstrate conclusively (63), and multiple mouse models were required to shed light on this issue.

Manifestations of p73 null mice

Mouse models with inactivation of p53 family members are an invaluable resource, providing clues to if and when p53, p63, and p73 act as tumor suppressors in vivo. *p63*$^{-/-}$ mice that do and do not develop cancers have been described in detail (64). For p73, there is greater consensus, as mice deficient for the TAp73 isoform of p73, and *p73* heterozygous mice, demonstrate that it is indeed a tumor suppressor.

The first p73 transgenic mice that were studied were deficient for all isoforms of p73 (28). These mice survived to birth and had severe developmental abnormalities including: 1) hippocampal dysgenesis, 2) hydrocephalus due to excessive neuronal death, 3) loss of pheromone sensing and lack of mating, 4) massive sinus inflammation and infection, 5) gastrointestinal erosion and excessive mucosecretion, and 6) runting (28). The deficient or faulty mechanisms behind many of these phenotypes remain unknown.

For example, it is unclear if immune infiltration in the nasal cavity is due to defects in the immune system, or epithelial dysfunction leading to excessive mucus secretion or infection. The majority of p73-deficient mice lived to be only 4-6 weeks old, dying from gastrointestinal or cerebral hemorrhage (28). During this shortened lifespan, there was no increase in spontaneous tumor formation.

According to the subsequent TA isoform-specific knockout p73 mouse model, p73-depleted animals may display complex tumor phenotypes due to the loss of both an oncogene (ΔNp73) and a tumor suppressor (TAp73) that can lead to a multitude of intermediate phenotypes. In addition, tumor analysis of p73-deficient animals is complicated by the severe developmental problems that lead to an early demise, largely attributed to loss of the ΔNp73 isoform that is expressed during development (28). Mak and colleagues circumvented these issues, using a gene targeting approach that deleted exons that specifically encode the transactivation domain of p73. Because the *p73* gene contains a second promoter from which ΔNp73 can be transcribed, this approach led to a selective deficiency of all TAp73 isoforms. The developmental defects of the resulting mice were less severe than their $p73^{-/-}$ counterparts. Subsequent analysis revealed an increased incidence of both spontaneous and carcinogen-induced tumors in the $TAp73^{-/-}$ mice, showing that TAp73 is a tumor suppressor (65).

In part, the $TAp73^{-/-}$ tumors provided critical validation of previous work that demonstrated an increased rate of spontaneous tumors in $p73^{+/-}$ mice (66). Interestingly, this same study demonstrated that $p63^{+/-}$ mice develop spontaneous tumors, and that $p53^{+/-}$ $p63^{+/-}$ mice have an enhanced rate of tumor formation compared to $p53^{+/-}$ mice (66). This is in contrast to another study using a distinct, inactivated *p63* allele that

demonstrated a lack of tumors in *p63* heterozygous mice (67). This second model also showed a *decreased* rate of tumor formation in mice heterozygous for both *p53* and *p63* (67). The contradictory results of this second study may be due to expression of truncated p63 proteins that appear to be expressed from the transgenic allele (68). Regardless, the opposing results in different p63-deficient mice heightened the need for validation and additional characterization of the p73-deficient phenotypes. Although there seem to be some differences in tumor spectrum, in general the TAp73-deficient mice recapitulated the tumor-prone phenotype of the $p73^{+/-}$ mice (65).

Decreased TAp73 inhibits p53 function in vitro in a context-dependent manner. For example, studies in E1A-transformed mouse embryonic fibroblasts (MEFs) suggested that p63 and p73 are required for p53-mediated apoptosis (69). This finding was contradicted by a second study in T-cells showing that p63 and p73 are dispensable for p53-mediated apoptosis (70). In the TAp73 null mice, E1A-transformed MEFs and T-cells did not demonstrate any alteration in p53 activity, suggesting that p73 is dispensable for p53 function, or that ΔNp73 compensates for the loss of TAp73 in E1A-transformed MEFs. It would be interesting to determine the effect of TAp73 loss on p53 function in an in vivo model in which p53 activity is dependent on both p63 and p73, such as during ionizing radiation-induced central nervous system apoptosis (69). This would be particularly relevant because all three p53 family members contribute to neuron development and function (71). Indeed, the $TAp73^{-/-}$ mice support a model that ascribes distinct roles for ΔNp73 in the survival of neurons after injury (71), and for TAp73 during hippocampal development. How this system is perturbed during genotoxic stress

would provide insight to the roles of the p53 family members in the nervous system and during tumorigenesis.

A possible mechanism for TAp73 tumor suppressive function came from a second phenotype of TAp73-deficient mice: infertility. Unlike the p73 heterozygotes, which do not mate due to lack of pheromone sensing (28), the *TAp73* null mice mate normally but are infertile (65). Female infertility was due to genomic instability of the oocyte. This genomic instability may have lead to retention during folliculogenesis and decreased viability, and may be similar in effect to the decreased oocyte quality that occurs with natural aging.

p63 also plays a role in the female oocyte; TAp63 is expressed and is essential for DNA damage-induced oocyte death that does not involve p53 (72). Thus, the p53 family emerges as a central player in maintaining fidelity of the female germ line. TAp73 prevents genomic stress, and loss of TAp73 during aging may contribute to the decline in oocyte viability. In contrast, TAp63 is activated by genotoxic agents to induce apoptosis in oocytes that have sustained genomic damage (72). Whether p73 cooperates with p63 during this process, and the roles that these family members may play in the male germ line (*TAp73*$^{-/-}$ male mice are also infertile), remains unknown.

Thus the two major phenotypes of the TAp73-deficient mice, cancer and infertility, are both associated with genomic instability. These data suggest that maintaining the fidelity of the genome is a key molecular function of TAp73 at least in some tissues. The balance between TAp73 and ΔNp73 protein levels may be the ultimate determinant of tumor formation. An understanding of the functions of ΔNp73 in adult

tissues, and how ΔNp73 alters tumor incidence, are unknown and await the development of conditional p73 mouse models.

p73 expression in human cancers

Additional in vivo analysis of p73 has come from the study of p73 in human tumors. These analyses are complicated by the poor quality of p73 antibodies and the number and complexity of p73 isoforms. *p73* loss of heterozygosity (LOH) has been observed in approximately 20% of examined patients; however, LOH does not correlate with a decrease in p73 expression level and seems to be driven by selection for allelic loss of another tumor suppressor near the *p73* locus (73). In addition, only very rare mutations of *p73* have been detected (~0.6% of reported patients in one meta-analysis) (74). Polymorphisms of *p73* have been reported to both increase and decrease tumor risk in different populations (74). Taken together, these data argue against p73 as a classic Knudson-like tumor suppressor.

In contrast, increased p73 RNA and protein levels have been detected in a number of cancer types. In addition, specific antibodies against accumulated p73 protein have been identified in cancer patients (75). Overexpression of p73 or ΔNp73 isoforms has been associated with poor prognosis in patients with hepatocellular, colorectal, breast, ovarian, and lung cancers (74). In malignant myeloproliferations, for example, overexpression of p73 is a frequent event. In one such disorder, chronic myeloid leukemia, overexpression specifically of the epsilon isoform of p73 is observed, an expression pattern that appears to be unique to this tumor type. In contrast, in malignant lymphoproliferative disorders the *p73* gene is hypermethylated resulting in decreased p73

expression relative to myeloproliferations (74). These studies highlight the diversity of p73 expression patterns in human tumors.

Large cohorts of breast and colon tumors have also been assessed for p73 RNA expression levels. One study revealed tumor-specific upregulation of both TAp73 and ΔNp73 (76). Interestingly, correlations between p73 levels and specific molecular alterations and tumor characteristics were observed. There was association between wild-type p53 and upregulation of p73 isoforms (TAp73 and ΔNp73 in colon cancer and ΔNp73 in breast cancer), suggesting that there may be redundancy in the functions of these family members, thus alleviating selective pressure for dysregulation of both p53 and p73 in the same tumor, or that ΔNp73 can inhibit p53. Correlations were also found between TAp73 and E2F-1 RNA levels, and indeed in vitro studies show that the *p73* promoter is regulated by E2F-1 (77,78). In colon cancer, ΔNp73 levels increased in parallel with increasing tumor stage. Correlations with tumor stage have also been observed in hepatocellular carcinoma, chronic lymphocytic leukemia, and lung cancer (76).

Interestingly, the increased p73 protein may alter tumor chemosensitivity, depending primarily on the ratio of p73 isoforms that are over-expressed. In most tumor types, ΔNp73 expression is associated with chemoresistance and TAp73 expression is associated with chemosensitivity (79,80). These results suggest that TAp73 is a potential therapeutic target in specific types of cancer, as discussed further below.

p73 target genes, with comparison to p53

p73 can activate the transcription of many p53 target genes such as *MDM2*, *p21*, *BAX*, and *GADD45A* (81), and hundreds of p53-bound genes can also be bound by p73 (82). This is in concordance with in vitro experiments that demonstrate that p73 regulates apoptosis and cell cycle arrest. Interestingly, there are some differences in transactivation efficiency between p53 and p73. For example, p73 mediates higher *14-3-3σ* and *GADD45A* induction and lower *p21* induction compared to p53 (81). Another interesting example is alpha fetoprotein (AFP), a target gene that is expressed during liver development. *AFP* is a target of p53 and p73 (but not p63) transcriptional repression (83). Both p53 and p73 bind to the promoter region of *AFP* simultaneously and modify surrounding chromatin to inhibit transcription initiation. However, there are some differences in the activities of p53 and p73; p73 has a decreased ability to repress *AFP* transcription compared to p53 (83).

Analysis of individual genes has made it clear that p73 regulates target genes distinct from those regulated by p53. For example, aquaporin 3 is a water and glycerol transporter whose expression is induced by p73 but only very weakly by p53 (84). This target gene contains three p53-responsive half-sites in its promoter. Similarly, *JAG1* and *JAG2*, which express ligands of the notch receptor, are p63 and p73 target genes that are not regulated by p53 (85). These genes contain four half-sites of the p53 responsive element in intron 2 that are likely used by p73 to regulate transcription. The full extent of shared versus unique p53 and p73 target genes is presented in Chapter IV.

Several high-throughput analyses of p53 and p63 target genes have been performed; these studies lay the groundwork for comparison to p73. One of the most

notable was a paired-end ditag ChIP-sequencing approach developed by Wei and colleagues that identified hundreds of p53 binding sites in Hct116 cells treated with 5-fluorouracil (86). As described in greater detail in later chapters, this study identified key determinants of p53 binding and function. It also provided a resource for further studies of p53 binding. For example, another group created an array for ChIP-on-Chip that only detects binding events at p53 target genes identified in the Wei *et al.* study. This focused array was used to confirm the results of the original study, and to study p53 binding in multiple cell types in response to cellular stresses (87).

In primary cells, two sets of p53 binding sites were identified (87). One set was bound by p53 both at baseline and after p53-inducing cellular stress, and the binding level of p53 did not change after stress. At the second much larger set of sites, p53 binding was only detected after stress. In contrast, in three established cell lines p53 bound to almost all of its target genes both at baseline and after a variety of p53-inducing cellular stresses. Importantly, the binding level at all sites correlated with the amount of p53 protein in the cell, both after induction and after RNAi-mediated depletion of p53 (87). In these cancer cell lines, binding did not seem to be the critical determinant of p53 transcriptional activity. It will be important to evaluate this model of p53 binding and activity in additional tissues and cancer cell lines, particularly because p53 occupancy of promoters at baseline has been observed in other normal cell types (88). Furthermore, we present a different model for p73 binding in response to cellular stress in Chapter IV.

Signaling pathways upstream of p73

The differential phenotypes of the p53 family mouse models suggest that different upstream signals regulate this family – temporal, tissue-specific, and context-dependent cues lead to separation of function in the p53 family. This might occur, for example, through the E3-ubiquitin ligase Mdm2 which triggers the degradation of p53 but not p73 (89). Or it may occur through the cofactor YAP, which binds to p73 but not p53, enhancing p73 activity as well as recruiting p73 to specific target genes during apoptosis (90-92). By mechanisms such as these, differential activation of p53, p63, and p73 isoforms can be achieved. Ultimately, the settings in which p53 family members are active will select for their inactivation in human tumors.

In terms of upstream signals, the DNA Damage Response (DDR) signaling pathway is the classic activator of p53. Initial analyses of DDR pathways were performed in the TAp73$^{-/-}$ mice. Intriguingly, DNA damaging agents such as irradiation, etoposide and cisplatin were ineffective at inducing TAp73-dependent cell death in either T-cells or MEFs, suggesting a clear differential response to DNA damage between p53 and p73 (65). This was in contrast to in vitro evidence that p73 can be activated by a subset of DDR-inducing agents, and regulated by kinases in the DNA Damage pathway such as Chk1 and Chk2 (93). Perhaps p73 responds to genotoxic stress in a tissue-specific or context-dependent manner, for example only in the absence of p53 (94).

There is evidence that the DNA damage response activates p73 through different mechanisms than p53. For example, cisplatin-mediated induction of p73 occurs at the protein level and, at least in some contexts, is dependent on an intact mismatch repair (MMR) pathway (32). It has been suggested that some proteins in the MMR complex act

as sensors of cisplatin-DNA adducts, while other proteins act as adaptors to recruit, modify, and stabilize p73 (95). The kinase c-abl is also required for cisplatin-mediated induction of p73 but not p53; c-abl phosphoryates p73 on tyrosine 99 in the transactivation domain (31,32,34). In Chapter III we show that mTOR inhibition leads to induction of p73 but not p53. Because genotoxic agents can inhibit mTOR (96), this may be an additional mechanism by which the DNA damage response regulates p73, and may explain some discrepancies in the literature about p73 activation.

Careful dissection of p73 changes in response to a variety of genotoxic stresses suggests that p73 can be induced by some agents, but not others such as ultraviolet radiation, and that different doses and time windows are needed to activate p73 in comparison to p53. For example, low doses but not high doses of several DNA damaging agents were found to activate p73 (97). Our preliminary data suggests that neither γ-irradiation nor adriamycin increases p73 levels in select mouse tissues (unpublished observations). Further inquiry in vivo is required to understand these conflicting data on p73 and genotoxic stress in multiple contexts.

There was clear evidence of tissue-specific function in the TAp73$^{-/-}$ mice. Loss of TAp73 led to the development of genomic instability, but only in select tissues. Cells isolated from the lung but not the thymus were aneuploid in the absence of TAp73. This correlated with the development of lung tumors but not thymic tumors, and was highly suggestive of a causal relationship (65). Through such data, a model has been proposed in which p53 is activated by environmental and/or genotoxic stress, and cells in this setting select for p53 mutations. In contrast, p73 may be activated by other types of stresses, in distinct contexts, leading to different routes of inactivation (98). Perhaps

lessons learned from p63/p73 biology will shed further light on p53 function. p53 inhibitory isoforms are expressed in human cancer types with lower p53 mutation rates: breast cancer, Acute Myeloid Leukemia, and HNSCC (99). Because different cancers are promoted by different environmental stresses, these correlations suggest that upstream signals determine if p53 family members are inactivated by mutation or by inhibitory isoforms.

What are the alternative upstream signals, outside of classic DDR signaling? Results from a fibroblast model of step-wise tumorigenesis suggest that TAp73 and ΔNp73 are engaged at different stages of tumorigenesis, and that the function of TAp73 is to contribute to contact inhibition in high density cell cultures (100). Loss of TAp73 enabled anchorage-independent growth, unlike p53 depletion that allowed cells to escape cell-cycle arrest and apoptosis. In this model, p53 and p73 performed different molecular functions that both lead to tumor suppression, and were activated during different stages of tumorigenesis.

As described in Chapter III, we developed an approach to identify upstream regulators of transcription factors using downstream gene signatures. Using this approach, mTOR was identified as a negative regulator of p73. Notably, pharmacologic inhibition of mTOR in primary human mammary epithelial cells resulted in differential regulation of p53 family members. Cells exhibited selective upregulation of TAp73, whereas ΔNp63 and p53 levels both decreased. Since mTOR is a master regulator of energy homeostasis and cell growth, and is often active in tumors (101,102), this suggests that mTOR may inhibit TAp73 in tumors. In general, cancer cells may use upstream

kinases or cofactors to inhibit p53 family members in different cellular contexts, ultimately maintaining proliferation and survival.

The mTOR Kinase Pathway

The two mTOR kinase complexes

The mammalian Target of Rapamycin (mTOR) kinase is a ubiquitous protein kinase that integrates multiple signals to control cellular growth and proliferation. There are two mTOR complexes, called mTORC1 and mTORC2, with different substrates and upstream regulators. Both complexes contain mLST8/GβL, an essential component that stabilizes the complex and contains potential protein docking sites, and FRAP1, the catalytic kinase subunit (103). mTORC1 also contains PRAS40, which is involved in Akt-dependent activation of mTOR, and Raptor, which contains the substrate docking site (104). mTORC2 also contains SIN1, which stabilizes the complex, PROTOR/PRR5, a protein of unknown function, and Rictor, which provides the substrate docking site (105,106). In this dissertation 'mTOR' refers to mTORC1 unless otherwise noted.

Two primary substrates of mTORC1 are the eIF-4E-binding protein 1 (4EBP1) and p70 S6 kinase (S6K) that play a role in the translation regulation of mRNAs, including those involved in G1-phase progression. mTORC1 also phosphorylates other substrates such as ULK1, a regulator of autophagy (107,108). Less is known about the substrates of mTORC2. Only two mTORC2 substrates have been identified to date: SGK1, involved in the cellular stress response, and Akt, a key protein that integrates growth factor signals (109).

mTORC2 phosphorylates Akt on Serine 473. However, two phosphorylation events are required for full activation of Akt. Insulin-like growth factor 1 (IGF1) binds to its receptor (IGFR), resulting in recruitment of phosphoinositide-3 kinase (PI3K) to the cell membrane, and an accumulation of phosphoinositides. PI3K is counteracted by a lipid 3' phosphatase, phosphatase and tensin homolog (PTEN). The lipid second messengers generated by PI3K serve as docking sites for a 3-phosphoinositide dependent protein kinase (PDK), PDK1, and for Akt, resulting in PDK1-mediated phosphorylation of Akt on Threonine 308 (110). mTORC2 is the previously elusive PDK2 that is also recruited to the cell membrane to phosphorylate Akt on Serine 473, resulting in full activation of Akt (111).

Interestingly, Akt activates mTORC1 by inhibiting its gatekeeper, the tuberous sclerosis complex (TSC) that contains two proteins called TSC1 and TSC2. (Akt specifically phosphorylates and inactivates TSC2.) The TSC complex is a GTP-Activating Protein (GAP) for the RHEB G-protein, which is an activator of mTOR (110). Through this mechanism, the TSC proteins serve as integrators of numerous signals that all feed into mTORC1; TSC-mediated inhibition of mTORC1 may be released depending on the status of these signals. The other major kinase that feeds into the TSC complex is AMPK, which is a major sensor of cellular AMP levels and thus energy status. Glucose deprivation results in an increase in AMP, which serves as a coactivator of AMPK, and in activation of the LKB1 tumor suppressor kinase, which phosphorylates AMPK. AMPK phosphorylates TSC2, but unlike Akt-mediated phosphorylation this is an activating signal (112). Through these upstream kinases, mTORC1 responds to low energy and

growth factor levels by inhibiting translation of specific mRNAs and increasing autophagy, a process described in greater detail below.

Thus, mTORC2 is upstream of mTORC1, but the factors that regulate mTORC2 activity are unknown. mTORC2 plays roles in cytoskeleton reorganization and fat metabolism (106,113,114). In addition, mouse models of prostate cancer in which PTEN is deleted demonstrated that mTORC2 activity is required for the formation of at least some tumor types, likely through its phosphorylation of Akt (115).

Cross-talk with p53

The p53 and mTOR signaling pathways are multiply inter-connected. In general, these connections comprise either a fast response or a slow response to DNA damage and cellular stress, resulting in a p53-dependent decrease in cell growth and proliferation and increase in cellular autophagy. The genes in these pathways (p53, PTEN, TSC2, PI3K, Akt, MDM2, AMPK, and mTOR) are the most frequently deregulated genes in human tumors, highlighting their importance as critical control mechanisms.

The fast response between mTOR and p53 occurs within minutes after cellular stress. Glucose starvation results in Ser-15 phosphorylation of p53, mediated by AMPK. A Ser-15 p53 phophatase, α-4 PP2A, is activated through phosphorylation by mTOR. Theoretically this should create a positive feedback loop resulting in sustained p53 activation, although in vitro experiments suggest that many time and dose-dependent variables affect this response (110). In contrast, after DNA damage, activated p53 activates AMPK. This occurs through sestrin-1 and sestrin-2, p53 target genes, that bind to both p53 and AMPK and promote AMPK activity (96). Thus, DNA damage activates

p53, which activates AMPK, and the latter downregulates mTOR, resulting in decreased translation of select mRNAs and increased autophagy levels.

There is also a slow response, due to inter-connections between p53 and mTOR that do not occur until hours after initiation of cellular stress. Both PTEN and TSC2 are p53 target genes, although their regulation by p53 appears to be highly cell type and context specific (116). The expression products of both of these genes, as described above, inhibit mTOR. In addition, REDD1 is a p53 target gene that is activated in response to hypoxia, and inhibits mTOR through TSC2 (117,118). Thus, these target genes cause decreased cellular growth and proliferation, often in a p53 and mTOR-dependent manner.

p53 can act both downstream and upstream of mTOR signaling. Hamartomas contain constitutively active mTOR signaling (in familial syndromes this occurs due to genetic inactivation of *TSC1* or *TSC2*), and also have high levels of active p53 (119). Elevated p53 levels may be due to downregulation of Mdm2 secondary to decreased translation of *Mdm2* mRNA. While the kinase Akt phosphorylates Mdm2, leading to Mdm2 activation and downregulation of p53 activity, $PTEN^{-/-}$ cells have increased p53 activity (110). Similary, we have observed a slight decrease in p53 levels after pharmacologic inhibition of mTOR (discussed in later chapters). The functional consequences of p53 downstream of mTOR remain unknown.

Role in tumorigenesis and cancer therapy

mTOR inhibitors are currently in clinical trials for a broad range of tumor types. As single agents, rapamycin analogs have generally not shown strong efficacy (102).

Given the importance of mTOR in tumorigenesis, three strategies have been proposed to improve clinical response to these agents. First, because mTOR inhibitors have the ability to synergize with a large number of genotoxic agents, they are being pursued in combination therapies. Second, since a small subset of patients show striking reductions in tumor volume after treatment with rapamycin analogues, marker-based prediction of patients that will respond to mTOR-targeting therapies could guide treatment regiments. Third, mTOR inhibitors evaluated in clinical trials were mTORC1 inhibitors. Based on feedback loops such as those described above, inhibitors that target FRAP1, the catalytic kinase subunit in both mTORC1 and mTORC2, may show greater efficacy as cancer therapies than rapamycin analogues and several pharmaceutical companies have these dual inhibitors under development.

mTOR inhibitors block cellular proliferation and in combination enhance apoptosis, particularly in synergy with other agents (120-123). Both of these functions would inhibit tumor cell growth. In addition, mTOR inhibitors increase autophagy, a catalytic process in which double-membrane vesicles surround proteins and organelles and digest them into components for re-use (reviewed in (124)). Autophagy allows cells to survive periods of starvation, as this catalytic process increases cellular nutrient pools. Autophagy is also a normal homeostatic process, and inactivation of key autophagy genes in transgenic mouse models causes either embryonic lethality, perinatal lethality from starvation, or severe tissue dysfunction from intracellular inclusions (124). Haploinsufficiency of some of the same genes leads to an elevated frequency of tumor formation; thus, autophagy is a critical process that maintains cellular fidelity. Finally,

autophagy can be associated with tumor cell death due to excessive catabolism, or as a supplemental process that occurs as a 'clean up' mechanism during apoptosis (124).

DNA damage-induced activation of p53 induces autophagy through the p53 target gene and lysosomal protein DRAM, and also through AMPK-mediated inhibition of mTOR (125). (Of note, cytoplasmic p53 inhibits autophagy at baseline, in a manner that does not seem to be induced by DNA damage (126).) Thus, autophagy will likely play a critical role in anti-tumor strategies that target mTOR or p53.

Anti-Cancer Strategies Targeting p73

Several anti-cancer approaches have targeted p53. However, there has been increasing interest in p73 as a target based on its expression in tumors that have inactivated p53. This is highlighted by two studies. First, a high-throughput based screen identified small molecules that activate p53 target genes and apoptosis in p53-null cells. Two of the small molecules mediated their activity through TAp73, as demonstrated using TAp73-specific RNAi (127). In a separate study, a novel p53-derived peptide (37AA) was identified that stimulates cell death through activation of p53 family target genes. It functions by preventing TAp73 from interacting with an inhibitor, iASPP, resulting in TAp73 activation in p53-null cell lines and xenografts (128). The discoveries from these two approaches show the promise of directly targeting p73 for therapeutic gain.

In vitro studies have used adenoviruses to grossly increase TAp73 levels, overcoming potential regulatory mechanisms and leading to apoptosis of cancer cells (129,130). However, a greater understanding of the signaling pathways upstream of

TAp73 could lead to approaches that selectively modulate TAp73 to engage tumor cell death and was a major goal of the dissertation research presented herein. In addition, it is thought that inhibitory signals such as ΔNp63 and ΔNp73, as well as unknown signals, are present in tumor cells and are inhibiting TAp73 function (37). Strategies that tip the balance of these isoforms and increase TAp73 levels and activity would be effective at eliciting a p53-type response in tumor cells that have inactivated p53. There is a critical need to understand genes and ncRNAs regulated by p73, and how they change during treatment regimens. We have identified mTOR as a regulator of p73, defined the p73 genomic binding profile, and demonstrated its modulation by the mTOR inhibitor rapamycin. mTOR-p73 gene signatures classified tumors by clinical subtype and outcome. Similar signatures might inform the use of cancer therapies such as mTOR inhibitors that engage p73 and are affected by differential p73 activities in tumor subtypes.

Understanding p73 Signaling

Transcription factors regulate highly complex gene networks. This is exemplified by the p53 gene family, which contains three members, p53, p63, and p73 that collectively can encode over 50 protein isoforms, all with the ability to bind DNA. A major goal of this dissertation research was to understand p73 biology through its essential function as a transcription factor, the gene expression that it regulates. In this thesis I analyzed p73 signaling using whole-genome technologies. As more researchers use advanced genomic technologies and make their findings publicly available, it becomes increasingly possible to perform meta-analyses, annotate datasets, and recognize

patterns of genes. This dissertation research has contributed significantly by using an integrative genomic approach in a mesenchymal cell line to define the p73 cistrome (the comprehensive set of binding sites of a transcription factor across the non-repetitive genome), and the p73 transcriptome (the comprehensive set of transcripts regulated by a transcription factor), creating valuable resources of p73 target genes.

How tumors tolerate over-expression of p73, a protein with tumor suppressive properties, is unclear. I had hypothesized that signaling pathways upstream of p73 inhibit its activity in tumors. In Chapter III I devised an approach, based on recognition of patterns within the p73 gene signature, that identified mTOR as an upstream regulator of p73. Regulation by mTOR may provide an explanation for the seemingly contradictory in vitro effects of p73 on apoptosis and autophagy, and in vivo status of p73 in human tumors. In Chapters IV and V, mTOR inhibition was shown to alter p73 binding and activity in a selective manner that was extensively detailed. In Chapter VI, I explored the mechanism by which the mTOR pathway regulates p73; kinases involved in mTOR signaling were tested for their ability to phosphorylate p73, and p73 was found to interact with FRAP1, the catalytic subunit of mTOR. Finally, in Chapter VII I created models that will be useful for dissection of the in vivo consequences of these findings. The mTOR and p73 gene signatures created herein have clinical utility, as they can predict outcome and classify tumor sub-types. In Chapter VIII I discuss the implications of these findings for transcription factor signaling, and describe a potential anti-cancer strategy that targets p73 using mTOR inhibitors in combination with other p73-inducing chemotherapies in predefined cancer subgroups.

CHAPTER II

MATERIALS AND METHODS

Cell culture and treatment

The rhabdomyosarcoma cell line Rh30 was provided by P. Houghton (St. Jude Children's Research Hospital, Memphis, TN), and cultured in RPMI Medium 1640 (Invitrogen, Carlsbad, CA). Human Mammary Epithelial Cells (HMECs) were purified from normal breast tissue obtained from the Vanderbilt-Ingram Cancer Center Human Tissue Acquisition and Pathology Shared Resource by Kimberly Johnson, and cultured in DMEM/F12 medium 1:1 supplemented with 1.0 μg/ml hydrocortisone (Sigma, St. Louis, MO), 10 μg/ml ascorbic acid (Sigma), 12.5 ng/ml human recombinant EGF (Gibco BRL, Gaithersburg, MD), 10 μg/ml apotransferrin (Sigma), 0.1 mM phospho-ethanolamine (Sigma), 2.0 nM β-estradiol (Sigma), 10 nM 3,3',5-triiodo-L-thronine sodium salt (Sigma), 15 nM sodium selenite (Sigma), 2.0 mM l-glutamine, 1% penicillin-streptomycin, 1 ng/ml cholera enterotoxin (ICN Biomedicals, Inc., Aurora, OH), 1% fetal bovine serum, and 35 μg/ml bovine pituitary extract (Gibco BRL). MDA-MB-231 cells [American Type Culture Collection (ATCC), Manassas, VA] were cultured in McCoy's 5A Medium (Invitrogen), MDA-MB-468 cells (ATCC) were cultured in 1:1 McCoy's 5A:DMEM (Invitrogen), and 293T cells (ATCC), 293A cells (ATCC), H1299 cells (ATCC), and HaCat cells (kindly provided by P Boukamp, Deutsches Krebsforschungszentrum, Heidelberg, Germany) were cultured in DMEM (Invitrogen)

(131,132). All medias were supplemented with 10% fetal bovine serum unless otherwise described.

Cisplatin (APP Biopharmaceuticals, Schaumburg, IL) was used at 25 μM, paclitaxel (Sigma) was used at 100 nM, and RAD001 (everolimus, Novartis, Basel, Switzerland) was used at 20 nM. Rapamycin (Calbiochem, Darmstadt, Germany), metformin (Sigma), and pyrvinium (United States Pharmacopeial Convention, Rockville, MD) were used as described. For experiments involving rapamycin, cells were plated at 3-4 x 10^5 cells per 10 cm^2 dish. (HMECs were plated at 5 x 10^5 cells per 10 cm^2 dish.) After cells attached, media was changed 12 h prior to addition of drug [to avoid experimental variation due to the effect of media replacement on mTOR (133)], or drug was added to serum-free media as described. Media without antibiotics was used for treatment.

For cell growth experiments, MDA-MB-231 cells were plated in triplicate and treated with shRNA-expressing lentivirus, as described below. After 2 d, cells were treated with 20 nM rapamycin or vehicle-control and total cell number was measured at the indicated times.

Cell transfection/infection and shRNA

The following sequences were used for small interfering RNA (siRNA): p73-1: 5'- GCAATAATCTCTCGCAGTA -3', p73-2: 5'- GAGACGAGGACACGTACTA -3', TAp73-1, 5'- GAACCAGACAGCACCTACT -3', TAp73-2, 5' - GGATTCCAGCATGGACGTC -3', GFP: 5'- GAAGGTGATACCCTTGTTA -3', mTOR (FRAP1): 5'- GCATTTACTGCTGCCTCCTAT -3', and p73β: 5'-

TCAAGGAGGAGTTCACGGA -3'. 293T cells were transfected using Fugene 6 (Roche, Indianapolis, IN). For knock-down of p73, the pSicoR lentivirus system was used (134). For knock-down of mTOR (FRAP1), the pGIPZ system was used according to the manufacturer's protocol (OpenBiosystems, Huntsville, AL). p70S6K was depleted using Dharmacon SmartPools, and Rictor and Raptor were depleted using Qiagen siRNAs, according to the manufacturer's instructions.

For microarray and ChIP, MDA-MB-231 cells were infected with adenovirus expressing HA–TAp73β (pAdEasy-1:HA-TAp73β) or with a control adenovirus, and the cells were harvested after 80% transduction efficiency was reached, as monitored by GFP fluorescence. The recombinant adenoviruses were generated using pAdEasy kindly provided by B Vogelstein (Johns Hopkins University, Baltimore, MD) (135). The cDNA of interest was cloned into the shuttle vector pAdTrack and transferred into the adenoviral vector pAdEasy-1 through recombination events in bacteria. 293A cells were transfected with adenoviral vector, cells were monitored by fluorescence, and once 100% of cells were fluorescing viral particles were harvested by freeze-thaw lysis of the cells. Over-expression of multiple p73 isoforms was performed using the pcDNA3 backbone [kindly provided by C. Backendorf and G. Melino (136,137)], and transfection was performed using Lipofectamine (Invitrogen) according to the manufacturer's instructions.

Protein lysate preparation and Western analysis

Cells were washed in ice-cold phosphate-buffer saline, and protein extrates were prepared by harvesting cells in radio immunoprecipitation assay (RIPA) buffer (150 mM NaCl, 1% Nonidet P-40, 0.5% deoxycholate, 0.1% SDS, 50 mM Tris [pH 8.0], 5 mM

EDTA). Lysis buffers were supplemented with phosphatase inhibitors 50 mM NaF, 0.2 mM NaVanadate, 10 mM p=nitrophenyl phosphate, and the protease inhibitors antipain (10 μg/ml), leupeptin (10 μg/ml), pepstatin A (10 μg/ml), chymostatin (10 μg/ml) (Sigma), and 4-(2-aminoethyl)-benzenesulfonylfluoride (200 μg/ml) (Calbiochem). Cells were incubated on ice 30-45 min, and the protein supernatant was cleared by centrifugation at 13,000 x *g* for 10 min at 4°C.

Protein lysates were boiled in 1x Laemmli sample buffer, separated by SDS-Page, and transferred them to Immobilon-P membranes (Millipore, Billerica, MA) for Western analysis. Membranes were blocked with 5% non-fat dry milk in TTBS (100 mM Tris-HCl [pH 7.5], 150 mM NaCl, 0.1% Tween-20) and incubated with the following antibodies: p73 monocolonal antibodies IMG-246, IMG-259, IMG-313 (Imgenex, San Diego, CA), p73 monoclonal antibody cocktail Ab-4 (Neomarkers, Fremont, CA), mdm2 monoclonal antibody SMP14, β-actin polyclonal antibody I-19, mTOR polyclonal antibody N-19 (α-FRAP), p63 monoclonal antibody 4A4, p53 monoclonal antibody DO-1 (Santa Cruz Biotechnology, Santa Cruz, CA), GAPDH monoclonal antibody MAB374 (Chemicon, Temecula, CA), p21 monoclonal antibody Ab-1 (Calbiochem, San Diego, CA), phospho-4EBP1 Thr37/46 polyclonal antibody, PARP antibody, Caspase-3 antibody, puma antibody, p70S6K antibody, phospho-p70S6K (Thr389) antibody, phospho-Akt (Ser473) antibody, Akt antibody, phospho-AMPKα (Thr172) antibody, AMPKα antibody, phospho-S6 Ser235/236 polyclonal antibody 2F9, total S6 monoclonal antibody 54D2 (Cell Signaling Technology, Danvers, MA), MAP1LC3B antibody (Abgent, San Diego, CA), and p73 antibody (Bethyl Laboratories, Montgomery, TX). p73 was immunoprecipitated for ChIP with Ab-4 or p73 antibody using conditions

previously described (138), and as outlined further below. mTOR complex components were immunoprecipitated as previously described (139). A Fluor-S Max MultiImager (Bio-Rad, Hercules, CA) was used to quantify Western signals.

For analysis of protein levels in ChIP-on-Chip duplicate samples, fixed cells were resuspended in cell lysis buffer (5 mM PIPES pH 8.0, 85 mM KCl, 0.5% NP40, and protease and phosphatase inhibitors [10 ug/ml chymostatin, 10 ug/ml leupeptin, 10 ug/ml antipain, 10ug/ml pepstatin A, 0.2 ug/ml AEBSF, 0.2 mM NaVanadate, and 8 mM NaFluoride]) and dounce homogenized. Nuclear pellets were resuspended in sonication buffer (50 mM Hepes pH 7.9, 140 mM NaCl, 1mM EDTA, 1% Triton X-100, 0.1% Na-deoxycholate, 0.1% SDS, and protease and phosphatase inhibitors as above), and Western analysis was performed on a chromatin-enriched fraction as above.

Systematic evolution of ligands by exponential enrichment

Systematic evolution of ligands by exponential enrichment (SELEX) was performed as described in (48). Briefly, a library of random-sequence 33-mer DNA oligonucleotides, flanked by fixed sequences complementary to PCR primers with *BglII* rescriction enzyme sites, was obtained from Carmen Perez. A pool of ~2 x 10^{14} random-sequence 87-mers was converted to a double-stranded DNA library by PCR. The PCR products were ethanol precipitated and resuspended in 100 µl of Annealing Buffer (20 mM Tris, 2 mM $MgCl_2$, 10 mM NaCl). p73-binding sequences were selected from this library by performing a DNA-binding assay using immunopurified p73 (from H1299 cells infected with adenovirus expressing HA-TAp73β as above), purified using

QIAquick PCR purification kit (Qiagen), digested with *BglII*, cloned into the pBluescript II SK vector (Stratagene), and a fraction of the clones were sequenced.

Flow cytometry

Flow cytometry was performed by incubating 1 x 10^6 cells in 20 μg/mL propidium iodide (Sigma-Aldrich) and measuring DNA content for 15,000 events with a FACSCaliber instrument (Becton, Dickinson & Co, Franklin Lakes, NJ). Flow cytometry data were plotted using CellQuest software (Becton, Dickinson & Co).

Quantitative reverse transcription-PCR

Total RNA was purified, reverse transcribed, and quantitative real-time PCR performed as follows. RNA was isolated using the Aurum Total RNA Mini kit (Bio-Rad), and reverse transcription of 100 ng of mRNA was performed using he TaqMan Reverse Transcription Reagents kit (Applied Biosystems, Carlsbad, CA) to generate cDNA samples. The cDNA samples were diluted at 1:5 and 2 μl were used for qRT-PCR. Reactions were performed using iQ SYBR-Green Supermix (BioRad). For qRT-PCR of MDA-MB-231 RNA, all primer sequences were obtained from the PrimerBank resource (140,141), and can be found at: (http://pga.mgh.harvard.edu/primerbank/). Using an iCycler Thermal Cycler (Bio-Rad), 40 cycles of PCR were performed after an initial 3 min at 95°C, each cycle consisting of 10 s at 95°C and 45 s at 54-60°C.

miRNA isolation and expression analysis

miRNA analyses were performed as follows: Rh30 cells were treated with vehicle or 40 nM rapamycin for 24 h after infection with lentivirus expressing shRNA targeting GFP or TAp73 for 3 d, and RNA was isolated using the miRVana minikit (Applied Biosystems). Duplicate samples were sent to the Vanderbilt-Ingram Cancer Center Microarray Shared Resource (VMSR) for quality control. The RNA was reverse transcribed, and cDNA hybridized to TaqMan Low Density Array version 2.0 cards A and B without pre-amplification for MultiPlex quantitative real-time PCR analysis, according to the manufacturer's instructions (Applied Biosystems). Data were analyzed and normalized using the ΔΔCT method, by averaging sample values from two independent experiments. miRNAs with low copy number (CT > 35) were excluded.

For miR-133b and RNU19 qRT-PCR analysis, RNA samples from three independent experiments were harvested as above, reverse transcription was performed using the TaqMan Reverse Transcription kit, and real-time PCR was performed using the TaqMan MicroRNA Assays according to the manufacturer's instructions (Applied Biosystems).

RNA isolation, microarray experiments, and statistical analyses

Over-expression microarray experiments were performed in duplicate as follows: H1299 cells were infected with adenoviruses expressing GFP or TAp73β for 5 h, RNA was isolated using the Aurum Total RNA Mini kit (Bio-Rad) and submitted to the VMSR for quality control. The RNA was processed and microarray was hybridized by VMSR. Microarray data analyses were performed using the ArrayAssist software platform

(Stratagene, La Jolla, CA). A list of probes was created with fold-change in gene expression for p73-overexpressing samples versus GFP controls. The following software programs were used for statistical analyses, gene annotations, and determination of categorical enrichment as indicated: ArrayAssist (Stratagene), WebGestalt (Bioinformatics Resource Center at Vanderbilt University) (142), Ingenuity Pathway Analysis (Ingenuity Systems, Redwood City, CA), NCBI DAVID, and the Connectivity Map (143). KEGG and gene ontology analyses was accessed through WebGestalt, using statistical tests coupled to the WebGestalt interface (142). Comparison of the over-expression p73 gene signature to publicly available datasets, and to gene expression data from the VICC 9936 clinical trial (provided by J. Bauer) was performed using ArrayAssist.

Rapamycin/ knock-down microarray experiments were performed in duplicate in Rh30 cells treated as above, and RNA was isolated using the Aurum total RNA minikit (Bio-Rad) and submitted to the VMSR for quality control. The RNA was processed, and Affymetrix Hu Gene 1.0 ST microarrays were hybridized according to VSMR/Affymetrix protocols (144).

Probe summarization algorithms (ExonPLIER16) were used to identify changes in transcript expression levels. Expression levels have been log transformed. GeneSpring GX software (Agilent, Santa Clara, CA) was used for statistical analyses and transcript annotations, and for algorithms involved in: hierarchical clustering, Venn analysis, classification, box plots, bar charts, statistical similarity of gene lists, and Benjamini-Hochberg multiple testing-corrected t- and ANOVA testing. Methods used for comparison to publicly available datasets and survival analyses are detailed below.

H1299 ChIP and ChIPSeq

Formaldehyde crosslinking, chromatin preparation and immunoprecipitation (ChIP) were carried out as follows. Growth media was aspirated from cells and replaced with a 1.6% formaldehyde (EM Science, Gibbstown, NJ) solution in PBS. Cells were incubated in formaldehyde for 10 min at room temperature, followed by inhibition of the crosslinking reaction by the addition of glycine for a final concentration of 0.125 M. After 2 min incubation, cells were washed twice with PBS. Exctracts were prepared by scraping cells in 1 ml of RIPA buffer, as above.

Sonication of the cell lysates was performed to yield chromatin fragments of ~500-1000 bp, and debris was pelleted by centrifugation for 10 min at 13,000 x *g*, and 1 to 1.5 mg of total protein extracts was pre-cleared with 10 μg of mouse immunoglobulin G (Pierce, Rockford, IL) bound to PAS for 1 h with rocking at 4°C. After centrifugation for 2 min at 13,000 x *g*, supernatants were transferred to a new tube. The extracts were immunoprecipitated with 1 μg of Ab-4 antibody (Calbiochem) by rocking overnight at 4°C. Immunocomplexes were washed twice with RIPA buffer, four times with wash buffer (100 mM Tris [pH 8.5], 500 mM LiCl, 1% Nonidet P-40, 1% deoxycholic acid), followed by two washes in RIPA buffer. The protein was degraded in digestion buffer (120 μg/ml Proteinase K, 10 mM Tris [pH 7.5], 5 mM EDTA, and 0.5% SDS) at 56°C overnight, and then incubated at 65°C for 30 min. The DNA was resuspended in 40 μl water, and 2 μl of each sample were used for PCR amplification. The *p21* and *mdm2* ChIP primers correspond to those previously published (145).

For ChIPSeq and semi-quantitative ChIP experiments, cells were crosslinked and submitted to GenPathway, Inc. (San Diego, CA) according to their FactorPath protocol. Potential response elements for p53 family members were identified by using the p53MH and p63MH algorithms to scan sequences for the p53 and p63 motifs (48,146).

Rh30 ChIP, ChIP-on-Chip, and the FactorPath protocol

The following antibodies were used for immunoprecipitation of p73-DNA complexes in Rh30 cells: anti-TAp73 A300-126A (Bethyl, Montgomery, TX) that recognizes an epitope within amino acids 1-62 of TAp73 isoforms, anti-p73α ER-13 (Ab-1, Calbiochem) that recognizes an epitope within amino acids 495-637 that is unique to p73α, and anti-p73β GC-15 (Ab-3, Calbiochem) that recognizes an epitope in amino acids 380-499 that is unique to p73β. Antibody specificity was confirmed using cells in which different p73 isoforms had been over-expressed as described above. For ChIP-on-Chip and semiquantitative ChIP experiments, cells were cross-linked and submitted to GenPathway, Inc., according to their FactorPath protocol.

For ChIP-on-Chip, probe signal and enrichment analysis was performed using Affymetrix Tiling Analysis Software (Affymetrix, Santa Clara, CA). An estimate of fold enrichment was obtained by computing the ratio of signal for each probe on the ChIP array to each corresponding probe on an input (unenriched) array. These ratios were made more significant by applying a series of averaging and ranking steps to probes within a 400 bp sliding window; p73 binding sites were those that exhibited > 2.5-fold enrichment for at least 180 bp of consecutive probes (GenPathway FactorPath Protocol).

The following software programs were used for statistical analyses, gene annotations, and determination of categorical enrichment as indicated: UCSC genome browser and tables (hg18; http://genome.ucsc.edu), Ingenuity Pathway Analysis (Ingenuity Systems, Redwood City, CA), Integrated Genome Browser (Affymetrix), NCBI DAVID, and WebGestalt (Bioinformatics Resource Center at Vanderbilt University) (142). De novo identification of enriched sequence motifs was performed using MEME (147). CEAS (148) was used for conservation analysis, annotation of functional elements, and identification of TRANSFAC and JASPAR enriched motifs.

Locations of rhabdomyosarcoma and related publicly available datasets

Publicly available data sets for analysis of rhabdomyosarcoma sub-types and clinical outcomes, and for comparisons to biologic processes, were obtained from various locations as follows. The Wachtel et al. (149) and Davicioni et al. (150) datasets are based on Affymetrix chips (HG-U133A) and are available at EBI ArrayExpress database (E-MEXP-121) and the National Cancer Institute Cancer Array Database (trich-00099) respectively. Oncomine Research Platform (151) was used to access and analyze the De Pitta et al. dataset (152), which is based on a custom muscle cDNA array. Mesenchymal Stem Cell and epithelial-to-mesenchymal transition datasets were obtained from the National Center for Biotechnology Information Gene Expression Omnibus under the accession numbers GSE9764, GSE6460, GDS3220, and GSE8240.

Survival analyses of rhabdomyosarcoma patient cohorts

A total of 134 patients in the Davicioni *et al.* cohort that had alveolar or embryonal rhabdomyosarcoma and a known survival time were included in survival analyses (150,153). These tumors had been profiled using Affymetrix HG U133A arrays. Expression data were extracted from the Davicioni et al. dataset for 18 probes (corresponding to 17 genes) that are indicated in orange text in Figure S9A; these are the direct p73 target genes from among all p73-regulated genes that clustered alveolar rhabdomyosarcomas by clinical outcome (alive versus deceased). The relationship between this 17-gene p73 signature and overall clinical survival time was examined further using 10,000 re-sampling tests.

Expression data for each Affymetrix probe set were treated as the independent variable, and the Cox proportional hazard model was used for survival analyses. The number of significant probes with Wald P value <= 0.01 was saved as the observed number of significant probes. Beta (from Cox model) and Wald statistics for each Affymetrix probe set were used along with expression data to build up a compound score for each patient. The compound score was used as the independent variable to perform overall survival analysis based on the Cox model. The compound score for patient i is defined as $\Sigma_j \ W_j \bullet X_{ij}$, where W_j = Wald statistic score for probe j, and $X_{ij} = \log_2$ probe j expression level for patient i. The Wald test P value was saved as the observed P value. For the re-sampling test, we randomly selected 18 probes without replacement among all possible Affymetrix probes in the array (22,283 probes), and repeated the above procedure of determining the number of significant probes, building up a compound score and calculating a Wald test P value. We repeated the re-sampling and survival

analysis procedure 10,000 times, generating 10,000 re-sampling numbers of significant probes and Wald test P values, to confirm that our observed values were outside of the range of values that occur by chance. For alveolar tumors, only 0.18% of the 10,000 re-sampling P values were smaller than the observed P value. In contrast, for embryonal tumors 73.5% of the 10,000 re-sampling P values were smaller than the observed P value and none of the probes were significant. Thus, the 18-probe p73 signature segregates alveolar rhabdomyosarcomas but not embryonal rhabdomyosarcomas by clinical outcome.

Next, we performed Kaplan-Meier analysis for the 64 patients with alveolar rhabdomyosarcoma in the cohort. For a given set of patients with compound scores, we divided the patients into two groups based on the median of the compound score. We plotted survival curves based on this grouping. The P value of the log-rank test based on this grouping was shown. Validation of the model was performed using the c-index, also indicated on the plot. The c-index is the probability of concordance between predicted and observed survival, with c = 0.5 for random predictions, and c = 1 for a perfectly discriminating model.

Purification of GST-fusion proteins

Bacterial expression was performed in BL21 codon plus *Escherichia coli* after electroporation of a bacterial expression plasmid (pBG101, Vanderbilt University Center for Structural Biology) encoding GST in-frame with the protein of interest. To induce expression, bacteria were grown at 37°C in 200 mL of LB until an OD_{600} of 0.5 was

reached, 200 μL of 1M IPTG was added and cultures were incubated at 25°C for 4 hours, and bacteria were pelleted.

Bacterial pellets were resuspended in 15 mL cold NET buffer (25 mM Tris pH 8.0, 100 mM NaCl, 0.1 mM EDTA, 5% Glycerol, 1 mM DTT) with protease inhibitors, sonicated for 20 sec 3 times, and mixed with 780 μL of 20% Triton X-100. This suspension was incubated for 30 min on ice, centrifuged at 5000 g for 15 minutes at 4°C, and the supernatant was incubated with 200 μL of pre-washed glutathione sepharose beads (GE Healthcare). The beads were recovered and washed three times with NET buffer. Proteins were eluted by incubation in elution buffer (75 mM Tris-Hcl, 15 mM glutathione, 0.1 μg/mL leupeptin) for serial elutions. Desired elutions were combined, dialyzed at a molecular weight cutoff of 10 kDa molecular weight, aliquoted and stored at -80°C.

Kinase assays

The following kinases were purchased for assessment of p53, p63 and p73 phosphorylation: the mTOR catalytic subunit FRAP1, Akt, AMPK, and RSK1 (Invitrogen), GSK3β and p70S6K (Cell Signaling, Beverly, MA). Kinase assays were performed in kinase buffer (10 mM HEPES at pH 7.5, 50 mM NaCl, 50 mM β-glycerol phosphate, 1 mM sodium vanadate, 1 mM DTT, 10 mM $MgCl_2$ or $MnCl_2$) with ATP and substrate, typically incubated at 30°C for 20 minutes. Kinase reactions were analyzed by SDS-PAGE and autoradiography.

Recombineering in EL350 bacteria

The recombineering-based method for generation of a p73 targeting vector is described in detail in Chapter VII. Restriction digests were performed to remove the cassette (containing loxP) to be introduced into the target sequence. The vector was treated with calf intestinal alkaline phosphatase (New England Biolabs, Ipswich, MA), and the linearized fragment was gel purified using the Qiagen gel purification kit according to the manufacturer's instructions. EL350 cells containing the target plasmid were grown in LB with antibiotics overnight at 32°C with shaking. The next day 1 mL of the overnight culture was transferred into a flask containing 20 mL of LB, and the mixture was incubated at 32°C with shaking for 2 hours.

Next, 10 mL of the culture was transferred to a new flask, with the remaining culture stored on ice to be used as a negative control for recombineering. The cells were heat-shocked for 15 minutes at 42°C to induce the production of proteins required for recombineering, then the cells were chilled immediately on ice. Both sets of cells (negative control and recombineering-ready) were centrifued at 4°C for 5 minutes, and each pellet was resuspended in 880 μl of ice cold water and transferred to an Eppendorf tube. The tubes were spun in a microcentrifuge at 5000 rpm for 4 minutes to pellet the cells. Cells were washed three times with ice cold water, and electroporated with 50 ng of the linearized, purified vector fragment. Bacteria were grown overnight at 32°C on LB plates containing antibiotics to select for bacteria in which recombineering was successful. Recovered plasmids were checked by sequencing across all junctions.

For arabinose-induction of Cre, EL350 cells were grown in 10 mL LB without antibiotics overnight at 32°C. The 10 mL culture was added to 500 mL of LB in a 2 L

flask. The culture was grown at 32°C with shaking at 180 rpm until an OD_{600} of 0.4 was reached (~2 hours). Then, 5 mL of 10% L(+)arabinose (Sigma) was added to the culture for a final concentration of 0.1%. After another hour of shaking cells were collected and made electrocompetent as above.

Analysis of p73 genomic sequences and Southern screening

The p73 genomic locus and our targeting vector were analyzed using Geneious (Biomatters Ltd, Auckland, New Zealand), VISTA homology (http://genome.lbl.gov/vista), and www.ensembl.org. Southern blots were performed as described in Chapter VII and as follows. A total of 12 μg of mouse genomic DNA was digested with *HindIII* (2 μl, New England Biolabs) in 38 μl total volume for 1.5 hours at 37°C, then adding 2 μl more enzyme and incubating for continued digestion overnight. Mouse BAC 176B7 was digested as well as a positive control. DNA was run on 0.8% agarose gel at < 75 volts and a photograph was taken with a ruler for reference.

Gels were depurinated for 20 minutes in 0.25M HCl with rocking, rinsed with water 3 times, and denatured for 20 minutes in 1.5M NaCl, 0.5M NaOh with rocking. DNA was transferred as follows. Glass plates were placed across a container full of 0.4M NaOH transfer buffer. A paper wick was placed across the plate with ends in the buffer. The agarose gel was inverted onto the paper wick, and a pre-wet Zeta probe membrane was placed on the gel followed by two pieces of blotting paper. A 4 inch stack of paper towels was tehn placed on top of the blotting papers, followed by glass plates. Transfer was allowed to continue overnight, after which the membrane was rinced in 2x saline-sodium citrate (0.3M NaCl, 0.03M Trisodium Citrate). The

membrane was air dried and UV crosslinked using a UV Stratalinker (Stratagene Cloning Systems, La Jolla, CA).

The strategy for designing the Southern probe was detailed in Chapter VII. Probe was PCR-amplified from BAC template using the forward primer: 5'-CTGACCAGTACCGTATGACC-3', and the reverse primer: 5'-AGTGGCTCTCTGTCTCTGTG-3'. Probes were run on a 1% agarose gel and gel purified using the Qiagen DNA gel purification kit (Qiagen, Germantown, MD). Probe was labeled using the Stratagene Prime-It Random Primer Labeling Kit.

Blots were incubated in Sigma PerfectHyb plus for 1 hour at 65°C. Probes were boiled for 10 minutes and then snap chilled on ice, and 2 x 10^6 counts per ml were used overnight at 65°C. Blots were washed briefly in 2x saline-sodium citrate, 1x in low stringency wash (2x SSC / 0.1% Sodium Dodecyl Sulfate) at 55-60°C, and 1x in high stringency wash (0.5x saline-sodium citrate / 0.1% Sodium Dodecyl Sulfate). Blots were covered with thick saran wrap and exposed to film at -80°C with an intensifying screen for 2 d.

CHAPTER III

A GENE-SIGNATURE BASED APPROACH IDENTIFIES MTOR AS A REGULATOR OF P73

Introduction

Mammalian transcription factors can bind to and regulate thousands of sites throughout the genome (13,15,86). The sheer complexities of these gene regulatory networks make conventional methods an unsuitable choice for comprehensive analysis. The advent of genomic technologies, in particular DNA microarray profiling and Chromatin Immunoprecipitation (ChIP) coupled with high-throughput sequencing (ChIPSeq) or ChIP-on-Chip, has led to the identification of target genes and transcriptional networks on a genome-wide scale (16,154). These techniques have been used to characterize the gene regulatory networks of a growing number of transcription factors (154).

The integral role of p53 in tumor suppression has prompted many laboratories to perform extensive analyses of signaling pathways downstream of the p53 family of sequence-specific DNA binding transcription factors (p53 and its homologs p63 and p73). It is estimated that p53 has 1,600 binding sites in the human genome, only 22% of which are near promoters (15,86). A more recent study has identified ~5,800 binding sites for p63 (13). Using integrative genomic tools, hundreds of novel target genes have been identified for all three family members (13,86,88,155-157). Similar analyses with many transcription factors have led to an explosion of genomic binding site and target gene expression data (154). These datasets hold great potential for much more than the

characterization of downstream pathways, in particular we predict that they can be used to define the signaling pathways that reside upstream of transcription factors of interest.

Despite the ability of p73 to regulate many p53 family target genes, little is known about the specific pathways that modulate p73 during development, tumorigenesis and tumor therapy (63). Unlike p53, which is mutated in more than 50% of human cancers, p73 is not mutated during tumorigenesis, but instead can be over-expressed (55,58,158-160). There has been much interest in modulating p73, due to its high expression level in p53 deficient tumors and its ability to activate p53 target genes leading to apoptosis of tumor cells (33,69,129,161-163). Given the above, drug-inducible pathways upstream of p73 are of therapeutic interest.

We used gene expression signatures downstream of p73 to identify novel upstream regulators. A p73 gene signature was created using a combination of genomic tools, and was queried against a database of drug-related profiles known as the Connectivity Map (143,164,165). Pattern-matching software (143) was used to identify potential p73-activating drugs. A link between p73 and mammalian target of rapamycin (mTOR), a kinase important in energy homeostasis and tumorigenesis, was identified and validated, demonstrating the utility of this approach to identify critical signaling nodes upstream of transcription factors.

Results

Generation of gene signatures for identifying upstream pathways

With an overall goal of developing a gene signature-based approach for connecting signaling pathways to transcription factors, we first sought to identify known pharmaceutical activators of transcription factor signaling using publicly available expression profile datasets and the Connectivity Map resource. Our ultimate goal was to use this strategy to identify novel upstream regulators of p73. However, we thought it prudent to use well-defined transcription factors with known upstream signaling pathways to confirm that such pathways can be identified using the Connectivity Map within reasonable parameters.

As a starting point for feasibility testing, we analyzed two publicly available expression profile datasets. In the first analysis, we made use of a list of genes up- or down-regulated by zinc-inducible p53 (166). In the second, we generated a gene list from raw microarray data generated from NIH-3T3 cells in which PPARγ had been overexpressed (167). The lists of genes both induced and repressed by these transcription factors were queried against the Connectivity Map resource (143). In brief, this resource consists of pattern-matching software that compares an input gene signature to a database of signatures from 164 small-molecule bioactive compounds (dubbed perturbagens), 85 of which are classified as pharmaceutical drugs. A connectivity score from +1 to -1 is assigned based on the degree of similarity or dissimilarity between the two signatures (143). Thus, a drug with a high connectivity score has a gene signature very similar to the query signature, and might be hypothesized to act on a pathway in parallel with the

transcription factor that generated the query signature. This score allows the user to choose perturbagens irrespective of p-value, which is of particular relevance because perturbagens are profiled at different doses, in different cell lines, or for a different number of experimental replicates (143). Both the average connectivity score, and the maximum connectivity score (from the best instance of treatment, dose, and cell line) are informative; for example some cell lines might not express the target of interest, and some doses might not be effective, bringing down the average.

In this manner we evaluated the gene signatures of p53 and PPARγ that we had created to test the feasibility of our approach. Many of the well-studied chemical agents that activate p53 are not included in the Connectivity Map. Nevertheless, when we analyzed the p53 gene signature, two known activators of p53 were identified: nocodazole, a microtubule inhibitor (168), and tioguanine, a chemotherapy drug known to induce p53-mediated autophagy (169,170). These agents were ranked 6 and 18 out of all 85 pharmaceutical perturbagens by average connectivity score. Analysis of the PPARγ signature resulted in the identification of the PPARγ activator, troglitazone, used to treat diabetes mellitus type 2. Troglitazone was ranked 22 out of 85 compounds. Given these results, we considered the thirty highest-ranking perturbagens to be of likely relevance in terms of modulating a transcription factor of interest.

Having ascertained the feasibility of the *in silico* arm of our approach, we sought to identify novel signaling upstream of the transcription factor p73. To establish a collection of p73-regulated genes, Affymetrix GeneChips were used to quantify transcript levels after ectopic p73 expression in the H1299 lung carcinoma cell line. This cell line does not have readily detectable expression of p53 family members (171), making it ideal

for an analysis of p73 without the confounding effect of its homologs. Since p73 can be expressed as multiple isoforms, we ectopically expressed an isoform designated TAp73β that is capable of strong transactivation (137). p73 transcriptional activity was evidenced by induction of known target genes p21 and Mdm2 (Figure 2), and 11 out of the top 20 regulated genes by microarray are known p53 family targets (Table 2).

In order to discriminate between direct and indirect regulation by p73, we also performed whole genome ChIP to identify sequences to which p73 is bound (ChIPSeq), using formaldehyde cross-linked samples that were replicates of those used for our microarray experiment. Over 4,000 p73-bound DNA sequences were isolated, sequenced, and mapped to the mammalian genome using GenPathway FactorPath technology. Tags that mapped within 10 kb of genes were considered for further analysis. Overlay of our microarray dataset (562 genes that increased or decreased two-fold with p73 overexpression) with our whole genome ChIP dataset (2,298 genes) gave a more refined list of candidate p73 target genes (121 genes) (Figure 3). In order to validate our technique for identifying novel p73 target genes, we performed semi-quantitative ChIP using a different p73 antibody from the original ChIPSeq dataset to immunoprecipitate DNA-protein complexes. p73 bound to the promoter elements of both *p21* and *MDM2* (Figure 2). Binding levels did not correlate with expression levels for these two genes (Figure 2), suggesting that other transcriptional modulators (e.g. transcription factors, cofactors) regulate gene expression in this system similar to what has been reported previously (13). We chose 15 additional genes that were present in both the microarray and ChIPSeq datasets, and were able to validate that p73 bound promoter or intronic regions in all 15 genes (Figure 3).

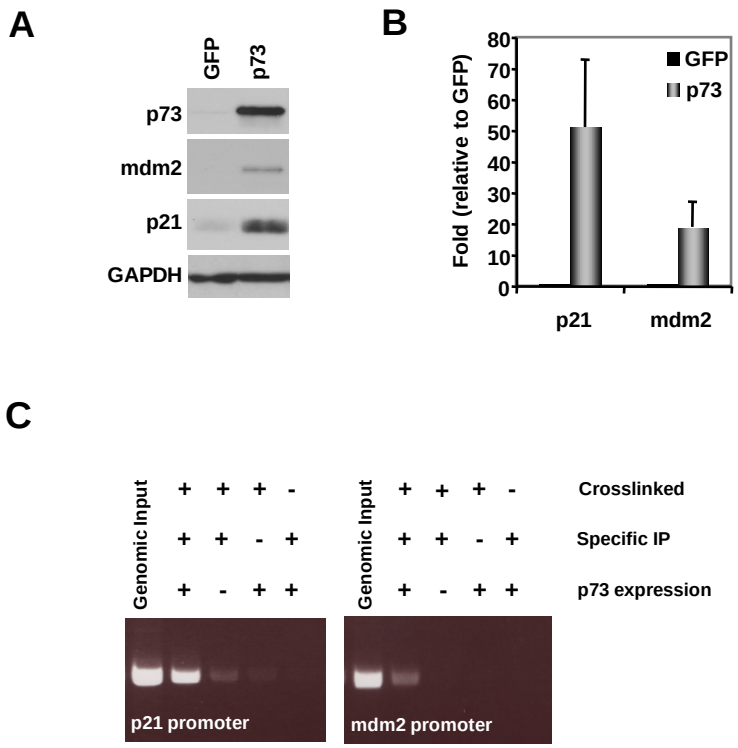

Figure 2: Analysis of ectopic p73 expression and resulting modulation of p21 and mdm2. H1299 cells were transduced with TAp73β or GFP expressing adenoviruses. A) Protein lysates were harvested after transduction and p73, GAPDH and downstream targets mdm2 and p21, were analyzed by Western blot. B-C) p73 regulates known target genes when expressed in H1299 cells. B) Total RNA was purified, reverse transcribed, and quantitative real-time PCR performed with primers to p21 and mdm2. The samples were normalized to GAPDH and the results are presented as fold-change over GFP control. Error bars represent standard deviation from three experiments. C) For ChIP analysis, p73 was immunoprecipitated (IP) from formaldehyde-crosslinked H1299 cells transduced with adenoviral p73 or a GFP control. Associated DNA fragments were PCR-amplified using primers flanking the p53 family response elements in *p21* and *mdm2*. Nonspecific binding was assayed by IP of p73 from non-crosslinked lysates or crosslinked lysates with an isotype-matched antibody ('-' specific IP).

Table 2: Top 20 genes identified by microarray analysis

Gene Title	Gene Symbol	Fold Change by Microarray	References for Known Targets*
stratifin (14-3-3sigma)	SFN	275	(Hermeking et al, 1997)
IBR domain containing 2	IBRDC2 (p53RFP)	99	(Huang et al, 2006)
S100 calcium binding protein A2	S100A2	61	(Tan et al, 1999) (Hibi et al, 2003)
transformed 3T3 cell double minute 2	MDM2	53	(Momand et al, 1992) (Michael et al, 2002) (Harms & Chen, 2006)
carboxypeptidase M	CPM	48	
microtubule-associated protein 2	MAP2	41	
basic helix-loop-helix domain containing	BHLHB2 (DEC1)	34	(Thin et al, 2007) (Qian et al, 2007)
jagged 2	JAG2	34	(Candi et al, 2007) (Sasaki et al, 2002)
p21	CDKN1A (p21)	32	(el-deiry et al, 1993) (Nozell et al, 2002)
DNA-damage-inducible transcript 4	DDIT4 (REDD1)	21	(Ellisen et al, 2002)
apoptotic peptidase activating factor 1	APAF1	17	(Moroni et al, 2001) (Gressner et al, 2005)
chromosome 11 open reading frame 17	C11orf17	17	
pantothenate kinase 1	PANK1	17	
SRY-box 7	SOX7	16	
RAP2B, member of RAS oncogene family	RAP2B	16	
ferredoxin reductase	FDXR	15	(Liu et al, 2002) (Hwang et al, 2001)
dystonin	DST (BPAG-1)	13	(Osada et al, 2005)
angiopoietin-like 4	ANGPTL4	13	
hypothetical protein MGC5370	MGC5370	12	
endothelial PAS domain protein 1	EPAS1	11	

***** Genes regulated by p53, p63, and/or p73 as described in (144).

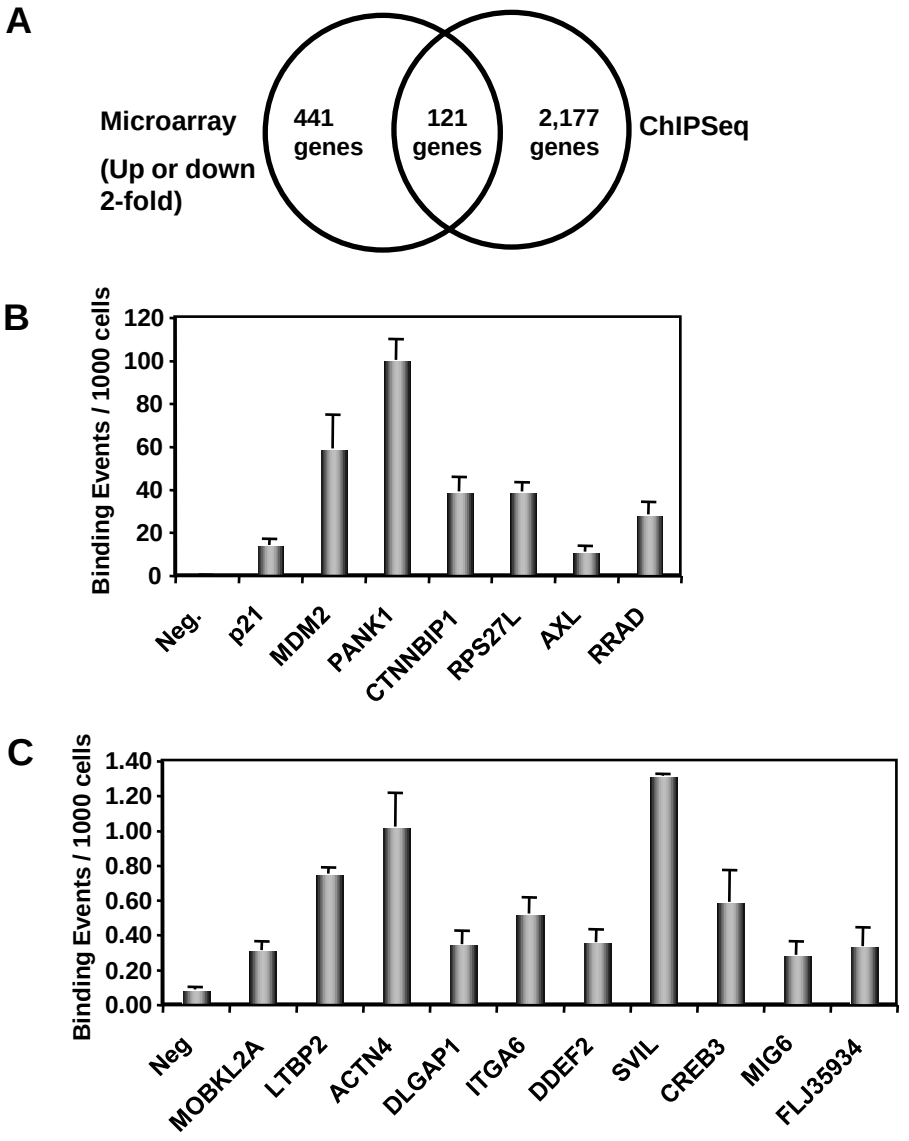

Figure 3: Generation of a multi-tiered p73 signature. A) Schematic showing the number of genes that increase or decrease after p73 over-expression relative to GFP control by microarray alone, the number of genes identified by ChIPSeq analysis alone, and the number of genes that are present in both datasets. B-C) DNA fragments were created from ChIP, and analysis of p73 binding at genomic regions near the indicated genes was performed by semi-quantitative PCR for genes showing high levels of binding (B), and lower levels of binding (C). Neg. represents a negative control region. Error bars represent standard deviation from three experiments.

Connectivity Map perturbagens increase p73 levels

Multiple tiers of information were used to create a rank-ordered list of target genes for further analysis, including: (i) presence in microarray dataset, (ii) fold change in expression level with p73 over-expression, (iii) presence in ChIP dataset, (iv) presence of a cluster of ChIP tags at gene locus, (v) number of tags per cluster, (vi) cluster length, and (vii) functional annotation by a variety of methods that are described in greater detail below. The microarray dataset was used to query the connectivity map because it contains a large number of genes analyzed in the proper format. However, we later used all tiers of information to choose target genes for follow-up analysis.

To begin our analysis, genes whose transcript levels increased or decreased two-fold after ectopic p73 expression were analyzed using the Connectivity Map. Because we were ultimately interested in connecting p73 to pathways rather than just drugs *per se*, we focused on the 'pharmaceutical' subset of 85 perturbagens, which we found to be better affiliated with known molecular targets and signaling pathways. Five of the top thirty perturbagens predicted to induce p73 activity were either direct or indirect inhibitors of mTOR signaling (Table 3). This includes sirolimus (known as rapamycin) a drug that binds to FKBP12 to form a complex that inhibits mTOR (101), as well as metformin, a drug widely used to treat diabetes mellitus type 2 activates AMPK and inhibits mTOR in cell culture (172). We also identified phenformin, a drug that is in the same class as metformin but is no longer used therapeutically, pyrvinium, an inhibitor of the Akt kinase that is an upstream activator of mTOR (173), and dexamethasone, known to inhibit mTOR in muscle cells (174).

Table 3: Top thirty pharmaceutical perturbagens identified through the Connectivity Map that induce a p73 signature

Pharmaceutical Perturbagen	Maximum Connectivity Score[a]	Rank[b]	Description
valproic acid	1	10	HDAC1 inhibitor
pyrvinium	**0.813**	**7**	**Inhibits carbohydrate metabolism[c]**
prazosin	0.801	8	Alpha-adrenergic blocker
sirolimus	**0.736**	**19**	**mTOR inhibitor[d]**
oxaprozin	0.727	1	COX inhibitor
carbamazepine	0.694	6	Sodium channel inhibitor
haloperidol	0.694	14	Antidopaminergic action
sodium phenylbutyrate	0.662	16	Orphan drug
deferoxamine	0.656	22	Iron chelator
fulvestrant	0.641	29	Estrogen receptor antagonist
mercaptopurine	0.617	2	Antimetabolite
felodipine	0.602	23	Calcium channel blocker
clozapine	0.585	13	Antiserotonergic / dopaminergic
diclofenac	0.519	15	COX inhibitor
exemestane	0.516	3	Aromatase inhibitor
dopamine	0.507	4	Neurohormone
copper sulfate	0.499	30	Copper treatment
clofibrate	0.487	18	PPAR activator
dexamethasone	**0.469**	**28**	**Steroid hormone[e]**
tamoxifen	0.466	17	Selective Estrogen Receptor Modulator
gefitinib	0.448	5	EGFR inhibitor
chlorpropamide	0.448	20	Augments beta-cell insulin secretion
ciclosporin	0.442	21	Inhibits calcineurin
metformin	**0.436**	**26**	**Improves insulin sensitivity[f]**
fluphenazine	0.404	24	GABA agonist
tomelukast	0.398	9	Leukotriene antagonist
imatinib	0.38	25	Tyrosine kinase inhibitor
phenformin	**0.35**	**11**	**Improves insulin sensitivity[g]**
pentamidine	0.35	12	Orphan drug - antimicrobial
colforsin	0.335	27	Stimulates adenylate cyclase

[a]Maximum connectivity score among all treatment instances
[b]Rank by average connectivity score
[c]Akt inhibitor, induces apoptosis in glucose-starved cancer cells (173)
[d]Known as rapamycin
[e]Inhibits mTOR in muscle cells (174)
[f]Inhibits mTOR in breast cells (172)
[g]Same drug class as metformin

Annotation of genes in the p73 signature by ontology (function) and pathway analyses generated additional evidence supporting a connection between mTOR and p73. Enrichment of functional categories in the p73 signature was determined by comparing the observed number of genes in that category to the number of genes expected by chance based on sample size (see Materials and Methods). Known p73 functions were enriched in our datasets, including regulation of the cell cycle and cell death (Figure 4). Interestingly, the p73 signature also showed enrichment for novel functions such as cellular metabolism (Figure 4). The Kyoto Encyclopedia of Genes and Genomes (KEGG), a compendium of genes annotated and organized by signaling pathway (175), was used to annotate p73-regulated genes by pathway. Both the mTOR pathway and the insulin signaling pathway [a canonical pathway upstream of mTOR (176)] were enriched in the p73 signature (Figure 4). Taken together, the data from the Connectivity Map and gene annotation analyses led us to hypothesize that mTOR is an upstream regulator of p73.

To validate p73 modulation by the mTOR inhibitors identified through the Connectivity Map, we focused on two drugs that are widely used therapeutically, rapamycin and metformin. MDA-MB-231 cells were treated with these drugs and mTOR inhibition was confirmed using phospho-4EBP1 as a marker of mTOR activity. Both agents caused an elevation in p73 protein levels (Figure 5). (Unless otherwise noted, p73 refers to the TAp73β isoform throughout.) To determine if the observed effects of these drugs on p73 levels were specific to breast cancer cell lines such as MDA-MB-231, we also treated the rhabdomyosarcoma cell line Rh30 with rapamycin and metformin using phospho-S6 as a marker of drug activity.

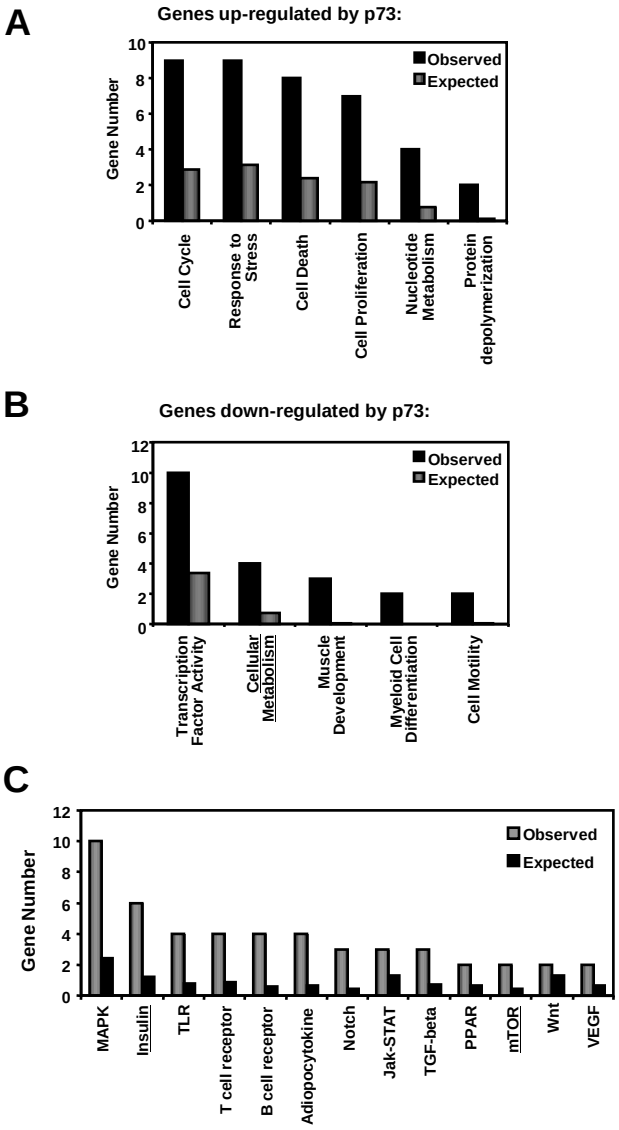

Figure 4: Enrichment of genes by function and signaling pathway in the p73 gene signature. A-B) Enrichment of major biological processes among genes regulated by p73. Gene Ontology enrichment is shown for sets of genes that are both present in the ChIP dataset, and increased (A) or decreased (B) 2-fold over GFP with p73 over-expression in H1299 cells by microarray. Processes with p-value by hypergeometric test of less than 0.01, and containing two or more genes as annotated by WebGestalt, are graphed. C) Analysis of KEGG signaling pathways enriched among all genes that were upregulated two-fold or more in p73-overexpressing H1299 cells by microarray. Enrichment is shown as the number of observed genes in the dataset, compared to the expected number of genes as calculated using the WebGestalt software.

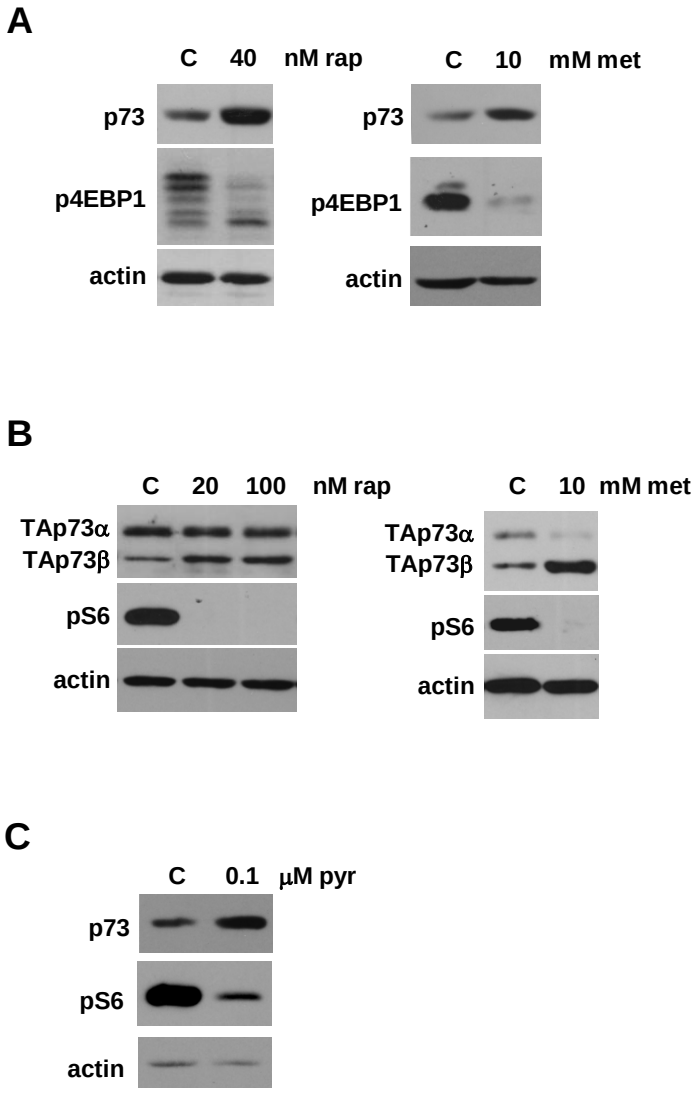

Figure 5: Western analysis of perturbagen effect on p73. A) p73 levels were increased in MDA-MB-231 cells treated with rapamycin (rap) (left panel), or metformin (met) (right panel) for 24 h. B) Rh30 cells treated with rap (left panel), or met (right panel) for 24 h. C) MDA-MB-468 cells treated with pyrvinium (pyr) for 36 h.

Unlike MDA-MB-231 cells that express one predominant p73 isoform (TAp73β), Rh30 cells express high levels of two p73 isoforms, TAp73α and TAp73β, that differ only in the presence or absence of a C-terminal Sterile Alpha Motif of unknown function (37). Only the TAp73β isoform is elevated after treatment with rapamycin and metformin in Rh30 cells (Figure 5). Pyrvinium pyruvate inhibits mTOR through the upstream kinase Akt (173). In a breast cell line expressing high levels of Akt (MDA-MB-468) (177) we also observed an increase in p73 protein levels 12 h after treatment with pyrvinium (Figure 5). Thus, drugs that inhibit mTOR by multiple mechanisms were found to induce p73 levels.

Serum-starvation is a model for energy depletion in cell culture, and leads to changes in mTOR signaling (178), and to differences in the effect of rapamycin on MDA-MB-231 cells (179). When rapamycin was added to MDA-MB-231 cells in media lacking serum, the elevation of p73 was synergistically enhanced at later time-points (Figure 6). The observed changes in p73 protein in MDA-MB-231 and Rh30 cells were not due to parallel changes in p73 RNA levels (Figure 7). In addition, because mutant p53 is a known regulator of p73 through physical interaction (97), we assessed both mutant p53 levels and the potential of mutant p53 to co-associate with p73 in both cell lines. The levels of mutant p53 protein did not change in response to rapamycin, nor was there detectable co-association between p73 and mutant p53 as assessed by co-immunoprecipitation analysis (data not shown).

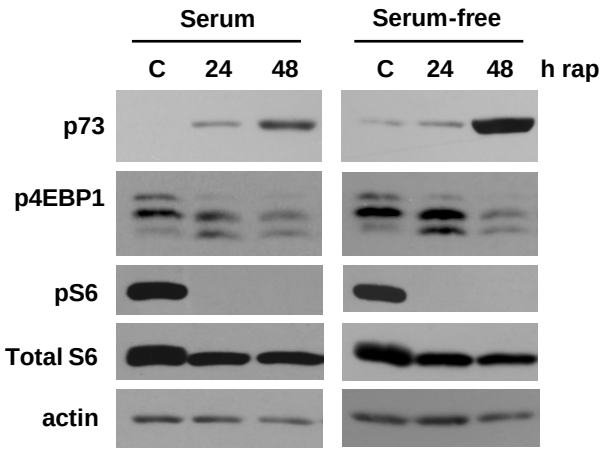

Figure 6: Serum-starvation enhances rapamycin-induced regulation of p73. Left panel: MDA-MB-231 cells were treated with 20 nM rapamycin 12 h after replacement of media containing 10% serum. Right panel: MDA-MB-231 cells were treated with 20 nM rapamycin in fresh serum-free media. C is vehicle control. Protein lysates were analyzed by Western blot for p73, pS6, total S6, and actin as indicated. Panels are representative of at least three independent experiments.

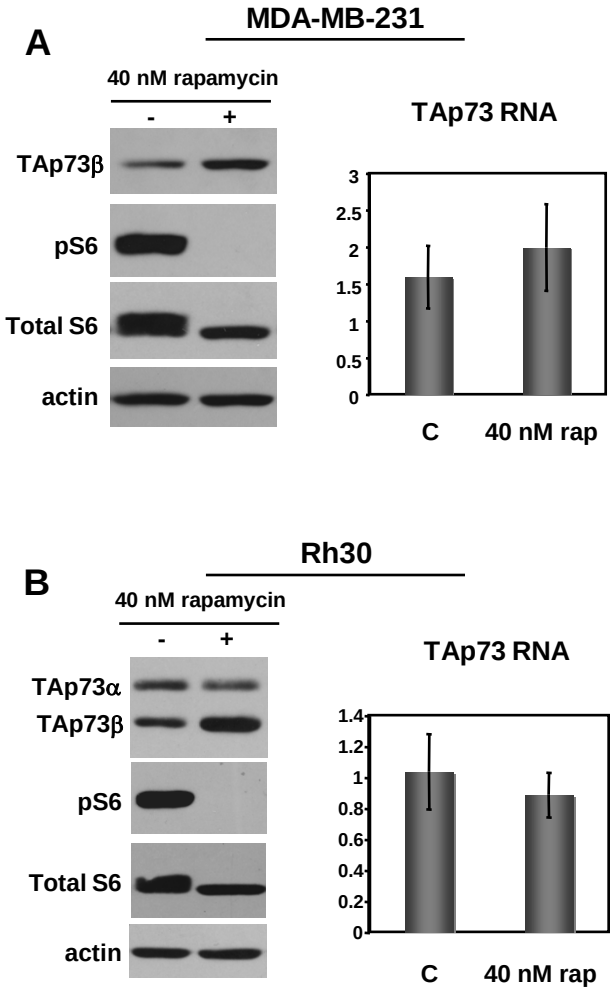

Figure 7: Changes in p73 protein levels do not correspond to changes in p73 RNA levels. A) MDA-MB-231 cells and (B) Rh30 cells were treated with rapamycin for 24 h in 10% serum and analyzed by Western Blot for p73, pS6, Total S6, and actin. Total RNA was purified 24 h after treatment, reverse transcribed, and quantitative real-time PCR performed with primers to TAp73. The samples were normalized to GAPDH and the results are presented as fold-change over vehicle-control. Error bars represent standard deviation from three experiments. Densitometry was performed on p73 western signals, followed by normalization to actin. The increase in TAp73β protein levels over vehicle-control was 2.2-fold in (A) and 4.3-fold in (B).

To determine if the rapamycin-induced elevation of p73 was an indirect consequence of rapamycin-induced cell cycle arrest (180), we treated MDA-MB-231 and Rh30 cells with the cell-cycle inhibitors hydroxyurea and mimosine. Cells were treated with the inhibitors for 24 h to achieve a G1/S phase arrest; however, TAp73β levels remained constant (Figure 8). These data show that p73 levels are responsive to cellular energy status but not general cell-cycle arrest.

MDA-MB-231 and Rh30 cells do not express detectable levels of p63 by Western blot, and in both cases p53 is known to be mutant (181,182). In contrast, experiments within the Connectivity Map were often performed in cell lines that express multiple family members. Because both p53 and p63 can regulate overlapping sets of target genes with p73 (37), we addressed the possibility that rapamycin-induced changes in gene expression are due to modulation of p53 and/ or p63. To assess the effect of rapamycin on protein levels of all three family members we used nontransformed HMECs. Only p73 increased in response to rapamycin in HMECs; p53 and p63 levels both decreased slightly (Figure 9). We tested additional cell lines that express functional p53 or p63 (UM-SCC-012, UM-SCC-6, UM-SCC-17b, and MCF-7); in no case did we observe an increase in p53 or p63.

mTOR regulates p73 signaling

To determine if the modulation of p73 by rapamycin was mTOR-dependent and to control for any off-target effects induced by rapamycin and metformin, we inhibited mTOR using a non-pharmaceutical approach. MDA-MB-231 cells were infected for three days with lentivirus expressing shRNA that targets mTOR (Figure 10).

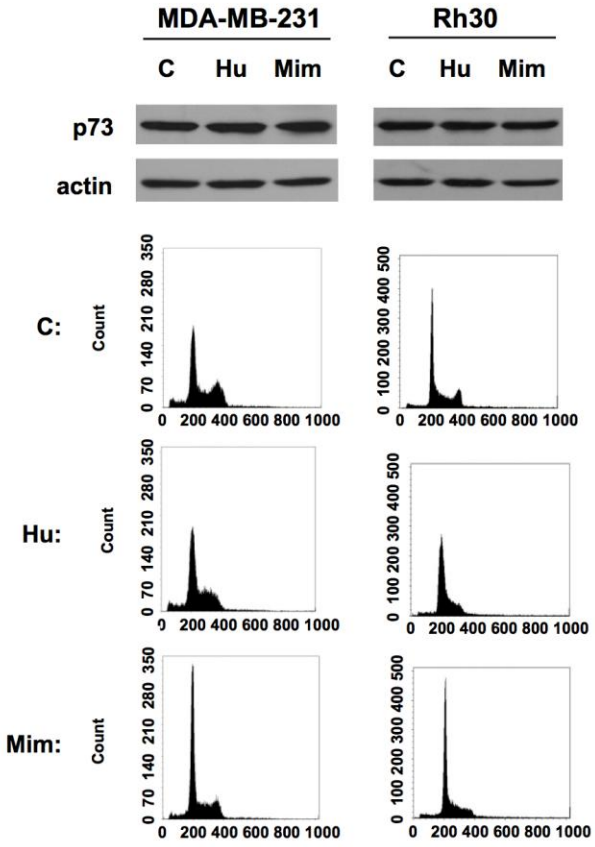

Figure 8: General cell-cycle inhibition does not increase p73 levels. MDA-MB-231 and Rh30 cells were treated with 100 nM hydroxyurea (Hu) or 500 μM mimosine (Mim), or the appropriate vehicle-control (C) for 24 h. Protein lysates were harvested and analyzed for p73 and actin by Western blot, and cells were analyzed by flow cytometry to assess cell cycle profile.

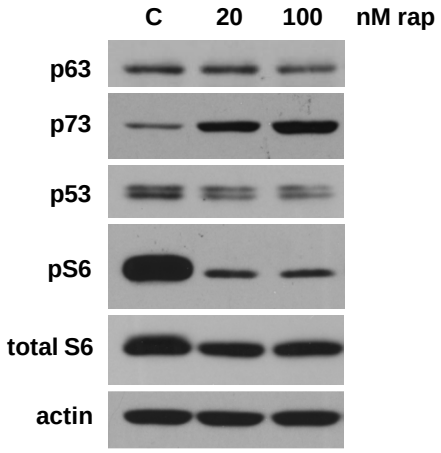

Figure 9: Differential regulation of p53 family members by rapamycin. HMECs were treated with vehicle control (C) or rapamcyin for 12 h. Protein lysates were analyzed by Western blot for p53, p63, p73, actin, pS6 and total S6. Representative of three independent experiments.

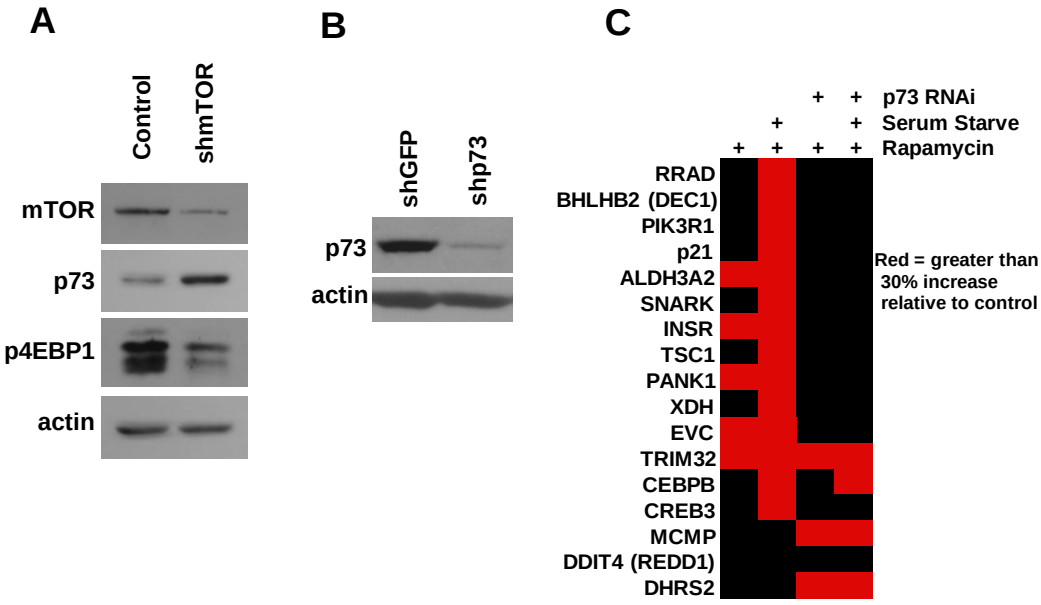

Figure 10: mTOR regulates p73 levels and activity. A) mTOR knock-down induces p73. MDA-MB-231 cells were transduced with lentivirus engineered to express shRNA against the FRAP1 subunit of mTOR, or with control lentivirus. Protein lysates were harvested three days after transduction, and mTOR, p73, p4EBP1, and actin were analyzed by Western blot to demonstrate knock-down of mTOR levels and activity and induction of p73 levels. Westerns are representative of three independent experiments. B) MDA-MB-231 cells were transduced with lentivirus engineered to express shRNA against GFP or p73. Protein lysates were harvested five days after transduction. C) p73 activity is induced in MDA-MB-231 cells treated with 20 nM rapamycin, with or without concurrent serum-starvation, verified using p73 RNAi. p73 RNAi was performed by transducing cells with lentivirus engineered to express shRNA against either GFP or p73 72 h before treatment. Total RNA was prepared 48 h after treatment, reverse transcribed, and quantitative real-time PCR performed with primers to the indicated genes. The samples were normalized to GAPDH, and the results are presented as fold-change over vehicle-control for an average of three experiments. Samples that exhibited a 30% or greater increase relative to control are indicated in red. Twelve of seventeen genes exhibited a p73-dependent increase in RNA levels after rapamycin treatment and serum-starvation.

Expression of the shRNA resulted in a significant decrement in mTOR protein levels and activity and an increase in p73 protein levels (Figure 10).

Since a signature of p73-regulated genes was the initial query that identified a link to mTOR, we hypothesized that several of these genes should be regulated by mTOR in a p73-dependent manner. To test our hypothesis, MDA-MB-231 cells were infected with lentiviral shRNA targeting p73 (Figure 10). RNA was harvested from these cells after treatment with rapamycin in the presence or absence of serum in the media. The target genes selected for further analysis were genes in the p73 signature with mTOR-related gene ontologies (e.g. involvement in insulin signaling), as well as genes with general metabolic functions if they exhibited a high fold-change after p73 expression, and if one or more ChIP tags mapped to the gene locus. All of the target genes that were selected are shown in Figure 10. We found that twelve out of the seventeen candidate target genes identified using our *ad hoc* selection method exhibited an increase in expression after treatment with rapamycin that was abrogated by depletion of p73 (Figure 10).

Three target genes further demonstrate our selection methods. The insulin receptor (INSR) was identified by both microarray and ChIP, and was selected based on known cellular function. Similarly, Tuberous Sclerosis 1 (TSC1) was identified by ChIP and is a known component of the mTOR signaling pathway (183). Finally, xanthine dehydrogenase (XDH) is an example of a target gene chosen both for its ontology and for its presence as a cluster of tags in the ChIPSeq dataset (data not shown). XDH regulates cellular metabolism and cellular response to reactive oxidative stress (184), a process that can by regulated by mTOR during hypoxia (118).

XDH, *TSC1*, and *INSR* are three examples of a larger subset of genes whose regulation by mTOR is p73-dependent at the transcriptional level. An increase in expression from all three genes after treatment with rapamycin in the absence of serum is abrogated by p73 knock-down, as depicted in Figure 11. In addition, semi-quantitative ChIP in Rh30 cells revealed an increase in p73 binding to promoter or intronic sequences in all three genes in response to rapamycin (Figure 11). These genes, that were selected using multiple criteria, thus serve as readout of an mTOR-p73 signaling axis.

Also consistent with mTOR being an upstream modifier of p73 signaling, knock-down of p73 prevented a decrease in cell growth rate in MDA-MB-231 cells after treatment with rapamycin (Figure 11). These data suggest that cellular processes affecting growth rate are modulated by mTOR and p73.

To assess more specific functions of p73 that might be regulated by mTOR, we focused on autophagy, a form of degradative cell death in response to energy starvation that is induced by p73 (185). Because our gene signature was generated using the TAp73β isoform, and only TAp73β is induced by rapamycin, we tested the effect of selective knock-down of this isoform on autophagy using two different RNAi constructs targeting either the N-terminal TA domain or the C-terminal β domain. In both cases, knock-down abrogated baseline autophagy as measured by detection of the cleaved forms of MAP1LC3 (LC-I and LC-II) by Western blot. MAP1LC3-II is the only protein known to be associated with the completed autophagolysosome, and is considered a marker of autophagy (186).

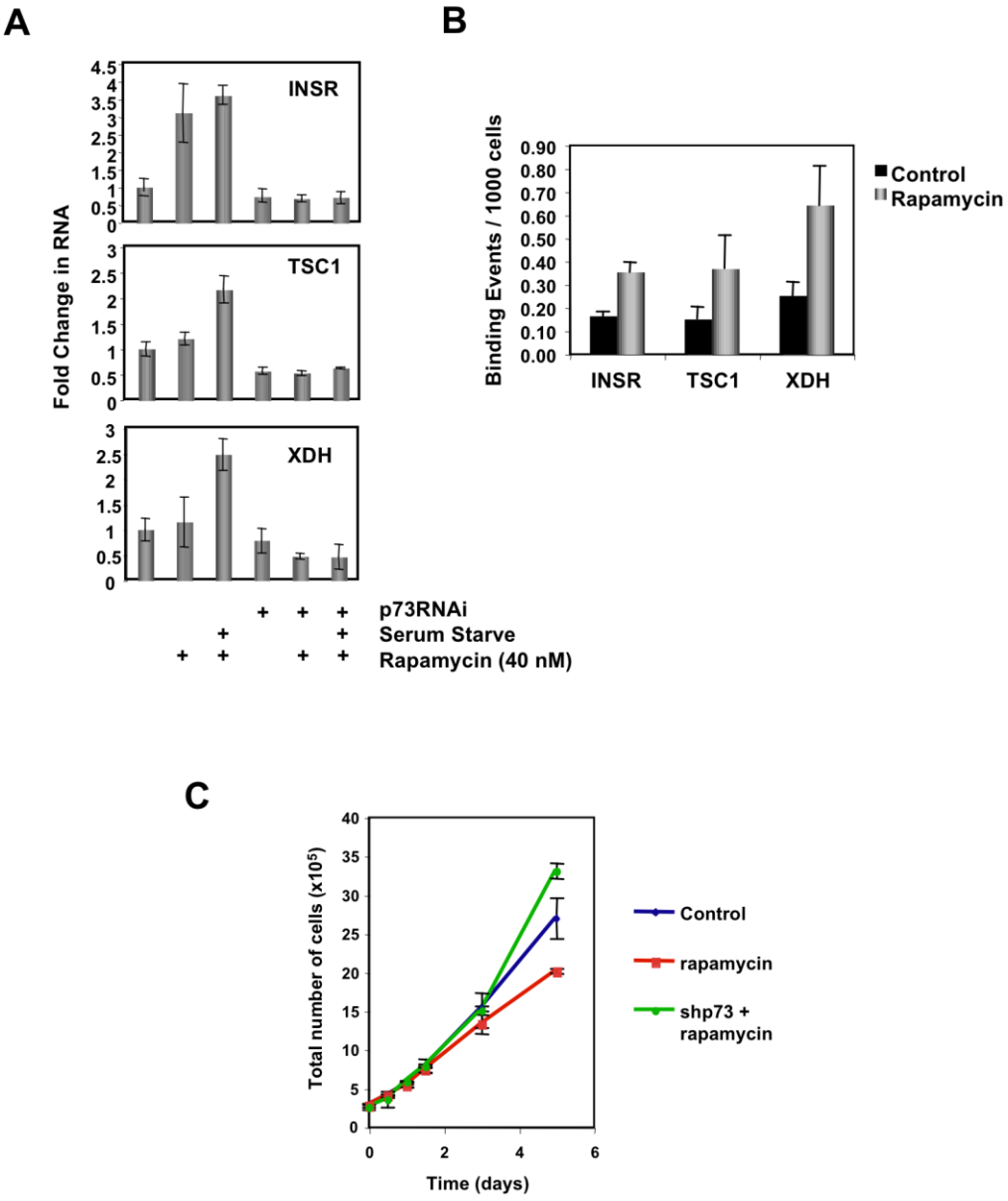

Figure 11: mTOR regulates p73 binding and activity. A) Fold change in RNA for INSR, TSC1, and XDH shows rapamycin/serum-starvation induced changes that are p73-dependent. Error bars represent standard deviation for three experiments. B) Semi-quantitative ChIP was performed to assess levels of p73 binding to genomic regions in *INSR*, *TSC1*, and *XDH* promoters or introns in Rh30 cells treated with vehicle or 40 nM rapamycin for 24 h. C) MDA-MB-231 cells were transduced with shRNA lentivirus and treated with 20 nM rapamycin or vehicle. At the indicated times cells from treated or control cultures were counted and changes in cell growth rates due to p73 and rapamycin are shown. Error bars represent standard deviation from three experiments.

We next sought to identify downstream factors that might mediate this effect on autophagy. p73-regulated genes were analyzed using publicly available datasets in which biological states involving mTOR modulation, such as nutrient deprivation and autophagy, were profiled using DNA microarrays (187,188). Several known p73 target genes showed increased expression in response to starvation and/or starvation-induced autophagy (Figures 12 and 13; orange font) (85,117,187-193). Two unknown genes in the p73 gene signature, Kelch-like 24 (KLHL24) and LOC153222, clustered with the known and functionally better-annotated target genes that were increased in these biological states (Figures 12 and 13; blue font). Both KLHL24 and LOC153222 RNA levels increased in MDA-MB-231 cells treated with rapamycin (Figure 13). For both genes, this increase was p73-dependent (Figure 13). Thus our approach resulted in the identification of new p73-regulated genes associated with autophagy and metabolism. A gene signature of p73 target genes, when queried using the Connectivity Map, allowed us to identify mTOR as a key signaling pathway upstream of p73.

mTOR and p73 in triple-negative breast cancers

We next explored the relevance of the mTOR-p73 signaling pathway to human cancer, focusing on a particular subtype of breast cancer that expresses p53 family members, is basal-like, and is associated with a poor prognosis (57). As described above, using a combination of microarray profiling and ChIPSeq, we generated a robust p73 gene signature. We also generated a p63 gene signature comprised of 299 genes that are regulated by p63 in squamous tissues, as measured by Barbieri *et al.* (131).

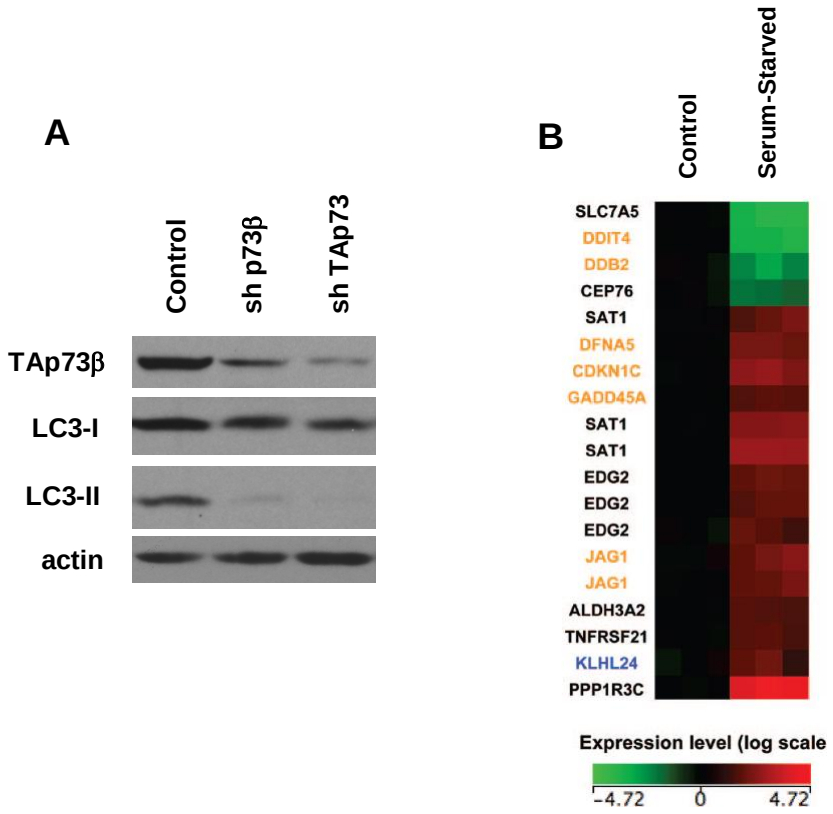

Figure 12: Analysis of p73-regulated genes in a profiling study of starvation. A) p73β knock-down decreases levels of autophagy markers. MDA-MB-231 cells were transduced with lentivirus engineered to express shRNA against TAp73 isoforms or against p73β isoforms. Protein lysates were prepared and p73, actin, and the autophagy markers LC3-I and LC3-II were detected by Western blot. B) Genes from the p73 signature were assessed using a publicly available dataset in which T98G glioblastoma cells were grown asynchronously or serum-starved for 3 d before RNA harvest and microarray analysis (187). Known p53, p63 and/or p73 target genes indicated in orange are: DDIT4 (117), DDB2 (193), DFNA5 (192), CDKN1C (191), GADD45A (190), and JAG1 (85). Cell lines are arranged in columns, grouped by treatment as indicated. Genes (annotated from Affymetrix probes) are in rows that are ordered based on hierarchical clustering results (data not shown). Color range shown indicates baseline transformed expression level on a log scale. Genes that are upregulated during serum-starvation that were selected for additional analysis are in blue.

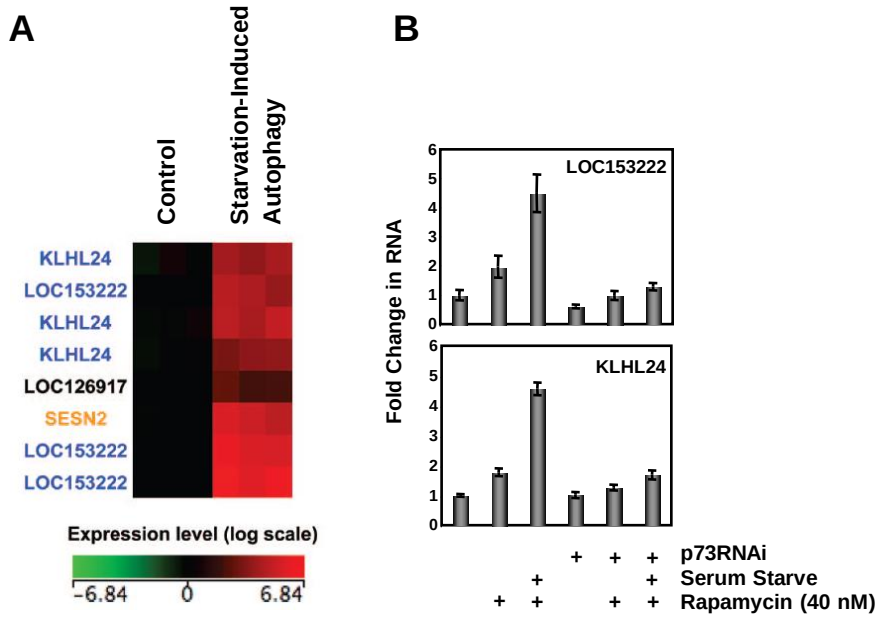

Figure 13: Analysis of p73-regulated genes in a profiling study of starvation-induced autophagy. A) Genes from the p73 signature were assessed using a publicly available dataset in which Awells B-lymphoblastoid cells were serum starved for 6 h or 24 h, inducing autophagy (188). A known p53, p63 and/or p73 target genes indicated in orange is SESN2 (189). Cell lines are arranged in columns, grouped by treatment as indicated. Genes (annotated from Affymetrix probes) are in rows that are ordered based on hierarchical clustering results (data not shown). Color range shown indicates baseline transformed expression level on a log scale. Genes that are upregulated during autophagy or serum-starvation that were selected for additional analysis are in blue. B) Fold change in RNA as in Figure 4 for KLHL24 and LOC153222 indicate increases in RNA levels after rapamycin treatment in a p73-dependent manner in MDA-MB-231 cells.

Because p63 expression is restricted to the triple negative, basal-like subtype of breast cancer, where it functions to inhibit TAp73-mediated apoptosis (37,57), we assessed the ability of our p63 and p73 signatures to segregate triple negative tumors into additional subtypes.

For this line of investigation we analyzed a dataset that was made available to us by Andrea Richardson (Brigham and Women's Pathology Department; GSE7904 in the Gene Expression Omnibus). Dr. Richardson generated microarray data from a collection of 22 basal-like tumors. We took this microarray data and filtered it through a p73 signature (comprised of 333 genes that increased more than 2-fold with p73 over-expression). We were able to cluster the 22 basal-like tumors into two groups of 8 and 14 tumors based on differential expression of genes from the p73 signature (Figure 14). These genes, when segregated by their tumor expression patterns, fell into distinct functional categories (Figure 14). Further, we filtered microarray data generated from 16 pretreatment biopsies isolated from patients enrolled on the VICC BRE9936 trial (concurrent neoadjuvant paclitaxel and radiation for locally advanced breast cancer patients (194)) through a subset of the p63 signature comprised of 44 genes repressed by p63. Of the 16 tumors, 8 were from triple negative breast cancer patients. The gene signature clustered 6 of 16 tumors and all 6 were triple negative (Figure 14). These data suggested that, with a larger cohort of patients, biological meaningful subtypes of basal-like tumors could be identified using p73 and/or p63 gene signatures.

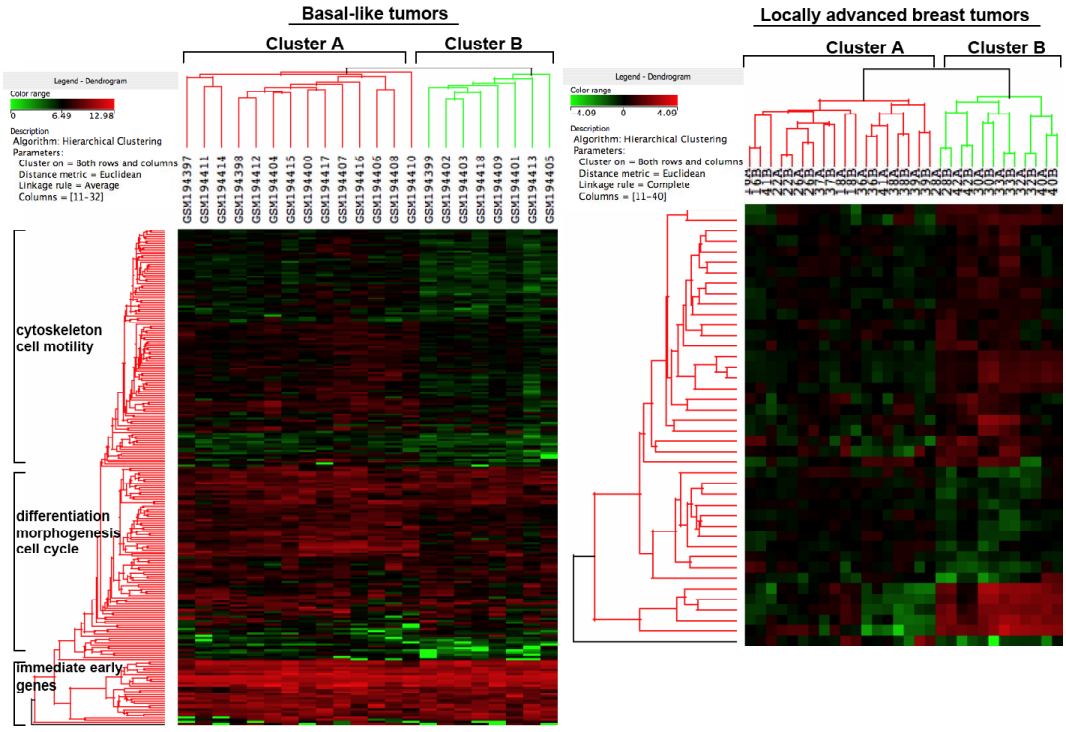

Figure 14: p63/p73 gene signatures can subclassify basal-like tumors and locally advanced tumors. (Left panel) Hierarchical clustering of GSE7904, microarray data from 22 basal-like tumors using a p73 gene signature (333 genes). Of the 22 tumors, 8 were classified based on the differential expression of genes regulated by the p63/p73 signaling axis. (Right panel) Hierarchical clustering of microarray data generated from 16 biopsies collected from patients with locally advanced breast cancer enrolled in VICC BRE9936 using a p63 gene signature (42 of original 299 genes in our signature). The gene signature clustered 6 of 16 tumors into one subgroup and all 6 were triple negative. Of the 16 tumors analyzed there were 8 triple negative tumors.

Given the induction of p73 by rapamycin in mammary epithelial cells, and the decrease in inhibitory p63 levels, we hypothesized that rapamycin would perturb the p63/p73 signaling axis to favor apoptosis. We further hypothesized that mTOR inhibitors would synergize with other agents that induce p73 and are used as neoadjuvant therapies in triple-negative breast cancers such as cisplatin and paclitaxel (32) (195). We examined the sensitivity of MDA-MB-231 cells as well as primary cultures of HMECs to various combinations of cisplatin, paclitaxel, and everolimus [RAD001, an FDA-approved rapamycin analog and mTOR inhibitor (Novartis)]. We found that RAD001 and cisplatin could elevate p73 levels when used as single agents and could decrease p63 levels in cells (HMECs) that expressed the protein (Figure 15). We observed a synergistic effect of the three drugs in combination as evidenced by increased expression of the p73 target gene Puma, cleavage of PARP and caspase-3, and apoptosis (Figure 15 and data not shown). These data serve as preclinical evidence supporting an ongoing clinical trial studying the activity of cisplatin and paclitaxel ± RAD001 in patients with triple negative breast cancer.

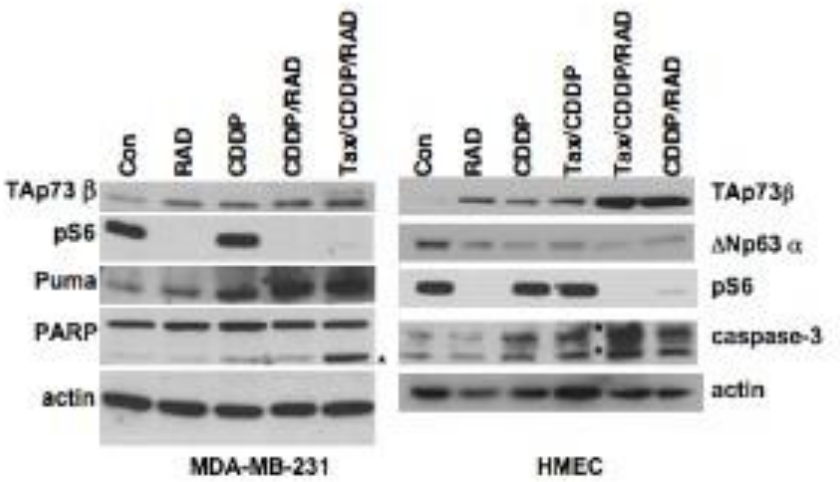

Figure 15: Drug modulation of p63/p73 signaling axis. The indicated cell lines were treated with RAD001 (20 nM), cisplatin (CDDP, 25 μM), or paclitaxel (Tax, 100 nM) alone or with the indicated combinations. Protein lysates were harvested at 24 h and Western analysis performed for p73, p63, pS6, Puma, PARP, caspase-3, or actin. The *s indicate cleaved products of PARP or caspase-3 found in cells undergoing apoptosis. Cell treatment and Western analysis were performed by Maria Pino and Lucy Tang.

Discussion

Through whole-genome ChIP coupled with gene expression profiling, we have created a p73 gene signature that contains multiple tiers of expression and genome location information. This signature was used to identify a novel connection between p73 and the upstream kinase mTOR. Further, select genes from the p73 signature exhibited mTOR-mediated, p73-dependent regulation. Our approach, using a downstream signature to identify upstream regulators, is based on straightforward cell culture methods and should be widely applicable to the study of many transcription factors.

Determinants of our approach include over-expression of the protein of interest in a cell line that does not express high levels of the protein. This should be easily applied to transcription factors that are not essential for cell cycle progression or proliferation. In addition, we predict that modifications of our approach such as using a knock-down instead of an over-expression technique would be successful. One of the striking findings from the completion of the Connectivity Map was the extent to which connections could be made across different cell lines and tissues (143,196). Likewise, we did not encounter any problems due to the cell lines that we chose for analysis, although this might be a significant issue for a modified knock-down approach. In our study, p73 was regulated by mTOR inhibitors in primary cells as well as multiple cancer cell lines.

The link between mTOR and p73 sheds new light on p73 biology, further demonstrating that p73 can be regulated by upstream pathways outside of canonical p53 signaling (77,78,93,197-200). For example, Akt can regulate p73 and p73-dependent apoptosis (162,201). It would be intriguing to determine the role of mTOR (and

additional members of the mTOR signaling pathway such as Akt) on canonical p53-family functions such as apoptosis and cell-cycle arrest. Because Akt directly regulates YAP, an activator of p73 (201), this mechanism may function in parallel with mTOR to affect p73-dependent transcriptional regulation.

Other functions downstream of mTOR may also be mediated by p73. Metformin induces apoptosis specifically in p53-null tumor cells (202). Given our results that metformin can induce p73 levels, additional studies are ongoing to test the role of p73 in metformin-induced apoptosis and tumor toxicity, in the presence or absence of p53.

It is the isoform TAp73β that is induced by rapamycin and metformin, with apparent coordinate downregulation of TAp73α (Figure 5). Few proteins that differentially modify the alpha versus beta isoforms of p73 have been identified (203,204). We identified a putative E3-ubiquitin ligase in our datasets, TRIM32. The RNA levels of TRIM32 increase 142% upon serum-free treatment with rapamycin (Figure 10 and data not shown). The increase is abrogated to 37% after treatment with concomitant p73 RNAi-mediated knockdown (Figure 10 and data not shown). Perhaps TRIM32 or another regulatory protein differentially modifies TAp73α and TAp73β isoforms in response to signaling from the mTOR pathway.

We demonstrated that endogenous regulation of caspase-independent cell death known as autophagy is a specific function of the TAp73β isoform (Figure 12). Although the mechanism that links p73 to autophagy is unknown (185), the p73 signature presented in this work contains candidate target genes, including unknown factors such as KLHL24 and LOC153222, that are increased in autophagy by microarray profiling (Figures 12 and 13). KLHL24 contains a BTB/POZ domain that can function in transcriptional

repression, and LOC153222 contains a basic-leucine zipper domain suggesting transcription factor activity (205). These factors may regulate a transcriptional program inhibited by mTOR but induced by p73 during autophagy.

Our study suggests a larger role for mTOR in regulating the p53 family as a whole. p53 is upstream of mTOR through regulation of *PTEN*, *TSC2*, and *IGFBP3* (116), as well as downstream of mTOR in vivo in hamartomas (119). In general the mTOR signaling pathway integrates multiple inputs, and can involve alteration of and feedback regulation by Akt and the mTORC2 complex (111,206-208). In later chapters we will explore the signaling mechanism(s) by which this pathway is connected to p73. Our data suggest that p73 is regulated by mTOR at the post-transcriptional level, either by altering protein stability or other mechanisms. For example, p53 family transcripts may have internal ribosomal entry sites that would allow for cap-independent translation (209-211). Cap-independent translation may play a role in mTOR regulation of the p53 family.

As has been suggested by Golub, Lamb and colleagues, our study demonstrates the potential impact of an expanded Connectivity Map as a community-wide resource that would include many more drugs and perturbagens than were included in the first build (143,196). Here we show utility for linking the pathways represented by the Connectivity Map to the study of transcription factors in particular, but the power of this approach is dependent on the number of drugs and drug-inducible pathways that are testable through this resource. In our study we chose to assess the top 30 compounds predicted to induce a p73 gene signature. This was based on our pilot study using transcription factors with known activators. In contrast, few compounds were identified

that would be predicted to repress p73 (i.e. compounds with a negative connectivity score), and we did not do a formal analysis of these drugs. However, one compound with a negative connectivity score was estradiol (data not shown), a known activator of the mTOR pathway (212). Preliminary data suggests that estradiol can decrease p73 levels (data not shown). Therefore, we predict that using our approach to identify compounds that inhibit transcription factors could also elucidate signaling connections. An expanded Connectivity Map that included more drugs that impact the same pathway at multiple levels would allow for more rigorous statistical testing, and thus increase an investigator's ability to look for enrichment of pathways and agents among their top hits.

Already, genomic technologies have created a wealth of information downstream of transcription factors. We propose that this information can be used not only to characterize downstream signaling pathways, but also to map upstream drug-inducible pathways. Using a genomic-based screening procedure and cell culture-based validation techniques, we identified a novel link between p73 and mTOR, an important kinase in energy homeostasis and tumorigenesis.

Because p73 isoforms are over-expressed in many tumors, they may provide effective targets for cancer treatment (161). Recent studies suggest that p73 may be present in an inactive form in select head and neck squamous cell carcinomas and basal-like breast tumors, and that activation of p73 would lead to tumor cell apoptosis (56-58). We explored the ability of p63 and p73 to define subtypes of triple-negative breast tumors. Given the synergistic effect of mTOR inhibition on cisplatin and paclitaxel-induced apoptosis and on p73 induction in basal-like tumors, p63 and p73 gene signatures may be useful for predicting patients that will respond to combination therapies that

include mTOR inhibitors. Thus, our results have implications for ongoing and future clinical trials examining the efficacy of mTOR inhibitors in tumors expressing p73.

CHAPTER IV

DIFFERENTIAL REGULATION OF THE P73 CISTROME BY MTOR REVEALS TRANSCRIPTIONAL PROGRAMS OF MESENCHYMAL DIFFERENTIATION AND TUMORIGENESIS

Introduction

It has become increasingly clear that no single target gene can explain more than a fraction of the tumor suppressive activity of p53. Instead, p53 regulates the transcription of an extensive network of genes involved in diverse functions such as cell cycle arrest, apoptosis, senescence, and autophagy (213). Genome-wide technologies such as chromatin immunoprecipitation (ChIP) coupled with sequencing (ChIP-Seq or ChIP-PET) or microarray (ChIP-on-Chip) have confirmed that p53 regulates highly complex gene networks (15,82,86,88). For example, a recent ChIP-PET study showed that p53, when activated, binds to hundreds of sites in the genome (86).

The complexity of the p53 response, however, extends beyond its genomic binding profile, and is reflected by the existence of many p53-like variant proteins that can also bind DNA. Alternative splicing and multiple promoter usage can generate p53 isoforms with variable N- and C-terminal domains (35). In addition, mammals have two homologs of p53: p63 and p73. All three p53 family members share a core structural architecture and significant sequence identity, and, although their precise roles remain unknown, p63 and p73 can also act as tumor suppressors (35).

It is clear that p63 and p73 can regulate many p53 functions. However, comprehensive whole-genome analyses are needed to identify the full extent of shared versus unique target genes that underlie these functions, as well as biochemical

determinants such as sequence-specificity, use of cofactors, and epigenetic context. Along these lines, a recent study used ChIP-on-Chip technology to create a complete, unbiased resource of p63 binding sites in cervical cancer cells (13). This work revealed both similarities and differences in the way that p53 and p63 regulate gene expression (13). Such insights into p53 and p63 highlight the need to investigate p73 upstream of transcriptional networks during development, tumorigenesis, and tumor therapy.

Herein we report the first comprehensive, whole genome analysis of p73 binding in human cells. Furthermore, we re-analyzed this p73 cistrome after perturbation with an upstream stressor, an mTOR inhibitor that induces p73 as shown in Chapter III. The p73 cistrome shows significant overlap with p53 and p63-regulated target genes. In addition, we identified determinants of p73 binding, activity, and function, some of which were modulated by mTOR. We created an mTOR-p73 gene signature that is enriched for genes, micro-RNAs (miRNAs), and non-coding RNAs (ncRNAs) involved in mesenchymal stem cell differentiation and rhabdomyosarcoma tumorigenesis.

Results

mTOR modulates the p73 cistrome

To perform a comprehensive analysis of p73 binding sites in the genome (the p73 cistrome), we sought a cell line that expresses abundant p73 with detectable binding to chromatin. We analyzed two cell lines in which we had observed an intact mTOR-p73 signaling pathway in Chapter III: the rhabdomyosarcoma line Rh30, and the breast cancer line MDA-MB-231. We used ChIP coupled with quantitative real-time PCR (ChIP-

qPCR) to compare the binding levels of endogenous p73 to representative target genes, identified in Chapter III, in these two cell lines after rapamycin treatment. p73 exhibited more robust binding in Rh30 cells (Figure 16), therefore we performed subsequent genomic analyses in that cell line. For genome-wide ChIP analysis and for the ChIP-qPCR in Figure 16, we used the A300-126A antibody that only recognizes p73 proteins that contain a transactivation domain. These TAp73 isoforms are considered 'active' as they are capable of inducing expression of target genes (214).

p73 also exhibits C-terminal diversity, and TAp73 can be expressed as any of nine variants (e.g. TAp73α, TAp73β, TAp73γ…). We detect two p73 isoforms in Rh30 cells at the protein level, TAp73α and TAp73β, which have the ability to form hetero-oligomers (Figure 17) (137). The levels of p73 are increased in rapamycin-treated Rh30 cells, and both isoforms are present and bind DNA (Figure 17). Therefore, protein-DNA complexes immunoprecipitated with the A300-126A antibody contain all of the active isoforms of p73 that are detectable in Rh30 cells, and this antibody was used for subsequent ChIP-on-Chip.

ChIP-on-Chip was performed in both control and rapamycin-treated samples. DNA recovered from ChIP was hybridized to oligonucleotide tiling arrays that cover the entire nonrepetitive human genome at 35 bp resolution, and p73 binding was measured as fold enrichment after ChIP compared to un-enriched input. A total of 7,678 sites in control cells, and 8,165 sites in rapamycin-treated cells, showed greater than 2.5-fold enrichment after p73 ChIP. Using the 'negative peaks' approach to estimate error, the false discovery rate at this cut-off is ~0.86%, giving us high confidence that these sites were indeed bound by p73 (215).

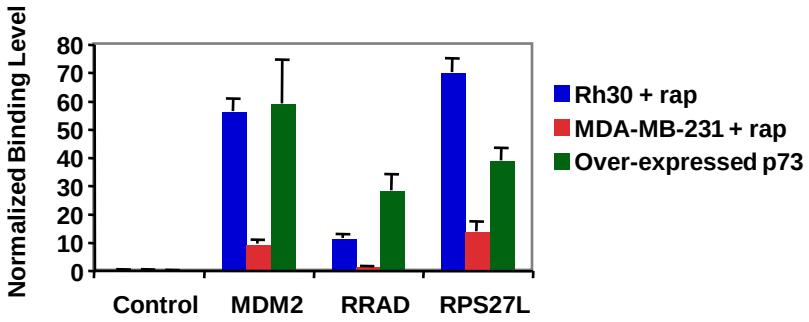

Figure 16: Assessment of p73 occupancy by qRT-PCR. ChIP-qPCR was performed to assess p73 occupancy at genomic regions in *MDM2*, *RRAD*, and *RPS27L* promoters in Rh30 or MDA-MB-231 cells treated with 40 nM rapamycin (rap) for 24 h. To facilitate comparison across cell lines, ChIP-qPCR was also performed in H1299 lung carcinoma cells transduced with an adenovirus that expresses high levels of p73. Binding levels were normalized to input, and "Control" represents a negative-control region.

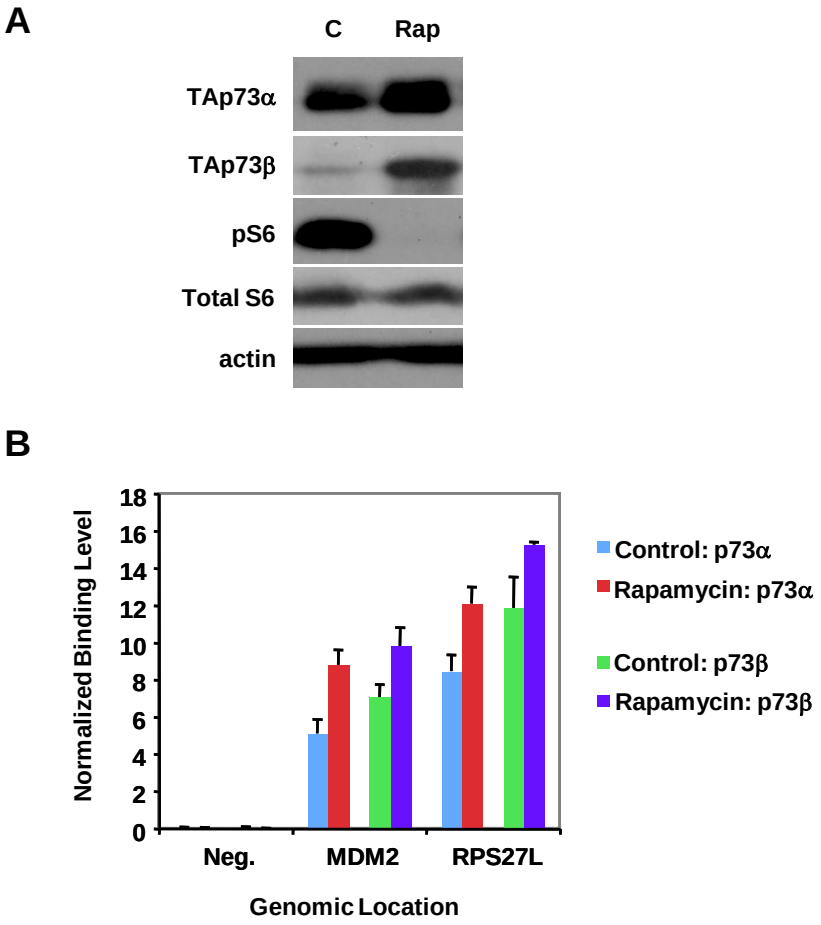

Figure 17: p73 levels and binding increase with rapamycin treatment in Rh30 cells. A) p73 protein levels increase in chromatin-enriched fractions from Rh30 cells treated with 40 nM rapamycin for 24 h, as analyzed by Western blot. p73 was detected using an antibody specific for TAp73 isoforms. "C" is vehicle control. pS6 was used as a marker of mTOR activity. B) ChIP-qPCR was performed to assess p73 occupancy at genomic locations in *MDM2* and *RPS27L* promoters using two unique antibodies that preferentially recognize either p73α or p73β. Error bars indicate standard deviation from triplicate analyses.

The accuracy of ChIP is highly reliant on antibody specificity. Thus, we validated our ChIP-on-Chip results on thirty randomly chosen p73-binding sites by performing ChIP-qPCR with two different p73 antibodies. p73 binding was observed at all thirty sites (Figure 18). The two antibodies used preferentially recognize either p73α or p73β, suggesting that both p73 isoforms bind to the same sites, either directly or through hetero-dimerization with the other p73 isoform. Previous studies suggest that TAp73α forms hetero-oligomers with TAp73β (De Laurenzi et al., 1998). However, we cannot formally distinguish between hetero-oligomers and mixed populations of TAp73α and TAp73β homo-dimer-DNA complexes. Currently, sequential ChIP that measures simultaneous co-occupancy of two proteins on a stretch of DNA is too technically challenging to pursue on a genome-wide scale (Geisberg and Struhl, 2005). Regardless, each p73 binding site as measured by ChIP-on-Chip is likely to reflect genuine binding by both TAp73α and TAp73β. Sites with higher enrichment as measured by ChIP-on-Chip also exhibited higher enrichment by ChIP-qPCR.

To further validate our ChIP-on-Chip results, we used the phastCons score as a measure of evolutionary conservation at every nucleotide in the genome (148). Sequence conservation is an established property of functional genomic elements. As expected, p73 binding sites were conserved relative to non-bound, distant regions (Figures 19 and 20). Thus, our ChIP-on-Chip method identified high-confidence p73 binding sites of likely functional significance.

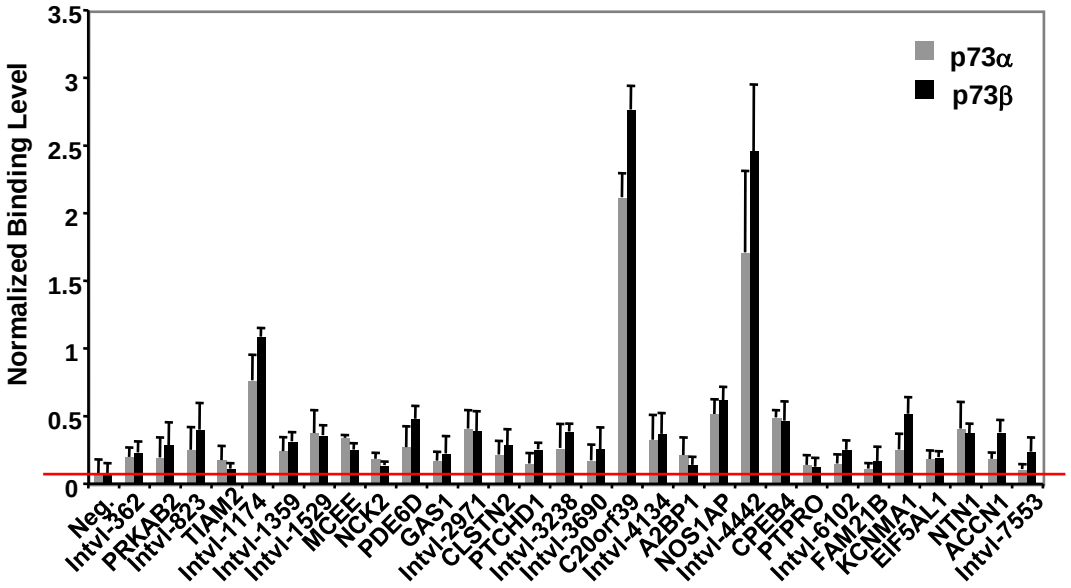

Figure 18: Verification of p73 binding by qRT-PCR. To confirm the ChIP-on-Chip results, p73 occupancy was re-measured using different antibodies and methodology. Thirty loci were chosen randomly from among all p73-bound regions. p73 binding was confirmed by immunoprecipitating either p73α or p73β from sonicated lysates prepared from formaldehyde-crosslinked Rh30 cells, and PCR-amplifying associated DNA fragments using primers flanking each of the thirty sites. The gene nearest each genomic interval ("Intvl") is indicated when located within 10 kb.

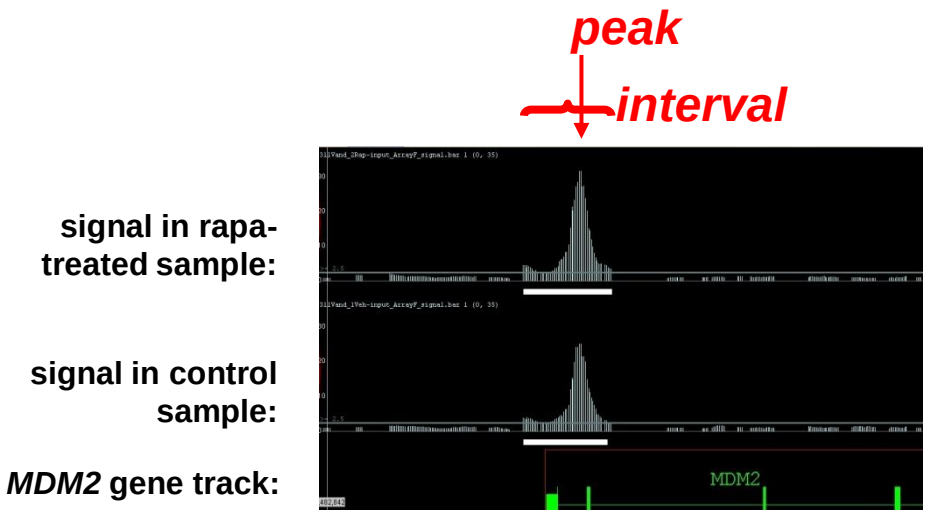

Figure 19: Dimensions of p73 binding. The *MDM2* gene is depicted using the Integrated Genome Browser in order to demonstrate two dimensions of p73 occupancy. The 'interval' is the region across which p73 binding exceeds threshold. The 'peak' is the location in the interval with the highest p73 binding level. These two dimensions are related - binding sites with higher peaks generally have longer intervals.

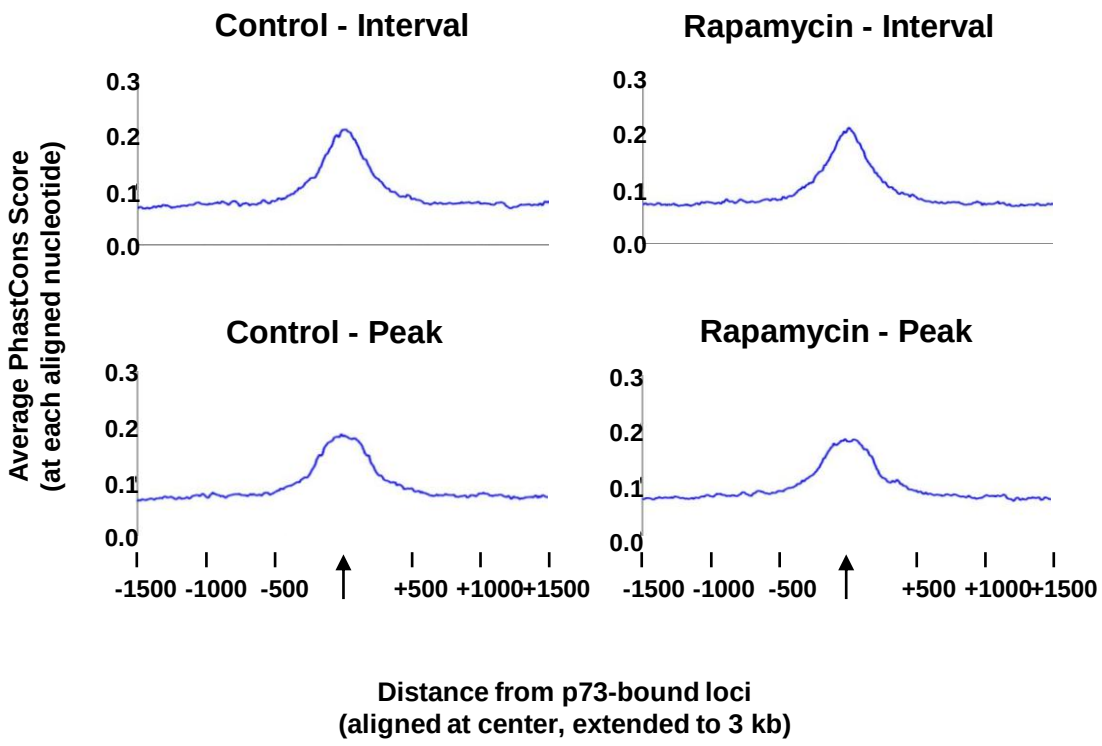

Figure 20: p73 binding sites are conserved. Sequence conservation was determined using phastCons scores from the UCSC GoldenPath genome resource in both control and rapamycin-treated samples. The conservation of broad p73-bound intervals and more sharply defined peaks was assessed. Regions were extended to 3 kb and aligned at their centers, and an average conservation score was calculated at each aligned nucleotide. Conservation is higher at p73-bound regions (center of each plot), compared to genomic background (at both ends of each plot).

We next examined whether inhibition of mTOR results in alteration of the p73 genomic binding profile. A second ChIP-on-Chip analysis was performed in Rh30 cells treated with 40 nM rapamycin for 24 h, conditions that induced p73 in Chapter III. We measured the effect of rapamycin on p73 binding relative to two different parameters. First, we measured the p73 cistrome by distance to nearest transcriptional start site. As shown in Figure 21, rapamycin treatment did not alter p73 binding distribution when measured relative to the start site of human genes. As a second measure of p73 occupancy, ChIP enrichment levels were compared before and after rapamycin treatment. There was a significant increase in p73 binding level after rapamycin treatment (Figure 21, $p<0.0001$, skew test). Thus, although the overall distribution of p73 binding location was unaffected by inhibition of mTOR, p73 occupancy increased in magnitude.

p73 binding did not increase uniformly at all sites in the genome. Instead, only 8.7% of p73 binding sites demonstrated greater than 50% increase in binding level after rapamycin treatment. Eighteen sites to which p73 exhibited greater than 2.5-fold increased binding are shown in Figure 22. Only nine of the eighteen sites shown are within 10 kb of known human genes, yet eight of the remaining nine sites have a high level of sequence conservation across vertebrate species (data not shown). Thus some of these sites may be functional elements such as enhancers that can regulate gene transcription across great distances. We hypothesize that as chromosome conformation capture-based technologies are developed to map long-range chromosome interactions, more p73-binding sites will be linked to mRNA transcripts.

Collectively, these data suggest that mTOR inhibition increases p73 protein levels, but does not significantly change the overall distribution of p73 binding sites

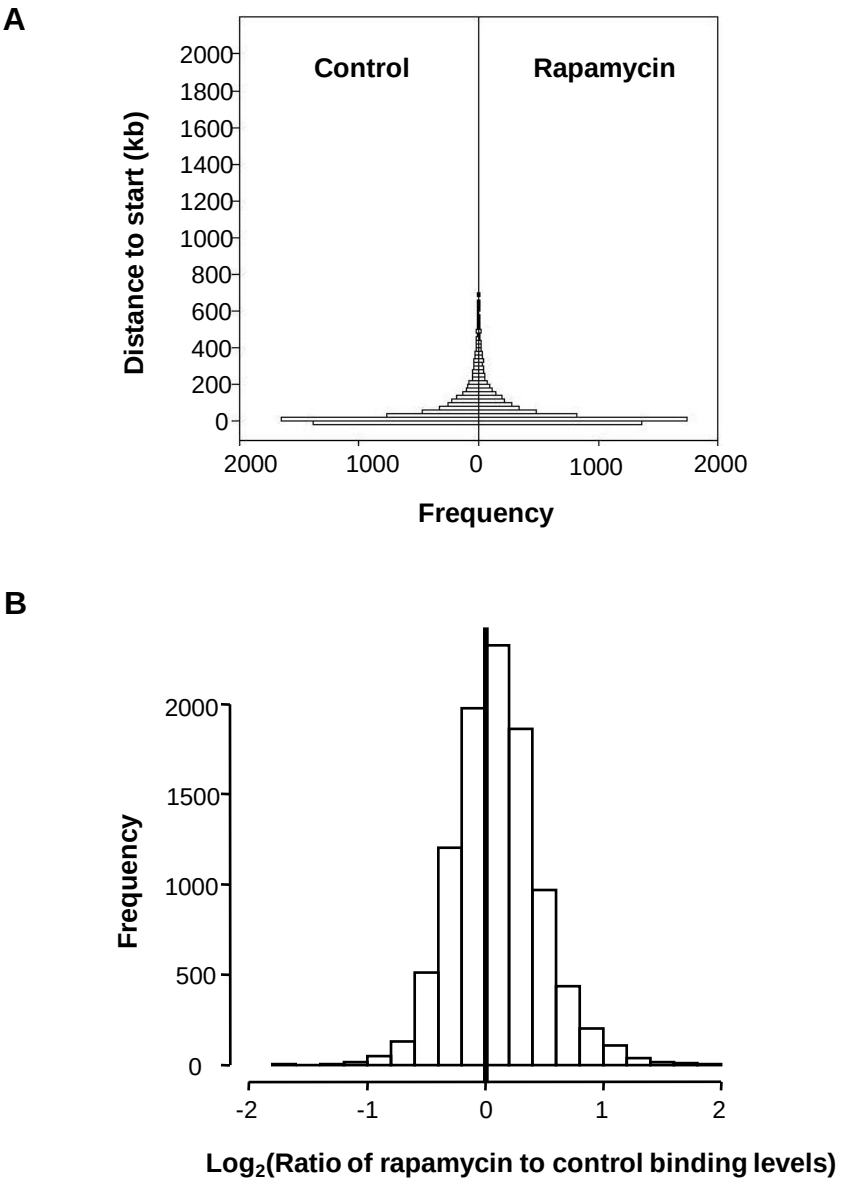

Figure 21: Rapamycin increases p73 occupancy levels. A) Histogram analysis was performed to assess the distribution of p73 binding sites relative to transcriptional start sites. The control sample (left half of plot) and rapamycin-treated sample (right half of plot) were compared using the two-sample Kolmogorov-Smirnov test. The p-value was 0.6, indicating that these distributions are not significantly different. B) Histogram analysis was performed to assess the impact of rapamycin on overall p73 binding level. The ratio of binding levels in rapamycin-treated versus control samples was calculated and log transformed. A skew to the right is evident in this plot, indicating higher binding in rapamycin-treated samples. The degree of skew is 0.34, with $p < 0.0001$. Statistical analysis was performed by Aixiang Jiang and Yu Shyr.

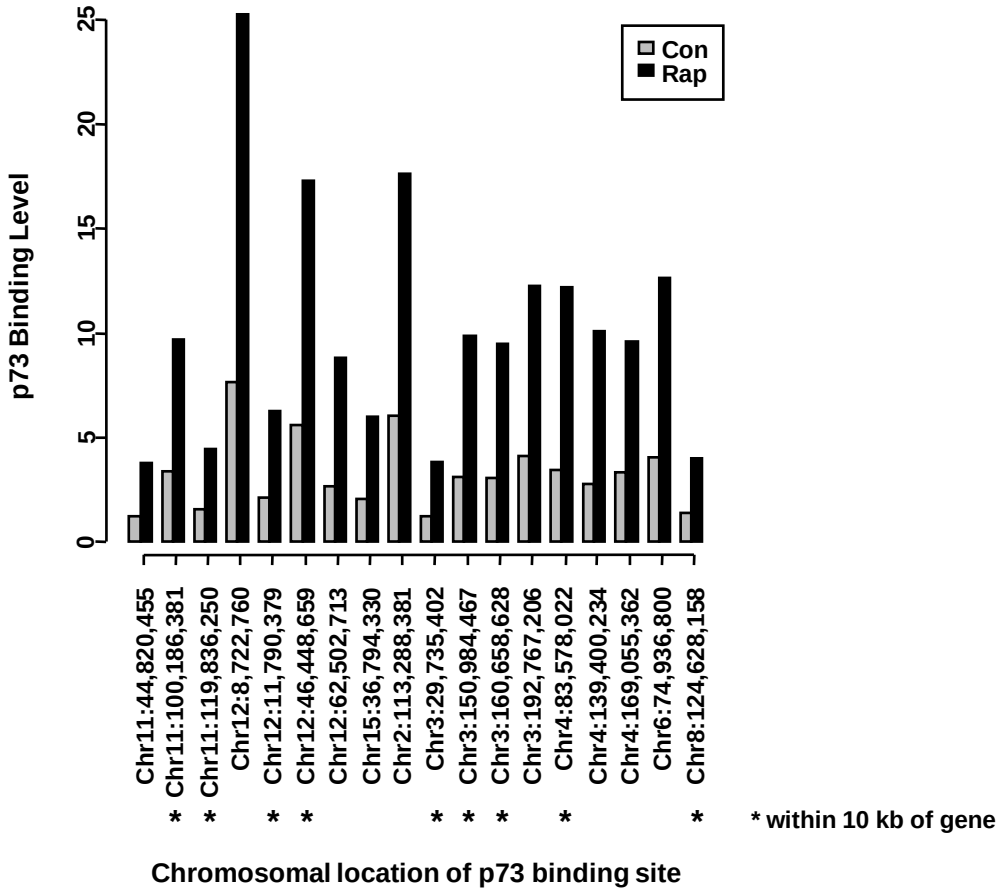

Figure 22: Rapamycin increases p73 binding to specific regions of the genome. p73 binding levels were plotted for 18 loci that exhibited the greatest increase in binding after rapamycin treatment. For comparison, the average p73-binding site exhibits only 1.1-fold higher binding after rapamycin treatment. Chromosomal locations that are within 10 kb of known genes are indicated by an asterisk. From left to right, these genes are: *FLJ32810*, *ARHGEF12*, *ETV6*, *RAPGEF3* / *FLJ20489*, *RBMS3*, *SCHIP1*, *HNRPDL* / *ENOPH1*, and *FBXO32*.

across the genome. Instead, the increased p73 protein is either recruited to specific sites in the genome, or undergoes a selective increase in affinity to specific loci. We next explored determinants of p73 binding, such as sequence-specificity or association with cofactors, which could be responsible for selective, mTOR-induced changes in p73 activity.

Annotation and analysis of the p73 cistrome reveals multiple determinants of p73 binding

We hypothesized that detailed annotation of the p73 cistrome would uncover determinants of p73 activity, some of which would be sensitive to mTOR signaling. First, we mapped all p73 binding sites to within 10 kb of human genes. A total of 4,083 genes in the genome are bound by p73, with some genes containing multiple p73 binding sites (Figure 23). Rapamycin treatment results in only an ~5% increase in p73-bound genes (Figure 23). In both treated and untreated cells, p73 binds predominantly to enhancers, introns, and proximal promoters (Figure 23). These findings suggest that p73 plays a primary role in the regulation of gene expression. p73-bound genes were assigned to functional and biochemical pathways using the Kyoto Encyclopedia of Genes and Genomes (KEGG) database (175). p73 binds genes associated with diverse signaling pathways and cancer types (Figure 24). Some of these associations, including all cancer pathways, had increased significance in rapamycin-treated samples (Figure 24), suggesting that mTOR selectively regulates p73 functions.

One mechanism transcription factors use to engage in selective binding is to recognize a specific DNA sequence, or motif. We used a *de novo* motif-finding algorithm to identify a sequence enriched in top p73-bound loci (Figure 25A),

A

	Control	Rapamycin
Total number of sites (FDR = 0.86%)	7678	8165
within 10kb of Gene	4911	5134
within 200 bp of CpG Islands	557	546
Total number of genes (p73 binding site within 10kb)	4083	4276
with CpGs and p73 binding site in promoter	1220	1198

B

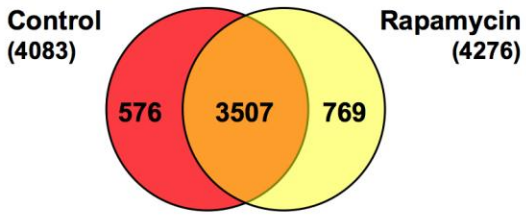

C

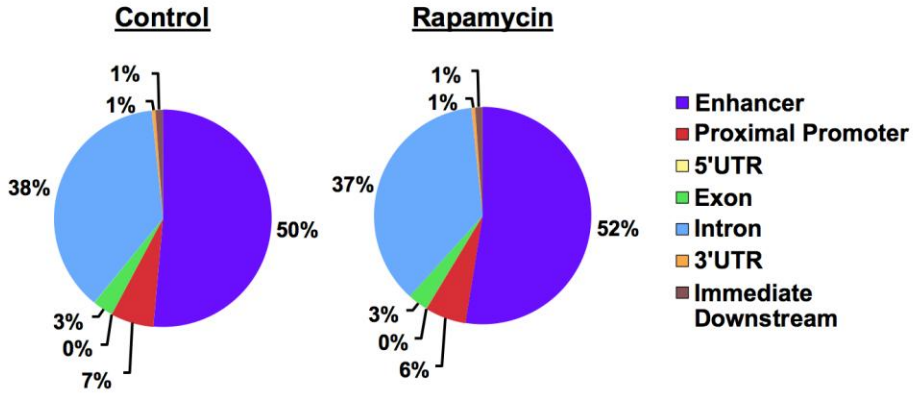

Figure 23: p73 binds the regulatory regions of genes. A) The total number of p73 binding sites (false discovery rate = 0.86%), the number of sites within 10 kb of genes, and the number of sites within 200 bp of CpG islands is listed for control and rapamycin-treated samples. The total number of genes within 10 kb of a p73 binding site, and the number with CpG islands and p73 binding site(s) in promoter regions (from -7500 to +2500 of gene start) is also indicated. B) Schematic showing that ~86% of p73-bound genes in control samples are also bound by p73 in rapamycin-treated samples. C) We determined the percentages of p73 binding sites that reside in proximal promoters (1 kb upstream from 5' gene start), immediate downstream regions (1 kb downstream from 3' gene end), 5' UTRs, 3' UTRs, coding exons, introns, and enhancers (more than 1 kb from gene). Pie charts depict the percentage of p73 binding sites that reside in the indicated functional elements in control and rapamycin-treated samples. The 'enhancers' category includes experimentally validated enhancers from the VISTA Enhancer Browser (http://enhancer.lbl.gov/).

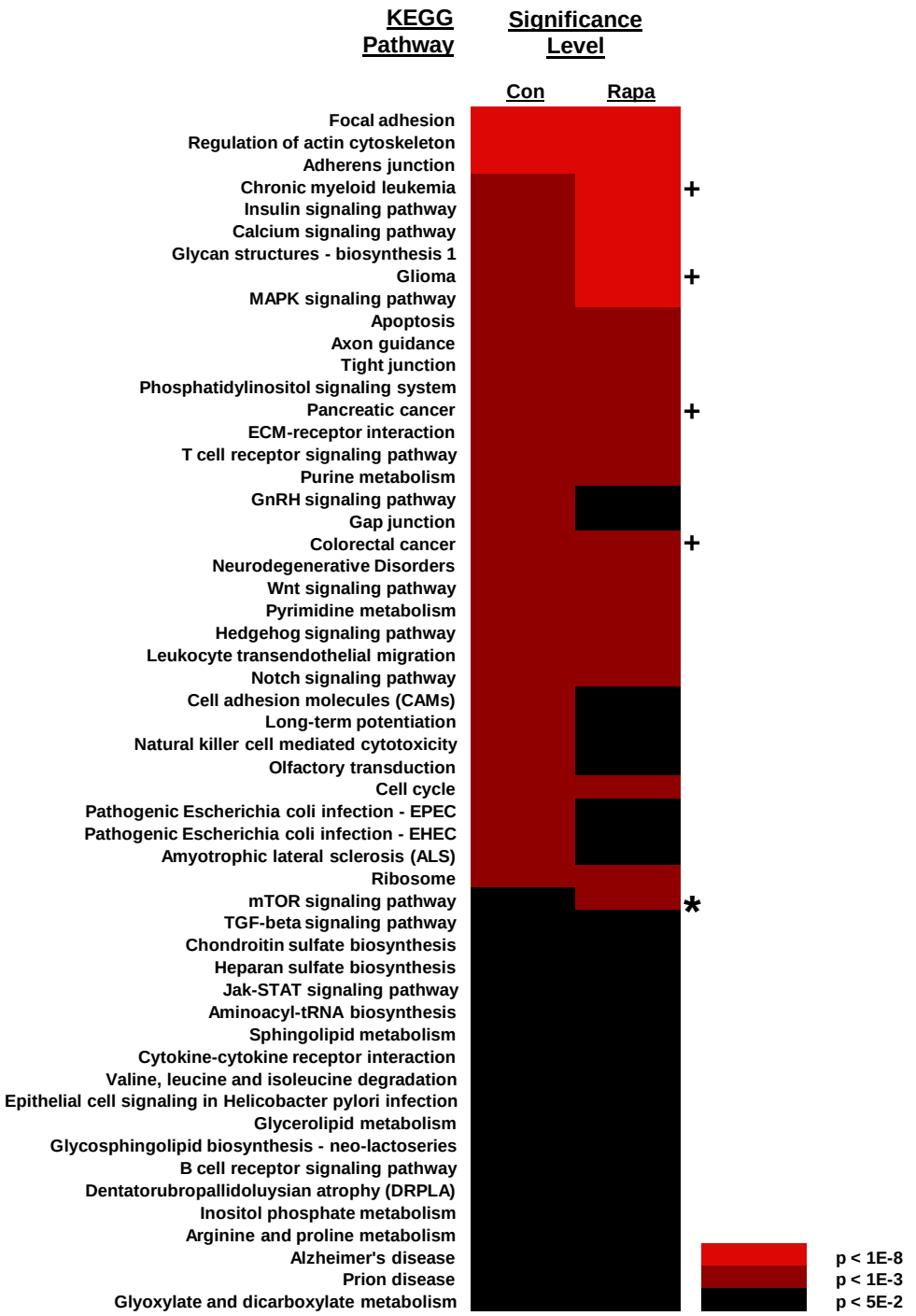

Figure 24: Enrichment of genes in the p73 cistrome by signaling pathway. KEGG signaling pathways that are enriched among genes within 10 kb of p73-binding sites are shown for control and rapamycin-treated samples. Significance is indicated by color, based on p-values from hypergeometric tests. The mTOR pathway is marked with an asterisk. Cancer pathways are marked with '+'; also of note the p-value for pancreatic cancer changes from 1E-4 to 4E-7 with rapamycin-treatment, and the p-value for colorectal cancer changes from 2E-5 to 2E-6 with rapamycin treatment.

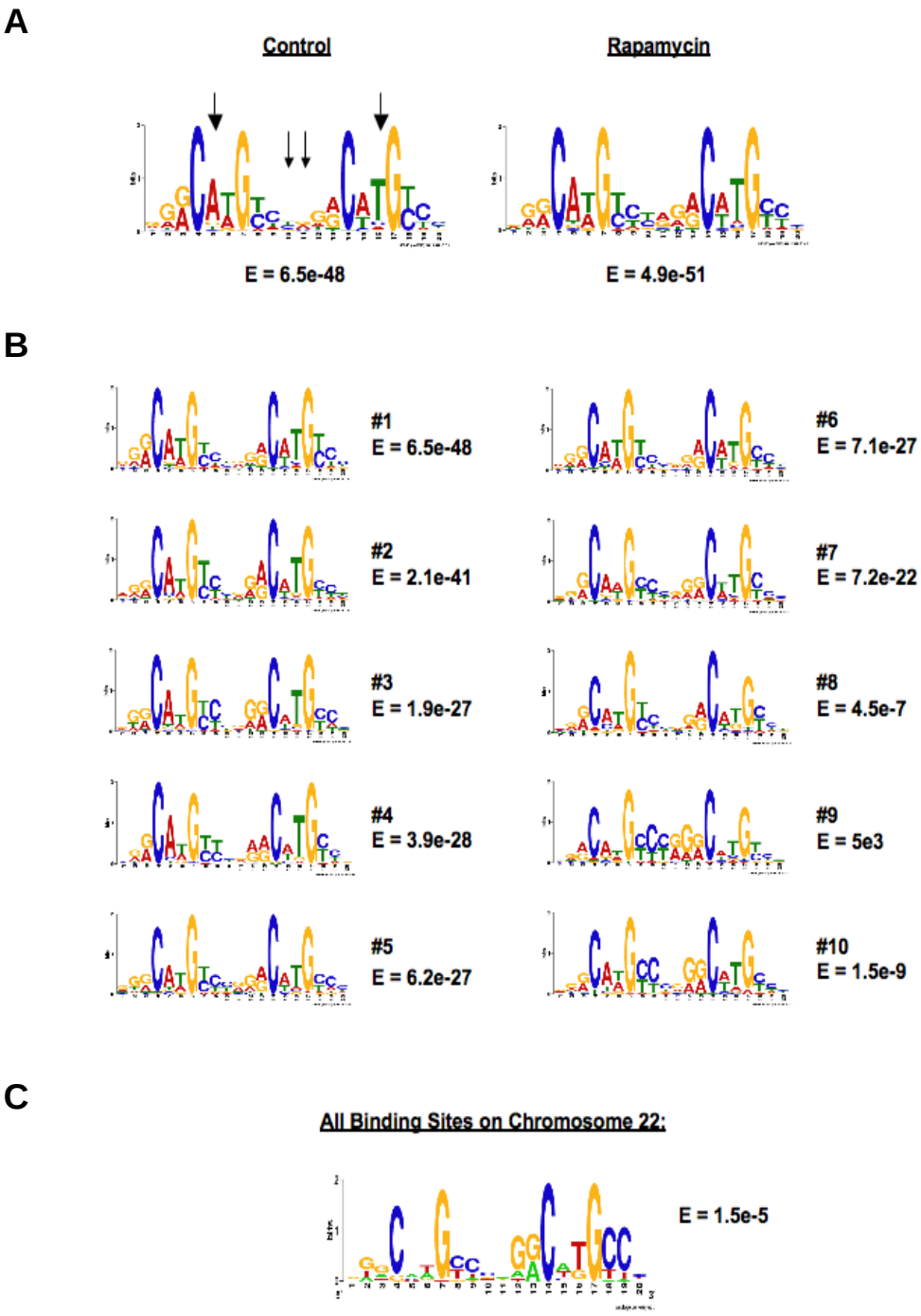

Figure 25: p73 binds a consensus DNA sequence similar to the p53 and p63 response elements. Motifs were identified *de novo* from A) the top fifty p73-bound sequences in control and rapamycin-treated samples, and validated in B) the top 500 p73-bound sequences in groups of 50 in control samples, and C) all p73 binding sites on chromosome 22. Arrows indicate similarities in the motifs of p63 and p73 that differ from p53. These results suggest that, like p53 and p63, p73 is capable of binding sequences that deviate from its consensus motif. The height of each nucleotide indicates its relative frequency at that position in the motif. The probability of identifying an equally well-conserved pattern in random sequences (E-value) is also indicated for each motif.

and validated it against less stringently bound loci (Figures 25B and C). We also validated the p73 consensus binding sequence by performing the systematic evolution of ligands by exponential enrichment technique (SELEX), in which the affinity of p73 for randomly generated oligonucleotide motifs is measured in vitro. SELEX did identify the p73 consensus binding sequence from a pool of random sequences.

The p73 binding motif is nearly identical to the p53 response element (86). However, as indicated by the arrows in Figure 25, p73 also shares certain motif elements with p63 that may decrease p63 selectivity of binding, leading to a larger pool of potential p63 binding sites (47,48). p63 and p73 share 87% sequence identity in their DNA binding domain, compared to only 63% for p53 and p73 (216), supporting our finding that p73 and p63 have highly similar DNA binding motifs. In addition, p73 binds ~4,000 genes, compared to ~3,000 for p63 and ~1,500 for p53 (13,82). Thus, within the p53 family, strictness of DNA motif conservation does seem to correlate with total number of loci bound, and p63 and p73 share more similarity in this regard than either do to p53. Still, the p53, p63, and p73 consensus binding sequences are highly similar, and all family members regulate highly overlapping sets of target genes (Figure 26). The identification of this novel consensus binding sequence will be useful for the future identification of response elements in novel p73 target genes.

p73 binds less than 10% of all its motifs that exist in the genome (data not shown). Thus, other determinants must specify whether or not p73 binds a particular motif both at baseline and during mTOR inhibition. One such determinant may be the association of p73 with other transcription factors and cofactors.

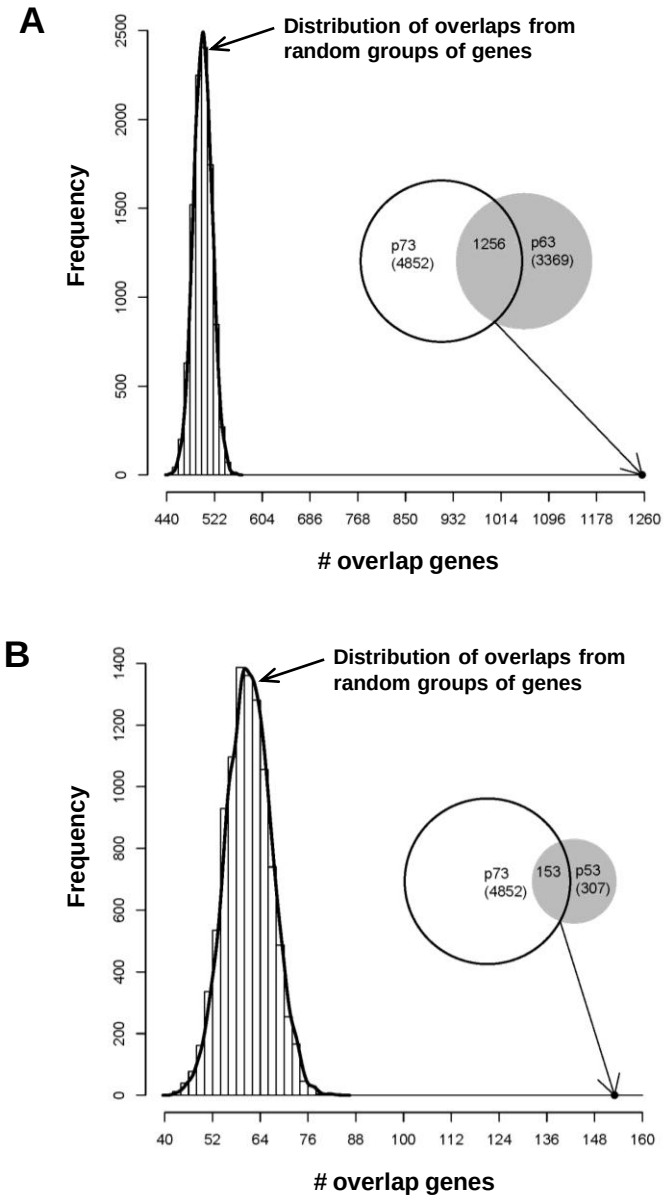

Figure 26: Regulation of common sets of genes by p53, p63, and p73. The observed overlap between p73-bound genes and A) p63-bound genes from Yang and colleagues (see text) or B) p53-bound genes Wei and colleagues (see text) is compared to the overlaps of 10,000 random groups of equivalent size. None of the random overlaps has a larger overlap than the observed data ($p < 0.0001$). Bootstrap analyses were performed by Aixiang Jiang and Yu Shyr.

To obtain a list of DNA-binding factors associated with p73-bound loci, we used the TRANSFAC and JASPAR databases of eukaryotic cis-acting regulatory DNA elements that contain a total of ~800 nucleotide distribution matrices (148). By searching for enriched motifs in p73-bound regions, 58 DNA-binding factors were found to have significant association with the p73 cistrome. As shown in Table 4, many of these factors are involved in tissue-specific functions such as neuron lineage specification, endocrine organ development, hematopoietic development, and muscle development. Interestingly, *p73*$^{-/-}$ mice suffer from a number of tissue-specific defects such as neuron cell death, loss of pheromone sensing, intestinal erosion, and immune cell infiltration (28).

Several cofactors show selective interaction with p73-bound loci in rapamycin-treated or untreated cells (Table 4). For example, Neuron Restrictive Silencing Factor (NRSF) is a transcription factor that binds to and represses neuronal genes in non-neuronal tissues (16). The NRSF motif was enriched in p73-bound loci, particularly in rapamycin-treated samples (Table 4). Because a comprehensive list of NRSF-bound genes was previously reported (16), we were able to identify genes bound by both p73 and NRSF. The overlap between NRSF and p73-bound loci was statistically significant when compared to 10,000 random groups of equivalent size (Figure 27A). Gene Ontology and KEGG analyses confirmed that NRSF and p73 co-associated genes are involved in neuron-specific processes such as axon guidance and neuropeptide hormone activity (Figure 27B). As more cistromes are identified and made publicly available, additional associations can be validated as we have done for NRSF and p73.

Table 4: Tissue-specific factors associated with p73-bound loci

DNA-binding factors with motifs over-represented in the p73 cistrome are organized by tissue-specific function (binomial test, $p<0.0001$). Marked factors have greater than 20% increased enrichment in rapamycin-treated samples, or greater than 20% decreased enrichment.

	Increase w/ rap	Decrease w/ rap
CNS/ Neuron lineage		
MYCN		
NRSF*	X	
TEAD2		
EGR2		
HEN1		X
ZIC2		X
Endocrine organ development		
PAX4		
PAX8	X	
GCM2	X	
Hematopoietic development		
RUNX1		
LMO2		
BACH2		
TAL1		X
MYB		
HOXA9		X
Muscle development		
MYF		
MYOD		
PAX3		
ELK1		
TEAD1	X	
ZEB1		

* Negative regulator of neurogenesis

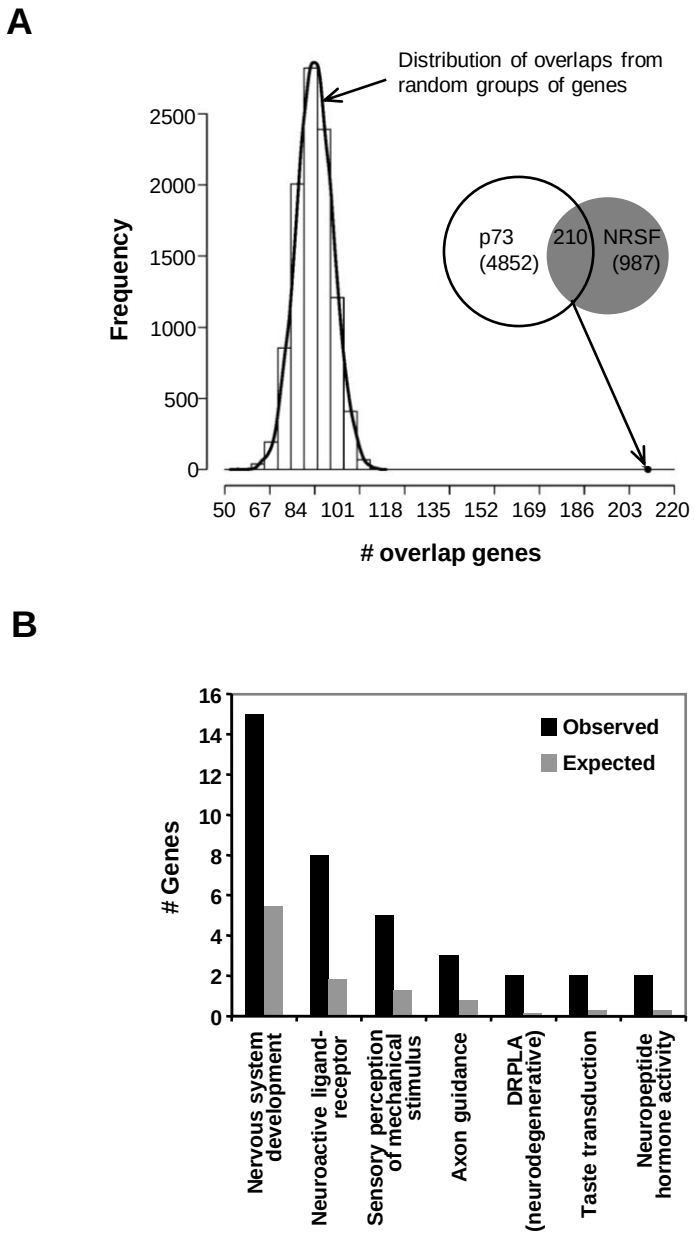

Figure 27: Tissue-specific transcription factors associate with p73-bound genomic regions. A) The observed overlap between p73-bound genes and NRSF-bound genes (from Johnson and colleagues, see text) is compared to the overlaps of 10,000 random groups of equivalent size. None of the bootstrap sampling results has a larger overlap than the observed data ($p < 0.0001$). B) Major nervous system processes are enriched among genes bound by both p73 and NRSF. The number of observed genes in the dataset is compared to the number of genes expected by chance for neuronal ontologies with $p < 0.05$ by hypergeometric test.

mTOR and p73 regulate the expression of genes, miRNAs, and ncRNAs

Microarray analyses were performed to determine which p73-binding sites are associated with transcriptional regulation by the mTOR-p73 axis. Rh30 cells were treated with vehicle or rapamycin as above. In addition, RNAi was used to deplete p73 to assess p73-dependence. Two different RNAi targeting sequences were used to deplete p73 in independent samples. One sequence depletes all p73 isoform mRNAs, and the other depletes only TAp73 mRNA. Knock-down of both TAp73α and TAp73β protein using these constructs was confirmed by Western blot in Chapter III.

Gene expression patterns using the two p73 RNAi constructs showed a high level of correlation (Pearson correlation coefficient r^2=0.996 in rapamycin-treated samples), and were treated as duplicates to calculate fold-change differences in expression. In Chapter III, we identified 12 genes that are transcriptionally activated by p73 when mTOR is inhibited. Consistent with those results, 118 transcripts in our whole-genome analysis were increased in a p73-dependent manner during mTOR inhibition. However, we were surprised to find that these genes were only a subset of those regulated by mTOR and p73. Figure 28 depicts these 118 transcripts (indicated as cluster B) combined with all genes that changed >50% with rapamycin treatment and/or p73 depletion. Clustering analysis reveals that 591 transcripts, which comprise an mTOR-p73 gene signature, segregated into discrete groups (Figure 28, clusters A-E). Cluster A contains transcripts that decreased after knockdown of p73 regardless of rapamycin treatment, including known targets of p73 such as *Mdm2* (81). Intriguingly, however, most genes in the signature increased rather than decreased after knockdown of p73, and thus were targets of p73-mediated repression (Figure 28, clusters C and D).

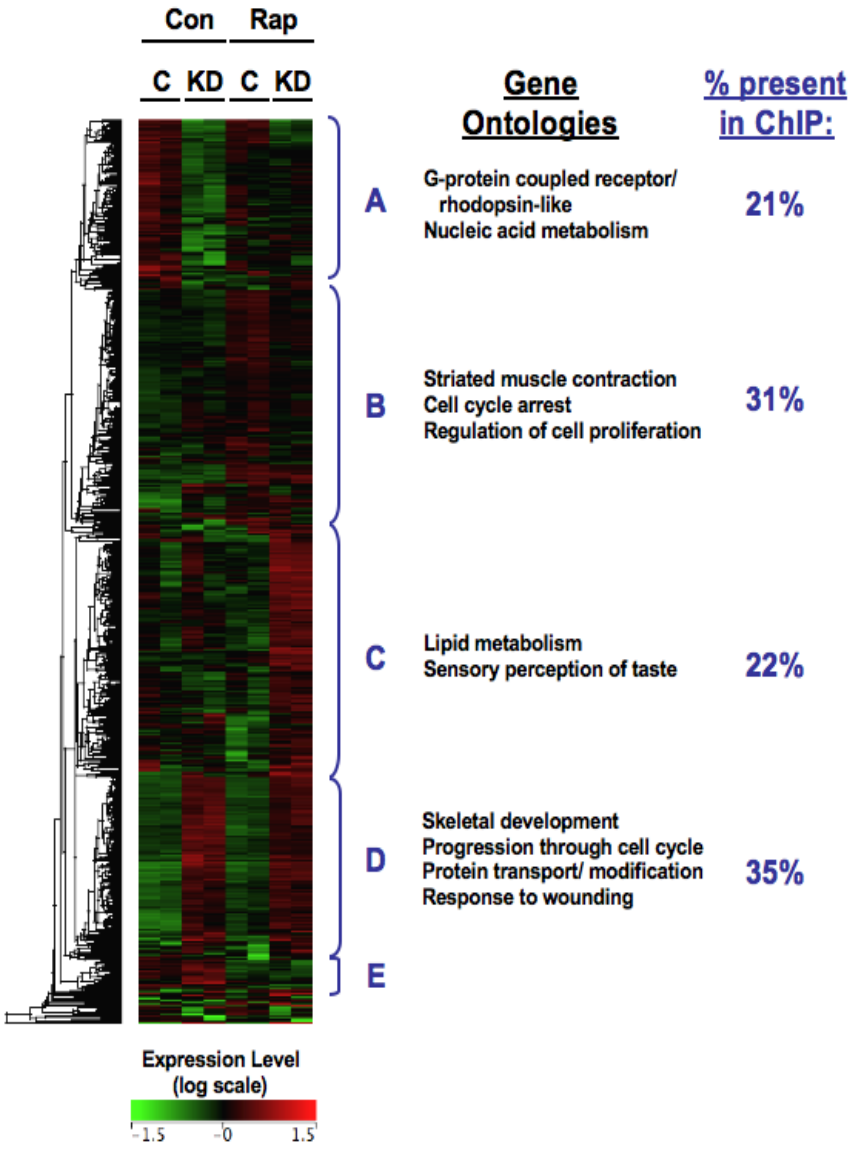

Figure 28: Genes regulated by mTOR and p73 display distinct patterns of regulation. Microarray analysis was performed in duplicate to assess gene expression patterns. Rh30 cells were transduced with lentivirus expressing shRNA targeting p73 (KD) or GFP (C) for 3 d, cells were treated with vehicle (C) or 40 nM rapamycin (Rap) for 24 h, and total RNA was harvested and hybridized to whole-genome oligonucleotide arrays. A total of 118 transcripts had p73-dependent log (expression level) increases > 20% after rapamycin treatment. These were combined with all transcripts that changed after either rapamycin treatment or p73 RNAi to create an mTOR-p73 signature of 591 transcripts. Hierarchical clustering reveals distinct groups of transcripts (A-E). Major gene ontologies (hypergeometric test, $p<0.05$) and the percentage of genes present in the ChIP-on-Chip dataset are indicated for each cluster. Cluster E was too small for additional statistical analysis.

This may be due to the presence of two isoforms of p73 in Rh30 cells, and is consistent with reports that domains exclusive to the TAp73α isoform prevent p73 from interacting with transcriptional co-activators (54). Cluster E contains transcripts regulated by mTOR alone, a group too small for additional statistical analysis (Figure 28). However, gene ontologies were used to functionally categorize the genes in the other four clusters (hypergeometric test, $p<0.05$).

Comparison of these p73-regulated genes to our ChIP-on-Chip database showed that 29% of p73-regulated genes were direct targets of p73. Interestingly, genes that were transcriptionally repressed by p73 contain a disproportionate number of genes with rapamycin-enhanced p73 occupancy (Figure 29). Thus, we generated a gene signature of the mTOR-p73 axis that has a highly modular architecture, demonstrating that p73 both activates and represses gene expression on a large scale. A comprehensive list of genes and ncRNAs directly regulated by p73 is presented in Table 5, and contains both known and novel p73 targets.

Finally, we addressed one class of transcript that is not covered by whole-genome oligonucleotide arrays: short miRNAs. p73 may regulate genes indirectly through direct modulation of miRNAs. Indeed, analysis of p73 ChIP data revealed p73 binding sites within 10 kb of 116 miRNAs (Table 6). Less is known about the regulatory regions of miRNAs than of genes. However, miRNA promoters were recently mapped across the human genome (217). We found that p73 bound within the promoters of eight of these miRNAs (Table 7). These data suggest that p73 could play an extensive role in regulation of gene expression through direct miRNA targets.

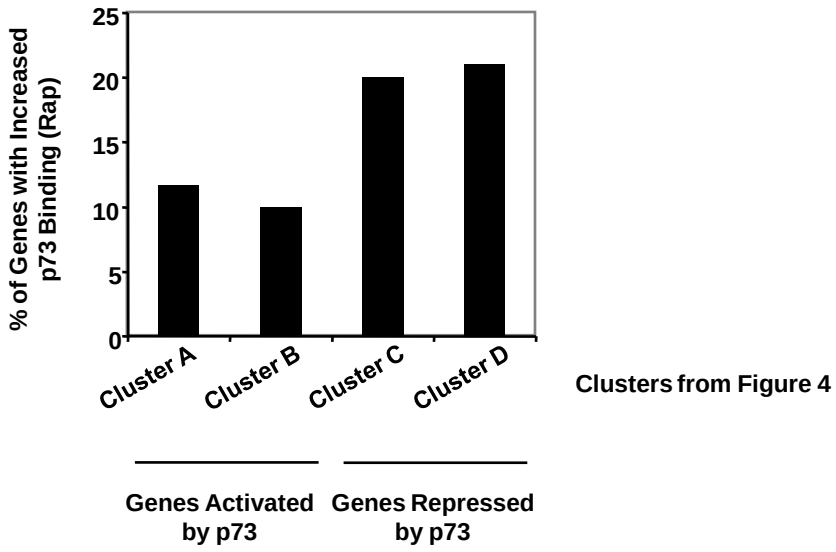

Figure 29: Analysis of p73-regulated gene clusters. Microarray analysis was performed in duplicate to assess gene expression patterns in Rh30 cells treated with p73 RNAi and/ or rapamycin. The percentage of genes in each cluster (from mTOR-p73 gene signature hierarchical clustering) to which p73 binding level increases > 50% after rapamycin treatment is plotted. Genes with expression repressed by p73 (clusters C and D) exhibit more frequent rapamycin-mediated inductions in p73 occupancy. (For comparison, 8.6% of total p73-bound loci exhibit increased occupancy after rapamycin treatment.)

Table 5: Genes and ncRNAs regulated by p73 and present in ChIP dataset

Organized by hierarchical cluster from mTOR-p73 microarray analyses

Affymetrix Transcript Cluster ID	Transcript Description or Gene Symbol
Cluster A	
7956989	MDM2
7918313	MYBPHL /// PSRC1
7920128	S100A11
7951593	FLJ45803
7970150	C13orf28
7980680	FOXN3
7997427	CMIP
8042346	FLJ16124
8050813	DNMT3A
8085393	TMEM40
8093997	SORCS2
8121794	SMPDL3A
8149953	ncRNA:snoRNA_pseudogene
7900350	ncRNA:tRNA_pseudogene
8085114	ncRNA:misc_RNA
Cluster B	
7935058	FER1L3
7942332	FOLR1
7945228	FLJ34521
7950235	STARD10
7952375	OR6M1 /// OR6X1
7957338	SYT1
7958377	BTBD11
7960654	ING4
7969677	MBNL2
7973314	OXA1L
7983630	FGF7
8030171	FTL
8036636	SIRT2
8077503	CAV3
8090098	MYLK
8095870	CCNG2
8099912	C4orf34
8100464	NMU
8115397	C5orf4
8116859	TMEM14C
8132055	C7orf41
8140534	SEMA3C
8146230	CHRNB3
8148059	DEPDC6
8149320	LOC157740
8152703	FBXO32
8156573	C9orf3
8179055	ZNRD1
8026292	pseudogene
8041642	ncRNA:snRNA_pseudogene
8124922	ncRNA:misc_RNA
8147038	ncRNA:scRNA_pseudogene

Affymetrix Transcript Cluster ID	Transcript Description or Gene Symbol
Cluster C	
7904414	HSD3B1 /// LOC440606
7904693	FLJ21272
7930559	hCG_1776259
7935776	PRO1933
7957835	NR1H4
8005446	LOC339240
8018860	EPR1
8074780	YPEL1
8106516	JMY
8124057	LOC728380
8135069	SERPINE1
8154563	ASAH3L
8157800	mir-181a-2
7924967	ncRNA:snRNA
7927773	ncRNA:snRNA
8025996	ncRNA:rRNA
8042466	snoRNA_pseudogene
8052231	ncRNA:snRNA
8099717	ncRNA:Mt_tRNA_pseudogene
Cluster D	
7910022	CNIH3
7915882	KIAA0494
7916928	ANKRD13C
7917649	TGFBR3
7924207	PTPN14
7930593	C10orf81
7934979	ANKRD1
7943998	NNMT
7946504	TMEM41B
7956867	HMGA2
7957759	APAF1
7959251	P2RX7
7965335	DUSP6
7970999	SPG20
7974870	SNAPC1
7975344	SLC39A9
7984259	RNU5B
7988467	FBN1
8009243	C17orf60
8024019	PTBP1
8032909	M6PRBP1
8046340	DYNC1I2
8047538	BMPR2
8052680	RAB1A
8057797	SDPR
8088979	VGLL3
8094460	RBPJ
8101429	PLAC8
8104234	TRIP13
8105585	RNF180
8112202	PLK2
8123744	F13A1
8124144	DEK
8132710	FLJ21075
8135218	LRRC17
8168622	KLHL4
8012854	snoRNA_pseudogene

Table 6: miRNAs within 10 kb of p73 binding sites

p73 binding sites were measured by ChIP-on-Chip. miRNAs whose expression levels changed >50% after p73 RNAi are indicated.

	Regulation by p73			Regulation by p73	
miRNA *	**Positive**	**Negative**	**miRNA** *	**Positive**	**Negative**
mir-200b			mir-453		
mir-200a			mir-485	x	
mir-429			mir-377	x	
mir-9-1			mir-656	x	
mir-205			mir-410	x	
mir-28			mir-369		x
mir-26a-1		x	mir-412		
mir-569			mir-409		
mir-128b	x		mir-541		
mir-568			mir-370	x	
mir-95			mir-376b		
mir-887			mir-376a-1	x	
mir-583			mir-300		
mir-580			mir-381		
mir-582			mir-654	x	
mir-548a-1			mir-376a-2	x	
mir-586			mir-368		
mir-206	x		mir-495	x	
mir-133b	x		mir-487b	x	
mir-590			mir-758	x	
mir-486_os			mir-323	x	
mir-151			mir-543	x	
mir-320	x		mir-494		
mir-601			mir-329-2	x	
mir-204			mir-329-1	x	
mir-24-1			mir-380	x	
mir-27b		x	mir-299		
mir-23b			mir-411	x	
mir-126			mir-379	x	
mir-602			mir-625	x	
mir-600			mir-190	x	
mir-505			mir-549_os		
mir-603			mir-193b	x	
mir-604			mir-365-1		
mir-606			mir-484		
mir-107			mir-634		
mir-146b			mir-21		
mir-125b-1			mir-744	x	
let-7a-2			mir-451		
mir-100			mir-144		
mir-611			mir-365-2		
mir-326			mir-193a	x	
mir-34b			mir-152	x	
mir-34c			mir-548d-2		
mir-619			mir-657		x
mir-620			mir-338	x	
mir-200c			mir-640		
mir-141			mir-7-3	x	
mir-616	x		mir-638		
let-7i	x		mir-330		
mir-623			mir-150		
mir-342			mir-645		
mir-382	x		mir-103-2	x	
mir-134			mir-1-1		
mir-496			mir-133a-2	x	
mir-154	x		mir-125b-2		
			let-7c		x
			mir-99a		
			mir-802		
			mir-648		

** organized by polycistron*

Table 7: miRNA promoters directly bound by p73

Chrom #	Promoter Start	Promoter End	miRNA	p73 binding level*	Nearby gene(s)+
5	59100080	59100279	miR-582	3.5	*PDE4E*
10	91395210	91395409	miR-107	7.6	*PANK1*
12	61282697	61282896	let-7i	3.7	*C12orf61*
12	93540063	93541288	miR-492	11.9	*TMCC3*
16	14309749	14312532	miR-365-1	3.7	*LOC10019781*
16	15643093	15645825	miR-484	18.9	*KIAA0430, NDE1*
17	76753312	76755359	miR-338	2.8	*NM_207389, KIAA0641*
17	76753312	76755359	miR-657	2.8	*NM_207389, KIAA0641*

* from the ChIP-on-Chip dataset
+ within 10 kb of the miRNA

Interrogation of 667 miRNA expression levels after rapamycin treatment and p73 depletion in Rh30 cells was performed using TaqMan Low-Density Arrays. p73 knock-down was performed with two different RNAi constructs. A total of 142 miRNAs were identified whose expression levels changed more than 50% with either p73 knockdown or rapamycin treatment. Unlike the p73-regulated genes in Figure 28, most of these miRNAs were transcriptionally activated by p73 (Figure 30A). In addition, 14 miRNAs were regulated by mTOR in a p73-dependent manner (Figure 30B).

We next mapped the 142 miRNAs that were modulated after p73 knockdown to p73-bound loci to identify direct miRNA targets. A total of 41 p73-regulated miRNAs were in the vicinity of p73 binding sites, and thus are likely directly regulated by p73, though in some cases this is due to the regulation of large polycistrons of miRNAs by p73 (Table 6). Of those miRNAs whose promoters were bound by p73 in Table 7, four were not expressed at detectable levels in Rh30 cells (miR-582, miR-107, miR-492, and miR-356-1), three were positively regulated by p73 (let-7i, miR-484 and miR-338), and one was negatively regulated by p73 (miR-657). Interestingly, both miR-338 and let-7i are associated with tumorigenesis, and let-7i regulates tumor cell chemosensitivity (218,219) in a manner reminiscent of p73 (220). As more regulatory regions of miRNAs are identified, additional annotation of p73 binding sites can be performed. These are the first miRNA targets of p73 to be identified.

p73-regulated genes classify rhabdomyosarcoma subtypes and are associated with differentiation of mesenchymal stem cells

Our genomic analyses gave us an unprecedented opportunity to explore p73 function using the mTOR-p73 gene signature.

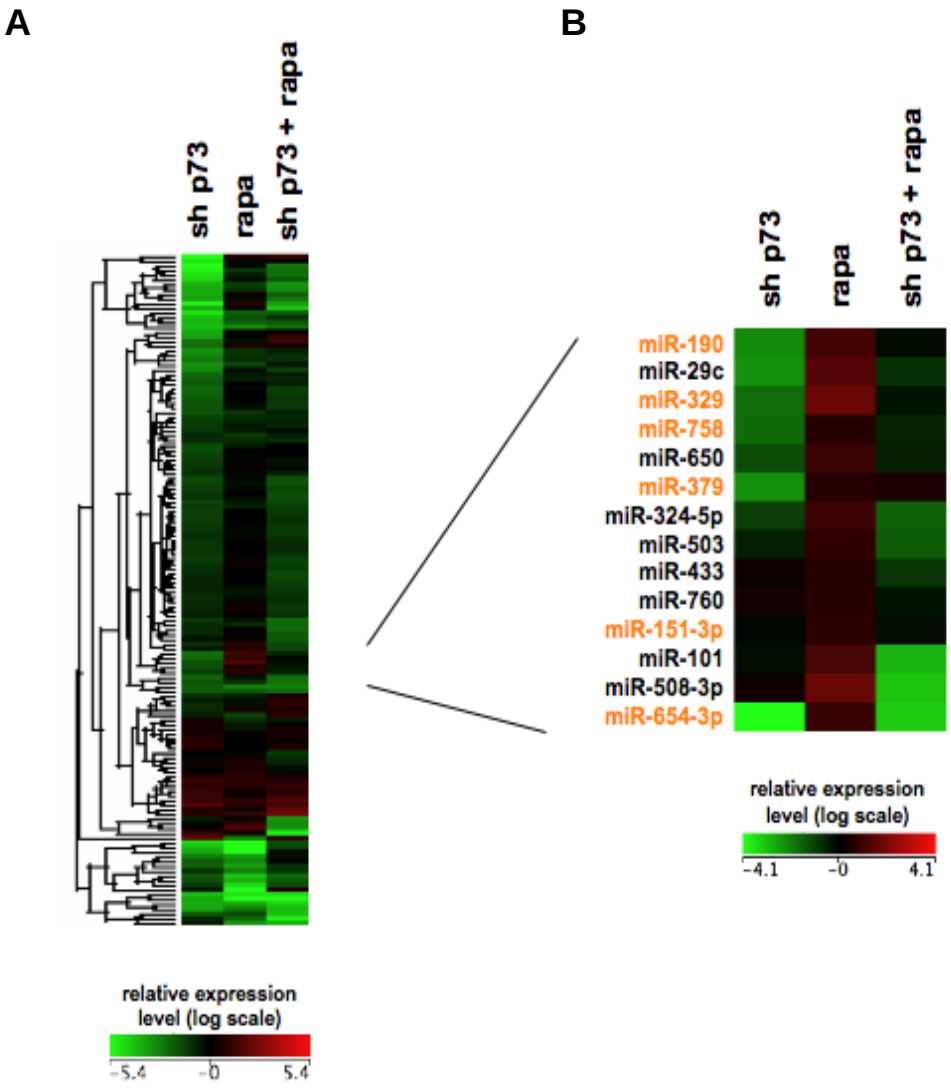

Figure 30: p73 regulates miRNA expression. A) Hierarchical clustering was used to segregate 142 miRNAs whose expression levels were regulated by mTOR or p73 into discrete groups. Mature miRNA levels were measured using TaqMan assays in Rh30 cells treated with p73 RNAi and/ or rapamycin, and the ΔΔCT method was used to calculate expression relative to control samples. B) A total of 14 miRNAs whose expression levels increase after rapamycin treatment in a p73-dependent manner are shown. Those miRNAs that are located within 10 kb of a p73 binding site are highlighted in orange text.

We were particularly intrigued by pathways enriched in p73-bound loci that are associated with muscle function and development (Table 8). p53, p63, and p73 play at least partially redundant roles in myogenic differentiation and rhabdomyosarcoma formation (159). Alteration of the p53 pathway, for example through a dominant-negative isoform of p73, can block skeletal muscle differentiation and promote transformation in vitro (159,221). The mTOR pathway, perhaps by acting upstream of p73, is a marker of rhabdomyosarcoma outcome (222).

We hypothesized that p73 leaves recognizable 'patterns' of gene expression in tissues in which it is active, allowing us to use our newly derived mTOR-p73 gene signature as a measure of p73 activity in rhabdomyosarcoma tumors. Wachtel and colleagues analyzed the gene expression patterns of 29 primary rhabdomyosarcomas (149). We filtered these data against the mTOR-p73 signature, and used hierarchical clustering to segregate tumors according to the status of the mTOR-p73 signature (Figure 31). The rhabdomyosarcoma patients segregated into two distinct clusters that were equivalent to the major rhabdomyosarcoma subtypes: alveolar and embryonal.

These two subtypes of rhabdomyosarcoma are associated with different outcomes, molecular alterations, age groups, and histologic appearances (223,224). While alveolar tumors (ARMS) are more common in older children and exhibit small round cells with primitive myoblast differentiation, embryonal rhabdomyosarcoma (ERMS) typically presents at an earlier age and is histopathologically analogous to embryonic skeletal muscle (223,224). We found that genes positively regulated by p73 (clusters A and B, Figure 28) were increased in ARMS (Figure 31). Conversely, genes transcriptionally repressed by p73 (clusters C and D, Figure 28) were decreased in ARMS (Figure 31).

Table 8: Muscle-related Biocarta pathways enriched among p73-bound genes ($p < 0.05^{+}$)	Enrichment Ratio*
Skeletal muscle hypertrophy is regulated via AKT/mTOR pathway	2.1
CUTL1	
IGF1	
IGF1R	
PPP2R4	
RPS6KB1	
EIF2B4	
Control of skeletal myogenesis by HDAC & calcium/calmodulin-dependent kinase (CaMK)	2.4
HDAC5	
CABIN1	
IGF1	
IGF1R	
INSR	
PPP3CA	
Actions of nitric oxide in the heart	2.6
CRAT	
PDE3B	
ACTA1	
BDKRB2	
TNNI2	
CAV1	
NFAT and hypertrophy of the heart (transcription in the broken heart)	2.0
CSNK1A1	
HBEGF	
GATA4	
IGF1	
LIF	
PPP3CA	
MAP2K1	
ACTA1	
RPS6KB1	
CAMK4	
Role of EGF receptor transactivation by GPCRs in cardiac hypertrophy	3.3
EGF	
EGFR	
FOS	
RHOA	
NFKB1	
PRKCA	
ADAM12	
ALK in cardiac myocytes	2.7
GATA4	
SMAD1	
SMAD5	
NPPB	
BMP5	
BMP7	
BMPR2	
TGFBR1	
TGFBR2	
TGFBR3	
AXIN1	
ACVR1	

+ calculated by hypergeometric test

* # observed genes in category / # genes expected by chance

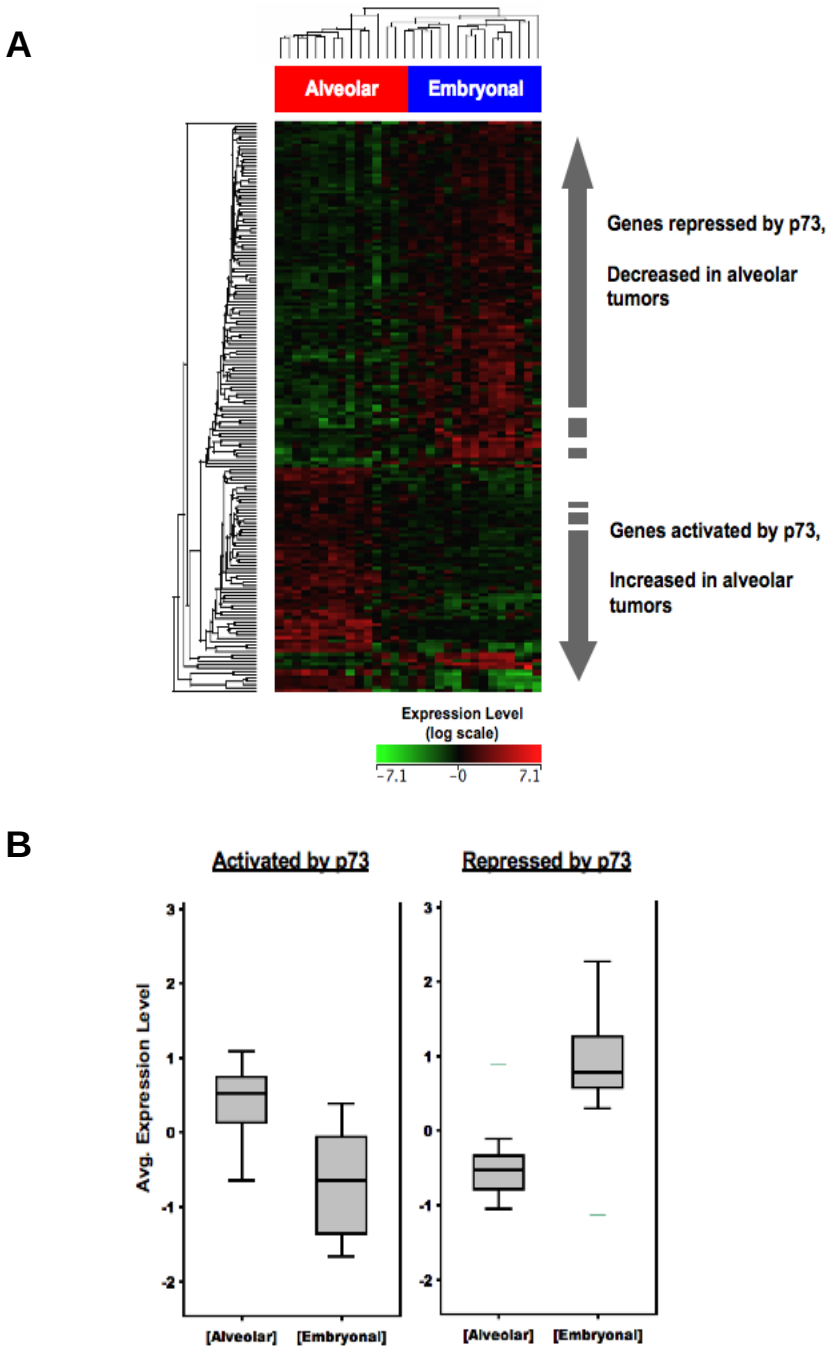

Figure 31: p73-regulated genes are differentially expressed in rhabdomyosarcoma subtypes. The mTOR-p73 gene signature was assessed using a publicly available dataset from Wachtel and colleagues (see text) in which 29 rhabdomyosarcoma tumors were profiled by microarray. A) All genes that changed >20% with rapamycin or p73 RNAi were included in this initial analysis to increase overlap across microarray platforms. Hierarchical clustering demonstrates that the mTOR-p73 gene signature segregates tumors into two classes, corresponding to the clinical alveolar and embryonal subtypes. B) Genes positively regulated > 50% by p73 and genes negatively regulated > 50% by p73 were analyzed in ARMS and ERMS subtypes. Box plots demonstrate opposing gene expression trends in these two tumor subtypes.

A similar effect was observed in an independent cohort containing 139 rhabdomyosarcoma patients, previously reported by Davicioni and colleagues (150) (Figure 32). As a control, we examined the ability of all genes (unfiltered) to segregate rhabdomyosarcomas and found that ARMS and ERMS were not segregated in either cohort as they were by p73-regulated genes. These data suggest that p73 is actively engaged in transcriptional regulation in the alveolar subtype that is associated with a worse prognosis.

Clinical outcome data was available for 134 rhabdomyosarcoma patients in the Davicioni *et al.* cohort (150). In this cohort we could identify genes in the p73 signature that correlated with 5-year survival after treatment for ARMS (Figure 33), but not ERMS (data not shown). Several of these p73 target genes were also associated with clinical outcome in an independent cohort of rhabdomyosarcomas deposited in the Oncomine database by De Pitta and colleagues (152). The four most significant genes, genes involved in muscle function, are plotted by survival outcome in Figure 34. These data strongly suggest a role for p73-regulated genes in ARMS disease progression.

We performed additional survival analyses by using the tumor expression levels of 17 direct p73 target genes, selected by t-test and shown in Figure 33 (orange text), to create a compound score model (described in Chapter II) that could segregate rhabdomyosarcoma patients into subgroups.

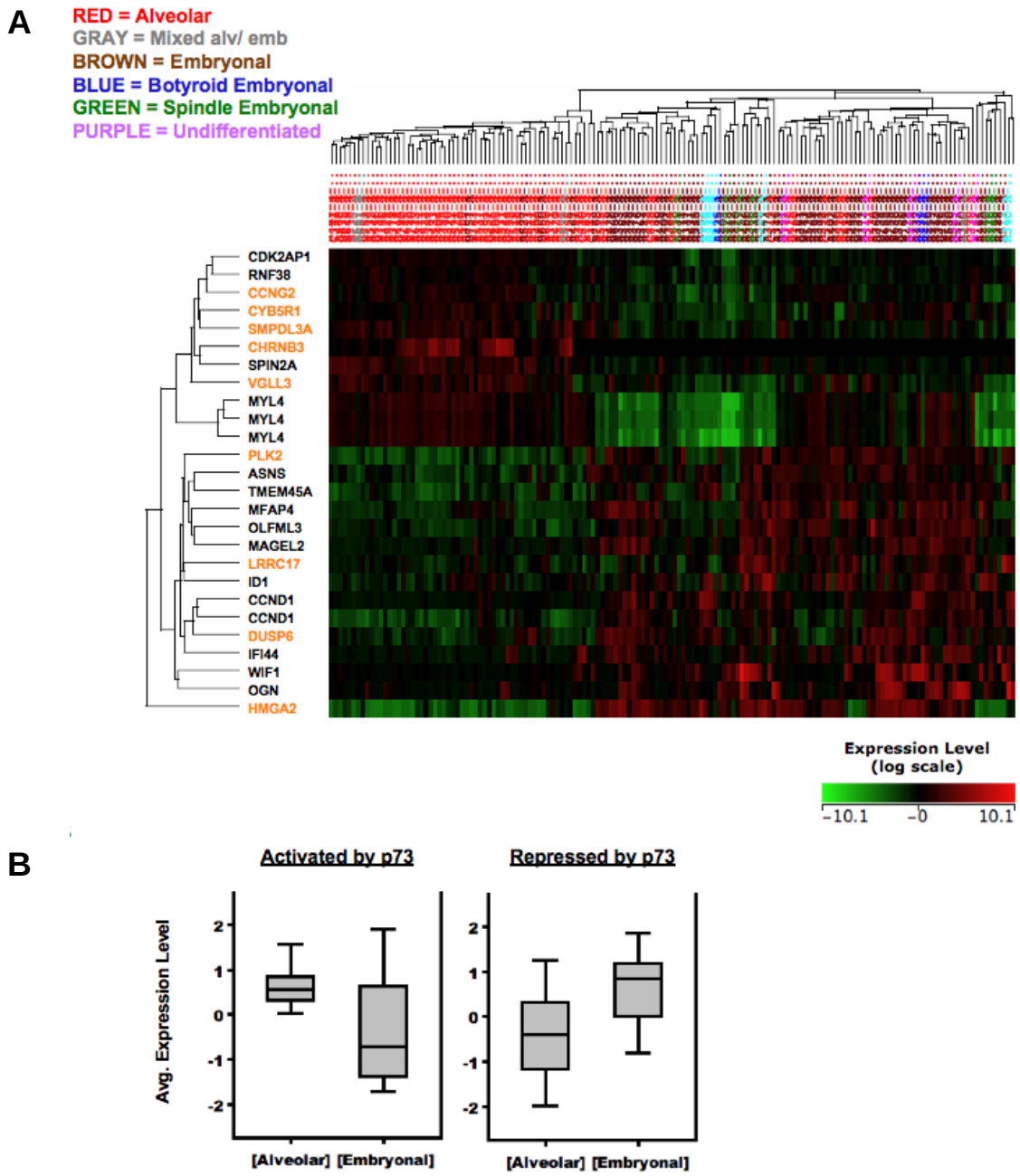

Figure 32: Differential expression of the p73 signature in an independent cohort of alveolar and embryonal rhabdomyosarcomas. The mTOR-p73 gene signature was assessed using a second publicly available data set, from Davicioni and colleagues (see text), in which 139 rhabdomyosarcoma tumors were profiled by microarray. A) Hierarchical clustering demonstrates that the mTOR-p73 gene signature segregates tumors into two classes, corresponding to the clinical alveolar and embryonal subtypes. (Botryoid and spindle tumors are subtypes of embryonal tumors.) Those p73-regulated genes that were most significantly associated with ARMS are shown. These 23 genes exhibit significant differential expression in the two subtypes (multiple testing-corrected p-value < 0.001, Fold Change > 2). Direct p73 target genes are highlighted in orange text. B) Genes positively regulated > 50% by p73 and genes negatively regulated > 50% by p73 were analyzed in ARMS and ERMS subtypes, demonstrating opposing gene expression patterns in these two tumor subtypes.

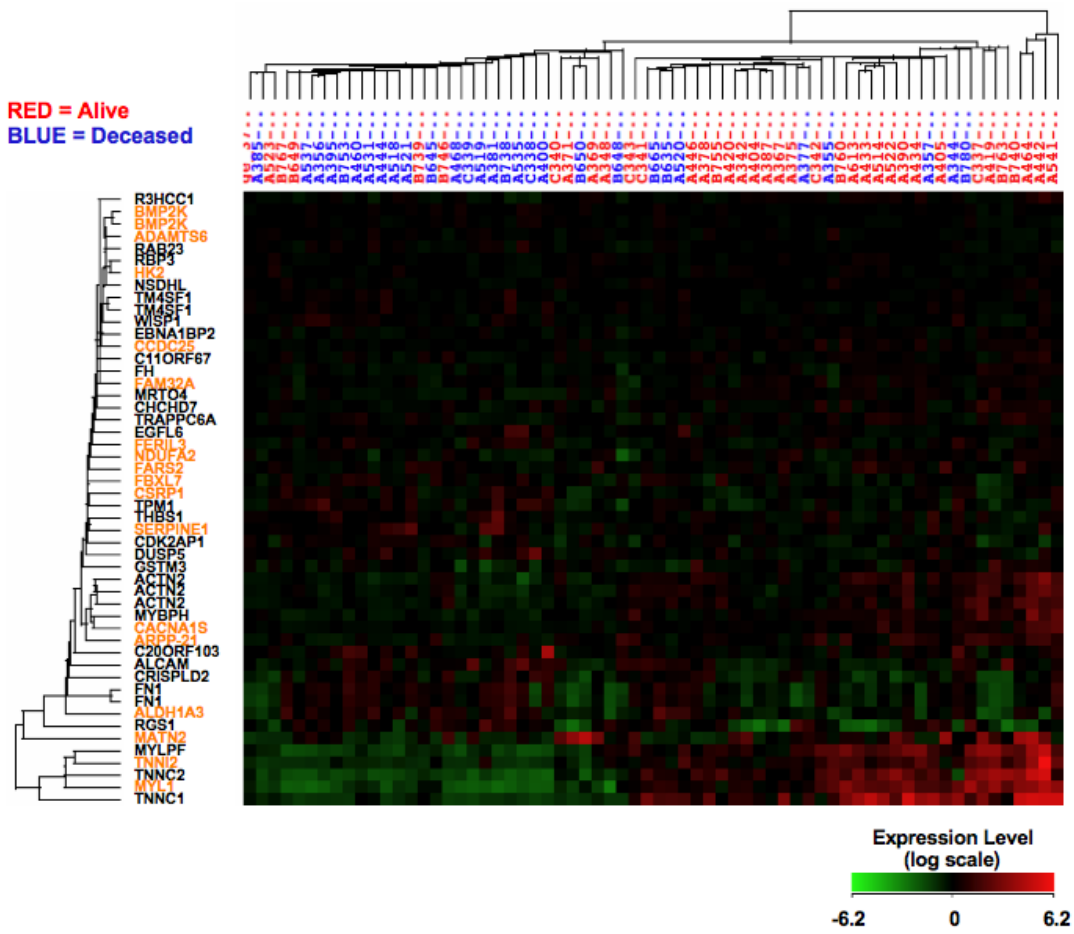

Figure 33: p73-regulated genes associated with clinical outcome in alveolar rhabdomyosarcoma patients. Alveolar rhabdomyosarcoma microarray data from Davicioni and colleagues were annotated by 5-year survival outcome (see text). In this cohort we could identify genes in our p73 signature that correlated with 5-year survival after treatment for ARMS. The probes in the p73 signature that exhibited the most significant association with clinical outcome (by Benjamini-Hochberg false discovery rate t-test) are shown by gene. Hierarchical clustering was performed with these probes, leading to partial segregation of tumors from alive and deceased outcomes. Genes present in the p73 ChIP-on-Chip dataset are indicated in orange text.

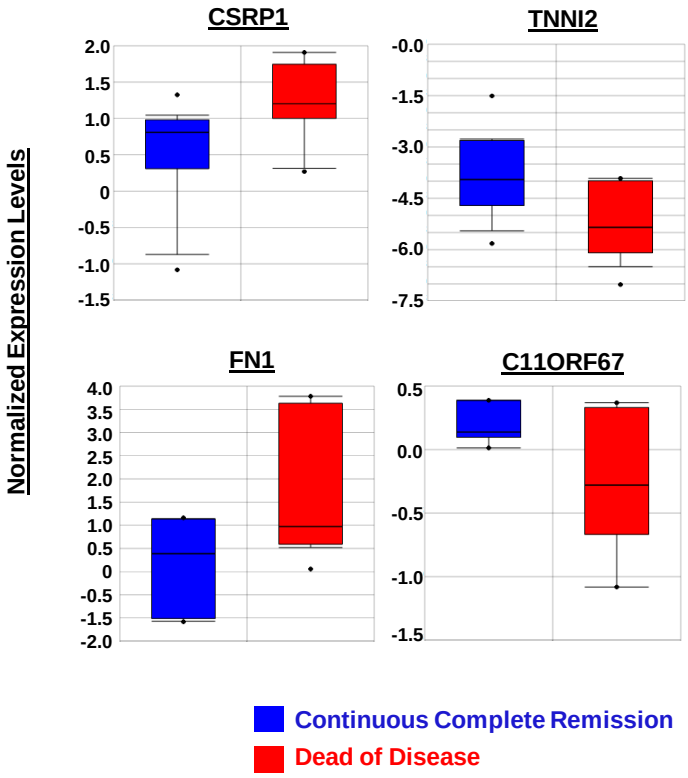

Figure 34: p73-regulated genes associated with clinical outcome. Additional data for a limited number of genes in our signature were available in the Oncomine database, using a third independent rhabdomyosarcoma cohort deposited by De and colleagues (see text). Two direct targets of p73, CSRP1 and TNNI2, and two indirect targets of p73, C11ORF67 and FN1, were the most significant p73-regulated genes associated with clinical outcome from those in both the Davicioni and De cohorts. Box plots for the four indicated genes demonstrate association with clinical outcome ($p < 0.05$) in the latter cohort. These plots were derived using the Oncomine data-mining tool.

Alveolar tumors with a low compound score for p73 target genes were associated with a 5-year survival rate of ~85%, whereas tumors with a high compound score were associated with a 5-year survival rate of ~20% (Figure 35). In contrast, there was no significant difference in survival from ERMS based on these genes. Thus, genes in the p73 signature influence clinical outcome, suggesting that the mTOR-p73 axis plays a role in ARMS pathogenesis.

We hypothesized that this role could be related to functions of p73 during myogenic differentiation (159). Supporting this hypothesis, genes in the p73 signature were differentially expressed in undifferentiated rhabdomyosarcoma tumors compared to other subtypes (Figure 36). We sought additional, more global data supporting a role for p73 as a major regulator of cellular differentiation. We took advantage of a recent observation that developmental genes are marked by two histone modifications (H3K4me3 and H3K27me3 – a bivalent mark) in embryonic stem cells (20). These findings were extended when histone methylations were mapped across the entire human genome (225,226). Genes generally fall into three categories: those that are modified by H3K4me3 and play a role in proliferation, metabolism, or housekeeping, those that are bivalently marked and are developmental, and those that are not marked at all and are lineage-specific (225,226). We hypothesized that if genes can be generally classified in this fashion, then transcription factors might be generally classified based on the genes that they regulate. Indeed, we found that both p73-bound genes and genes regulated by p73 at the expression level were highly associated with the bivalent category, as indicated by p-value in Table 9. These data supported the hypothesis that p73 plays a role in development through the transcriptional programs that it regulates.

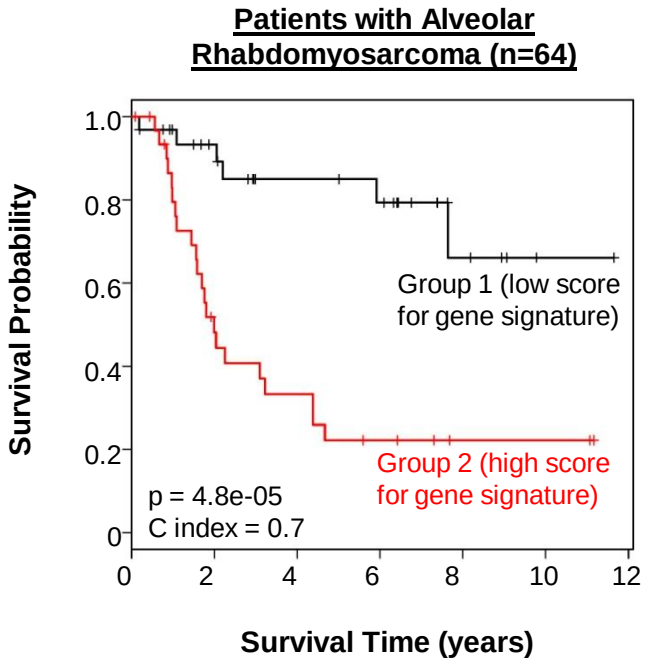

Figure 35: A 17-gene p73 signature segregates patients by clinical outcome. The expression levels of 17 direct p73 target genes were used to segregate an independent cohort of 64 ARMS patients into two groups, using Cox proportional hazards modeling and Kaplan-Meier analysis. This 17-gene p73 signature segregates patients with alveolar but not embryonal tumors by clinical survival time (see Chapter II for additional methodology). Statistical analysis was performed by Aixiang Jiang and Yu Shyr.

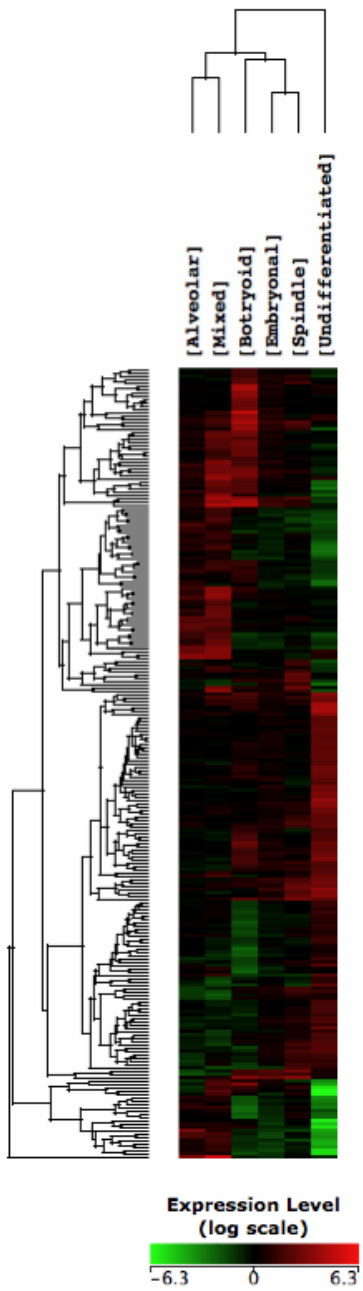

Figure 36: p73-regulated genes associated with undifferentiated rhabdomyosarcoma tumors. A total of 139 rhabdomyosarcoma tumors profiled by microarray by Davicioni and colleagues, were grouped by histology. The p73 signature was assessed for average expression level in each of these tumor subtypes (alveolar, mixed alveolar & embryonal, botryoid, spindle, embryonal, and undifferentiated). From among mTOR and p73-regulated probes, 239 probes were identified that exhibit a fold change > 5 in undifferentiated versus other tumor subtypes and used for hierarchical clustering.

Table 9: Gene categories defined by epigenetic marks

	H3K4me3 only	Bivalent	No Marks
gene #	7539	1295	3505
All ChIP-on-Chip Genes*	$p = 8.9 \times 10^{-10}$	$p = 1.7 \times 10^{-10}$	p = 0.01
gene #	1969	317	548
All p73-regulated genes*	p = 1.0	$p = 1.3 \times 10^{-9}$	$p = 7.0 \times 10^{-10}$
gene #	110	21	59
Cluster A*	p = 0.99	p = 0.080	p = 0.029
Cluster B	p = 0.029	p = 0.58	p = 0.40
Cluster C	p = 1.0	p = 0.83	p = 0.95
Cluster D*	$p = 8.1 \times 10^{-8}$	p = 0.19	p = 0.29

* significant associations are highlighted
(hypergeometric test)

We explored this concept further with a focus on differentiation associated with ARMS. Studies of molecular translocations in ARMS provide growing evidence that mesenchymal stem cells (MSCs) are the cell of origin for this tumor subtype (223). This is in contrast to ERMS, where committed muscle progenitor cells are thought to be the cell of origin (223). Thus, we decided to analyze the fate of p73-regulated genes during MSC differentiation. MSCs can be induced to differentiate along the myogenic lineage by treating them with 5-azacytidine (5AZA) (227,228). We identified a group of p73 target genes, both direct and indirect, whose expression levels changed during MSC differentiation (corrected p-value < .05, Figure 37A). Interestingly, the expression of many direct p73 target genes changed more than 50% during myogenic differentiation, or during myofibroblast-like differentiation induced by tumor conditioned medium (TCM) (227) (Figure 37B). This suggests that a conserved set of genes are altered during mesenchymal differentiation programs.

To gain greater insight into the roles such transcriptional programs might play during rhabdomyosarcoma tumorigenesis, we sought a minimal set of p73 target genes that correlate with both differentiation status and rhabdomyosarcoma subtype. We identified nine direct p73 target genes from among those regulated by 5AZA in Figure 37 that are sufficient to segregate alveolar and embryonal rhabdomyosarcoma subtypes (Figure 38A). A Support Vector Machine model derived from these nine genes was able to predict alveolar subtype in a cohort of rhabdomyosarcoma tumors with an accuracy of ~82%. These nine genes include potential tumor suppressors (*FBLN1*, *DUSP6*, *KLF6*, and *CCNG2*) and genes with documented expression in mesenchymal tumors (*OXTR*, *FAM129A*, *NMI*, and *HMGA2*) (229-236).

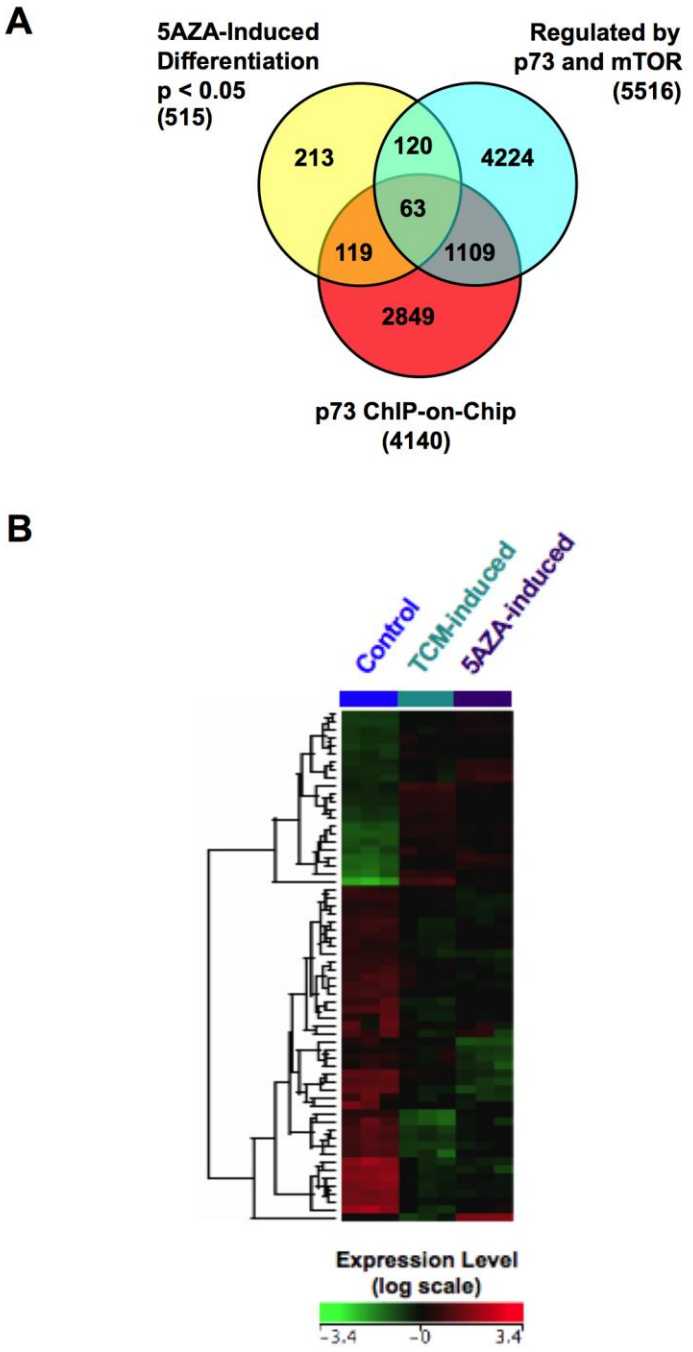

Figure 37: Genes regulated during mesenchymal stem cell differentiation. A) p73/mTOR-regulated genes, p73-bound genes (ChIP-on-Chip), and genes significantly altered during 5-azacytidine (5AZA)-induced myogenic differentiation of MSCs (multiple testing corrected p-value < 0.05) were compared. MSC microarray data was publicly available from Mishra and colleagues (see text). The Venn diagram shows the number of Affymetrix probes in each category. B) p73-regulated transcripts were identified from (A) that change more than 50% during differentiation of MSCs in response to two different stimuli: Tumor Conditioned Medium (TCM) and 5AZA. Hierarchical clustering of MSCs before and after differentiation is shown.

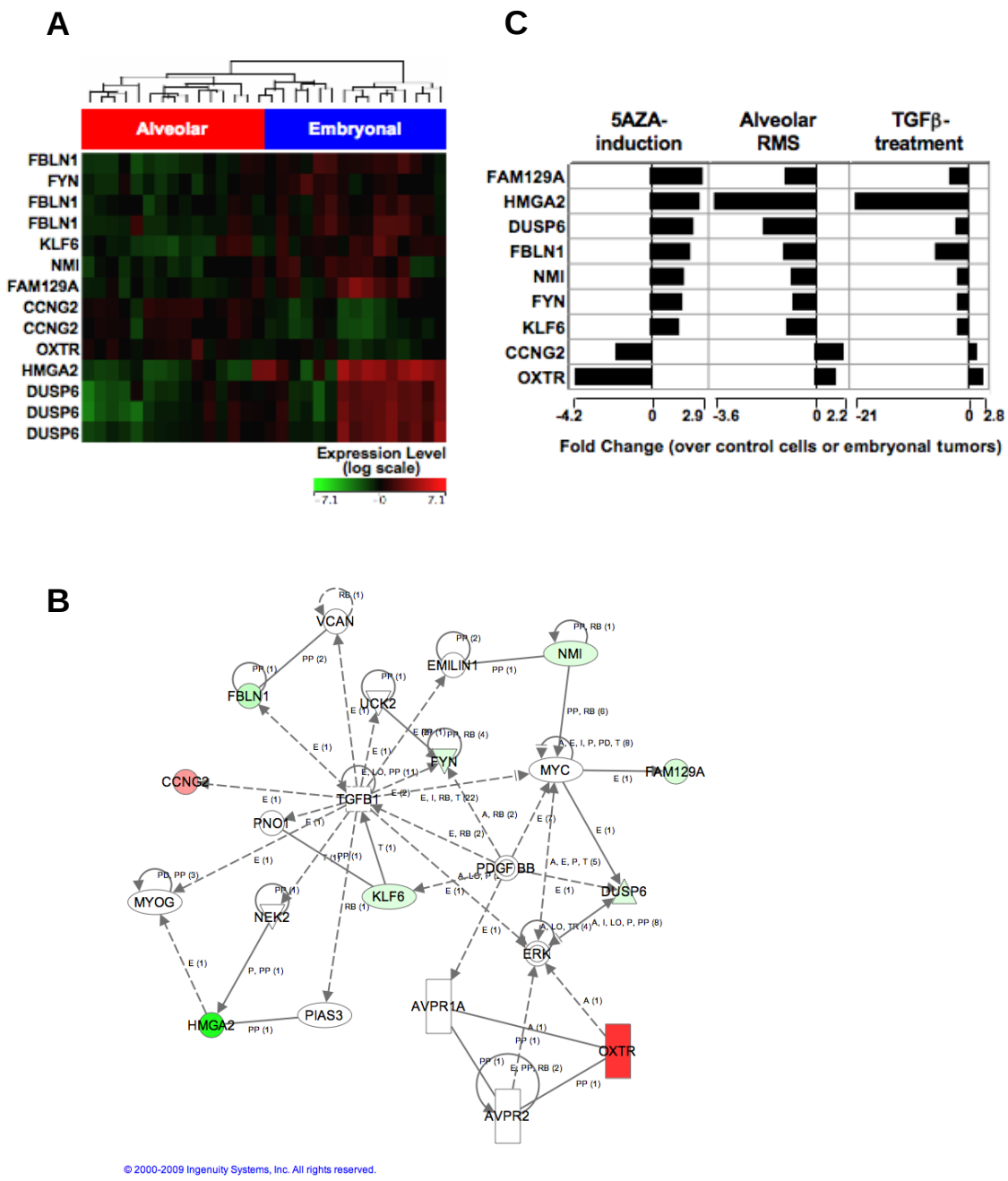

Figure 38: Conserved patterns of p73 target genes in mesenchymal processes. A) A core set of nine direct p73 target genes from those regulated by 5AZA was sufficient to segregate ARMS and ERMS by hierarchical clustering. These nine genes were identified from among those regulated during MSC differentiation. B) Ingenuity software was used to identify literature-based connections between the nine genes. In the Ingenuity network, these genes are colored by expression level in TGFβ-treated MSCs relative to control. C) Fold changes are indicated in three bar charts for: 5AZA-treated MSCs relative to control (left panel), ARMS relative to ERMS (middle panel), and TGFβ-treated MSCs relative to control (right panel). TGFβ microarray data was obtained from Sachetti and colleagues (see text).

Interestingly, an Ingenuity network connects all nine p73 target genes to the transforming growth factor β (TGFβ) signaling pathway, with at most one degree of separation between TGFβ and each gene (Figure 38B).

We analyzed these nine genes further by comparing fold changes in expression after MSC differentiation, and in alveolar versus embryonal tumors (Figure 38C). We also examined the expression levels of these genes after treatment of MSCs with TGFβ, a known inhibitor of MSC proliferation and differentiation (237,238) (Figure 38C). Patterns of gene expression during these three mesenchymal processes suggest a common mechanism of regulation.

Interestingly, many genes indirectly regulated by p73 were also associated with mesenchymal differentiation (120 genes, Figure 37A). p73 might regulate the expression of these genes through direct regulation of miRNAs. Three miRNAs with established roles in myogenic differentiation, miR-133b, miR-133a-2, and miR-1-1 (239), mapped to p73-bound loci. These three miRNAs are upregulated in certain human sarcomas including ARMS (240). miR-133b was the closest of the three to a p73 binding site (~5 kb upstream of miR-133b transcriptional start site). We used real-time PCR and three different p73 RNAi constructs to confirm that p73 regulates miR-133b expression levels in Rh30 cells (Figure 39). Taken together, these data strongly suggest that p73 regulates transcriptional programs common to both MSC differentiation and rhabdomyosarcoma tumorigenesis.

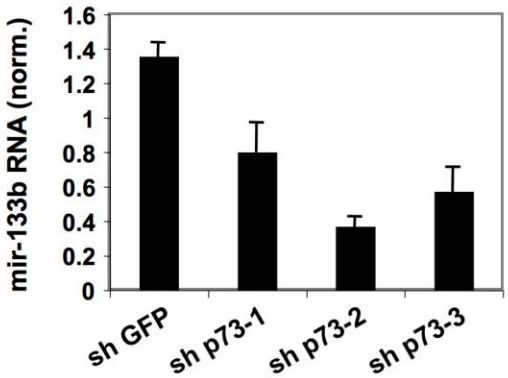

Figure 39: p73 regulates miR-133b levels. qRT-PCR analysis of mature miR-133b levels was performed in Rh30 cells treated with lentivirus expressing control RNAi (sh GFP), or three different RNAi constructs that target p73 (sh p73-1, 2, and 3), normalized to RNU19 levels. Error bars represent standard deviations from three independent experiments.

Discussion

Herein we demonstrate that, like p53 and p63, p73 exhibits complex patterns of binding and activity across the genome. In addition, we show that mTOR modulates p73 occupancy in a selective, locus-specific manner. While p73 has affinity for a particular 20 bp DNA motif, this only loosely defines the boundaries of the p73 cistrome. Numerous cofactors associate with p73-bound loci, and likely serve as additional determinants of transcriptional specificity. These interactions provide the potential for exquisite control of p73 binding, and are both regulated by mTOR, and restricted to specific tissues and cell lineages. The end product of this intricate regulation is the expression of genes and ncRNAs, for which we demonstrate functional significance through analysis of MSC differentiation and rhabdomyosarcoma tumorigenesis.

Generation of a p73 genomic binding profile

Unlike previous studies of p73 binding, we used ChIP-on-Chip to obtain a comprehensive view of p73 occupancy (144,155). The advantages of this technique include reproducibility, and avoidance of potential biases in some sequencing-based technologies (14). In addition, previous analyses of p73-bound loci relied on ectopic p73 expression (144,155), and over-expressed transcription factors can bind inappropriately to DNA, titrate inhibitors, and inappropriately alter cellular signaling pathways. Here, we focused on endogenous p73, using the following methods to ensure specificity: 1) use of an antibody that recognizes only 'active' isoforms of p73, 2) validation with two additional p73 antibodies, 3) analysis of a cell line with robust p73 binding, and 4) perturbation with a stressor that engages the p73 signaling pathway.

p73 regulates genes and miRNAs associated with mesenchymal phenotypes

We coupled our ChIP data to microarray analyses, in essence mapping regions of transcriptional activity to p73-bound loci. We hypothesized that p73 leaves recognizable 'patterns' of gene expression in tissues in which it is active. p73 is frequently over-expressed in human cancers (54); however, in some tumor types p73 is over-expressed concomitantly with a protein inhibitor that prevents it from functioning (37). The ability to detect a p73 signature is thus critical for measuring p73 activity in tumors in which it is expressed.

Based on this concept, we determined that p73 is functional in ARMS, using two independent cohorts of patients. This disease is characterized by cells that have both engaged a myogenic program and experienced a differentiation block (223,224). We analyzed gene expression patterns in MSCs, the likely cell of origin of ARMS. p73 directly regulates a set of nine target genes that are involved in both MSC differentiation and rhabdomyosarcoma tumorigenesis, suggesting a common role in both processes.

The p73 cistrome can be used to expand on previous studies of p53 family members in myogenic differentiation. For example, in one study an inhibitory isoform of p73 was over-expressed in a mouse myogenic cell line undergoing differentiation (159). By microarray, this p73 isoform modulated the expression of a large number of genes; however, due to lack of information on the p73 cistrome the authors were unable to identify which of these genes were direct targets (159). By mapping the mouse genes in this microarray study to human orthologs, and comparing them to the p73 cistrome, we were able to identify 76 target genes that are directly regulated by p73 in this system.

In addition to genes, several miRNAs involved in mesenchymal differentiation and tumorigenesis are present in the p73 cistrome (e.g. miR-1-1, miR-133a-2, and miR-133b), suggesting extensive regulation of the mesenchymal transcriptome by p73. Work from our laboratory has shown that p63 is not only a master regulator of epithelial phenotype, but also inhibits genes that are normally expressed in mesenchymal tissues (131,241). Our data suggest that this may occur through inhibition of p73 in mammalian cells. Consistent with a role for p73 in regulating mesenchymal phenotype, we identified a number of genes in the p73 cistrome associated with epithelial-to-mesenchymal transition (Figure 40) (242). Thus, p73 may regulate mesenchymal programs both in human sarcomas and in epithelial tumors that have transitioned to an invasive state.

Clinical utility of p73 transcriptional programs

p73 can be engaged to activate p53 apoptotic pathways in tumor cells that have mutated p53 (161), thus there has been substantial interest both in drugs that target p73, and in potential prognostic markers of p73 activity (128). We have shown that mTOR inhibition induces p73 and selectively alters the p73 cistrome. Even more striking, the majority of transcriptional changes that followed rapamycin treatment were dependent on p73. mTOR inhibitors are currently in clinical trials for a number of human cancers, and it will be interesting to see if these drugs activate p73, or synergize with other drugs that can activate p73.

A

Transcription Factors	Biomarkers	miRNAs	Other
PSIP1	E-cadherin	hsa-mir-7-3	TGFβ receptors
FSIP1	N-cadherin	hsa-mir-200c	Wnts
LGL2	WNT2		MMPs
ZEB2	SPARC		EGF
SNAI2	SPARCL1		IGF1
FSP1			PDGFC
			PDGFD

BioCarta Pathways (hypergeometric test, p<0.05)

Integrin
HGF
EGF
CXCR4
TNFR1
Rho cell motility
PDGF
Rac1 cell motility
IGF-1
AKT
TGFβ
Insulin
mTOR
TNFR2
Cell to cell adhesion
Inhibition of MMPs

B

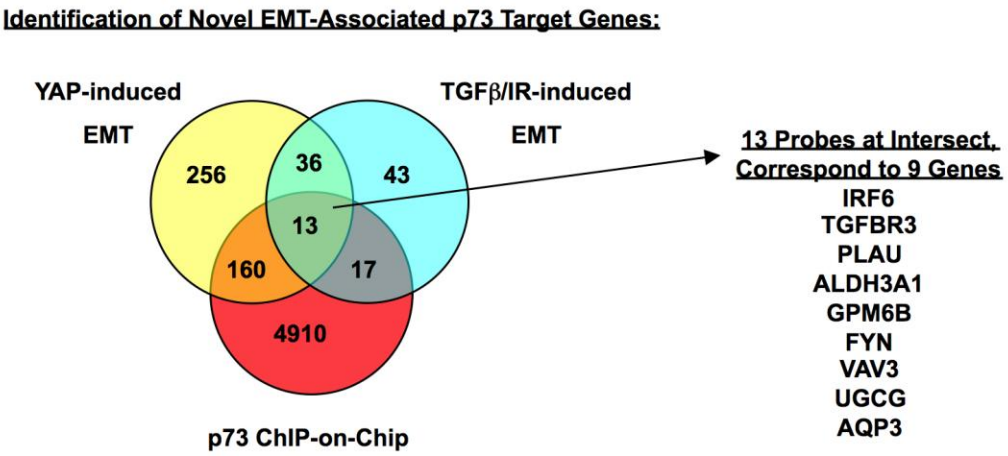

Figure 40: p73-regulated genes associated with epithelial-to-mesenchymal transition (EMT). A) Genes and pathways enriched in the p73 cistrome that are associated with EMT, from those listed in the review by Sabbah and colleagues (242). B) Subsets of the p73 cistrome are associated with EMT transcriptional programs, as identified using publicly available microarray datasets (302,303) during which MCF10A cells were subjected to YAP over-overexpression, or TGFβ and ionizing radiation treatment, resulting in induction of EMT.

We have developed an mTOR-p73 gene signature, demonstrated that p73 is active in certain human sarcomas, and importantly, shown that p73 target genes influence clinical outcome. Because p73 is not mutated in tumors, key to a p73-based treatment approach will be the ability to predict response based on the isoforms of p73 that are present, the modifying proteins that are inhibiting its activity, and the other p53 family members that are interacting with it in any given tumor. The complexity of p73 in cancers makes it particularly amenable to using gene signatures as biomarkers of its activity. Such signatures might find utility in the molecular profiling of sarcomas and other tumor types for therapeutic decision-making.

CHAPTER V

METABOLIC FUNCTIONS OF P73

Introduction

One function of mTOR is to regulate the bulk degradation system, autophagy, which occurs through the concerted, step-wise efforts of a number of proteins that are conserved from yeast to man. First, an isolation membrane forms to engulf cytoplasmic material and organelles into a phagophore. This process is often initiated through inhibition of mTOR. This inhibition results in dephosphorylation of the regulatory subunit Atg13, allowing Atg13 to associate with the kinase Atg1/ULK1 and stimulate its kinase activity, leading to initiation of phagophore nucleation (243). One of the first steps in vesicle nucleation involves phosphorylation and activation of the class III phosphatidylinositol 3-kinase Vps34. Vps34 activation depends on a multiprotein complex including Beclin-1 and its cofactors such as UVRAG and Bif1 (243).

Elongation of the phagophore results in complete engulfment of the cytoplasmic materials into a double-membraned vesicle called the autophagosome. This is accomplished by a ubiquitin-like conjugation system. Although the enzymes in this system resemble E1, E2, and E3 ubiquitin ligases, they typically only have one or a limited number of substrates in the autophagy pathway. First, ubiquitin-like Atg12 is covalently conjugated to Atg5 through the activities of the E1-like enzyme Atg7 and the E2-like enzyme Atg10. In parallel, phosphatidylethanolamine is conjugated to ubiquitin-like LC3/Atg8 after protealytic cleavage of LC3 by Atg4, through the activities of the E1-

like Atg7, the E2-like Atg3, and the Atg12-Atg5-Atg16 complex which has E3-like activity (244,245).

Of note, there are additional mammalian homologs of LC3 such as GATE-16 and GABARAP that may be associated with autophagosome membranes in specific contexts. For example, GABARAP-phospholipid conjugates are activated during myoblast differentiation (246). Lipidated LC3 is inserted into the developing autophagosome membrane, and can be used as a marker to detect autophagy, because the lipid moiety causes faster electrophoretic mobility on a gel and exhibits a distinctive puncate distribution in cells undergoing autophagy. The final stage of autophagy is fusion of the autophagosome with a lysosome to form an autophagolysosome, in which the engulfed components as well as the inner membrane are degraded.

The above cascades allow rapid regulation of autophagy at the protein level. However, gene expression changes are also associated with autophagy (144,247,248). The mechanisms by which transcription is regulated during and to induce autophagy are largely unknown, thus there is interest in identifying transcription factors associated with autophagic processes.

Discoveries linking p53 to autophagy, and to core metabolic pathways, marked a shift in our understanding of p53 as a tumor suppressor. p63 and p73 likely coordinate with p53 during select cellular responses to environmental and developmental cues (37). All three p53 family members are subject to a variety of post-translations modifications and can exist as multiple protein isoforms, so there is the potential for substantial complexity in the p53 family transcriptional response (37,54,98). Indeed, each family member can regulate thousands of target genes (13,82,86).

In Chapter III genome-wide technologies were used to identify a p73 gene signature. This signature was compared to pathway-associated gene signatures in the Broad Institute Connectivity Map (143,144). Using this approach, mTOR was identified and validated as a negative regulator of p73 (144). Further analysis of subcomponents of the p73 gene signature revealed autophagy-associated genes that were regulated by mTOR in a p73-dependent manner (144). In addition, a reported link between p73 and autophagy was confirmed, and a transactivation-competent isoform of p73 was identified as a positive regulator of autophagy (144,185).

These data suggest that there are both similarities and differences between p53 and p73 in relation to mTOR. While our data showed that mTOR negatively regulates p73, in multiple contexts mTOR is a positive regulator of p53 (119,126). Consistent with these observations, we observed a simultaneous increase in p73 and decrease in p53 and p63 protein levels in primary human mammary epithelial cells treated with rapamycin (144). Of note, at least in some basal cell types, p63 is expressed as an isoform that can inhibit p73 (37,57). Thus, a coordinate upregulation of p73 and downregulation of p63 may be needed to fully activate p73 in response to metabolic stress. Given the critical role of mTOR as a regulator of autophagy, we hypothesized that analysis of the mTOR-p73 gene signature generated in Chapter IV would identify additional target genes involved in both autophagy and cellular metabolism.

Results

mTOR regulates autophagy-associated genes downstream of p73

We first explored potential mechanisms by which p53 family members engage metabolic stress responses such as autophagy. p53 itself plays opposing roles (125,126). Cytoplasmic p53 inhibits autophagy in multiple cell types and organisms (126). Nuclear p53 activates autophagy by upregulating genes such as DRAM (125). The cytoplasmic function of p53 is a basal activity of p53, while the nuclear function of p53 seems to require activating signals such as genotoxic stress (125,126). In addition, p53 can act upstream of mTOR, inhibiting mTOR by activating AMPK (96,116), and this may alter cellular autophagy levels as well.

Like p53, transactivation-competent p73 isoforms can activate autophagy, presumably through nuclear activity (185). However, the upstream signals that regulate p73 to do so, and the target genes that mediate autophagy downstream of p73 have been largely unknown. Unlike p53, p73 induces autophagy in a DRAM-independent manner (185). In addition, it is unknown whether p73 translocates to the cytoplasm to regulate autophagy as p53 does.

To explore the nuclear function of p73 further, we focused on p73-regulated genes that we had identified in the Rh30 cell line. ChIP-on-Chip experiments demonstrated that p73 bound to genomic sites near genes associated with autophagy or with lysosomal function (Figure 41A). Both of the p73 isoforms expressed in Rh30 cells bound to sites near autophagy-associated genes such as *ATG5* and *ATG7*, and in some cases binding level was enhanced after treatment with rapamycin (Figure 41B).

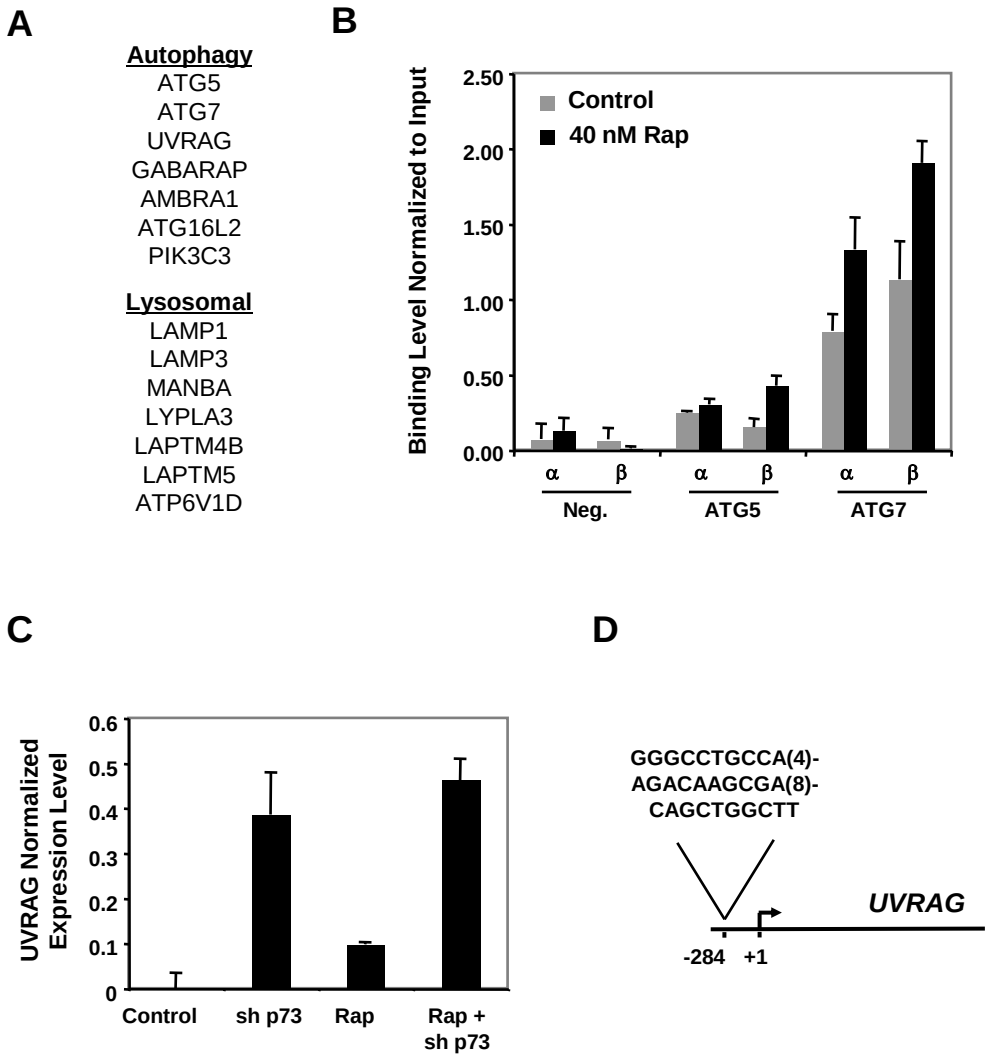

Figure 41: Analysis of autophagy-associated, p73-regulated genes. A) ChIP-on-Chip was performed in Rh30 cells, and p73 binding was detected within 10 kb of the indicated autophagy-associated and lysosome-associated genes. B) ChIP-qPCR was used to measure p73 binding at a negative control region, or at sites within 10 kb of the *ATG5* and *ATG7* genes, using antibodies specific for either the α or β isoform of p73. Cells were pre-treated +/- 40 nM rapamycin (Rap) in serum-free medium for 24 h before formaldehyde cross-linking and isolation of protein-DNA complexes. C) Microarray analysis of duplicate samples was used to assess UVRAG RNA levels in Rh30 cells treated with vehicle or 40 nM rapamycin (Rap) for 24 h and/or lentivirus expressing p73 sh RNA. D) Location of a p73-bound p53 response element in relation to the UVRAG transcriptional start site.

Thus, p73 regulates a network of genes, and the cumulative effect of this network may be to enhance and/or fine-tune the autophagic response.

These data suggest a role for p73 that is similar to that of nuclear p53, to activate target genes that regulate autophagy. However, the role of p73 may not be entirely straightforward. In the case of at least one autophagy-associated gene (*UVRAG*), microarray analysis revealed that p73 knock-down increased *UVRAG* expression levels (Figure 41C). In addition, ChIP showed that p73 bound to a region upstream of the *UVRAG* transcriptional start site that contains a p53 family response element (Figure 41D). p73 may directly suppress *UVRAG* expression, perhaps through recruitment of transcriptional repressors such as histone deacetylases. In this case, p73 would be expected in inhibit autophagosome nucleation and maturation (249,250). Our recent studies have revealed an entire network of autophagy-associated genes that are regulated by p73, and suggests multiple mechanisms by which this pattern of genes may alter the autophagic process.

p73 influences metabolic phenotypes

The above results suggest that p73 regulates metabolic processes such as autophagy in response to cellular stress. We tested this hypothesis in cell culture, and treated Rh30 and MDA-MB-231 cells with 40 nM rapamycin, resulting in an increase in lipidated LC3 as detected by Western blot. This was the expected result for Rh30 cells that are highly sensitive to rapamycin (182); however, MDA-MB-231 cells are relatively insensitive to the effect of rapamycin on cell proliferation (177). Our experiments in Chapter III demonstrated that mTOR signaling is intact in MDA-MB-231 cells from the

mTOR kinase to downstream targets such as 4EBP1 and S6K and secondary targets such as S6. In Chapter III, rapamycin inibited the growth of these cells but failed to cause complete cell cycle arrest. However, mTOR signaling seemed to be intact and we observed an increase in autophagy in response to rapamycin, which suggested that the intrinsic resistance to cell cycle arrest may be mediated by a different downstream signaling pathway.

We next treated cells with rapamcyin after RNAi-mediated depletion of p73. In Rh30 cells we observed only a slight decrease in the levels of rapamycin-induced autophagy in cells after p73 knockdown (data not shown). These data suggest that p73 signaling may be only one of many pathways through which mTOR regulates autophagy. This is consistent with the observation that mTOR inhibition causes both transcriptional and translational changes that induce autophagy (110,125).

We further hypothesized that p73 plays a role in the ability of cells to adapt and respond to metabolic stresses in general. To test this hypothesis, we measured the growth of Rh30 cells incubated in serum-free media. There was a decrease in the total number of viable cells after three days of incubation in serum-free media (Figure 42), likely due to cell death from metabolic stress arising from lack of nutrients and growth factors that are present in serum. However, concurrent RNAi-mediated depletion of p73 abrogated this effect (Figure 42). These data suggest that p73 is required for tumor cell death that occurs as a slow response to metabolic stress.

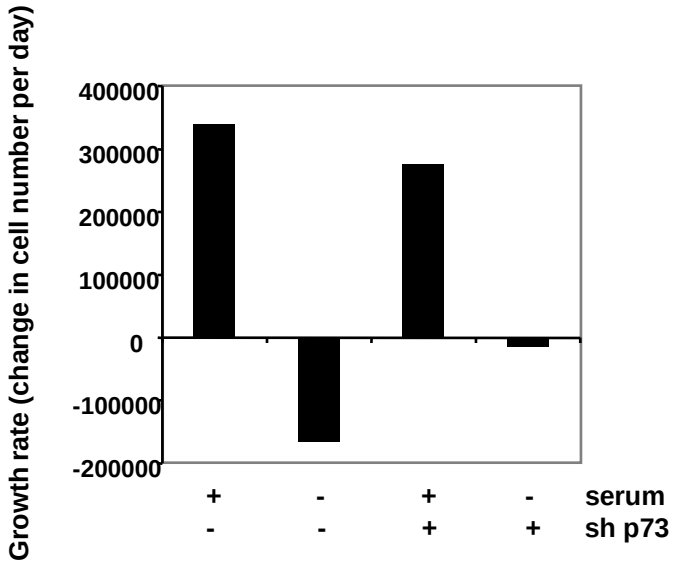

Figure 42: p73 mediates a cellular response to serum starvation. Rh30 cells were grown in medium with 10% fetal bovine serum or serum-free medium, in the presence of lentivirus that expresses shRNA targeting GFP or p73. The change in total cell number per day after 3 d growth in these conditions was plotted for each condition, demonstrating a p73-dependent decrease in cell number, likely due to cell death from metabolic stress during serum starvation.

Metabolic networks in the p73 cistrome

We used Ingenuity Pathway Analysis to explore additional networks among the p73 target genes identified in Rh30 cells. As described in Chapter IV, Ingenuity Analysis uses literature-based curations to connect genes into functional pathways. Three key pathways, linked to metabolic processes, emerged from our analysis. The first pathway was related to lipid metabolism (Figure 43A), and included five triacylglycerol lipases (DAGLI, PNPLA3, CEL, LIPC (helpatic lipase), and LIPG (endothelial lipase)). These lipases were connected to lipid transport mechanisms; the LDL receptor is one of the genes that exhibited the greatest p73 occupancy (~20-fold enrichment over input by ChIP-on-Chip). This network also consisted of enzymes that regulate the metabolism of fatty acids (Figure 43A).

The other two Ingenuity pathways are related to glucose metabolism (Figures 43B and C). Several phosphatidylinositol kinases and genes related to insulin and the insulin receptor were bound by p73 (Figure 43B). Other p73 target genes regulate glycolysis levels and are specific to muscle cells (Figure 43C). These pathways highlight the potential importance of p73 not only for cellular metabolic processes such as autophagy, but also for metabolism on a whole-organism level. This role would be best elucidated through in vivo analysis of p73 in adult tissues (see Chapter VII).

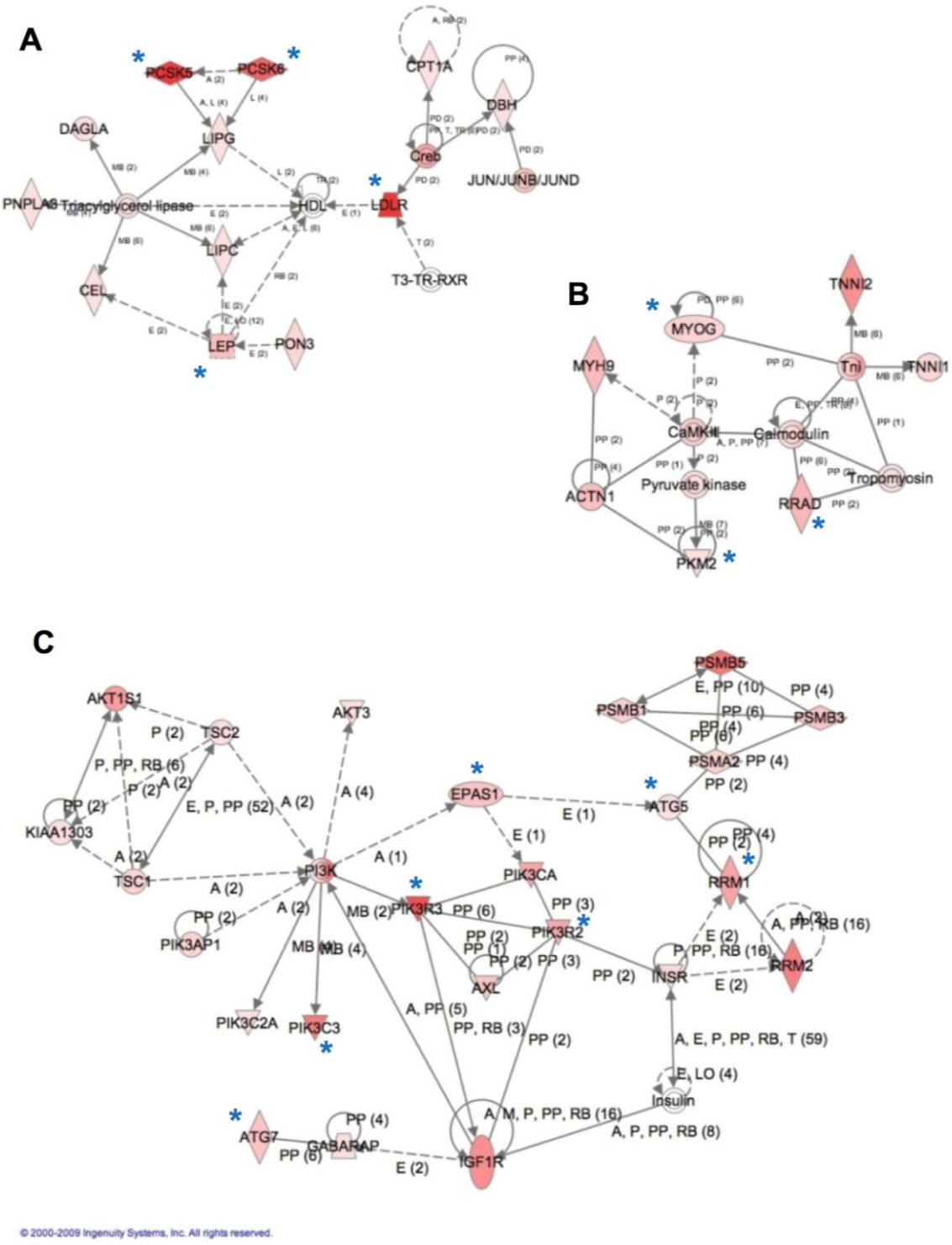

Figure 43: Key Ingenuity Pathways derived from p73 target genes identified in Rh30 cells. Three key pathways with literature-based connections include: A) a pathway connecting five triacylglyerol lipases, LDLR, and enzymes involved in fatty acid metablism, B) a pathway connecting muscle-specific genes to muscle-specific pyruvate kinase and glycolysis control, and C) a pathway connecting several PIK3 genes, receptors for insulin and insulin-like growth factor, and autophagy genes. For genes indicated with a blue asterisk, p73 binding was validated using ChIP-qPCR and two additional p73 antibodies in control and rapamycin-treated cells.

Discussion

Our observations that mTOR negatively regulates p73, and that p73 regulates many genes associated with autophagy, suggest both similarities and differences in the ways that p53 family members respond to metabolic stress and regulate autophagy. The role of autophagy in the different in vivo functions of the p53 family remains to be determined. p53 is one of the most frequently mutated genes in human cancer. Whether p63 and p73 are also tumor suppressors has long been controversial, although a recent isoform-specific p73 mouse model suggests that it is indeed a bona fide tumor suppressor (65). Thus, p53 family members may regulate autophagy to maintain genome integrity or suppress necrosis and inflammation that promotes tumorigenesis.

In addition, p63 and p73 play critical roles during development (37). p63 plays an essential role in the development of the epidermis and mammary gland (27). Loss of p73 leads to hippocampal dysgenesis, gastrointestinal erosion, hemorrhage, and an increased propensity for neurodegenerative disease in mice (28,251), phenotypes that are associated with dysregulation of autophagic pathways (252-254). Interestingly, we have identified p73 target genes such as GABARAP, an LC3 homolog expressed in neurons and muscle cells, that are important for tissue- and context-specific regulation of autophagy (246). Further, all three p53 family members have been associated with aging or aging-related pathology (251,255,256). In fact, the effect of the p53 orthologue CEP-1 on the life-span of C. elegans is mediated by autophagy (257). Thus, the discovery that p53 family members regulate autophagy may have implications for a wide range of human diseases.

Our results also provide another link between metabolic stress and tumor suppression. It has been suggested that p53 is required for induction of a metabolic

checkpoint in response to glucose deprivation (96). Low energy levels activate AMPK, but p53 can also activate AMPK by increasing the expression of sestrins that bind to AMPK and promote its phosphorylation (96). Cells that have undergone p53-mediated cell cycle arrest can still maintain high levels of metabolic processes. By inhibiting mTOR, p53 decreases the energy requirements of cells that have arrested (96,258). Interestingly, in Chapter III we identified sestrins as target genes of p73. Could p73, like p53, play roles both downstream and upstream of mTOR? Our data show that both p53 and p73 regulate cellular responses to metabolic stress, and raise many intriguing questions about the mechanisms by which they do so.

CHAPTER VI

MTOR-RELATED KINASES DIFFERENTIALLY PHOSPHORYLATE P53 FAMILY MEMBERS

Introduction

The p53 family of transcription factors contains three members, p53, p63, and p73, that share significant homology and evolved from a common ancestral gene. Yet the divergent expression patterns of these family members, both during development and in human tumors, are suggestive of key differences in their upstream regulators. p53 and its family members play critical roles by checking inappropriate cell growth in response to a wide range of stresses such as hypoxia, DNA damage, viral infection, loss of contact inhibition, glucose deprivation and activated oncogenes (100,259,260). Many of these cellular stresses also regulate mammalian target of rapamycin (mTOR), a serine/threonine kinase that is a master modulator of cellular growth. The mTOR pathway can be thought of as kinase-centric. mTOR integrates multiple signals that feed into it through upstream kinases such as Akt (responsive to growth factors) and AMP-activated protein kinase (AMPK, responsive to energy levels) (261). Output is achieved in part through kinases such as p70S6K, which is phosphorylated by mTOR to regulate protein synthesis (262), and glycogen synthase kinase 3-β (GSK3β), which is inhibited by both Akt and p70S6K to regulate energy metabolism (263).

The p53 family and the mTOR pathway are connected through many signaling nodes (98,110). p53 inhibits mTOR in response to genotoxic stress through target genes (sestrin-1 and sestrin-2) that interact with and activate AMPK (96). p53 is also

downstream of mTOR, as hamartomas containing constitutively activated mTOR have increased levels of wild-type p53, and p53 can suppress apoptosis caused by the mTOR inhibitor rapamycin (119,264). In contrast, in Chapter III we showed that p73 is inhibited by mTOR. Rapamycin treatment (as well as other methods of mTOR inhibition) resulted in increased p73 levels and activity. In Chapter IV we demonstrated that mTOR inhibition resulted in an altered p73 genomic binding profile.

Other kinases in the mTOR pathway can also regulate p53 family members. AMPK can phosphorylate p53, resulting in induction of p53 and thus an apoptotic response to glucose deprivation (260,265). AMPK can bind to p73, and this is thought to inhibit the ability of p73 to transactivate target genes in a kinase-independent manner (266). Evidence suggests that both p63 and p73 can act upstream of Akt. In one study, treatment of cells with the plant lectin ConA resulted in apoptosis that was dependent on p73-mediated inhibition of Akt (162). In another, p63 blocked UV-induced keratinocyte apoptosis by activating Akt (267). Finally, kinases downstream of mTOR interact with p53 family members, such as GSK3β which phosphorylates and activates p53 after DNA damage (268,269).

The mechanisms of many of the above interactions are unknown, and in cases where a mechanism is known it is usually unclear if only one or multiple p53 family members are involved. In previous chapters we explored the inhibition of p73 by mTOR; treatment of primary cells with rapamycin led to an increase in p73 but not p53 or p63 levels. Other agents such as cisplatin induce p73 through c-abl-mediated phosphorylation of Y-99 (31,32,34), and we questioned whether mTOR inhibitors induced p73 through similar, synergistic, or unrelated mechanisms. In Chapter III we demonstrated increased

p73 levels after treatment of cells with a combination of rapamycin and cisplatin compared to treatment with cisplatin alone. Understanding the mechanism by which mTOR regulates p73 could yield insight into potentially synergistic drug combinations, combinations that would be effective in tumor cells with inactivated p53.

To explore the mechanism by which mTOR regulates p73, and to study the inter-connections between the p53 family and mTOR pathway in general, we performed a candidate kinase approach. Key kinases in the mTOR pathway were assessed for their ability to phosphorylate p53 family members and isoforms. Phosphorylation patterns appeared to be both member and isoform-specific. Through this method we identified p73 as a substrate of mTOR, and confirmed a physical interaction between the mTOR kinase and p73 in cells.

Results

Development of a candidate kinase approach

In Chapter III we showed that rapamycin enhanced the induction of p73 and of apoptotic markers by cisplatin and taxol. While there are as many as 35 potential p73 protein isoforms, we observed an increase specifically in the levels of TAp73β, the isoform that has the strongest ability to transactivate target genes such as those involved in apoptosis (137). As a single agent, rapamycin usually elicits cell cycle arrest in the G1 phase (102), although it can induce apoptosis in some cell lines with inactivated p53 (182). Our data in Chapter III are consistent with reports that, when used in combination, rapamycin enhances the efficacy of a number of cytotoxic agents (120).

We explored the role of p73 during mTOR inhibition by treating Rh30 cells with rapamycin, and by depleting p73 with RNAi targeting either the TA domain or a C-terminal domain specific to p73β isoforms, as in Chapter III. Rapamycin caused an increase in PARP cleavage that was dependent on TAp73β (Figure 44A). While the amount of PARP cleavage that we observed seemed insufficient for robust induction of apoptosis, it may contribute to the ability of rapamycin to 'prime' cells for apoptosis in response to cytotoxic drugs.

We reasoned that mTOR regulates p73 by a distinct mechanism that allows for synergy with DNA damage pathways. In Chapter III we showed that rapamycin increased p73 protein levels but not RNA levels. Given the many kinases in the mTOR pathway, and the fact that some kinases in the pathway such as AMPK and GSK3β are known to phosphorylate p53 (260,265,268,269), we decided to test the ability of mTOR-related kinases to phosphorylate p73. As shown in Figure 44B, we chose three tiers of kinases to analyze. mTOR exists as two complexes, mTORC1 and mTORC2, with mTORC2 acting upstream of mTORC1 (Tier 1) (261). As mentioned above, Akt and AMPK transmit growth factor and nutrient signals to mTORC1 (Tier 2), and p70S6K and GSK3β are downstream of these kinases (Tier 3).

We tested the ability of these kinases to phosphorylate not only p73, but also p53 and p63, in order to gain insight into common versus distinct methods of regulation of these family members. We chose to test the ΔNp63α isoform, because this is the predominant isoform expressed in human tissues (270). We also assessed three different isoforms of p73: TAp73α, TAp73β, and TAp73γ.

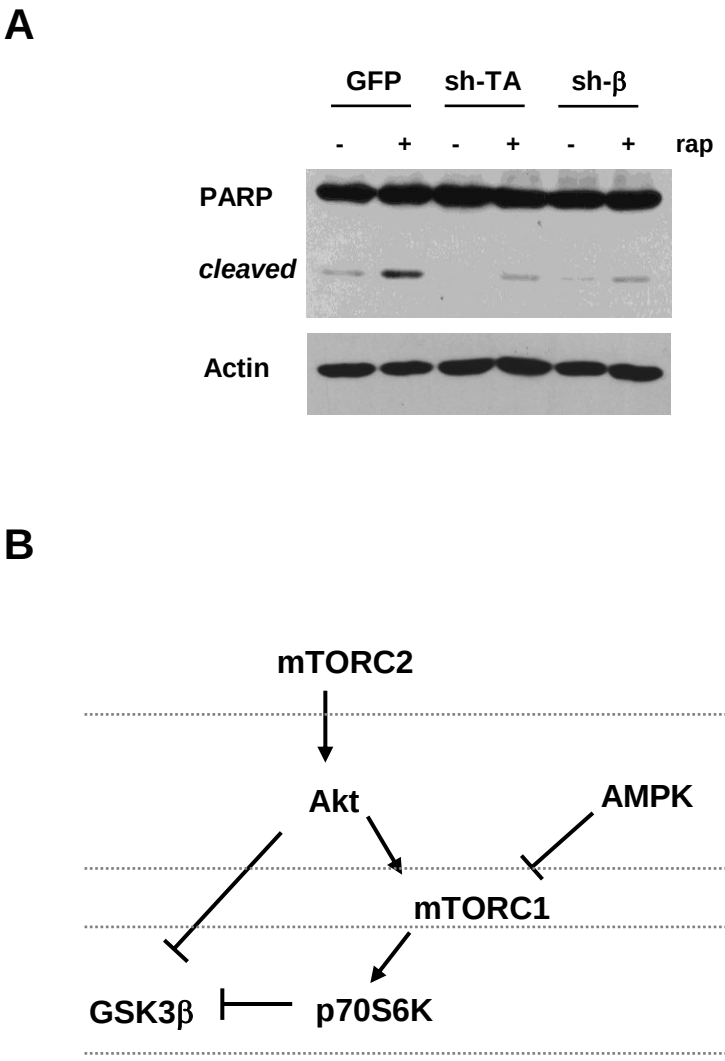

Figure 44: Rationale for a candidate kinase approach. A) Rapamycin induces PARP cleavage in Rh30 cells in a p73-dependent manner. Rh30 cells were treated with 40 nM rapamycin (rap) or vehicle control for 24 h in serum-free media, and treated with lentivirus expressing shRNA targeting GFP, TAp73, or p73β for 3 d. Western blot analysis was performed for PARP and actin; the blots shown are representative of three independent experiments. B) The mTOR pathway is depicted as three tiers of kinases (mTOR exists as two complexes, mTORC1 and mTORC2) that were chosen for assessment in a candidate kinase approach.

Theoretically, phosphorylation of one isoform but not another would help define a region of the protein required for phosphorylation. This region could have domains needed for interaction with kinase(s) and/or contain the actual phophorylates site(s). We generated recombinant proteins for each of these family members in *E. coli*; these proteins were GST fusion proteins containing a protease cleavage site for removal of the GST tag, if needed (Figure 45).

Kinases in the mTOR signaling pathway phosphorylate p53 family members

p53 is a known substrate of GSK3β and we observed phosphorylation of both p53 and p63 by GSK3β in vitro (Figure 46A). By comparison GSK3β did not phosphorylate any of the three p73 isoforms analyzed (Figure 46A). In contrast, in vitro kinase assays using p70S6K resulted in phosphorylation of all p53 family members (Figure 46B). Although we observed modulation only of p73 and not p53 or p63 by rapamycin, we considered that p70S6K might specifically target p73 due to selective mechanisms that exist in cells. Therefore, we used RNAi to deplete p70S6K levels and measured p73 protein by Western blot. We did not observe regulation of p73 levels by p70S6K in Rh30 cells, BPH prostate cells, or MDA-MB-231 breast cells (Figure 47). Thus, p70S6K-mediated signaling does not appear to be the mechanism by which mTOR regulates p73.

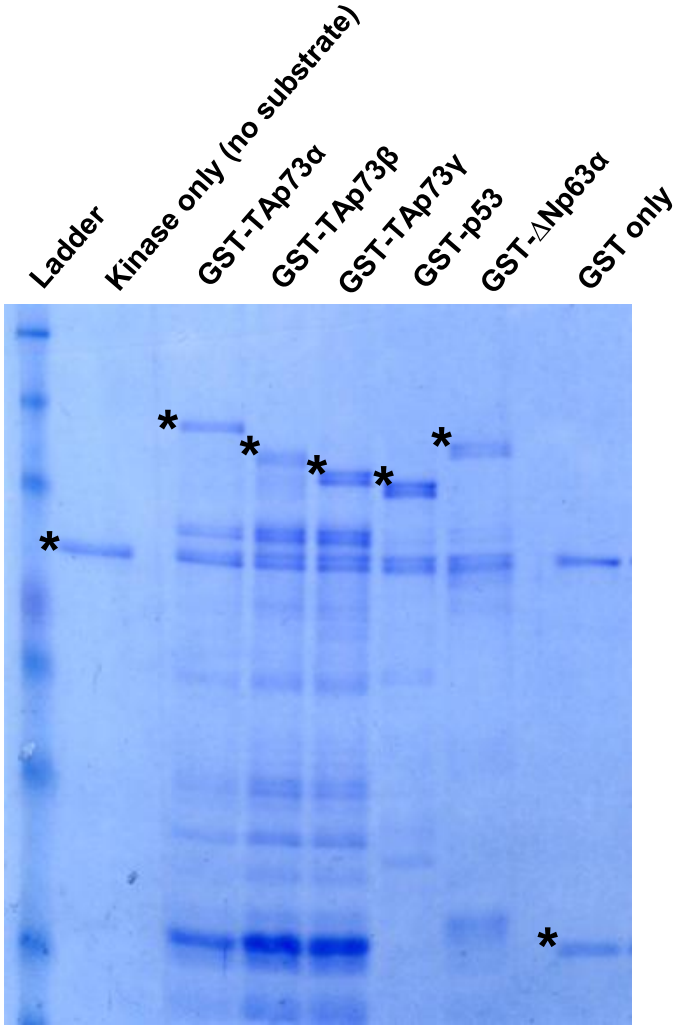

Figure 45: Substrates for in vitro kinase assays. Recombinant glutathione S transferase (GST) fusion proteins were generated in bacteria as described in Chapter II (Materials & Methods) with the assisstance of Peter Knowlton. p53, p63, and three different p73 isoforms were generated as GST fusion proteins, separated by SDS-PAGE and stained with Coomassie blue by Lucy Tang.

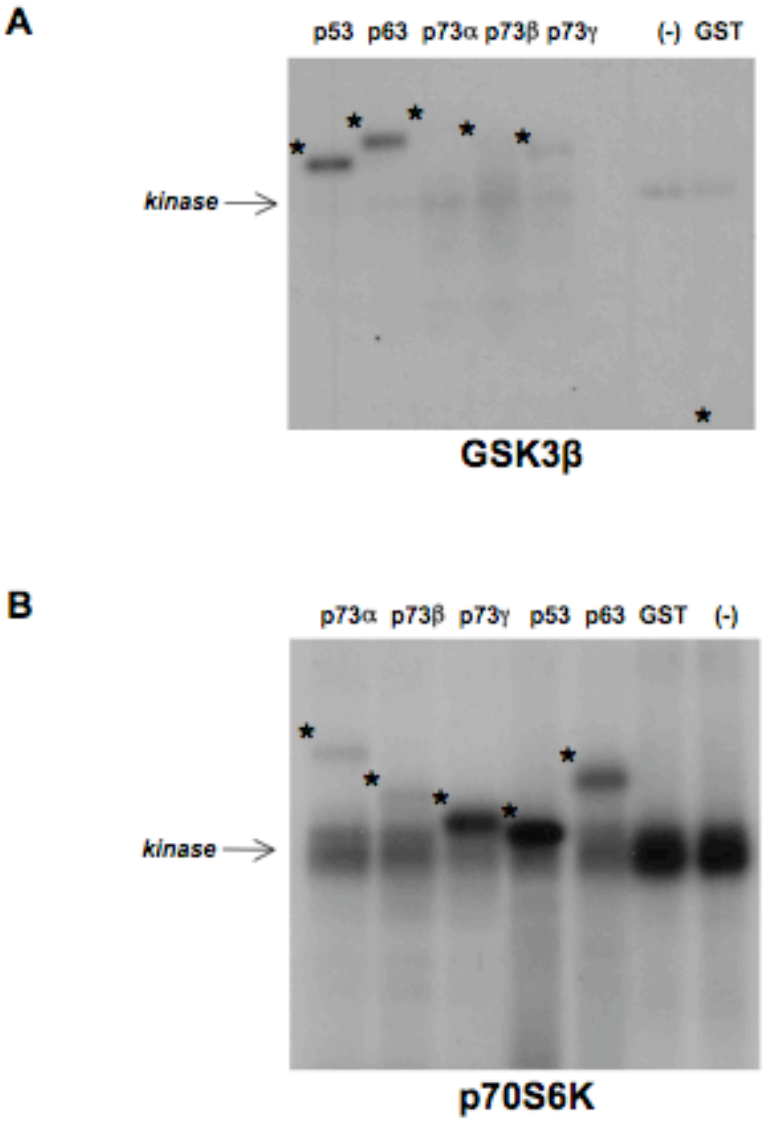

Figure 46: GSK3β and p70S6K differentially phosphorylate p53 family members. GSK3β (A) and p70S6K (B) kinases were incubated with the indicated GST-fusion p53 family member proteins or GST alone and γ-^{32}P-ATP. Kinase reactions were separated by SDS-PAGE, stained with coomassie blue and exposed to film. (-) indicates a negative control reaction without substrate (kinase only). Kinase assays were performed by Lucy Tang.

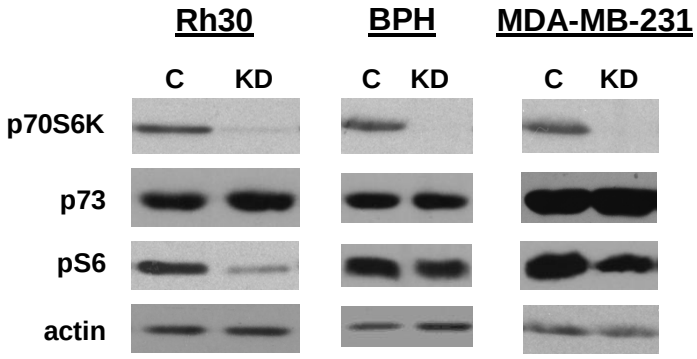

Figure 47: Depletion of p70S6K does not alter p73 levels. Rh30, BPH, and MDA-MB-231 cells were transfected with siRNA targeting p70S6K and harvested 3 d later. Cell lysates were prepared and analyzed by Western blot for p70S6K, p73, phospho-S6 (pS6), and actin levels.

We next assessed whether p53 family members can be substrates for AMPK and Akt. AMPK phosphorylated p53, p63, TAp73α, and TAp73β but not TAp73γ in an AMP-dependent manner (Figure 48A). Interestingly, there is a potential AMPK consensus sequence (NxxNxxxNxxBNxBxxS/TxxBN where N is a hydrophobic residue, B is a basic residue, and x is any residue (271)) within the residues that are present in TAp73α and TAp73β but not TAp73γ. In contrast, Akt showed very weak activity against p53 family members (Figure 48B). We measured the phosphorylation status of Akt and of AMPK in Rh30 cells treated with rapamycin to induce p73 (Figure 49). We used phosphorylated Thr-172 AMPKα as a marker of active AMPK. The activity of AMPK did not change with rapamycin treatment, suggesting that AMPK-mediated signaling is not the mechanism by which mTOR regulates p73. However, the levels of Akt phosphorylated on Ser-473 did increase after rapamycin treatment.

Ser-473 is one of two residues on which Akt needs to be phosphorylated for maximal activity, though for many years the kinase responsible remained elusive. mTORC2 is the long-sought kinase that phosphorylates Ser-473 on Akt (261). We found that multiple p53 family members are substrates of mTOR in vitro (Figure 50A). Given our results that rapamycin modulates both mTORC1 and mTORC2 activity, we next determined if a physical interaction exists between mTOR and p73 in cells. Co-immunoprecipitation experiments demonstrated that mTOR forms a complex with p73 in Rh30 cells, as well as with rictor and raptor (Figure 50B). These data suggest that p73 is a substrate of mTOR. In Chapter III we found that knock-down of mTOR increased p73 levels (Figure 10A); overall our data suggest that mTOR mediates rapamycin-induced changes in p73 levels by phosphorylating p73.

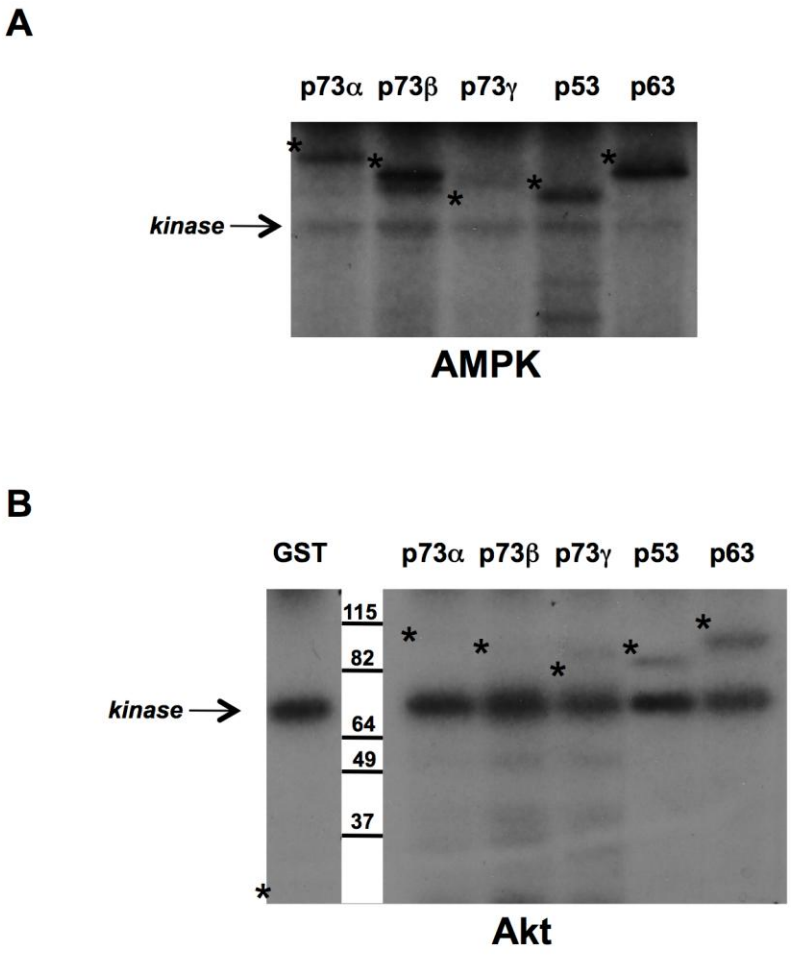

Figure 48: AMPK and Akt differentially phosphorylate p53 family members. AMPK (A) and Akt (B) kinases were incubated with the indicated GST-fusion p53 family member proteins or GST alone and γ-^{32}P-ATP. Kinase reactions were separated by SDS-PAGE, stained with coomassie blue and exposed to film. AMP was added to the kinase reaction in (A) and was necessary for phosphorylation of p53 family members. A molecular weight ladder marked in kDa is shown in (B). Kinase assays were performed by Lucy Tang.

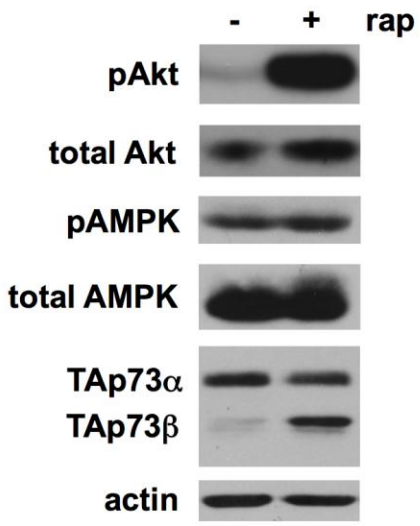

Figure 49: Phospho-Akt but not phospho-AMPK increases with rapamycin treatment. Rh30 cells were treated with 40 nM rapamycin (rap) in serum-free media for 48 h and whole cell lysates were harvested. Western blot analysis was performed to detect phosphorylated Akt on S-473 (pAkt), total Akt, phosphorylated AMPKα on T-172 (pAMPK), total AMPKα, p73 (the two predominant isoforms are indicated), and actin.

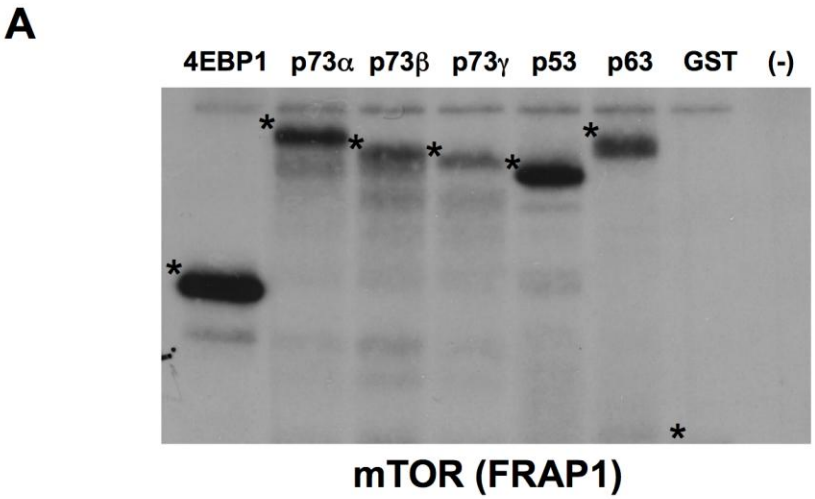

Figure 50: mTOR phosphorylates and interacts with p73. A) An in vitro kinase assay demonstrating phosphorylation of the indicated substrates by the mTOR catalytic subunit (FRAP1) was performed as in Figure 49 by Lucy Tang. B) Rh30 whole cell lysates (4 mg) were incubated with an antibody recognizing FRAP1, and immunoprecipitated ('IP') proteins were separated by SDS-PAGE and detected by Western blot for p73, mTOR (FRAP1), rictor, and raptor. Long and short exposures of p73 are shown and are representative of three independent experiments. 'Input' is 50 μg of Rh30 whole cell lysate. Immunoprecipitation with anti-mTOR was performed by Lucy Tang.

Discussion

Based on our finding that p73 is a substrate of mTOR, we propose future experiments to determine if mTOR phosphorylates p73 in cells and if this event is causally linked to the observed modulation of p73 protein levels after inhibition of mTOR by chemical inhibition or RNA knockdown. For example, we can determine if p73 exhibits a differential mobility shift by 1D and 2D electrophoresis after rapamycin treatment. A positive result, with a change after phosphatase treatment, would be consistent with phosphorylation and would lead to additional avenues of exploration. Identification of the phosphorylation site on p73 would allow us to make p73 mutants and generate phospho-specific antibodies. These tools, in combination with protein stability studies, would confirm and more precisely define the regulation of p73 by mTOR. A key goal of such studies would be to determine whether p73 phosphorylation is required for rapamycin-induced PARP cleavage in cells with inactivated p53. It would also be interesting to over-express catalytically active versus kinase dead mutants of mTOR, to assess whether high levels of mTOR activity are capable of suppressing p73 levels (the reverse of our rapamycin experiments), and whether such changes are dependent on mTOR kinase activity.

We found that rapamcyin treatment not only altered mTORC1, but also mTORC2, as evidenced by increased phosphorylation of Akt on Ser-473. It is important to consider whether or not cellular levels of Ser-473 phospho-Akt accurately reflect levels of mTORC2 activity. While mTORC2 is the primary kinase responsible for phosphorylation of Akt on this site, it has been suggested that increased phospho-Akt may be due instead to negative feedback loops that increase PI3K activity and therefore

increase recruitment of Akt to cell membranes (261). However, our results are consistent with studies that show increased Akt Ser-473 phosphorylation after mTORC1 inhibition in multiple cell lines (272). These studies confirmed that rictor is required for the increased phosphorylation of Akt on this residue, thus it is likely that mTORC2 activity correlates with p73 levels in our assays. Interestingly, although rapamycin treatment can modulate (perhaps variably) the ability of mTORC2 to phosphorylate its substrates, there does not appear to be any relationship between the resulting phospho-Akt and the phosphorylation of Akt substrates (272).

Thus, to identify whether p73 is in a complex with mTORC1, mTORC2, or FRAP1 alone, it will be important to perform additional co-immunoprecipitation experiments with rictor and raptor. If p73 does not associate with either of these proteins, it may be part of a previously unidentified mTOR complex. However, we consider it more likely that p73 interacts with mTORC1 and/or mTORC2, because of preliminary data suggesting that RNAi-mediated depletion of raptor and rictor alters p73 levels in cells. Identification of mTOR complex components associated with FRAP1 and p73 will be critical for understanding this signaling axis.

Another remaining question is: In what subcellular compartment does mTOR phosphorylate p73? p73 contains nuclear export and nuclear localization signals that allow it to shuttle between the nucleus and cytoplasm (50). When in the cytoplasm, p73 can interact with the tumor suppressor WWOX (273), but the functional consequences of cytoplasmic p73 remain unknown. mTOR has primarily been studied in the cytoplasm where it phosphorylates targets such as p70S6K and 4EBP1, however some studies found

that mTOR can shuttle between the nucleus and cytoplasm (274,275), thus it could potentially phosphorylate p73 in either compartment.

mTOR contains a nuclear localization signal (274). Furthermore, when cells are treated with leptomycin B, a specific inhibitor of the export receptor Crm1, mTOR accumulated in the nucleus (276). In some cell lines, including Rh30 cells, Houghton and colleagues have found that mTOR is predominantly nuclear (275). In addition, Rag proteins have been proposed to localize mTOR to perinuclear vesicles after amino acid stimulation (277). p73 has also been detected in a perinuclear extranuclear compartment (278,279), but it is unclear if this is the same compartment as mTOR or a side-effect of apoptotic nuclear blebbing. Localization studies will shed significant light on the regulation of mTOR-p73 complexes.

Finally, we took a general approach and tested the ability of mTOR-related kinases to phosphorylate p53 and p63 in addition to p73. Our results highlight previous findings about p53, p63, or p73 that might be extended to the other family members. For example, GSK3β phosphorylates p53 following DNA damage and activates it (269). However, we found that GSK3β can phosphorylate both p53 and p63; thus the role of p63 in this pathway should be examined. Similarly, we identified specific isoforms of p73 that can be substrates for AMPK. A previous report showed that AMPK inhibits p73 transactivation activity, but suggested that this occurred in a kinase-independent manner (266). Our data show that reassessment of this model is warranted, and should include comparison to p53 and p63. All three family members are substrates of mTOR and p70S6K, adding to the multiple layers of inter-connection that seem to exist between the p53 family and mTOR signaling pathway.

CHAPTER VII

GENERATION OF A CONDITIONAL P73 NULL MOUSE

Introduction

Although p63- and p73-deficient mouse models have been extremely informative for assessing the in vivo role of these proteins, the profound developmental defects, the perinatal lethality of the *p63*$^{-/-}$ mice and the early death of the *p73*$^{-/-}$ mice limit the utility of these models for examining the function of these proteins at later stages in the adult or during tumorigenesis. Engineered mice that allow conditional knockout of either *p63* or *p73* are needed to circumvent the limitations of the 'globally' deficient animals. Mice expressing a conditional *p63* allele (*p63*^{flox}) have been generated (280). With the goal of generating a conditional *p73* null mouse model, as part of this dissertation research we created a targeting vector and screened gene-targeted embryonic stem cells for generation of a mouse line expressing a conditional allele of *p73*.

Previous p63 and p73 mouse models informed our strategy for inactivation of *p73*. Two groups have generated *p63* knockout mouse lines using different embryonic stem cell-ablation technologies. The *p63*$^{-/-}$ mice generated by McKeon and colleagues contained a neomycin resistance (*Neo*) cassette instead of exons 6, 7, and 8, which encode part of the p63 DNA-binding domain that is common to all p63 isoforms (27). *p63*^{Brdm2} were generated by Bradley and colleagues using a gap-repair methodology to insert a cassette into and disrupt the *p63* allele (281). The *p63* gene in the *p63*^{Brdm2} mice

is disrupted after exon 10 by an inserted region that includes a puro resistance cassette and a duplication of the region of homology (exons 5 through 10).

The *p63*$^{-/-}$ and *p63*^{Brdm2} mice yielded similar developmental defects (complete lack of epidermal structures) with some key differences (retention versus lack of basal skin cell patches) and highly divergent tumor phenotypes (increased tumor susceptibility in the *p63*$^{-/-}$ but not *p63*^{Brdm2} mice). The majority of subsequent studies by a number of laboratories used the *p63*^{Brdm2} mice, and major conclusions were drawn under the assumption that these mice were *p63* null. However, additional in-depth analysis of the *p63*^{Brdm2} mice showed that, instead of being a global knock-out line, these mice retained expression of a p63 isoform similar to p63γ that lacks the C-terminal SAM domain (68).

In contrast, only one group has generated a mouse model deficient for all isoforms of p73. (As discussed in the Introduction, a second mouse line that lacks TAp73 but retains ΔNp73 isoforms has been generated. However, direct comparison is complicated as it remains unclear if ΔNp73 can compensate for TAp73 loss in some contexts.) The *p73*$^{-/-}$ mice were generated by replacing two exons in the DNA-binding domain with a *Neo* cassette. As discussed in Chapter I, homozygotes exhibited severe developmental defects and heterozygotes had an increased frequency of spontaneous tumor formation. The complex alternative splicing of the *p73* gene, and the retention of the *Neo* cassette in the *p73*$^{-/-}$ line warranted generation of a second p73-deficient mouse model using alternative methodology. Thus, our aim is to generate a conditional *p73* null mouse for comparison to the existing *p73*$^{-/-}$ mice, and for analysis of p73 function in adult tissues and during tumorigenesis.

Results

Strategy and bacterial artificial chromosome screening

Our strategy for creation of a mouse model with a conditional *p73* allele included targeting exons 7, 8, and 9 ($p73^{floxE7\text{-}9}$). Removal of these three exons ensured disruption of two key functional domains of the p73 protein that are common to all isoforms, both the 3' end of the DNA-binding domain (DBD), as well as the oligomerization domain (OD). Previous p63 and p73 mouse models demonstrated the feasibility of removing the DBD. We chose to remove the OD to prevent alternative expression of any truncated p73 proteins that could oligomerize with and affect other p53 family members. This is relevant given that generation of small protein fragments containing the p73 OD cannot be ruled out in the previously generated p73 knockout mouse model (28).

The entire *p73* targeting region is 1.5 kb, and removal of this region was designed so that the 3' sequence was no longer in the *p73* open reading frame. The RPCl-22 Mouse 129S6/SvEv Taconic BAC library was hybridized to filters and screened for *p73* genomic sequences using a probe in exon 8 (5'-gtcctgggccgccggtctttcgagggtcgcatctgtgcct). Two bacterial artificial chromosome (BAC) clones were obtained that contained this region of the p73 gene. These two BACs were screened by PCR to identify the extent of *p73* genomic sequence present, and one BAC was chosen (176-B7) because it contained sequence > 10 kb upstream and downstream of exon 8. The primers used to generate the BAC probes and to screen by PCR are listed in Table 10.

Table 10: Primers used for generation of conditional p73 null mouse

Primer Name	Primer Sequence (5' -> 3')	Notes
DNp73-F	GTCCTGGGCCGCCGGTCTTTCGAG	BAC probe primer
DNp73-R	AGGCACAGATGCGACCCTCGAAAG	BAC probe primer
TAp73.P1	ACAGCTACAGTGTACTTATGT	for screening BAC by PCR
TAp73.P2	CTTCCTGTGTGTCTGTGAGAT	for screening BAC by PCR
TAp73.P3	TGCATCTTCTCATGTAGAGTG	for screening BAC by PCR
TAp73.P4	TGAGGAATCATAATATGCCTG	for screening BAC by PCR
TAp73.P5	AGCTGGAGCATCATACAGCAA	for screening BAC by PCR
TAp73.P6	ACATAATGAAGTGTCTGTACA	for screening BAC by PCR
TAp73.P7	ACTGATGAGGTACAGGTGTGT	for screening BAC by PCR
TAp73.P8	AGGCTACATAGACTCCAGTGT	for screening BAC by PCR
TAp73.P9	AGCCGTTCTCAGAGACGGAAC	for screening BAC by PCR
TAp73.P10	AGCCTCGTGCGAAATACCT	for screening BAC by PCR
TAp73.P11	TCATGTGTAACAGCAGCTGTG	for screening BAC by PCR
TAp73.P12	TAGCCTCAGAGCATAGACA	for screening BAC by PCR
FragA.top	agtcgcggccgcTCAGAGATCAGAAACTCTCACA	PCR fragment A from BAC
FragA.bottom	agtcaagcttCGCCACAGTCCAAGATGGGCC	PCR fragment A from BAC
FragB.top	atgcaagcttCTAGAGTCTAACACCTGCAT	PCR fragment B from BAC
FragB.bottom	agtcactagtCTGCAAGAGCGATGGGCAC	PCR fragment B from BAC
FragC.top:	AGTCggtaccGACTGGGGTTTATGGCGTTTG	PCR fragment C from BAC
FragC.bottom:	agtcgaattcCCCACTCACTTGCCGGTC	PCR fragment C from BAC
FragD.top:	agtcggatccGTAGGTGGATACGTGGGTGTG	PCR fragment D from BAC
FragD.bottom:	agtcccgcggGAATGCCCACCGAGGAGAGC	PCR fragment D from BAC
FragE.top:	agtcctcgagCCTTCCAGCCTAGGTTTG	PCR fragment E from BAC
FragE.bottom:	agtcgtcgacAGGCTGAACCCTATAGGATC	PCR fragment E from BAC
FragF.top:	agtcggatccGTGTTTAAATCCATGGTCC	PCR fragment F from BAC
FragF.bottom:	agtcccgcggCTATAGGACCATGGATTTAAAC	PCR fragment F from BAC
FragCOut2:	CAAACTCTGTACCTCCCCTA	used to sequence final construct
New3:	GGGAAGGGCTTAGTATCAGT	used to sequence final construct
New7:	GACTCACAGGCAAGGAAATA	used to sequence final construct
SeqE1:	GGTACCAACGTGAAGAAGAG	used to sequence final construct
452RevOut:	CACGAGACTAGTGAGACGTG	used to sequence final construct
451Out2:	GATTGGGAAGACAATAGCAG	used to sequence final construct

These screens were performed in collaboration with the laboratory of Dr. Mark Magnuson, Professor of Molecular Physiology and Biophysics, Professor of Medicine, and Director of the Transgenic Mouse and ES Cell Core at Vanderbilt. The 176-B7 BAC was used to generate a targeting vector in the pL253 backbone as described below.

Construction of a p73 targeting vector

The p73 targeting vector was generated using a highly efficient recombineering-based method generated by Copeland and colleagues. Recombineering is a form of chromosome engineering based on homologous recombination in *Escherichia coli* that takes advantage of proteins encoded in the λ phage (282). In the EL350 *E. coli* strain, the λ phage genes that mediate homologous recombination are under the control of a temperature-sensitive repressor. Thus, a brief heat induction causes expression of a 5'-3' exonuclease (Exo), a pairing / annealing protein (Beta), and an inhibitor of the RecBCD exonuclease (Gam), to promote gap repair of linear dsDNA into DNA cloned on plasmids. EL350 cells also express Cre under the control of an arabinose-inducible promoter.

In the first recombineering step, a 14.1 kb fragment of the *p73* gene locus was transferred from the BAC described above to the high-copy plasmid vector pL253. This backbone was used because the alternative strategy, introducing *loxP* sites into the BAC, would necessitate both the removal of *loxP* sites already present in the BAC and the time-consuming confirmation of BAC integrity after every modification. The 14.1 kb *p73* segment contained the 1.5 kb targeted region, as well as 7.3 kb of upstream DNA (long arm) and 4.3 kb of downstream DNA (short arm). The long arm included exons 5 and 6,

and the short arm included exons 10, 11, 12, and 13. Two 500 bp sequences (Fragment A and Fragment B generated using primers in Table 10) that flank the 14.1 kb segment were subcloned into the pL253 backbone. The resulting vector was electroporated into EL350 cells along with the p73 BAC, and recombineering was induced (Step 1, Figure 51).

The next step was to introduce a *loxP* site 5' of *p73* exon 7 (Figure 51). Homologous recombination was used to introduce a floxed *Neo* cassette (pL452) using Fragments C and D (500 bp each, see Table 10 for primers) that flank the appropriate region as in Figure 51. Then, arabinose was used to induce Cre expression in the EL350 cells, resulting in removal of the *Neo* gene leaving only a single *loxP* site upstream of exon 7. The second *loxP* site was introduced 3' of exon 9, along with an upstream selection cassette that contains *Neo* floxed by two *Frt* sites and a bacterial EM7 promoter in between the PGK promoter and the coding sequence of *Neo* to allow for selection in both bacterial and murine ES cells with either kanamycin or G418 (Figure 51). (The *Frt* sites that surround the *Neo* cassette allow removal of the selection cassette once the conditional allele is introduced into the mouse germ line, by breeding the mice with a strain that expresses Flpe recombinase in the germ line. This is important because the *Neo* cassette can have untoward effects on expression from nearby genomic loci.) Of note, the pL253 vector already contained an *MC1-TK* negative selection marker.

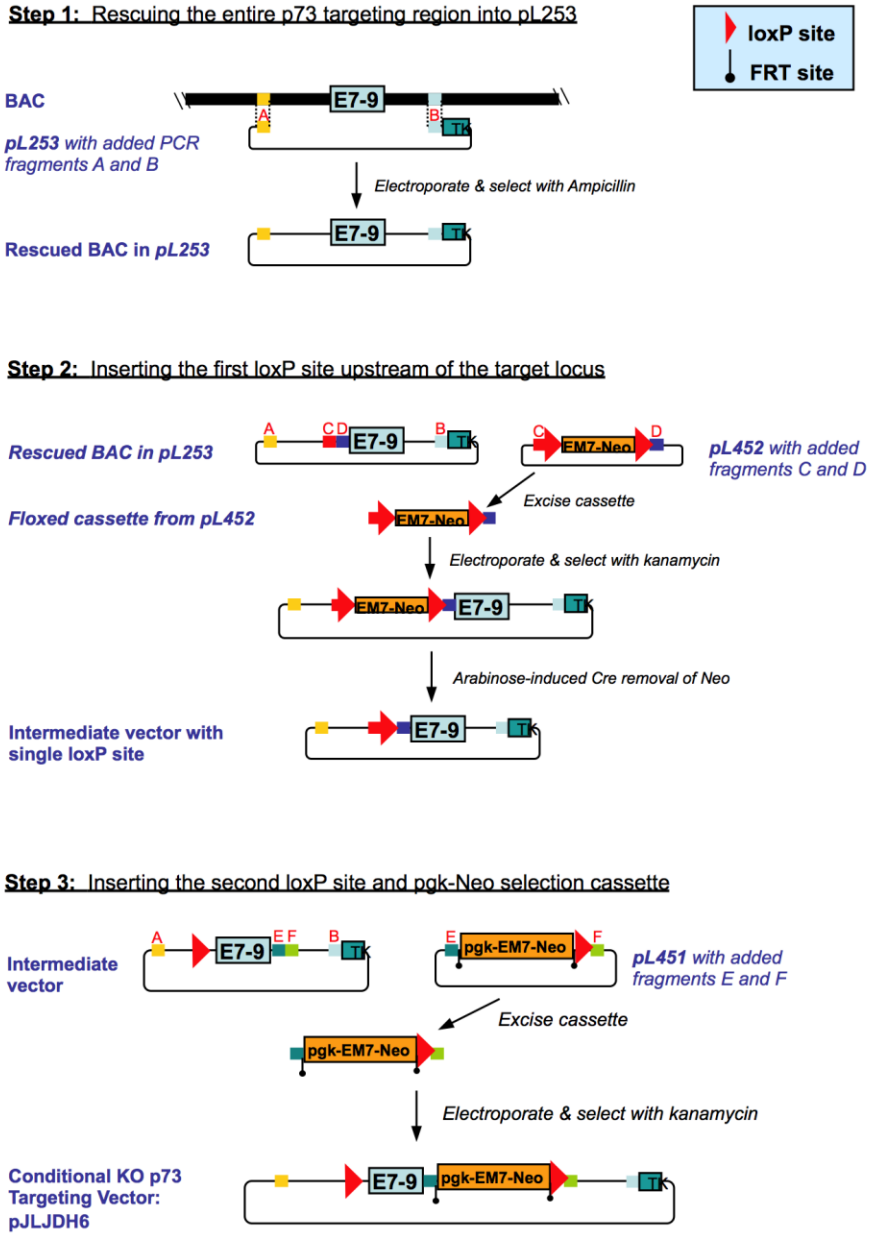

Figure 51: Recombineering-based method for generation of p73 targeting construct. The above schematic depicts the three stages used to insert a *loxP* site upstream of exons 7-9 of *p73*, and a *loxP* site and *pgk-Neo* cassette downstream of exons 7-9 of *p73*. The methodology is based on work described by Copeland and colleagues (see text), modified for p73 in collaboration with the Magnuson laboratory. Lucy Tang performed the PCR amplification, electroporation, and preparation of DNA for sequence analysis.

These recombineering steps generated a vector, pJLJDH6, as depicted in Figure 52, that was sequenced across every junction in both directions to verify its integrity using the primers listed in Table 10. The vector contains a long arm of 7.3 kb homologous to *p73*, a *loxP* site, the targeted region (exons 7, 8, and 9), the pgk-EM7-*Neo* cassette flanked by *Frt* sites, a second *loxP* site, a short arm of 4.3 kb homologous sequence, and a negative selection MC1-TK cassette.

Southern and PCR-based screening and generation of chimeric mice

There was approximately 13 kb total of *p73* sequence contained in the targeting vector. The vector was linearized using a unique *NotI* site and electroporated into the 129S6 TL1 XL ES cell line (isogenic to the BAC clone we used to generate the vector). G418 and gancyclovir-resistant ES cell colonies were picked, expanded, and confirmation of targeting confirmed by Southern hybridization (probes shown in Figure 53). Two ES clones containing the targeted allele were chosen (see representative Southern blot in Figure 54) for microinjection into 129S6 blastocysts.

After successful germline transmission of our engineered *p73* allele ($p73^{floxE7\text{-}9}$) using the mouse with the highest degree of chimerism, the resulting animals will be bred to a global *FlpE* 'deleter' mouse line, B6;SJL-Tg(ACTFLPe)9205Dym/J. *FlpE* is under the control of the actin promoter and these mice have been used routinely for the purpose of selectable marker deletion after germline transmission is achieved (http://jaxmice.jax.org/strain/003800.html). Efficient deletion of genomic material between *frt* sites, in our case the *Neo* gene, is typically observed.

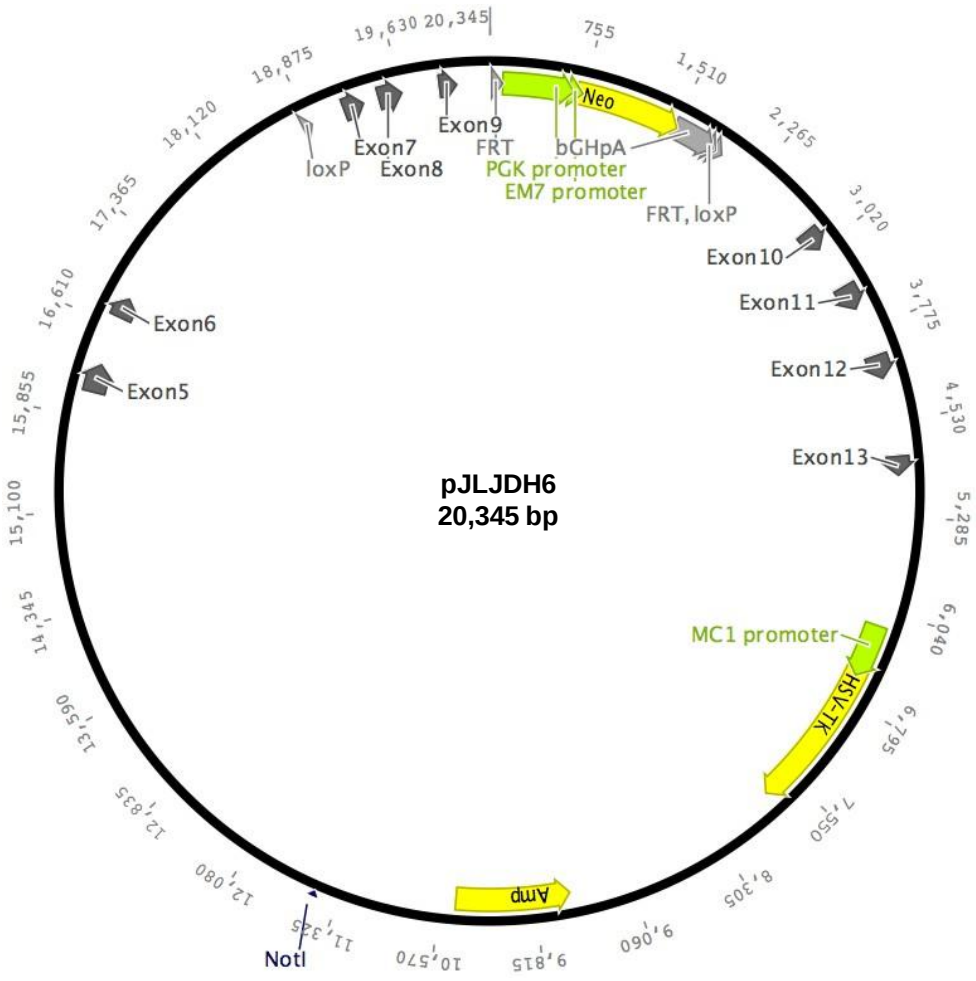

Figure 52: Vector map of p73 targeting construct. *LoxP* sites flank exons 7, 8, and 9 of *p73*. The positive selection cassette *Neo* and negative selection cassette *TK* are indicated. A unique *NotI* restriction site was used to linearize the vector prior to electroporation into ES cells.

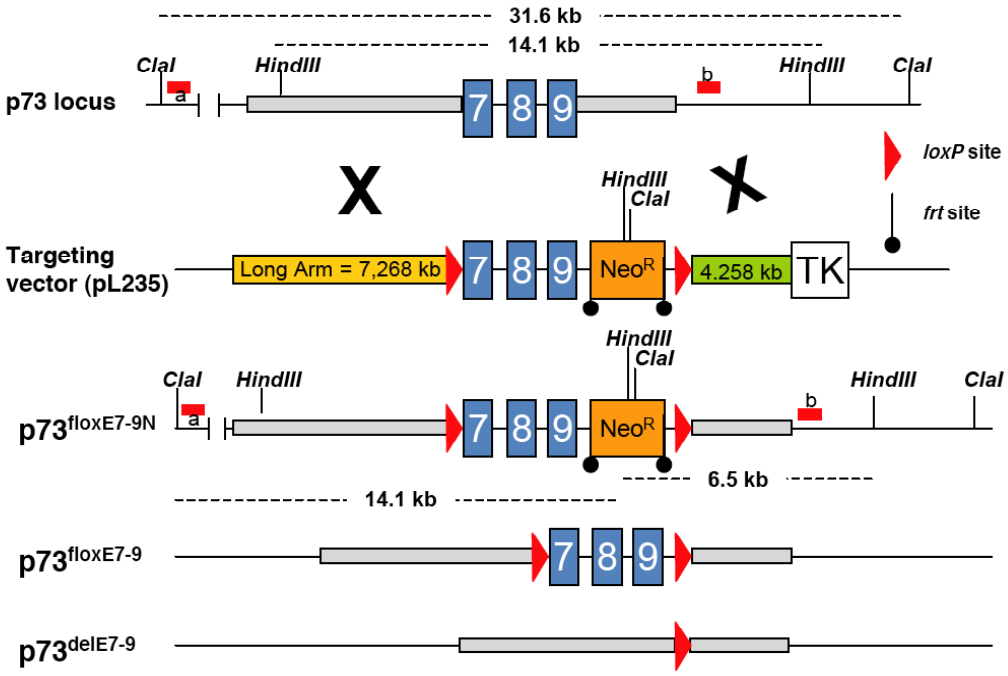

Figure 53: Targeting strategy for disruption of murine *p73* gene. The *p73* locus and targeting vector (pL253) are shown. The 129S6 TL1 ES cells were targeted to have deletion of exons 7, 8, and 9 of p73. Also shown are the predicted lengths of the restriction fragments of the targeted allele that we observed by Southern analysis. The location of the hybridizing probes used for Southern are indicated by red boxes labeled a and b. Neo^R, neomycin-resistance; TK, thymidine kinase. The yellow box is the long arm, and the green box is the short arm.

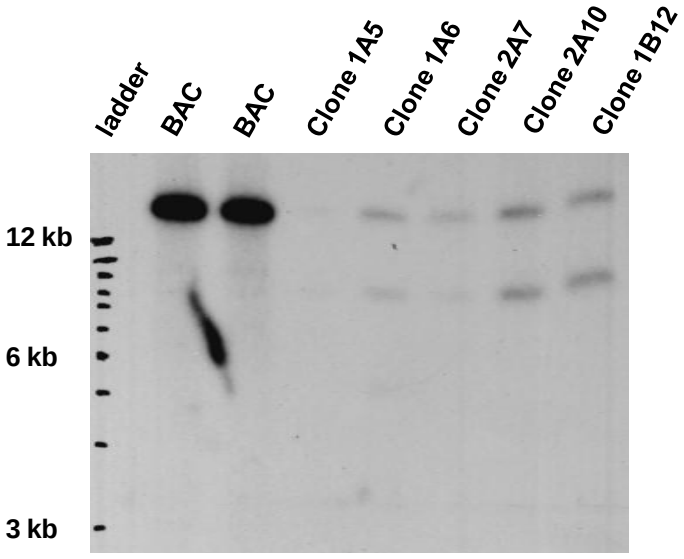

Figure 54: Southern blot analysis to screen for recombinant clones. Five representative murine embryonic stem cell clones are shown as an example of our Southern screening procedures. Genomic DNA was isolated, digested with *HindIII*, and fragments separated by gel electrophoresis. Southern blotting was performed using a probe located in exon 14 of *p73*. As indicated by differential digest patterns, all five clones have both a wild-type (~14 kb) and a floxed (~8 kb) genomic allele. Probe preparation, DNA digestion, and Southern blot analysis were performed by Deborah J. Mays.

In a few subsequent breedings, we will segregate out the *FlpE* gene and have a resulting mouse line that carries the $p73^{floxE7\text{-}9}$.

Discussion

Here I will discuss our plans for analysis of these conditional *p73* null mice. This includes both analysis of mice with global knockout of *p73* and tissue-specific, conditional targeting of *p63* and *p73* in the mammary gland. Global knockout of *p73* will be achieved by crossing the $p73^{floxE7\text{-}9}$ strain to the 'global deleter' mouse line B6.FVB-Tg(Ella-cre)C5379Lmgd/J that have been used extensively (http://jaxmice.jax.org/strain/003724.html). Male $+/p73^{delE7\text{-}9}$ mice will be established and crossed to 129s6 females and their progeny genotyped by Southern analysis. We will determine that $p73^{floxE7\text{-}9}$ is an efficient substrate for Cre if all possible forms of this allele are recovered in these crosses. $+/p73^{delE7\text{-}9}$ mice will be intercrossed to generate $p73^{delE7\text{-}9}/p73^{delE7\text{-}9}$ progeny. Given the previously published mouse model, we predict that breeding $+/p73^{delE7\text{-}9}$ mice will show Mendelian distribution consistent with *p73*, like *p53*, not being required for embryogenesis (28). RNA from mouse embryonic fibroblasts (MEFs) will be analyzed by RT-PCR as well as by sequencing to confirm disruption of the *p73* gene. The simple mouse genotypes of $p73^{+/+}$, $p73^{+/-}$, and $p73^{-/-}$ will then be used for analysis of p73 function.

In order to analyze mice with global knockout of *p73*, ten males and ten females from $p73^{+/+}$, $p73^{+/-}$ and $p73^{-/-}$ mice will be sacrificed at birth, 1, 3, and 5 months and analyzed for gene expression, histopathology, and phenotypes. A complete metabolic profiling of blood and select tissues will be performed by the Mouse Metabolic

Phenotyping Center at Vanderbilt. Analyses will involve various metabolic pathophysiology assays including determination of blood glucose levels, glucose utilization, and insulin secretion in these mice. This is particularly relevant given our findings that p73 regulates genes associated with insulin, glucose and lipid metabolism (as described in Chapter V). Interestingly, mTORC1/Akt is a well-known regulator of insulin signaling, and mTORC2 has been shown to regulate fat deposition and lipid metabolism in *C.* elegans (114). In addition to those mice analyzed at 1, 3, and 5 months, we will carry out necropsies on ten additional mice at 7, 10, 12, and 15+ months (depending on life span) to determine if there is any tendency to develop spontaneous tumors or if there are other gross tissue defects.

Based on the previous mouse model we predict the *p73* null pups will show a runting phenotype and high rates of mortality. We will examine the gastrointestinal tract and central nervous system for hemorrhages. A striking phenotype of the previously described *p73* null mice was severe rhinitis and purulent otitis media due to neutrophil infiltrates that persisted throughout adulthood. Lymphoid and granulocyte populations will be examined during the blood analysis. The most highly noted phenotypes of the previous *p73* null mouse was neurologic defects including hippocampal dysgenesis, hydrocephalus, and abnormalities in the pheromone sensing pathways (28). All neurological tissue will be examined with focus on choroid plexus, lateral ventricles, hippocampus, pyramidal cell layer, the dentate gyrus, and the vomeronasal organ. Confirmation of the phenotypes originally reported will underscore the requirement for p73 in the processes of pheromone detection and neurogenesis. We are most interested in

the overlap of genes and signaling pathways that are involved in metabolic processes (see Chapter V) to any noted phenotypes, whether similar to the previously described or not.

In addition to global knockdown of p73, and given our analyses of p73 activity in triple-negative breast cancers (as described in Chapter III), we will focus on p73 depletion that is specific to the mammary gland. A previous study demonstrated an increased incidence of mammary adenocarcinomas in $p63^{+/-}$;$p73^{+/-}$ mice (66). In human breast tumors, p73 exhibits significant over-expression (158). In the basal-like subtype of breast cancer, p63 is variably expressed and in those tumors it functions as an inhibitor of pro-apoptotic p73 function (37). Mouse models that analyzed p63 and p73 in breast tumors did not use histopathological analysis to define type. In addition, previous p63 and p73 mouse models had confounding variables such as a deficiency in gene expression from embryogenesis onward and potential compensatory roles of the other family members. Thus, crossing our floxed *p73* allele with those expressing Cre driven by the MMTV LTR promoter will allow us to address many of these unresolved issues. The MMTV promoter responds to estrogen, so when the mice reach puberty Cre mRNA will be expressed in the estrogen-sensitive tissues such as the mammary gland.

In addition, we have received *p63* conditional null mice, in which the *p63* DNA-binding domain is flanked by *loxP* sites (280). As mentioned above, mice in which *p63* has been globally deleted do not form mammary glands and die shortly after birth (27). We will be able to determine the effect of loss of p63 or p73 or both family members *after* development of the rudimentary mammary gland. For example, we hypothesize that Cre-mediated excision of both *p63* alleles at 5-7 weeks in the mammary gland will lead to loss of the basal, myoepithelial cells and the entire architecture of the mammary gland

will be disrupted. Whether or not such loss would depend on or be modulated by p73 (ΔNp63, the predominant isoform expressed during development, is an inhibitor of p73) could also be determined. Loss of myoepithelial cells could either confound tumor studies or it could provide a growth advantage for the luminal cells given reports about the 'natural' tumor suppressor properties of this basal cell population (283,284). Finally, we can perform a detailed histopathologic analysis to classify the subtype of breast cancer. We can examine the effect of complete loss of either p63 or p73 to maintenance and function of the adult mammary gland under control and stress-induced conditions.

The studies outlined above highlight the import that a conditional *p73* null mouse model would have on our understanding of the tissue- and temporal-specific roles of p73. In combination with *p63* and *p53* conditional null mice that have previously been generated, these mice would allow analysis of the coordinated and complementary functions of p53 family members.

CHAPTER VIII

SUMMARY & SIGNIFICANCE

p53 family isoforms inhibit p73 in tumors

p53 family members exhibit differential tumor expression patterns. Whereas p53 is frequently mutated in human cancers, reflecting its well-characterized role as a tumor suppressor, p63 is over-expressed or amplified in a subset of carcinomas derived from stratified tissues (tissues with both basal and luminal / squamous layers) (285). The predominant p63 isoform that is expressed in these carcinomas is the 'inhibitory' ΔNp63α isoform; this isoform is critical for the development, growth and maintenance of stratified tissues (285). Thus the opposing statuses of p53 and p63 in tumors matches their respective suppressive and oncogenic functions. In contrast, multiple isoforms of p73 are over-expressed in tumors despite the fact that many of these isoforms act as tumor suppressors in vitro (35,54).

Part of the above discrepancy may be explained by the concurrent expression of p73 inhibitors in tumors that express p73. The specific inhibitor or set of inhibitors that are engaged may be context-dependent. In select tumor types (HNSCC and basal-like carcinoma), ΔNp63α has been proposed to bind to TAp73β and sequester it from apoptotic promoters (56-58). Because p63:p73 hetero-dimerization is weaker than p73:p73 homo-dimerization (286), sequestration is likely limited to tumors in which the number of p63 molecules significantly outweighs the number of p73 molecules. Thus, we would hypothesize that this phenomenon is limited to carcinomas derived from basal

epithelium or that have developed squamous-like characteristics. Of note, our analyses suggest that a p63 antibody commonly used for IHC work, 4A4, can cross-react with p73 (Appendix). Therefore, we suggest that future analyses of p63 and p73 co-expression in tumors be validated with additional p63 antibodies.

Several studies suggest that ΔNp73 also plays a role as an inhibitor of TAp73. The balance of p73 isoforms expressed in any given tumor may thus dictate p73 function (54). Our understanding of ΔNp73 function is hampered by a general over-reliance on RNA analysis to detect p73 isoforms in tumors. In the Appendix, we evaluated commercially available p73 antibodies, identified a need for ΔNp73-specific antibodies, and generated new antibodies specific for ΔNp73. These antibodies can be used to assess ΔNp73 protein levels in human tumors. If ΔNp73 is the predominant inhibitor of TAp73 function, then its expression should be tightly correlated with TAp73 levels.

Finally, a few select mutations in p53 (specific hot-spot mutations that occur frequently in cancers) give p53 the ability to bind to p73 through weak interactions in the DNA-binding domain (59). Molecules have been developed that disrupt the mutant p53-p73 complex, freeing p73 to elicit tumor cell death or increase chemosensitivity (287,288). Overall, the above studies suggest that all three family members have the ability to inhibit p73. Whether they do so in vivo, the contexts under which p73 inhibition takes place, and whether these methods of inhibition are redundant remains unknown.

mTOR signaling inhibits p73

We were intrigued by several cancer cell lines in which TAp73 was robustly expressed in the absence of detectable p63 or ΔNp73, or detectable interaction between TAp73 and mutant p53. We hypothesized that either apoptotic pathways downstream of TAp73 were disabled, or unknown p73 inhibitors were engaged. In Chapter III, we sought to identify signaling pathways upstream of TAp73 in these cell lines. An example of the type of pathway we were searching for is the Rb pathway. Rb is an inhibitor of E2F, and E2F can bind to the p73 promoter and activate p73 transcription (a mechanism that may prevent p73 from being engaged in quiescent cells) (289). Rb can also inhibit c-abl, a kinase that mediates cisplatin-induced p73 stabilization (290,291). Thus, one hypothesis is that Rb prevents p73 from engaging tumor suppressor pathways in cancer cells (289). In Chapter III, we devised a gene-signature based approach to identify similar pathways upstream of p73, using pattern-matching algorithms to identify pharmacologic agents that induce gene expression signatures similar to the p73 signature (144).

Our approach took advantage of the Broad Institute Connectivity Map resource of drug signatures (143). First, we generated a p73 signature based on gene expression changes induced by ectopic p73 in H1299 lung carcinoma cells. By comparing the p73 signature to those in the Connectivity Map, we identified five drugs that target the mTOR pathway and induce a p73 gene signature. We validated mTOR as an inhibitor of TAp73β through both pharmacologic treatment of cell lines with mTOR inhibitors, and RNAi-mediated depletion of mTOR. The connection between p73 and mTOR was not due to general cell cycle inhibition, because treatment of the same cell lines with

mimosine or hydroxyurea did not result in p73 elevation. Finally, we demonstrated that p73 target genes are involved in mTOR-regulated processes such as autophagy (292).

mTOR is a master regulator of cellular growth across tissue types. As such, it is frequently activated in cancers through deregulation of upstream regulators like PTEN and PI3K. Thus, mTOR may serve as an inhibitor of p73 in tumor cells, preventing p73 from inhibiting cell growth or activating cell death pathways. Interestingly, in some cell lines such as MDA-MB-468 basal-like breast cancer cells, we detect both TAp73β and high levels of phospho-Akt, but not ΔNp63 or ΔNp73. Immunohistochemistry experiments are ongoing to determine whether phospho-Akt or phospho-S6, markers of mTORC2 or mTORC1 activation, correlate with p73 expression in human tumors.

In Chapter III, we further hypothesized that the mTOR-p73 signaling axis could be used as a therapeutic target. As shown in Chapter VI, rapamycin induced an increase in PARP cleavage that was dependent on TAp73β. We hypothesized that TAp73β may be 'priming' cells for apoptosis. This 'priming' effect could explain the synergy of rapamycin with other genotoxic agents that increase p73 levels. The kinase c-abl, which phosphorylates p73 on Y-99 in response to genotoxic stress (31,32,34), may tip the balance and lead to more robust induction of cell death.

We explored this hypothesis in triple-negative breast cancers, which are sensitive to cisplatin but lack targeted therapeutic options. As shown in Chapter III, the combination of cisplatin, paclitaxel, and everolimus (RAD001, a rapamycin analog) induced the levels of p73 and several apoptotic markers in basal-like breast cells. These preclinical results suggest that adding RAD001 to cisplatin and paclitaxel combination treatment regimens may increase clinical efficacy, and a phase II clinical trial has been

initiated at the Vanderbilt-Ingram Cancer Center to evaluate this hypothesis. We also found that our p73 gene signature could segregate triple-negative tumors into additional subgroups, and we posit that signatures of p73 activity could be used as tools to predict responsiveness of tumors to RAD001. This is particularly relevant because previous clinical trials involving rapamycin analogs, while not effective on a large scale, did result in tumor regression in select patients (102,293). Using gene signatures to predict clinical responders may be the key to an mTOR-based anti-cancer strategy.

A selective model for p73 binding and activity

In Chapter III we demonstrated that mTOR modulated p73 activity at 14 target genes involved in cellular metabolism and autophagy. However, our genomic analyses identified hundreds of p73 target genes, suggesting that our more traditional analysis provided too limited a window to p73 activity. Therefore, we asked whether mTOR altered p73 activity at all or only a subset of the target genes in its cistrome. In Chapter IV, we used comprehensive ChIP-on-Chip technology to answer this question, and to further examine the effect of mTOR inhibition on p73 binding and function at gene regulatory regions.

Our results generated a model for the regulation of p73 binding in response to cellular stresses. In total, we found that p73 bound constitutively to the regulatory regions of almost 4,000 genes. While mTOR inhibition resulted in an increase in p73 levels, the distribution of p73 binding sites did not change. Instead, p73 occupancy increased at ~9% of all p73-bound loci.

Our analyses of p73 binding suggested both similarities and differences with other p53 family members. p53 activates different subsets of its target genes depending on the specific cellular context and stressor. For example, nutlin-3 induces p53-dependent cell-cycle arrest, apoptosis or senescence in different cell types (294,295). In addition, the same colon carcinoma cell line undergoes arrest in response to doxorubicin, and apoptosis in response to 5-FU (296). For p73, we similarly found that rapamycin induced only a subset of its target genes, and this subset did not include several target genes known to be induced in response to other agents such as cisplatin (90).

Two models have been proposed to explain the selectivity of target gene activation by p53 (297). In the 'Selective Binding Model' p53 exhibits different affinities for different DNA sequences or response elements, resulting in differential binding to target genes. This model is supported by detailed kinetics analyses performed in our laboratory, that showed that p53 has different affinities for the response elements in different promoters (138). Furthermore, ChIP-on-Chip analyses in primary cells demonstrated that p53 binds the majority of its target genes only after genotoxic stress (87). In contrast, the 'Selective Context Model' posits that p53 binds to all of its target genes, but resultant activity is modulated by differential histone modifications, coactivator availabilities, and RNA Pol II loading. ChIP-on-Chip analyses in established cell lines demonstrated that p53 bound to target genes both before and after genotoxic stress, and the level of p53 binding correlated only with the amount of p53 in the cell (87). Analyses of p63 binding performed in our laboratory similarly showed constitutive p63 binding to many of its target promoters (145).

By defining a comprehensive p73 binding profile we set the stage for further evaluation of these models. Rapamycin resulted in an increase in p73 occupancy at specific loci. Interestingly these loci were enriched for genes that were transcriptionally repressed by p73. Could this be due to changes in p73 binding affinity? We defined a p73 consensus binding motif from among all p73-bound loci. This motif was very similar to the p53 and p63 response elements. The p53 family motif is notably long (20 bp) compared to other transcription factors, suggesting the potential for a high degree of regulatory diversity (297). Differences in the motifs bound by p73 at baseline and after rapamycin treatment were very subtle (the binding site is slightly more conserved after rapamycin treatment at positions 9-12), and while we consider it unlikely that such differences mediate selectivity of binding we cannot rule that out. Future studies that measure p73 binding after additional p73-inducing agents, or mere overexpression of p73, would yield significant insight. If all agents that increase p73 levels result in increased occupancy at the same sites, then this would suggest that the affinity of p73 for different DNA sequences is the primary determinant of its transcriptional activity.

In contrast, many of the p73 target genes that we identified in Chapter IV exhibited p73-dependent changes in expression without any change in p73 binding level. These data are strong support for a Selective Context Model for p73 function; factors outside of p73 binding must be regulating its activity. It is important to note that these types of studies are hampered by a frequent inability to link a binding site to its cognate target gene. The best one can do is annotate a binding site by its closest gene in terms of two-dimensional proximity. Many p73 binding sites may be regulating genes >10kb away but close in three-dimensional space. Nonetheless, our results suggest that

contextual cues influence p73 activity. Along these lines, we identified several tissue-specific factors that were associated with p73-bound loci in control and/or rapamycin-treated cells.

Integration of various facets of the p73 cistrome leads us to suggest the following model for p73 binding. Like p53 and p63, p73 exhibits extensive binding at baseline in cancer cells, and all three family members share a highly similar consensus binding sequence. However, p73 and p63 share additional similarities in their response elements that impart an ability to bind to a larger potential pool of target genes than p53. Certain types of cellular stress increase p73 occupancy at selective binding sites, and this may be driven in part by subtle differences in the response elements at these sites. Of greater impact, stress-induced changes in gene expression are modulated by the relative levels of the other p53 family members and by the availability of a variety of tissue-specific cofactors.

p73 regulates mesenchymal target genes

Our investigation of the p73 cistrome in Chapter IV revealed a significant number of target genes associated with muscle development and function. This led us to investigate the role of p73 in the pathogenesis of rhabdomyosarcoma, a disorder of skeletal muscle differentiation and growth. p53, p63, and p73 play redundant roles during myogenic differentiation by activating Rb (159). Moreover, inhibition of all three family members (by mutation of p53 and expression of dominant-negative ΔNp73) is required during rhabdomyosarcoma pathogenesis to block terminal differentiation (159). Interestingly, however, there are two types of rhabdomyosarcoma, ARMS and ERMS,

with different cells of origin and pathologies. The impact of p53 family members on these tumor subtypes is of interest given their distinct properties and pathways of formation.

ARMS are associated with gene translocations; ~70% of ARMS tumors harbor a gene fusion product that combines the PAX3 or PAX7 DNA-binding domain with the FKHR (or FOXO1) transactivation domain (223). Similar translocations have not been identified in ERMS, which are associated with a better prognosis. ARMS and ERMS occur in different age populations, likely due to differences in the number of second hits required for tumorigenesis, or in the available pool of target cells.

In Chapter IV, we generated an mTOR-p73 gene signature by performing gene expression profiling in Rh30 cells treated with rapamycin and/or RNAi targeting p73. We explored the status of this signature in two independent cohorts of rhabdomyosarcomas, and in both cases identified the signature only in the alveolar subtype. In addition, subsets of the p73 signature could predict clinical outcome for 64 patients with ARMS, but were unable to predict clinical outcome for patients with ERMS. Thus, p73 is functionally engaged in transcriptional activity in the alveolar subtype. Our analysis of p73 target genes revealed many involved in muscle differentiation / function and cell cycle progression that are potentially relevant to ARMS tumorigenesis.

We present two potential models to explain these data. First, a block in a signaling pathway downstream of or parallel to p73 may occur in ARMS resulting in retention of p73 activity in these tumors. Under such circumstances, p73 would not be a good therapeutic target in ARMS tumors. However, in this same scenario p73 may be

repressed in ERMS, and reactivation of p73 might lead to terminal differentiation and cell-cycle arrest of ERMS cells. In the second hypothesis, specific patterns of p73 isoforms may be expressed in ARMS tumors, and contextual cues may be present, that result in p73 activity at muscle-specific but not apoptotic gene promoters. As a result, treating ARMS tumors with molecules that activate p73, such as genotoxic agents and mTOR inhibitors, would alter p73 isoform ratios leading to induction of p73-mediated apoptosis. Along these lines, Rh30 xenografts treated with a rapamycin analog displayed a profound growth reduction (222). Comparison of p73-inducing treatment regiments in ARMS and ERMS cell lines would yield insight into the role of p73 in these two sarcoma subtypes.

Studies of ARMS pathogenesis and the role of p53 provide a framework for understanding the role of p73 (298, 299). Mesenchymal stem cells (MSCs) are thought to be the cell of origin for ARMS, as opposed to more committed muscle satellite cells that are thought to be the cell of origin for ERMS (223). It is clear that gene translocation products play an important role in the genesis of ARMS; however, mouse models that stably overexpress these fusion products have been difficult to establish. For most cell types, these oncogenic fusion products are lethal. It is only in more 'permissive' cells such as MSCs that their expression can be tolerated. Interestingly, attempts to establish xenografts from MSCs harboring ectopic expression of PAX3-FKHR were not successful without concurrent loss of p53 or ARF (298). Transgenic mouse models gave similar results. Conditional expression of PAX3-FKHR generated only 1 ARMS tumor out of 228 mice, but simultaneous loss of either p53 or ARF lead to accelerated tumorigenesis and increased incidence (299). It is thought that embryonal tumors, derived from more

committed cells, can only tolerate weaker oncogenes such as activated RAS (223). In both tumor subtypes second hits, such as those in the ARF-p53 pathway, are likely required for cells to tolerate oncogenic activation.

In Chapter IV, we used our gene signature to explore p73 activity in MSCs. Interestingly, gene patterns in the p73 signature were altered during differentiation of MSCs into the myogenic lineage. One key target gene that was present in the ChIP dataset and was regulated by p73 was myogenin. Myogenin plays a critical role during muscle differentiation - it is part of a cascade of transcription factors that converts myoblasts to myotubes to terminally differentiated muscle cells (300). Interestingly, unlike other core factors such as MyoD and Myf5, Myogenin is non-redundant and transgenic mice lacking it do not develop any skeletal muscles (301), suggesting that multiple potentially compensatory signals converge on myogenin during development. Myogenin plays a role in later parts of the differentiation cascade (300), thus if p73 regulates myogenin it may play a role during terminal differentiation that is altered during tumorigenesis. We demonstrated that p73 activates myogenin expression in a rhabdomyosarcoma cell line. These data suggest that mTOR inhibition could be used to terminally differentiate cancer cells by activating p73. Future examination of additional target genes in the p73 cistrome may yield additional insight to the role of p73 in MSCs, cells that are the origin of multiple tumor types.

We also identified many p73 target genes and miRNAs that are known to regulate epithelial-to-mesenchymal transition (EMT) suggesting a role for p73 that extends beyond human sarcomas. Furthermore, components of the p73 signature were altered in MCF10A breast cells induced to undergo EMT following different treatments (302,303).

Work by Piccolo and colleagues has shown that a complex containing mutant p53, p63 and Smad proteins inhibits p63, resulting in expression of genes such as cyclin G2 that promote tumor metastasis (304). Given that mutant p53 and p73 can interact (305), that p73 expression correlates with stage and invasion in some human tumors (76,306), and that we have identified cyclin G2 and other TGFβ-related genes as targets of p73, future studies on the contribution of p73 to EMT are warranted.

Thus, we propose that p73 plays a larger role in regulating a mesenchymal phenotype. Whether the p73 transcriptional program is the same in human sarcomas and in epithelial cells that have transitioned to a mesenchymal state remains to be determined. Interestingly, our analysis of p73-regulated genes in basal-like breast cancers in Chapter III may be related to this phenomenon, because basal-like breast carcinomas have increased expression of mesenchymal markers and a greater proclivity for EMT as compared to other breast cancer sub-types (307).

We performed additional functional analysis in Chapter III, demonstrating that p73 regulates cellular autophagy, a catabolic process that can provide nutrients for cells or accompany cell death. In Chapter V we analyzed the p73 cistrome further and identified networks of target genes related to lipogenesis and glucose utilization. We validated p73 binding at key target genes in each of these networks using ChIP-qPCR. Interestingly, a meta-analysis of several rhabdomyosarcoma microarray and SAGE studies found that a key defining phenotype of rhabdomyosarcomas was general down-regulation of energy production pathways (308). It is interesting to speculate that p73 regulates such metabolic pathways in rhabdomyosarcomas and other tumor types.

Mechanistic analysis of the mTOR-p73 axis

In Chapter III we demonstrated that mTOR inhibition increased p73 protein levels, but not p73 mRNA levels. In Chapter VI, we further explored the mechanism by which mTOR regulates p73 by assessing kinases in the mTOR pathway for their ability to phosphorylate p73. Because there are likely many inter-connections between the mTOR and p53 family pathways, as described in Chapter I, we generated recombinant p53, p63, and p73 for use as substrates. Our results showed that GSK3β, p70S6K, Akt, AMPK, mTOR and RSK1 differentially phosphorylate p53 family members in vitro. In some cases we can identify regions of the protein that are phosphorylated or required for phosphorylation. For example, AMPK phosphorylated p73α and p73β but not p73γ, therefore we hypothesize that AMPK phosphorylates a motif that is present in the short amino acid stretch that is absent in p73γ. We combined our kinase assay results with analyses of activation of kinases in cell lysates after various pharmacological treatments to narrow down the mechanism by which mTOR regulates p73. Our results suggested that mTOR phosphorylates p73 directly, and co-immunoprecipitation analyses suggest a physical interaction between the mTOR kinase and p73 in cells.

Several questions remain about the interaction between mTOR and p73. It is unknown whether p73 binds to components of the mTORC1 complex or mTORC2 complex. Rapamycin has traditionally been categorized as an inhibitor of mTORC1 based on its mechanism of action. However, other laboratories have disputed this finding, suggesting that rapamycin does inhibit mTORC2 after prolonged treatment in select cell lines, or that rapamycin induces mTORC2 activity due to mass action effect

(206,309). A key substrate of mTORC2 is Akt, which is phosphorylated on Ser-473. We analyzed phospho-Akt in multiple cell lines after treatment with rapamycin and found that mTORC2 activity increased concomitant with increasing p73 levels. We propose two models that explain rapamycin-mediated induction of p73: 1) mTORC1 phosphorylates p73 leading to its degradation, or 2) mTORC2 phosphorylates p73 leading to its accumulation. The experimental testing of these hypotheses in relation to the different p73 isoforms using co-immunoprecipitation- and RNAi-based metholdogy is ongoing in the laboratory.

In what subcellular compartment might mTOR phosphorylate p73? Most studies of mTOR and its substrates have focused on cytoplasmic activity. However, multiple reports have observed mTOR nuclear localization including in Rh30 cells (274,275). The major known substrates of mTOR are restricted to the cytoplasm, and the identity of potential nuclear targets of mTOR remain unknown (275). Work by Sabatini and colleagues showed that mTOR can localize to perinuclear vesicles upon activation (277). As described in Chapter I, p73 contains a NLS and a NES and has been detected in the cytoplasm where it interacts with the tumor suppressor WWOX (273). Interestingly, p73 has also been detected in a cytoplasmic perinuclear compartment (278,279). We have observed gene expression changes implying nuclear localization of p73 after rapamycin treatment. Thus, we hypothesize that mTOR phosphorylates p73 in the cytoplasm or perinuclear region, regulating shuttling of p73 to the nucleus, protein stability, and/or transcriptional activity. Alternatively, in some cell types p73 may be a substrate for nuclear mTOR.

p73 associates with distinct subnuclear compartments (278). For example, c-abl phosphorylates p73 resulting in increased association with a nuclear matrix (or insoluble fraction) (278,279). p73 is also associated with PML Organizing Bodies (PODs), regions of the nucleus where transcription factors can interact with cofactors and modifying proteins (278). We have observed p73 in the insoluble nuclear fraction of cell lysates. It would be of interest to determine whether rapamycin alters p73 cytoplasmic:nuclear distribution and p73 sub-nuclear distribution, and whether these distributions (or the mere phosphorylation of p73) results in changes in p73 protein stability.

Although we have detected phosphorylation of p73 by mTOR in vitro, and association of p73 with mTOR kinase in cells, there may be additional mechanisms by which mTOR regulates p73 levels and activity. Most notably, mTOR may cause differential initiation of p73 protein translation. The global regulation of cap-dependent translation is mediated by the mTORC1 signaling cascade (310). IRES-dependent translation has been shown to be involved in numerous cellular events, including proliferation, differentiation, and stress responses, such as heat shock, DNA damage and starvation, apoptosis, and cell cycle regulation (311,312) - all events to which p53 family members have been linked. Recent studies suggest that p53 family transcripts may have IRESs that would allow for cap-independent translation (209,211). Melino and colleagues have identified a motif that is implicated in IRES-dependent translation in the second exon of the p73 transcript, unique for p73 but not in p53 or p63 (211). Furthermore, the fifth methionine in TAp73 contains a strong Kozak sequence that may be used for translation. Therefore, cap-independent translation may play a role in the regulation of p73 by mTOR. Finally, it is possible that mTOR alters the association between p73 and

other modifying enzymes or cofactors. Our identification of an interaction between mTOR and p73, and our analyses of other mTOR-related kinases and p53 family members, lay the foundation for more detailed studies of the inter-connections between the mTOR and p53 family pathways.

The in vivo status of p73 was evaluated in 20 primary rhabdomyosarcomas at the RNA level (159). Two tumors expressed TAp73 without detectable ΔNp73, whereas two tumors expressed ΔNp73 without detectable TAp73. One tumor did not express p73, and fifteen tumors expressed both TAp73 and ΔNp73. A variety of C-terminal isoforms were evident that were not identified in the study. While it is clear that multiple isoforms of p73 RNA are being expressed in rhabdomyosarcomas, our analysis of the mTOR-p73 signaling axis in rhabdomyosarcoma cell lines highlights the need for detection of p73 protein in vivo. In the Appendix, we generated new p73 antibodies and thoroughly evaluated commercial p73 antibodies for use in immunohistochemistry. Correlative studies of p73 protein levels with phospho-S6 and phospho-Akt levels would help identify contexts in which the mTOR-p73 signaling axis is active. In Chapter VII, we described the generation of a conditional p73 null mouse that could be used for follow-up analyses of p73 function downstream of mTOR signaling.

Implications for cancer therapies and transcription factor signaling

We consider p73 to be particularly amenable for gene signature-based analysis. Although it is a p53 homolog with high expression levels in multiple tumor types, analysis of p73 in vivo is hampered by the large number of potential protein isoforms,

and the cross-reactivity and poor performance of many commercial antibodies. p73 gene signatures are thus attractive alternative methods for assessment of p73 status in tumors.

Furthermore, a model is emerging whereby p73 is expressed with at least one of many potential inhibitors or modifiers that may prevent it from engaging apoptotic pathways. Gene signatures can be thought of as collections of gene expression patterns or modules. Each p73 inhibitor may selectively change p73 activity, resulting in an altered p73 'status'. It may be possible to distinguish between relative levels of p73 activity or 'status' in a tumor based on its resultant gene signature. As a demonstration of this process, we identified four categories of p73 target genes in Chapter IV: genes transcriptionally activated by p73, genes transcriptionally repressed by p73, genes transcriptionally repressed by mTOR in a p73-dependent manner, and genes that are only expressed during concurrent mTOR inhibition and p73-depletion. Then we detected these gene signature modules in multiple tumor cohorts. By defining the p73 cistrome and creating a comprehensive resource of p73-bound genes and miRNAs, our work facilitates future analysis of p73 transcriptional programs.

Transcription factors can determine therapeutic outcome and thus can be viable predictors of clinical response as well as targets for cancer drug development. In order to understand how transcription factor signaling predicts patient response or can be modified to benefit the patient, it will be necessary to understand the mechanisms by which cellular stresses modify transcriptional responses. We have presented a model in which upstream signals converge on a transcription factor, causing increased occupancy at selective binding sites. This model highlights the multiple layers of regulation that ultimately allow for exquisite control of gene expression.

Many strategies to identify chemotherapy targets have focused on a 'druggable' part of the genome that is amenable to conventional small-molecule screening but does not include transcription factors. We have developed an approach to identify 'druggable' signaling pathways upstream of transcription factors, identifying and studying mTOR inhibitors such as rapamycin and metformin that modulate p73 (144). Other agents identified in our gene signature-based screen are also potent activators of p73, such as cyclooxygenase that has subsequently been validated as a p73 inhibitor by Irwin and colleagues (313). The advantage to using a gene signature as a readout of a complex cellular change lies not only in the ability to connect pathways, but also in the detection of signaling modules that can stratify tumors into clinically relevant subtypes. From this prospect transcription factors are no longer intractable therapeutic targets, but instead are utilized for their high degree of 'connectivity'.

APPENDIX A

GENERATION AND CHARACTERIZATION OF P73 ANTIBODIES

p73 exists as an array of protein isoforms due to alternative splicing and the presence of a cryptic promoter. These isoforms are a manifestation of its role as a node in a signaling network, a node that can connect multiple inputs into multiple outputs and thus requires a high degree of structural complexity. However, analysis of p73 isoforms, and indeed of p73 in general, is made difficult by a lack of robust and isoform-specific p73 antibodies. Most p73 isoforms have only been detected at the RNA level in vivo, thus their functional significance is unknown.

We provided insight to this issue by asking three questions: 1) Are commercially available p73 antibodies specific or do they cross-react with p53 or p63? 2) Are there adequate antibodies to differentiate the various p73 isoforms, in particular those containing the N-terminal transactivation domain? 3) Can p73 antibodies be used for in vivo detection of p73 protein? As described below, we developed a rigorous system for testing commercial p73 antibodies, and generated new ΔN-specific p73 antibodies that are more robust than their commercial counterparts. We also found that the commonly used p63 antibody, 4A4, can cross-react with p73, which has implications for many studies in the p63 field.

N- and C-terminal p73 antibodies

We assessed antibody specificity by ectopic expression of p63 and p73 isoforms in H1299 lung carcinoma cells that do not express detectable levels of endogenous p53 family proteins. p73 cDNAs were subcloned into the pcDNA3 vector and expressed as hemagluttinin (HA)-tagged TAp73α, TAp73β, TAp73γ, TAp73δ, TAp73ε, ΔNp73α, or ΔNp73β. p63 cDNAs were subcloned into the pCEP4 vector and expressed as untagged TAp63γ or ΔNp63α. We generated protein lysates containing abundant levels of each of these protein isoforms, and immobilized them on Western blots. We fixed parallel cultures of engineered H1299 cells with formalin, and created paraffin-embedded cell pellets that we used to make a cell/tissue microarray (p73 C/TMA). This C/TMA contains punches from H1299:p73 cell blocks, in addition to formalin-fixed, paraffin-embedded cancer cell lines and punches from human tumors (see Figure A1 for C/TMA map). Our parallel approaches allowed us to screen p73 antibodies by Western, immunohistochemistry (IHC), and immunofluorescence (IF). The assessment of p73 antibodies by Western is exemplified by Figure A2; the p73 antibody Ab4 was highly specific for the α and β C-terminal isoforms of p73.

Several p73 RNA isoforms are expressed at low levels in normal cell types (137,314,315). Our over-expression approach allowed us to obtain information about the specificity and sensitivity of antibodies for these isoforms. We first tested the TA and ΔN classes of p73 proteins.

BEVELED EDGE OF BLOCK

pcDNA3	Tap73 Alpha	TAp73 Beta	TAp73 Gamma	TAp73 Delta	DNp73 Alpha	DNp73 Beta	DNp73 Epsilon
PCEP4	TAP63 Gamma	DNp63 Alpha	MDA231-M	MDA231-R	RH30-M	RH30-R	T47D Methanol
T47D Rapamycin	SW620	SCC1	SCC6	SCC17B	Tongue SCC	pcDNA3	Tap73 Alpha
TAp73 Beta	TAp73 Gamma	TAp73 Delta	DNp73 Alpha	DNp73 Beta	DNp73 Epsilon	PCEP4	TAP63 Gamma
DNp63 Alpha	MDA231-M	MDA231-R	RH30-M	RH30-R	T47D Methanol	T47D Rapamycin	SW620
SCC1	SCC6	SCC17B	Tongue SCC	pcDNA3	Tap73 Alpha	TAp73 Beta	TAp73 Gamma
TAp73 Delta	DNp73 Alpha	DNp73 Beta	DNp73 Epsilon	PCEP4	TAP63 Gamma	DNp63 Alpha	MDA231-M
MDA231-R	RH30-M	RH30-R	T47D Methanol	T47D Rapamycin	SW620	SCC1	SCC6
SCC17B	Tongue SCC						

Figure A1: Map of C/TMA used for antibody screening. H1299 lysates expressing the indicated p63 or p73 isoforms, cell lines (M = treated with methanol vehicle, R = treated with 40 nM rapamycin for 24 h), and a tongue squamous cell carcinoma are represented on the block in triplicate. Subsequent versions of the p73 C/TMA (similar to the above) were constructed by Tracy Triplett and Kimberly Johnson.

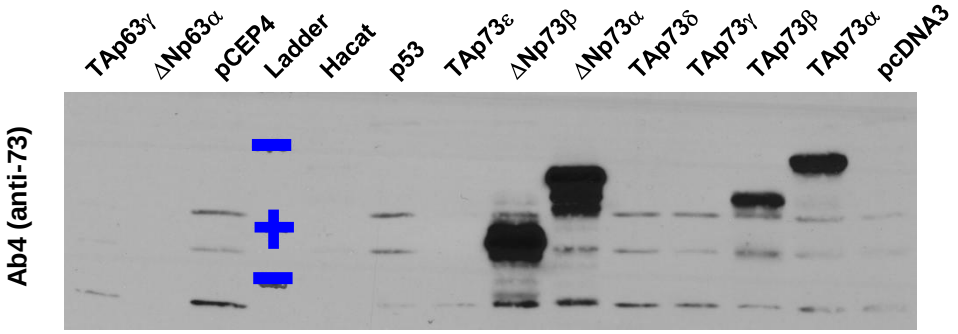

Figure A2: Western blot analysis of Ab4 reactivity against p63 and p73 isoforms. Lysates from H1299 cells transiently transfected with the indicated vectors (control or expressing p63 or p73 isoforms) were analyzed by Western blot. An antibody targeting C-terminal domains was assessed. This antibody, Ab4, is a cocktail of three monoclonal antibodies that recognize domains specific to α or β C-terminal domains. The blue bars indicate the molecular weight marker (82 kDa = top, 64 kDa = cross, 49 kDa = bottom mark). Western blot analysis was performed by Tracy Triplett.

In Chapters III-V we focused our studies on the TAp73 isoforms, because these isoforms were shown to have potent transactivation capability (137). Based on our results, future studies on the impact of the mTOR pathway on ΔNp73 are warranted. We therefore tested the ability of commercial antibodies, raised against N-terminal epitopes, to distinguish between TAp73 and ΔNp73.

As shown in Figure A3, two commercial antibodies were specific for TAp73 by Western blot: A300-126A (Bethyl) and IMG-246 (Imgenex). IMG-246 generated no detectable signal when tested by IHC, however there were other commercially available antibodies that were specific for TAp73 by IHC (Bethyl-IHC and H-79). As the experiments described in this Appendix were underway, there was only one commercially available antibody against the ΔNp73-specific epitope (clone 38C674; available through either Calbiochem or Imgenex). This antibody was specific but only weakly detected ΔNp73α and ΔNp73β (Figure A3). Detection was significantly hampered by the presence of a non-specific cross-reacting protein that migrates slightly slower than ΔNp73α (Figure A3).

Because of the apparent deficiency in ΔNp73-specific antibodies, we contracted with two groups to generate new antibodies in both mice (the Vanderbilt Monoclonal Antibody Core) and rabbits (Bethyl Laboratories). Animals were immunized with a peptide containing unique residues at the N-terminus of ΔNp73 (MLYVGDPARHLA). We used our over-expression screening system to test polyclonal sera and monoclonal supernatants during the production process by both Western blot and IHC.

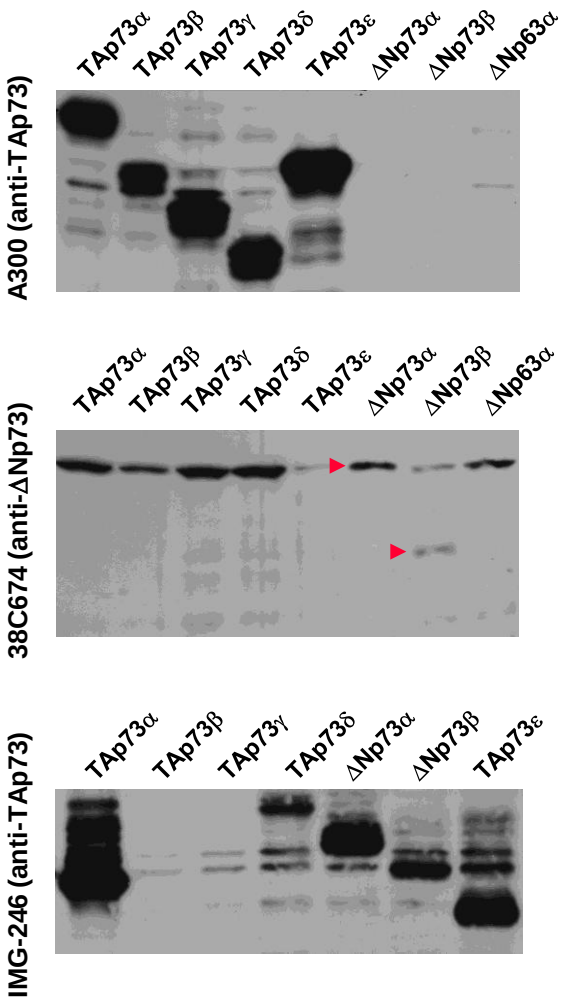

Figure A3: Western blot analysis of A300, 38C674, and IMG-246 reactivity against p63 and p73 isoforms. Lysates from H1299 cells transiently transfected with the indicated vectors (control or expressing p63 or p73 isoforms) were analyzed by Western blot. Three antibodies targeting N-terminal domains were assessed: A300 (top panel, anti-TAp73), 38C674 (middle panel, anti-ΔNp73), and IMG-246 (bottom panel, anti-TAp73). The red arrowheads show the locations of ΔNp73α and ΔNp73β. Additional Westerns were performed to confirm lack of reactivity of A300 and IMG-246 with TAp63. Western blot analysis was performed by Tracy Triplett.

Polyclonal mouse and rabbit antibodies were highly specific for ΔNp73 protein isoforms by Western blot (Figure A4). While polyclonal mouse antibodies were also specific and robust by IHC, polyclonal rabbit antibody did not give any signal by IHC.

We repeatedly attempted to generate monoclonal mouse antibodies but were unsuccessful, only polyclonal antibodies were able to detect ΔNp73 protein. Therefore, we terminally bled the remaining mice to collect ~2 mls of antibody from each mouse, representing a limited supply of antibody that could be used at 1:1000 for Western blotting. TAp73-specific polyclonal mouse antibodies were similarly generated for comparison studies of the two isoforms (data not shown). The polyclonal antibodies that were collected are listed in Table A1.

Cross-reactivity of pan-p63 and p73 antibodies

As shown in Figures A2 and A3, N- and C-terminal p73 antibodies are highly specific for the appropriate isoforms of p73, and do not cross-react with p63. However, p63 and p73 only share 30% sequence identity at the N-terminus (Table 1). In contrast, p63/p73 homology is 87% in the DNA-binding domain (Table 1). Therefore we assessed the reactivity of pan-p63 and pan-p73 antibodies, raised against DNA-binding domain epitopes, with p63 and p73 proteins. Interestingly, the pan-p73 antibody (IMG-259) detected p63 isoforms, and the pan-p63 antibody (4A4) detected p73 isoforms (Figure A5).

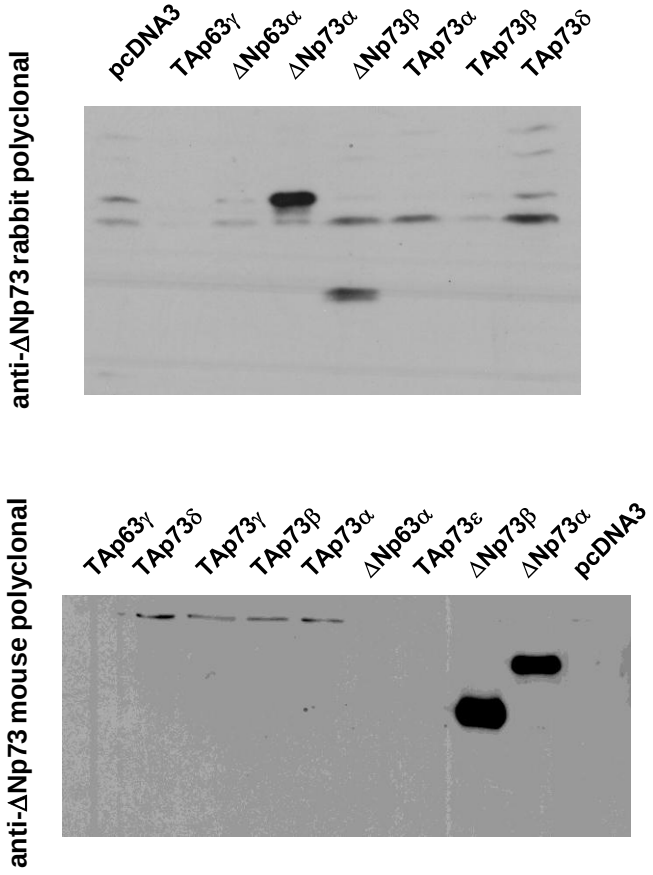

Figure A4: Assessment of custom polyclonal antibodies by Western blot. Antibodies were generated against a peptide specific to the N-terminus of ΔNp73 isoforms only. Both rabbit (top panel) and mouse (bottom panel) polyclonal antibodies were used to probe Western blots. Westerns blotting was used to analyze lysates from H1299 cells transiently transfected with vectors, either control or expressing p63 or p73 isoforms as indicated. Western analysis with mouse polyclonal antibodies was performed by Tracy Triplett.

Table A1: Mouse polyclonal sera, anti-TAp73 or anti-ΔNp73. Twenty-eight mice were immunized with peptides specific to either TAp73 or ΔNp73, and polyclonal sera were collected after each boost and tested by immunohistochemistry and Western blot. Antibodies were specific by Western, and cross-reactivity by IHC was only observed as indicated. Sera collected before immunization (pre-bleeds) were all negative for reactivity with p73 proteins. * = weak positive signal. + = strong non-specific band runs near ΔNp73α on Western blot. IHC analyses were performed by Melinda Sanders, Violeta Sanchez, Maria Olivares, and Kimberly Johnson.

Mouse (antigen, strain, tag)	Cross-reactivity?	Background?	Fusion for monoclonal attempted (otherwise terminally bled)
- 2007, ΔNp73 polyclonal sera			
AJ L			
AJ RL	minimal with TAp73 by IHC	None	
BALB 0		None	2nd fusion attempt (parvovirus infection prevented class-switching)
BALB RL	yes, with TAp73 by IHC		
BALB L		None	
BALB R		None	1st fusion attempt (contamination)
AJ R			
AJ 0	minimal with p63 by IHC		
- 2007, TAp73 polyclonal sera			
BALB RL		Yes	
BALB 0	minimal with ΔNp73 by IHC		
AJ R	yes, with ΔNp73 by IHC		
BALB L		Yes	
AJ 0			
BALB R		Yes	
AJ L			
AJ RL		Yes	
- 2008, ΔNp73 polyclonal sera			
Balb L - Test			Yes, but no monoclonals resulted
Balb 0 - Test			
Balb R - Test*			
Balb RL - Test*	yes, with TAp73		
AJ RL	yes, with TAp63		
BALB R+			
AJ L*			
AJ R*	yes, with TAp73		
BALB RL			Yes, but no monoclonals resulted
BALB L			
BALB 0	minimal with TAp73	Yes	
AJ 0			

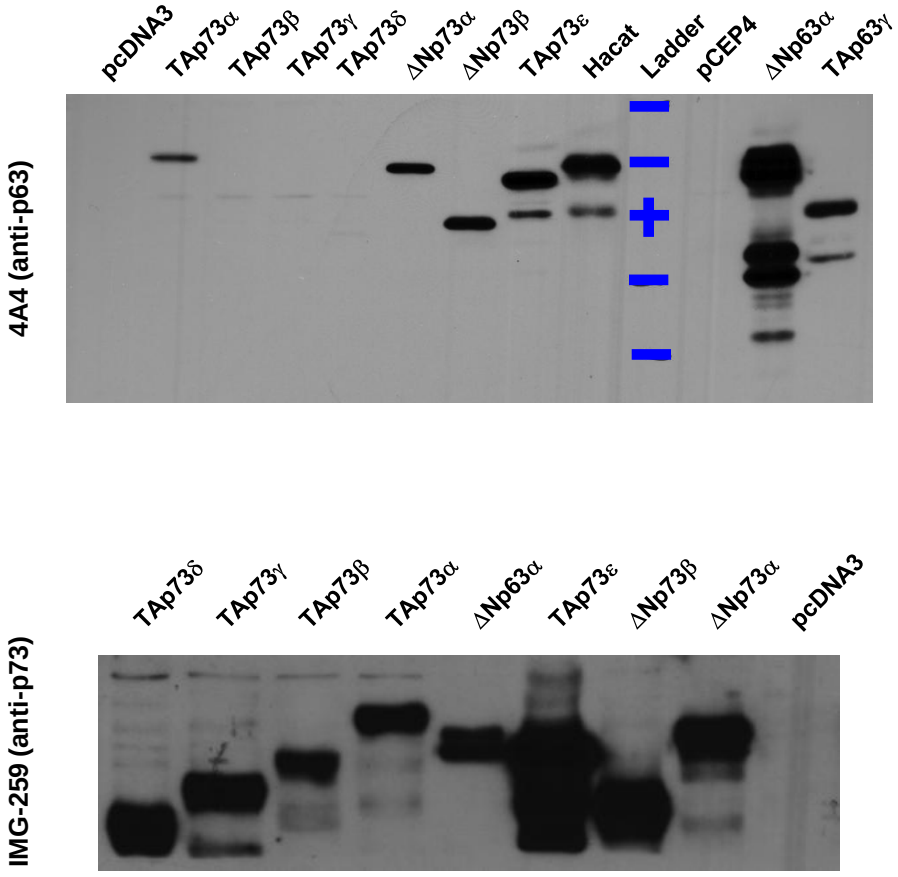

Figure A5: Western blot analysis of 4A4 and IMG-259 reactivity against p63 and p73 isoforms. Lysates from H1299 cells transiently transfected with vectors (expressing the indicated p63 or p73 isoforms) were analyzed by Western blot. Two antibodies recognizing epitopes in the DNA-binding domains were assessed: 4A4 (top panel, anti-p63) and IMG-259 (bottom panel, anti-p73). Blue bars indicate molecular weight markers (cross = 64 kDa). Western analysis was perfomed by Tracy Triplett.

These results are particularly notable for the p63 antibody, 4A4, as this antibody has been widely used to study p63. Many studies were performed when there were fewer commercially available alternatives for detection of p63 protein, due in part to the robustness of 4A4. The cross-reactivity of 4A4 with p73 thus has potential wide-ranging implications, particularly for studies of p63 and p73 correlative expression in human tumors. Of note, we tested 4A4 by IHC, and again saw cross-reactivity with p73 protein.

Immunofluorescence analyses

We assessed the ability of commercially available antibodies to detect p73 by IF, using paraffin-embedded cell blocks as above. TAp73-specific antibodies (Bethyl-IHC and IMG-246), a ΔNp73-specific antibody (38C674), and a pan-p73 antibody (IMG-259) all detected only the appropriate p73 isoforms and did not cross-react with p63 (Figure A6A). C-terminal p73 antibodies that preferentially recognize α or β isoforms (components of the Ab4 monoclonal antibody cocktail) were also relatively specific for either p73α or p73β respectively (Figure A6B). We assessed endogenous p73 in BPH prostate cells grown on glass coverslips and fixed with paraformaldehyde. The IMG-259 antibody was positive by IF in BPH nuclei, and the signal both increased after rapamycin treatment and correlated with expression of a p73 cofactor, YAP (Figure A7).

Thus, the results presented above have significant implications for a variety of techniques and methods that analyze members of the large collection of p53 family proteins. We propose re-evaluation of studies that relied on 4A4 or IMG-259, particularly IHC and IF studies. p63 and p73 antibodies, particularly those that recognize the DNA-binding domain, should be carefully evaluated for cross-reactivity.

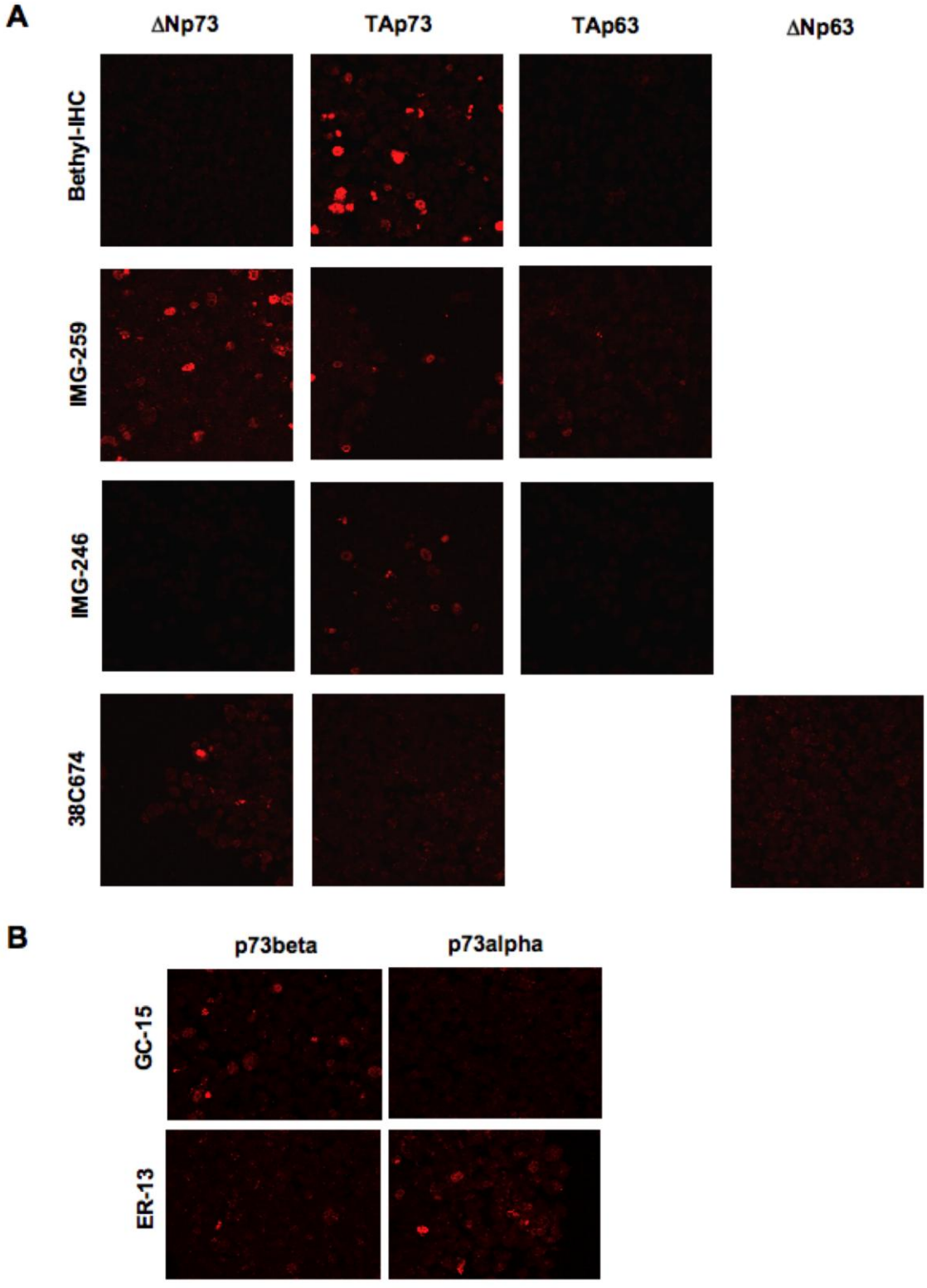

Figure A6: Assessment of commercial p73 antibodies by immunofluorescence. The indicated p73 isoforms were over-expressed in H1299 cells. Cells were fixed, paraffin embedded, and immunofluorescence performed using the indicated antibodies to determine cross-reactivity against other p73 isoforms (A and B), or against p63 (A).

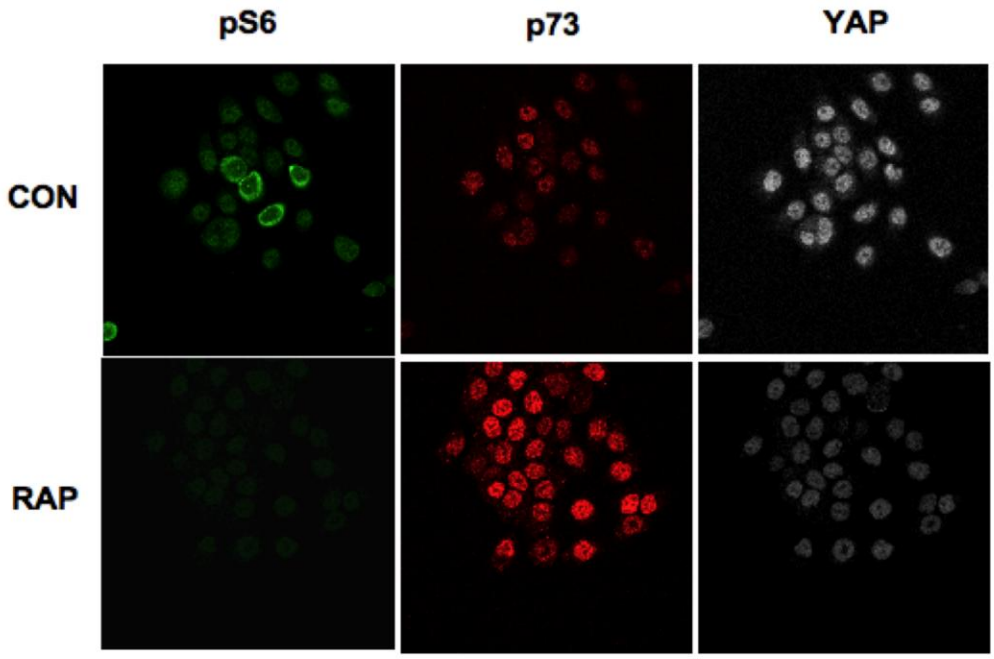

Figure A7: Immunofluorescence analysis of BPH cells. BPH cells grown on coverslips were treated in serum-free media with 40 nM rapamycin (RAP) or vehicle (CON) for 32 h. Immunofluorescence was performed with three antibodies that detect phospho-S6 (pS6), p73, and YAP, and confocal microscopy was performed.

REFERENCES

1. Babu, M. M., Luscombe, N. M., Aravind, L., Gerstein, M., and Teichmann, S. A. (2004) *Current opinion in structural biology* **14**(3), 283-291

2. Wilson, D., Charoensawan, V., Kummerfeld, S. K., and Teichmann, S. A. (2008) *Nucleic acids research* **36**(Database issue), D88-92

3. Mees, C., Nemunaitis, J., and Senzer, N. (2009) *Cancer gene therapy* **16**(2), 103-112

4. Krueger, C., and Osborne, C. S. (2006) *Trends Genet* **22**(12), 637-639

5. Fullwood, M. J., and Ruan, Y. (2009) *Journal of cellular biochemistry* **107**(1), 30-39

6. Xu, M., and Cook, P. R. (2008) *The Journal of cell biology* **181**(4), 615-623

7. Xu, M., and Cook, P. R. (2008) *Biochimica et biophysica acta* **1783**(11), 2155-2160

8. Odom, D. T., Dowell, R. D., Jacobsen, E. S., Gordon, W., Danford, T. W., MacIsaac, K. D., Rolfe, P. A., Conboy, C. M., Gifford, D. K., and Fraenkel, E. (2007) *Nature genetics* **39**(6), 730-732

9. Wilson, M. D., Barbosa-Morais, N. L., Schmidt, D., Conboy, C. M., Vanes, L., Tybulewicz, V. L., Fisher, E. M., Tavare, S., and Odom, D. T. (2008) *Science* **322**(5900), 434-438

10. Takahashi, K., Tanabe, K., Ohnuki, M., Narita, M., Ichisaka, T., Tomoda, K., and Yamanaka, S. (2007) *Cell* **131**(5), 861-872

11. Kocaefe, Y. C., Israeli, D., Ozguc, M., Danos, O., and Garcia, L. (2005) *Experimental cell research* **308**(2), 300-308

12. Cretekos, C. J., Wang, Y., Green, E. D., Martin, J. F., Rasweiler, J. J. t., and Behringer, R. R. (2008) *Genes & development* **22**(2), 141-151

13. Yang, A., Zhu, Z., Kapranov, P., McKeon, F., Church, G. M., Gingeras, T. R., and Struhl, K. (2006) *Molecular cell* **24**(4), 593-602

14. Johnson, D. S., Li, W., Gordon, D. B., Bhattacharjee, A., Curry, B., Ghosh, J., Brizuela, L., Carroll, J. S., Brown, M., Flicek, P., Koch, C. M., Dunham, I., Bieda, M., Xu, X., Farnham, P. J., Kapranov, P., Nix, D. A., Gingeras, T. R., Zhang, X., Holster, H., Jiang, N., Green, R. D., Song, J. S., McCuine, S. A., Anton, E., Nguyen, L., Trinklein, N. D., Ye, Z., Ching, K., Hawkins, D., Ren, B.,

Scacheri, P. C., Rozowsky, J., Karpikov, A., Euskirchen, G., Weissman, S., Gerstein, M., Snyder, M., Yang, A., Moqtaderi, Z., Hirsch, H., Shulha, H. P., Fu, Y., Weng, Z., Struhl, K., Myers, R. M., Lieb, J. D., and Liu, X. S. (2008) *Genome research* **18**(3), 393-403

15. Cawley, S., Bekiranov, S., Ng, H. H., Kapranov, P., Sekinger, E. A., Kampa, D., Piccolboni, A., Sementchenko, V., Cheng, J., Williams, A. J., Wheeler, R., Wong, B., Drenkow, J., Yamanaka, M., Patel, S., Brubaker, S., Tammana, H., Helt, G., Struhl, K., and Gingeras, T. R. (2004) *Cell* **116**(4), 499-509

16. Johnson, D. S., Mortazavi, A., Myers, R. M., and Wold, B. (2007) *Science* **316**(5830), 1497-1502

17. Wingender, E., Dietze, P., Karas, H., and Knuppel, R. (1996) *Nucleic acids research* **24**(1), 238-241

18. Robertson, A. G., Bilenky, M., Tam, A., Zhao, Y., Zeng, T., Thiessen, N., Cezard, T., Fejes, A. P., Wederell, E. D., Cullum, R., Euskirchen, G., Krzywinski, M., Birol, I., Snyder, M., Hoodless, P. A., Hirst, M., Marra, M. A., and Jones, S. J. (2008) *Genome research* **18**(12), 1906-1917

19. Schones, D. E., and Zhao, K. (2008) *Nat Rev Genet* **9**(3), 179-191

20. Bernstein, B. E., Mikkelsen, T. S., Xie, X., Kamal, M., Huebert, D. J., Cuff, J., Fry, B., Meissner, A., Wernig, M., Plath, K., Jaenisch, R., Wagschal, A., Feil, R., Schreiber, S. L., and Lander, E. S. (2006) *Cell* **125**(2), 315-326

21. Lupien, M., Eeckhoute, J., Meyer, C. A., Wang, Q., Zhang, Y., Li, W., Carroll, J. S., Liu, X. S., and Brown, M. (2008) *Cell* **132**(6), 958-970

22. Blandino, G., and Dobbelstein, M. (2004) *Cell cycle (Georgetown, Tex* **3**(7), 886-894

23. Moll, U. M., and Slade, N. (2004) *Mol Cancer Res* **2**(7), 371-386

24. Bjorkqvist, A. M., Husgafvel-Pursiainen, K., Anttila, S., Karjalainen, A., Tammilehto, L., Mattson, K., Vainio, H., and Knuutila, S. (1998) *Genes, chromosomes & cancer* **22**(1), 79-82

25. Hibi, K., Trink, B., Patturajan, M., Westra, W. H., Caballero, O. L., Hill, D. E., Ratovitski, E. A., Jen, J., and Sidransky, D. (2000) *Proc Natl Acad Sci U S A* **97**(10), 5462-5467

26. Massion, P. P., Taflan, P. M., Jamshedur Rahman, S. M., Yildiz, P., Shyr, Y., Edgerton, M. E., Westfall, M. D., Roberts, J. R., Pietenpol, J. A., Carbone, D. P., and Gonzalez, A. L. (2003) *Cancer Res* **63**(21), 7113-7121

27. Yang, A., Schweitzer, R., Sun, D., Kaghad, M., Walker, N., Bronson, R. T., Tabin, C., Sharpe, A., Caput, D., Crum, C., and McKeon, F. (1999) *Nature* **398**(6729), 714-718

28. Yang, A., Walker, N., Bronson, R., Kaghad, M., Oosterwegel, M., Bonnin, J., Vagner, C., Bonnet, H., Dikkes, P., Sharpe, A., McKeon, F., and Caput, D. (2000) *Nature* **404**(6773), 99-103

29. Yang, A., Kaghad, M., Wang, Y., Gillett, E., Fleming, M. D., Dotsch, V., Andrews, N. C., Caput, D., and McKeon, F. (1998) *Molecular cell* **2**(3), 305-316

30. Stiewe, T., and Putzer, B. M. (2000) *Nature genetics* **26**(4), 464-469

31. Agami, R., Blandino, G., Oren, M., and Shaul, Y. (1999) *Nature* **399**(6738), 809-813

32. Gong, J. G., Costanzo, A., Yang, H. Q., Melino, G., Kaelin, W. G., Jr., Levrero, M., and Wang, J. Y. (1999) *Nature* **399**(6738), 806-809

33. Jost, C. A., Marin, M. C., and Kaelin, W. G., Jr. (1997) *Nature* **389**(6647), 191-194

34. Yuan, Z. M., Shioya, H., Ishiko, T., Sun, X., Gu, J., Huang, Y. Y., Lu, H., Kharbanda, S., Weichselbaum, R., and Kufe, D. (1999) *Nature* **399**(6738), 814-817

35. Murray-Zmijewski, F., Lane, D. P., and Bourdon, J. C. (2006) *Cell Death Differ* **13**(6), 962-972

36. Bourdon, J. C., Fernandes, K., Murray-Zmijewski, F., Liu, G., Diot, A., Xirodimas, D. P., Saville, M. K., and Lane, D. P. (2005) *Genes & development* **19**(18), 2122-2137

37. Deyoung, M. P., and Ellisen, L. W. (2007) *Oncogene* **26**(36), 5169-5183

38. Harms, K. L., and Chen, X. (2006) *Cell Death Differ* **13**(6), 890-897

39. Scoumanne, A., Harms, K. L., and Chen, X. (2005) *Cancer biology & therapy* **4**(11), 1178-1185

40. Ghosh, A., Stewart, D., and Matlashewski, G. (2004) *Mol Cell Biol* **24**(18), 7987-7997

41. Harms, K., Nozell, S., and Chen, X. (2004) *Cell Mol Life Sci* **61**(7-8), 822-842

42. Liu, G., Nozell, S., Xiao, H., and Chen, X. (2004) *Mol Cell Biol* **24**(2), 487-501

43. Oswald, C., and Stiewe, T. (2008) *Cell cycle (Georgetown, Tex* **7**(12), 1726-1731

44. Brunner, H. G., Hamel, B. C., and Van Bokhoven, H. (2002) *Journal of medical genetics* **39**(6), 377-381

45. el-Deiry, W. S., Kern, S. E., Pietenpol, J. A., Kinzler, K. W., and Vogelstein, B. (1992) *Nature genetics* **1**(1), 45-49

46. Jordan, J. J., Menendez, D., Inga, A., Nourredine, M., Bell, D., and Resnick, M. A. (2008) *PLoS genetics* **4**(6), e1000104

47. Osada, M., Park, H. L., Nagakawa, Y., Yamashita, K., Fomenkov, A., Kim, M. S., Wu, G., Nomoto, S., Trink, B., and Sidransky, D. (2005) *Mol Cell Biol* **25**(14), 6077-6089

48. Perez, C. A., Ott, J., Mays, D. J., and Pietenpol, J. A. (2007) *Oncogene*

49. Liang, S. H., and Clarke, M. F. (1999) *Oncogene* **18**(12), 2163-2166

50. Inoue, T., Stuart, J., Leno, R., and Maki, C. G. (2002) *J Biol Chem* **277**(17), 15053-15060

51. Chene, P. (2001) *Oncogene* **20**(21), 2611-2617

52. Qiao, F., and Bowie, J. U. (2005) *Sci STKE* **2005**(286), re7

53. Barrera, F. N., Poveda, J. A., Gonzalez-Ros, J. M., and Neira, J. L. (2003) *J Biol Chem* **278**(47), 46878-46885

54. Vilgelm, A., El-Rifai, W., and Zaika, A. (2008) *Drug Resist Updat* **11**(4-5), 152-163

55. Zaika, A. I., Slade, N., Erster, S. H., Sansome, C., Joseph, T. W., Pearl, M., Chalas, E., and Moll, U. M. (2002) *J Exp Med* **196**(6), 765-780

56. Rocco, J. W., Leong, C. O., Kuperwasser, N., DeYoung, M. P., and Ellisen, L. W. (2006) *Cancer Cell* **9**(1), 45-56

57. Leong, C. O., Vidnovic, N., DeYoung, M. P., Sgroi, D., and Ellisen, L. W. (2007) *The Journal of clinical investigation* **117**(5), 1370-1380

58. Deyoung, M. P., Johannessen, C. M., Leong, C. O., Faquin, W., Rocco, J. W., and Ellisen, L. W. (2006) *Cancer Res* **66**(19), 9362-9368

59. Di Como, C. J., Gaiddon, C., and Prives, C. (1999) *Mol Cell Biol* **19**(2), 1438-1449

60. Anensen, N., Oyan, A. M., Bourdon, J. C., Kalland, K. H., Bruserud, O., and Gjertsen, B. T. (2006) *Clin Cancer Res* **12**(13), 3985-3992

61. Boldrup, L., Bourdon, J. C., Coates, P. J., Sjostrom, B., and Nylander, K. (2007) *Eur J Cancer* **43**(3), 617-623

62. Ebrahimi, M., Boldrup, L., Coates, P. J., Wahlin, Y. B., Bourdon, J. C., and Nylander, K. (2008) *Oral oncology* **44**(2), 156-161

63. McKeon, F., and Melino, G. (2007) *Cell cycle (Georgetown, Tex* **6**(3), 229-232

64. Mills, A. A. (2006) *Curr Opin Genet Dev* **16**(1), 38-44

65. Tomasini, R., Tsuchihara, K., Wilhelm, M., Fujitani, M., Rufini, A., Cheung, C. C., Khan, F., Itie-Youten, A., Wakeham, A., Tsao, M. S., Iovanna, J. L., Squire, J., Jurisica, I., Kaplan, D., Melino, G., Jurisicova, A., and Mak, T. W. (2008) *Genes & development* **22**(19), 2677-2691

66. Flores, E. R., Sengupta, S., Miller, J. B., Newman, J. J., Bronson, R., Crowley, D., Yang, A., McKeon, F., and Jacks, T. (2005) *Cancer Cell* **7**(4), 363-373

67. Keyes, W. M., Vogel, H., Koster, M. I., Guo, X., Qi, Y., Petherbridge, K. M., Roop, D. R., Bradley, A., and Mills, A. A. (2006) *Proc Natl Acad Sci U S A* **103**(22), 8435-8440

68. Wolff, S., Talos, F., Palacios, G., Beyer, U., Dobbelstein, M., and Moll, U. M. (2009) *Cell Death Differ*

69. Flores, E. R., Tsai, K. Y., Crowley, D., Sengupta, S., Yang, A., McKeon, F., and Jacks, T. (2002) *Nature* **416**(6880), 560-564

70. Senoo, M., Manis, J. P., Alt, F. W., and McKeon, F. (2004) *Cancer Cell* **6**(1), 85-89

71. Jacobs, W. B., Kaplan, D. R., and Miller, F. D. (2006) *Journal of neurochemistry* **97**(6), 1571-1584

72. Suh, E. K., Yang, A., Kettenbach, A., Bamberger, C., Michaelis, A. H., Zhu, Z., Elvin, J. A., Bronson, R. T., Crum, C. P., and McKeon, F. (2006) *Nature* **444**(7119), 624-628

73. Bagchi, A., Papazoglu, C., Wu, Y., Capurso, D., Brodt, M., Francis, D., Bredel, M., Vogel, H., and Mills, A. A. (2007) *Cell* **128**(3), 459-475

74. Pluta, A., Nyman, U., Joseph, B., Robak, T., Zhivotovsky, B., and Smolewski, P. (2006) *Leukemia* **20**(5), 757-766

75. Zaika, A. I., and El-Rifai, W. (2006) *Cell Death Differ* **13**(6), 935-940

76. Dominguez, G., Garcia, J. M., Pena, C., Silva, J., Garcia, V., Martinez, L., Maximiano, C., Gomez, M. E., Rivera, J. A., Garcia-Andrade, C., and Bonilla, F. (2006) *J Clin Oncol* **24**(5), 805-815

77. Irwin, M., Marin, M. C., Phillips, A. C., Seelan, R. S., Smith, D. I., Liu, W., Flores, E. R., Tsai, K. Y., Jacks, T., Vousden, K. H., and Kaelin, W. G., Jr. (2000) *Nature* **407**(6804), 645-648

78. Lissy, N. A., Davis, P. K., Irwin, M., Kaelin, W. G., and Dowdy, S. F. (2000) *Nature* **407**(6804), 642-645

79. Muller, M., Schleithoff, E. S., Stremmel, W., Melino, G., Krammer, P. H., and Schilling, T. (2006) *Drug Resist Updat* **9**(6), 288-306

80. Liu, S. S., Chan, K. Y., Cheung, A. N., Liao, X. Y., Leung, T. W., and Ngan, H. Y. (2006) *Clin Cancer Res* **12**(13), 3922-3927

81. Zhu, J., Jiang, J., Zhou, W., and Chen, X. (1998) *Cancer Res* **58**(22), 5061-5065

82. Smeenk, L., van Heeringen, S. J., Koeppel, M., van Driel, M. A., Bartels, S. J., Akkers, R. C., Denissov, S., Stunnenberg, H. G., and Lohrum, M. (2008) *Nucleic acids research* **36**(11), 3639-3654

83. Cui, R., Nguyen, T. T., Taube, J. H., Stratton, S. A., Feuerman, M. H., and Barton, M. C. (2005) *J Biol Chem* **280**(47), 39152-39160

84. Zheng, X., and Chen, X. (2001) *FEBS Lett* **489**(1), 4-7

85. Sasaki, Y., Ishida, S., Morimoto, I., Yamashita, T., Kojima, T., Kihara, C., Tanaka, T., Imai, K., Nakamura, Y., and Tokino, T. (2002) *J Biol Chem* **277**(1), 719-724

86. Wei, C. L., Wu, Q., Vega, V. B., Chiu, K. P., Ng, P., Zhang, T., Shahab, A., Yong, H. C., Fu, Y., Weng, Z., Liu, J., Zhao, X. D., Chew, J. L., Lee, Y. L., Kuznetsov, V. A., Sung, W. K., Miller, L. D., Lim, B., Liu, E. T., Yu, Q., Ng, H. H., and Ruan, Y. (2006) *Cell* **124**(1), 207-219

87. Shaked, H., Shiff, I., Kott-Gutkowski, M., Siegfried, Z., Haupt, Y., and Simon, I. (2008) *Cancer Res* **68**(23), 9671-9677

88. Hearnes, J. M., Mays, D. J., Schavolt, K. L., Tang, L., Jiang, X., and Pietenpol, J. A. (2005) *Mol Cell Biol* **25**(22), 10148-10158

89. Zeng, X., Chen, L., Jost, C. A., Maya, R., Keller, D., Wang, X., Kaelin, W. G., Jr., Oren, M., Chen, J., and Lu, H. (1999) *Mol Cell Biol* **19**(5), 3257-3266

90. Strano, S., Monti, O., Pediconi, N., Baccarini, A., Fontemaggi, G., Lapi, E., Mantovani, F., Damalas, A., Citro, G., Sacchi, A., Del Sal, G., Levrero, M., and Blandino, G. (2005) *Molecular cell* **18**(4), 447-459

91. Levy, D., Adamovich, Y., Reuven, N., and Shaul, Y. (2007) *Cell Death Differ* **14**(4), 743-751

92. Strano, S., Munarriz, E., Rossi, M., Castagnoli, L., Shaul, Y., Sacchi, A., Oren, M., Sudol, M., Cesareni, G., and Blandino, G. (2001) *J Biol Chem* **276**(18), 15164-15173

93. Urist, M., Tanaka, T., Poyurovsky, M. V., and Prives, C. (2004) *Genes & development* **18**(24), 3041-3054

94. Talos, F., Nemajerova, A., Flores, E. R., Petrenko, O., and Moll, U. M. (2007) *Molecular cell* **27**(4), 647-659

95. Shimodaira, H., Yoshioka-Yamashita, A., Kolodner, R. D., and Wang, J. Y. (2003) *Proc Natl Acad Sci U S A* **100**(5), 2420-2425

96. Budanov, A. V., and Karin, M. (2008) *Cell* **134**(3), 451-460

97. Irwin, M. S., Kondo, K., Marin, M. C., Cheng, L. S., Hahn, W. C., and Kaelin, W. G., Jr. (2003) *Cancer Cell* **3**(4), 403-410

98. Rosenbluth, J. M., and Pietenpol, J. A. (2008) *Genes & development* **22**(19), 2591-2595

99. Bourdon, J. C. (2007) *British journal of cancer* **97**(3), 277-282

100. Beitzinger, M., Hofmann, L., Oswald, C., Beinoraviciute-Kellner, R., Sauer, M., Griesmann, H., Bretz, A. C., Burek, C., Rosenwald, A., and Stiewe, T. (2008) *The EMBO journal* **27**(5), 792-803

101. Guertin, D. A., and Sabatini, D. M. (2007) *Cancer Cell* **12**(1), 9-22

102. Mita, M. M., Mita, A., and Rowinsky, E. K. (2003) *Clinical breast cancer* **4**(2), 126-137

103. Kim, D. H., Sarbassov, D. D., Ali, S. M., Latek, R. R., Guntur, K. V., Erdjument-Bromage, H., Tempst, P., and Sabatini, D. M. (2003) *Molecular cell* **11**(4), 895-904

104. Loewith, R., Jacinto, E., Wullschleger, S., Lorberg, A., Crespo, J. L., Bonenfant, D., Oppliger, W., Jenoe, P., and Hall, M. N. (2002) *Molecular cell* **10**(3), 457-468

105. Pearce, L. R., Huang, X., Boudeau, J., Pawlowski, R., Wullschleger, S., Deak, M., Ibrahim, A. F., Gourlay, R., Magnuson, M. A., and Alessi, D. R. (2007) *The Biochemical journal* **405**(3), 513-522

106. Sarbassov, D. D., Ali, S. M., Kim, D. H., Guertin, D. A., Latek, R. R., Erdjument-Bromage, H., Tempst, P., and Sabatini, D. M. (2004) *Curr Biol* **14**(14), 1296-1302

107. Jung, C. H., Jun, C. B., Ro, S. H., Kim, Y. M., Otto, N. M., Cao, J., Kundu, M., and Kim, D. H. (2009) *Molecular biology of the cell* **20**(7), 1992-2003

108. Hosokawa, N., Hara, T., Kaizuka, T., Kishi, C., Takamura, A., Miura, Y., Iemura, S., Natsume, T., Takehana, K., Yamada, N., Guan, J. L., Oshiro, N., and Mizushima, N. (2009) *Molecular biology of the cell* **20**(7), 1981-1991

109. Garcia-Martinez, J. M., and Alessi, D. R. (2008) *The Biochemical journal* **416**(3), 375-385

110. Levine, A. J., Feng, Z., Mak, T. W., You, H., and Jin, S. (2006) *Genes & development* **20**(3), 267-275

111. Sarbassov, D. D., Guertin, D. A., Ali, S. M., and Sabatini, D. M. (2005) *Science* **307**(5712), 1098-1101

112. Shaw, R. J., Bardeesy, N., Manning, B. D., Lopez, L., Kosmatka, M., DePinho, R. A., and Cantley, L. C. (2004) *Cancer Cell* **6**(1), 91-99

113. Jones, K. T., Greer, E. R., Pearce, D., and Ashrafi, K. (2009) *PLoS biology* **7**(3), e60

114. Soukas, A. A., Kane, E. A., Carr, C. E., Melo, J. A., and Ruvkun, G. (2009) *Genes & development* **23**(4), 496-511

115. Guertin, D. A., Stevens, D. M., Saitoh, M., Kinkel, S., Crosby, K., Sheen, J. H., Mullholland, D. J., Magnuson, M. A., Wu, H., and Sabatini, D. M. (2009) *Cancer Cell* **15**(2), 148-159

116. Feng, Z., Hu, W., de Stanchina, E., Teresky, A. K., Jin, S., Lowe, S., and Levine, A. J. (2007) *Cancer Res* **67**(7), 3043-3053

117. Ellisen, L. W., Ramsayer, K. D., Johannessen, C. M., Yang, A., Beppu, H., Minda, K., Oliner, J. D., McKeon, F., and Haber, D. A. (2002) *Molecular cell* **10**(5), 995-1005

118. Deyoung, M. P., Horak, P., Sofer, A., Sgroi, D., and Ellisen, L. W. (2008) *Genes & development* **22**(2), 239-251

119. Lee, C. H., Inoki, K., Karbowniczek, M., Petroulakis, E., Sonenberg, N., Henske, E. P., and Guan, K. L. (2007) *The EMBO journal* **26**(23), 4812-4823

120. Mondesire, W. H., Jian, W., Zhang, H., Ensor, J., Hung, M. C., Mills, G. B., and Meric-Bernstam, F. (2004) *Clin Cancer Res* **10**(20), 7031-7042

121. Calabro, A., Tai, J., Allen, S. L., and Budman, D. R. (2008) *Anti-cancer drugs* **19**(7), 705-712

122. Tam, K. H., Yang, Z. F., Lau, C. K., Lam, C. T., Pang, R. W., and Poon, R. T. (2009) *Cancer letters* **273**(2), 201-209

123. Shi, Y., Frankel, A., Radvanyi, L. G., Penn, L. Z., Miller, R. G., and Mills, G. B. (1995) *Cancer Res* **55**(9), 1982-1988

124. Mizushima, N., Levine, B., Cuervo, A. M., and Klionsky, D. J. (2008) *Nature* **451**(7182), 1069-1075

125. Crighton, D., Wilkinson, S., O'Prey, J., Syed, N., Smith, P., Harrison, P. R., Gasco, M., Garrone, O., Crook, T., and Ryan, K. M. (2006) *Cell* **126**(1), 121-134

126. Tasdemir, E., Maiuri, M. C., Galluzzi, L., Vitale, I., Djavaheri-Mergny, M., D'Amelio, M., Criollo, A., Morselli, E., Zhu, C., Harper, F., Nannmark, U., Samara, C., Pinton, P., Vicencio, J. M., Carnuccio, R., Moll, U. M., Madeo, F., Paterlini-Brechot, P., Rizzuto, R., Szabadkai, G., Pierron, G., Blomgren, K., Tavernarakis, N., Codogno, P., Cecconi, F., and Kroemer, G. (2008) *Nature cell biology* **10**(6), 676-687

127. Wang, W., Kim, S. H., and El-Deiry, W. S. (2006) *Proc Natl Acad Sci U S A* **103**(29), 11003-11008

128. Bell, H. S., Dufes, C., O'Prey, J., Crighton, D., Bergamaschi, D., Lu, X., Schatzlein, A. G., Vousden, K. H., and Ryan, K. M. (2007) *The Journal of clinical investigation* **117**(4), 1008-1018

129. Das, S., Nama, S., Antony, S., and Somasundaram, K. (2005) *Cancer gene therapy* **12**(4), 417-426

130. Oshima, Y., Sasaki, Y., Negishi, H., Idogawa, M., Toyota, M., Yamashita, T., Wada, T., Nagoya, S., Kawaguchi, S., Yamashita, T., and Tokino, T. (2007) *Cancer biology & therapy* **6**(7), 1058-1066

131. Barbieri, C. E., Tang, L. J., Brown, K. A., and Pietenpol, J. A. (2006) *Cancer Res* **66**(15), 7589-7597

132. Boukamp, P., Petrussevska, R. T., Breitkreutz, D., Hornung, J., Markham, A., and Fusenig, N. E. (1988) *The Journal of cell biology* **106**(3), 761-771

133. Chang, S. B., Miron, P., Miron, A., and Iglehart, J. D. (2007) *The Journal of surgical research* **138**(1), 37-44

134. Ventura, A., Meissner, A., Dillon, C. P., McManus, M., Sharp, P. A., Van Parijs, L., Jaenisch, R., and Jacks, T. (2004) *Proc Natl Acad Sci U S A* **101**(28), 10380-10385

135. He, T. C., Zhou, S., da Costa, L. T., Yu, J., Kinzler, K. W., and Vogelstein, B. (1998) *Proc Natl Acad Sci U S A* **95**(5), 2509-2514

136. Niemantsverdriet, M., Vermeij, W. P., and Backendorf, C. (2005) *Leukemia* **19**(9), 1685-1686

137. De Laurenzi, V., Costanzo, A., Barcaroli, D., Terrinoni, A., Falco, M., Annicchiarico-Petruzzelli, M., Levrero, M., and Melino, G. (1998) *J Exp Med* **188**(9), 1763-1768

138. Szak, S. T., Mays, D., and Pietenpol, J. A. (2001) *Mol Cell Biol* **21**(10), 3375-3386

139. Thedieck, K., Polak, P., Kim, M. L., Molle, K. D., Cohen, A., Jeno, P., Arrieumerlou, C., and Hall, M. N. (2007) *PLoS ONE* **2**(11), e1217

140. Spandidos, A., Wang, X., Wang, H., Dragnev, S., Thurber, T., and Seed, B. (2008) *BMC genomics* **9**, 633

141. Wang, X., and Seed, B. (2003) *Nucleic acids research* **31**(24), e154

142. Zhang, B., Kirov, S., and Snoddy, J. (2005) *Nucleic acids research* **33**(Web Server issue), W741-748

143. Lamb, J., Crawford, E. D., Peck, D., Modell, J. W., Blat, I. C., Wrobel, M. J., Lerner, J., Brunet, J. P., Subramanian, A., Ross, K. N., Reich, M., Hieronymus, H., Wei, G., Armstrong, S. A., Haggarty, S. J., Clemons, P. A., Wei, R., Carr, S. A., Lander, E. S., and Golub, T. R. (2006) *Science* **313**(5795), 1929-1935

144. Rosenbluth, J. M., Mays, D. J., Pino, M. F., Tang, L. J., and Pietenpol, J. A. (2008) *Mol Cell Biol* **28**(19), 5951-5964

145. Schavolt, K. L., and Pietenpol, J. A. (2007) *Oncogene* **26**(42), 6125-6132

146. Hoh, J., Jin, S., Parrado, T., Edington, J., Levine, A. J., and Ott, J. (2002) *Proc Natl Acad Sci U S A* **99**(13), 8467-8472

147. Bailey, T. L., and Elkan, C. (1995) *Proceedings / ... International Conference on Intelligent Systems for Molecular Biology ; ISMB* **3**, 21-29

148. Ji, X., Li, W., Song, J., Wei, L., and Liu, X. S. (2006) *Nucleic acids research* **34**(Web Server issue), W551-554

149. Wachtel, M., Dettling, M., Koscielniak, E., Stegmaier, S., Treuner, J., Simon-Klingenstein, K., Buhlmann, P., Niggli, F. K., and Schafer, B. W. (2004) *Cancer Res* **64**(16), 5539-5545

150. Davicioni, E., Finckenstein, F. G., Shahbazian, V., Buckley, J. D., Triche, T. J., and Anderson, M. J. (2006) *Cancer Res* **66**(14), 6936-6946

151. Rhodes, D. R., Yu, J., Shanker, K., Deshpande, N., Varambally, R., Ghosh, D., Barrette, T., Pandey, A., and Chinnaiyan, A. M. (2004) *Neoplasia (New York, N.Y* **6**(1), 1-6

152. De Pitta, C., Tombolan, L., Albiero, G., Sartori, F., Romualdi, C., Jurman, G., Carli, M., Furlanello, C., Lanfranchi, G., and Rosolen, A. (2006) *Int J Cancer* **118**(11), 2772-2781

153. Davicioni, E., Anderson, M. J., Finckenstein, F. G., Lynch, J. C., Qualman, S. J., Shimada, H., Schofield, D. E., Buckley, J. D., Meyer, W. H., Sorensen, P. H., and Triche, T. J. (2009) *The American journal of pathology* **174**(2), 550-564

154. Hawkins, R. D., and Ren, B. (2006) *Human molecular genetics* **15 Spec No 1**, R1-7

155. Fontemaggi, G., Kela, I., Amariglio, N., Rechavi, G., Krishnamurthy, J., Strano, S., Sacchi, A., Givol, D., and Blandino, G. (2002) *J Biol Chem* **277**(45), 43359-43368

156. Osada, M., Park, H. L., Nagakawa, Y., Begum, S., Yamashita, K., Wu, G., Kim, M. S., Trink, B., and Sidransky, D. (2006) *Biochem Biophys Res Commun* **339**(4), 1120-1128

157. Vigano, M. A., Lamartine, J., Testoni, B., Merico, D., Alotto, D., Castagnoli, C., Robert, A., Candi, E., Melino, G., Gidrol, X., and Mantovani, R. (2006) *The EMBO journal* **25**(21), 5105-5116

158. Zaika, A. I., Kovalev, S., Marchenko, N. D., and Moll, U. M. (1999) *Cancer Res* **59**(13), 3257-3263

159. Cam, H., Griesmann, H., Beitzinger, M., Hofmann, L., Beinoraviciute-Kellner, R., Sauer, M., Huttinger-Kirchhof, N., Oswald, C., Friedl, P., Gattenlohner, S., Burek, C., Rosenwald, A., and Stiewe, T. (2006) *Cancer Cell* **10**(4), 281-293

160. Dominguez, G., Silva, J. M., Silva, J., Garcia, J. M., Sanchez, A., Navarro, A., Gallego, I., Provencio, M., Espana, P., and Bonilla, F. (2001) *Breast cancer research and treatment* **66**(3), 183-190

161. Bell, H. S., and Ryan, K. M. (2007) *Cell cycle (Georgetown, Tex* **6**(16), 1995-2000

162. Amin, A. R., Paul, R. K., Thakur, V. S., and Agarwal, M. L. (2007) *Cancer Res* **67**(12), 5617-5621

163. Melino, G., Bernassola, F., Ranalli, M., Yee, K., Zong, W. X., Corazzari, M., Knight, R. A., Green, D. R., Thompson, C., and Vousden, K. H. (2004) *J Biol Chem* **279**(9), 8076-8083

164. Hieronymus, H., Lamb, J., Ross, K. N., Peng, X. P., Clement, C., Rodina, A., Nieto, M., Du, J., Stegmaier, K., Raj, S. M., Maloney, K. N., Clardy, J., Hahn, W. C., Chiosis, G., and Golub, T. R. (2006) *Cancer Cell* **10**(4), 321-330

165. Wei, G., Twomey, D., Lamb, J., Schlis, K., Agarwal, J., Stam, R. W., Opferman, J. T., Sallan, S. E., den Boer, M. L., Pieters, R., Golub, T. R., and Armstrong, S. A. (2006) *Cancer Cell* **10**(4), 331-342

166. Zhao, R., Gish, K., Murphy, M., Yin, Y., Notterman, D., Hoffman, W. H., Tom, E., Mack, D. H., and Levine, A. J. (2000) *Genes & development* **14**(8), 981-993

167. Akerblad, P., Mansson, R., Lagergren, A., Westerlund, S., Basta, B., Lind, U., Thelin, A., Gisler, R., Liberg, D., Nelander, S., Bamberg, K., and Sigvardsson, M. (2005) *Physiological genomics* **23**(2), 206-216

168. De Brabander, M., De May, J., Joniau, M., and Geuens, G. (1977) *Cell biology international reports* **1**(2), 177-183

169. Tishler, R. B., Lamppu, D. M., Park, S., and Price, B. D. (1995) *Cancer Res* **55**(24), 6021-6025

170. Zeng, X., Yan, T., Schupp, J. E., Seo, Y., and Kinsella, T. J. (2007) *Clin Cancer Res* **13**(4), 1315-1321

171. Liu, G., and Chen, X. (2002) *Oncogene* **21**(47), 7195-7204

172. Zakikhani, M., Dowling, R., Fantus, I. G., Sonenberg, N., and Pollak, M. (2006) *Cancer Res* **66**(21), 10269-10273

173. Esumi, H., Lu, J., Kurashima, Y., and Hanaoka, T. (2004) *Cancer Sci* **95**(8), 685-690

174. Wang, H., Kubica, N., Ellisen, L. W., Jefferson, L. S., and Kimball, S. R. (2006) *J Biol Chem* **281**(51), 39128-39134

175. Ogata, H., Goto, S., Fujibuchi, W., and Kanehisa, M. (1998) *Bio Systems* **47**(1-2), 119-128

176. Avruch, J., Lin, Y., Long, X., Murthy, S., and Ortiz-Vega, S. (2005) *Current opinion in clinical nutrition and metabolic care* **8**(1), 67-72

177. Yu, K., Toral-Barza, L., Discafani, C., Zhang, W. G., Skotnicki, J., Frost, P., and Gibbons, J. J. (2001) *Endocrine-related cancer* **8**(3), 249-258

178. Vander Haar, E., Lee, S. I., Bandhakavi, S., Griffin, T. J., and Kim, D. H. (2007) *Nature cell biology* **9**(3), 316-323

179. Gadir, N., Jackson, D. N., Lee, E., and Foster, D. A. (2007) *Oncogene*

180. Heitman, J., Movva, N. R., and Hall, M. N. (1991) *Science* **253**(5022), 905-909

181. Runnebaum, I. B., Nagarajan, M., Bowman, M., Soto, D., and Sukumar, S. (1991) *Proc Natl Acad Sci U S A* **88**(23), 10657-10661

182. Hosoi, H., Dilling, M. B., Shikata, T., Liu, L. N., Shu, L., Ashmun, R. A., Germain, G. S., Abraham, R. T., and Houghton, P. J. (1999) *Cancer Res* **59**(4), 886-894

183. Feng, Z., Zhang, H., Levine, A. J., and Jin, S. (2005) *Proc Natl Acad Sci U S A* **102**(23), 8204-8209

184. Anderson, R. F., Patel, K. B., Reghebi, K., and Hill, S. A. (1989) *British journal of cancer* **60**(2), 193-197

185. Crighton, D., O'Prey, J., Bell, H. S., and Ryan, K. M. (2007) *Cell Death Differ*

186. Rubinsztein, D. C., Gestwicki, J. E., Murphy, L. O., and Klionsky, D. J. (2007) *Nat Rev Drug Discov* **6**(4), 304-312

187. Cam, H., Balciunaite, E., Blais, A., Spektor, A., Scarpulla, R. C., Young, R., Kluger, Y., and Dynlacht, B. D. (2004) *Molecular cell* **16**(3), 399-411

188. Dengjel, J., Schoor, O., Fischer, R., Reich, M., Kraus, M., Muller, M., Kreymborg, K., Altenberend, F., Brandenburg, J., Kalbacher, H., Brock, R., Driessen, C., Rammensee, H. G., and Stevanovic, S. (2005) *Proc Natl Acad Sci U S A* **102**(22), 7922-7927

189. Budanov, A. V., Sablina, A. A., Feinstein, E., Koonin, E. V., and Chumakov, P. M. (2004) *Science* **304**(5670), 596-600

190. Hollander, M. C., Sheikh, M. S., Bulavin, D. V., Lundgren, K., Augeri-Henmueller, L., Shehee, R., Molinaro, T. A., Kim, K. E., Tolosa, E., Ashwell, J. D., Rosenberg, M. P., Zhan, Q., Fernandez-Salguero, P. M., Morgan, W. F., Deng, C. X., and Fornace, A. J., Jr. (1999) *Nature genetics* **23**(2), 176-184

191. Blint, E., Phillips, A. C., Kozlov, S., Stewart, C. L., and Vousden, K. H. (2002) *Proc Natl Acad Sci U S A* **99**(6), 3529-3534

192. Masuda, Y., Futamura, M., Kamino, H., Nakamura, Y., Kitamura, N., Ohnishi, S., Miyamoto, Y., Ichikawa, H., Ohta, T., Ohki, M., Kiyono, T., Egami, H., Baba, H., and Arakawa, H. (2006) *Journal of human genetics* **51**(8), 652-664

193. Hwang, B. J., Ford, J. M., Hanawalt, P. C., and Chu, G. (1999) *Proc Natl Acad Sci U S A* **96**(2), 424-428

194. Chakravarthy, A., Nicholson, B., Kelley, M., Beauchamp, D., Johnson, D., Frexes-Steed, M., Simpson, J., Shyr, Y., and Pietenpol, J. (2000) *Clinical breast cancer* **1**(1), 68-71

195. Lin, K. W., Nam, S. Y., Toh, W. H., Dulloo, I., and Sabapathy, K. (2004) *Neoplasia (New York, N.Y* **6**(5), 546-557

196. Lamb, J. (2007) *Nature reviews* **7**(1), 54-60

197. Jones, E. V., Dickman, M. J., and Whitmarsh, A. J. (2007) *The Biochemical journal* **405**(3), 617-623

198. Sanchez-Prieto, R., Sanchez-Arevalo, V. J., Servitja, J. M., and Gutkind, J. S. (2002) *Oncogene* **21**(6), 974-979

199. Toh, W. H., Siddique, M. M., Boominathan, L., Lin, K. W., and Sabapathy, K. (2004) *J Biol Chem* **279**(43), 44713-44722

200. Wan, Y. Y., and DeGregori, J. (2003) *Immunity* **18**(3), 331-342

201. Basu, S., Totty, N. F., Irwin, M. S., Sudol, M., and Downward, J. (2003) *Molecular cell* **11**(1), 11-23

202. Buzzai, M., Jones, R. G., Amaravadi, R. K., Lum, J. J., DeBerardinis, R. J., Zhao, F., Viollet, B., and Thompson, C. B. (2007) *Cancer Res* **67**(14), 6745-6752

203. Hosoda, M., Ozaki, T., Miyazaki, K., Hayashi, S., Furuya, K., Watanabe, K., Nakagawa, T., Hanamoto, T., Todo, S., and Nakagawara, A. (2005) *Oncogene* **24**(48), 7156-7169

204. Munarriz, E., Barcaroli, D., Stephanou, A., Townsend, P. A., Maisse, C., Terrinoni, A., Neale, M. H., Martin, S. J., Latchman, D. S., Knight, R. A., Melino, G., and De Laurenzi, V. (2004) *Mol Cell Biol* **24**(24), 10593-10610

205. Apweiler, R., Attwood, T. K., Bairoch, A., Bateman, A., Birney, E., Biswas, M., Bucher, P., Cerutti, L., Corpet, F., Croning, M. D., Durbin, R., Falquet, L., Fleischmann, W., Gouzy, J., Hermjakob, H., Hulo, N., Jonassen, I., Kahn, D., Kanapin, A., Karavidopoulou, Y., Lopez, R., Marx, B., Mulder, N. J., Oinn, T.

M., Pagni, M., Servant, F., Sigrist, C. J., and Zdobnov, E. M. (2000) *Bioinformatics (Oxford, England)* **16**(12), 1145-1150

206. Sarbassov, D. D., Ali, S. M., Sengupta, S., Sheen, J. H., Hsu, P. P., Bagley, A. F., Markhard, A. L., and Sabatini, D. M. (2006) *Molecular cell* **22**(2), 159-168

207. Wan, X., Harkavy, B., Shen, N., Grohar, P., and Helman, L. J. (2007) *Oncogene* **26**(13), 1932-1940

208. Sun, S. Y., Rosenberg, L. M., Wang, X., Zhou, Z., Yue, P., Fu, H., and Khuri, F. R. (2005) *Cancer Res* **65**(16), 7052-7058

209. Ray, P. S., Grover, R., and Das, S. (2006) *EMBO reports* **7**(4), 404-410

210. Yang, D. Q., Halaby, M. J., and Zhang, Y. (2006) *Oncogene* **25**(33), 4613-4619

211. Sayan, A. E., Roperch, J. P., Sayan, B. S., Rossi, M., Pinkoski, M. J., Knight, R. A., Willis, A. E., and Melino, G. (2007) *Annals of the New York Academy of Sciences* **1095**, 315-324

212. Yu, J., and Henske, E. P. (2006) *Cancer Res* **66**(19), 9461-9466

213. Murray-Zmijewski, F., Slee, E. A., and Lu, X. (2008) *Nat Rev Mol Cell Biol* **9**(9), 702-712

214. Ozaki, T., and Nakagawara, A. (2005) *Cancer Sci* **96**(11), 729-737

215. Johnson, W. E., Li, W., Meyer, C. A., Gottardo, R., Carroll, J. S., Brown, M., and Liu, X. S. (2006) *Proc Natl Acad Sci U S A* **103**(33), 12457-12462

216. Marin, M. C., and Kaelin, W. G., Jr. (2000) *Biochimica et biophysica acta* **1470**(3), M93-M100

217. Marson, A., Levine, S. S., Cole, M. F., Frampton, G. M., Brambrink, T., Johnstone, S., Guenther, M. G., Johnston, W. K., Wernig, M., Newman, J., Calabrese, J. M., Dennis, L. M., Volkert, T. L., Gupta, S., Love, J., Hannett, N., Sharp, P. A., Bartel, D. P., Jaenisch, R., and Young, R. A. (2008) *Cell* **134**(3), 521-533

218. Roehle, A., Hoefig, K. P., Repsilber, D., Thorns, C., Ziepert, M., Wesche, K. O., Thiere, M., Loeffler, M., Klapper, W., Pfreundschuh, M., Matolcsy, A., Bernd, H. W., Reiniger, L., Merz, H., and Feller, A. C. (2008) *British journal of haematology* **142**(5), 732-744

219. Blower, P. E., Chung, J. H., Verducci, J. S., Lin, S., Park, J. K., Dai, Z., Liu, C. G., Schmittgen, T. D., Reinhold, W. C., Croce, C. M., Weinstein, J. N., and Sadee, W. (2008) *Molecular cancer therapeutics* **7**(1), 1-9

220. Concin, N., Hofstetter, G., Berger, A., Gehmacher, A., Reimer, D., Watrowski, R., Tong, D., Schuster, E., Hefler, L., Heim, K., Mueller-Holzner, E., Marth, C., Moll, U. M., Zeimet, A. G., and Zeillinger, R. (2005) *Clin Cancer Res* **11**(23), 8372-8383

221. Molchadsky, A., Shats, I., Goldfinger, N., Pevsner-Fischer, M., Olson, M., Rinon, A., Tzahor, E., Lozano, G., Zipori, D., Sarig, R., and Rotter, V. (2008) *PLoS ONE* **3**(11), e3707

222. Petricoin, E. F., 3rd, Espina, V., Araujo, R. P., Midura, B., Yeung, C., Wan, X., Eichler, G. S., Johann, D. J., Jr., Qualman, S., Tsokos, M., Krishnan, K., Helman, L. J., and Liotta, L. A. (2007) *Cancer Res* **67**(7), 3431-3440

223. Charytonowicz, E., Cordon-Cardo, C., Matushansky, I., and Ziman, M. (2008) *Cancer letters*

224. Parham, D. M. (2001) *Mod Pathol* **14**(5), 506-514

225. Zhao, X. D., Han, X., Chew, J. L., Liu, J., Chiu, K. P., Choo, A., Orlov, Y. L., Sung, W. K., Shahab, A., Kuznetsov, V. A., Bourque, G., Oh, S., Ruan, Y., Ng, H. H., and Wei, C. L. (2007) *Cell stem cell* **1**(3), 286-298

226. Pan, G., Tian, S., Nie, J., Yang, C., Ruotti, V., Wei, H., Jonsdottir, G. A., Stewart, R., and Thomson, J. A. (2007) *Cell stem cell* **1**(3), 299-312

227. Mishra, P. J., Mishra, P. J., Humeniuk, R., Medina, D. J., Alexe, G., Mesirov, J. P., Ganesan, S., Glod, J. W., and Banerjee, D. (2008) *Cancer Res* **68**(11), 4331-4339

228. Wakitani, S., Saito, T., and Caplan, A. I. (1995) *Muscle & nerve* **18**(12), 1417-1426

229. Difeo, A., Martignetti, J. A., and Narla, G. (2008) *Drug Resist Updat*

230. Furukawa, T., Sunamura, M., Motoi, F., Matsuno, S., and Horii, A. (2003) *The American journal of pathology* **162**(6), 1807-1815

231. Arachchige Don, A. S., Dallapiazza, R. F., Bennin, D. A., Brake, T., Cowan, C. E., and Horne, M. C. (2006) *Experimental cell research* **312**(20), 4181-4204

232. Cheng, Y. Y., Jin, H., Liu, X., Siu, J. M., Wong, Y. P., Ng, E. K., Yu, J., Leung, W. K., Sung, J. J., and Chan, F. K. (2008) *British journal of cancer* **99**(12), 2083-2087

233. Sendemir, A., Sendemir, E., Kosmehl, H., and Jirikowski, G. F. (2008) *Gynecol Endocrinol* **24**(2), 105-112

234. Kannangai, R., Diehl, A. M., Sicklick, J., Rojkind, M., Thomas, D., and Torbenson, M. (2005) *Human pathology* **36**(4), 341-347

235. Bao, J., and Zervos, A. S. (1996) *Oncogene* **12**(10), 2171-2176

236. Italiano, A., Bianchini, L., Keslair, F., Bonnafous, S., Cardot-Leccia, N., Coindre, J. M., Dumollard, J. M., Hofman, P., Leroux, A., Mainguene, C., Peyrottes, I., Ranchere-Vince, D., Terrier, P., Tran, A., Gual, P., and Pedeutour, F. (2008) *Int J Cancer* **122**(10), 2233-2241

237. Yamaguchi, A. (1995) *Seminars in cell biology* **6**(3), 165-173

238. Sacchetti, B., Funari, A., Michienzi, S., Di Cesare, S., Piersanti, S., Saggio, I., Tagliafico, E., Ferrari, S., Robey, P. G., Riminucci, M., and Bianco, P. (2007) *Cell* **131**(2), 324-336

239. Chen, J. F., Mandel, E. M., Thomson, J. M., Wu, Q., Callis, T. E., Hammond, S. M., Conlon, F. L., and Wang, D. Z. (2006) *Nature genetics* **38**(2), 228-233

240. Subramanian, S., Lui, W. O., Lee, C. H., Espinosa, I., Nielsen, T. O., Heinrich, M. C., Corless, C. L., Fire, A. Z., and van de Rijn, M. (2008) *Oncogene* **27**(14), 2015-2026

241. Barton, C. E., Tahinci, E., Barbieri, C. E., Johnson, K. N., Hanson, A. J., Jernigan, K. K., Chen, T. W., Lee, E., and Pietenpol, J. A. (2009) *Developmental biology*, In press.

242. Sabbah, M., Emami, S., Redeuilh, G., Julien, S., Prevost, G., Zimber, A., Ouelaa, R., Bracke, M., De Wever, O., and Gespach, C. (2008) *Drug Resist Updat* **11**(4-5), 123-151

243. Maiuri, M. C., Zalckvar, E., Kimchi, A., and Kroemer, G. (2007) *Nat Rev Mol Cell Biol* **8**(9), 741-752

244. Geng, J., and Klionsky, D. J. (2008) *EMBO reports* **9**(9), 859-864

245. Hanada, T., Noda, N. N., Satomi, Y., Ichimura, Y., Fujioka, Y., Takao, T., Inagaki, F., and Ohsumi, Y. (2007) *J Biol Chem* **282**(52), 37298-37302

246. Tanida, I., Wakabayashi, M., Kanematsu, T., Minematsu-Ikeguchi, N., Sou, Y. S., Hirata, M., Ueno, T., and Kominami, E. (2006) *Autophagy* **2**(4), 264-271

247. Young, A. R., Narita, M., Ferreira, M., Kirschner, K., Sadaie, M., Darot, J. F., Tavare, S., Arakawa, S., Shimizu, S., Watt, F. M., and Narita, M. (2009) *Genes & development* **23**(7), 798-803

248. Chiacchiera, F., and Simone, C. (2009) *Methods in enzymology* **453**, 305-324

249. Liang, C., Lee, J. S., Inn, K. S., Gack, M. U., Li, Q., Roberts, E. A., Vergne, I., Deretic, V., Feng, P., Akazawa, C., and Jung, J. U. (2008) *Nature cell biology* **10**(7), 776-787

250. Liang, C., Feng, P., Ku, B., Dotan, I., Canaani, D., Oh, B. H., and Jung, J. U. (2006) *Nature cell biology* **8**(7), 688-699

251. Wetzel, M. K., Naska, S., Laliberte, C. L., Rymar, V. V., Fujitani, M., Biernaskie, J. A., Cole, C. J., Lerch, J. P., Spring, S., Wang, S. H., Frankland, P. W., Henkelman, R. M., Josselyn, S. A., Sadikot, A. F., Miller, F. D., and Kaplan, D. R. (2008) *Neuron* **59**(5), 708-721

252. Yu, S. W., Baek, S. H., Brennan, R. T., Bradley, C. J., Park, S. K., Lee, Y. S., Jun, E. J., Lookingland, K. J., Kim, E. K., Lee, H., Goudreau, J. L., and Kim, S. W. (2008) *Stem cells (Dayton, Ohio)* **26**(10), 2602-2610

253. Kuballa, P., Huett, A., Rioux, J. D., Daly, M. J., and Xavier, R. J. (2008) *PLoS ONE* **3**(10), e3391

254. Ling, D., and Salvaterra, P. M. (2009) *Autophagy* **5**(5)

255. Matheu, A., Maraver, A., and Serrano, M. (2008) *Cancer Res* **68**(15), 6031-6034

256. Keyes, W. M., Wu, Y., Vogel, H., Guo, X., Lowe, S. W., and Mills, A. A. (2005) *Genes & development* **19**(17), 1986-1999

257. Tavernarakis, N., Pasparaki, A., Tasdemir, E., Maiuri, M. C., and Kroemer, G. (2008) *Autophagy* **4**(7), 870-873

258. Hay, N. (2008) *Cell metabolism* **8**(3), 184-185

259. Gomez-Lazaro, M., Fernandez-Gomez, F. J., and Jordan, J. (2004) *J Physiol Biochem* **60**(4), 287-307

260. Jones, R. G., Plas, D. R., Kubek, S., Buzzai, M., Mu, J., Xu, Y., Birnbaum, M. J., and Thompson, C. B. (2005) *Molecular cell* **18**(3), 283-293

261. Huang, J., and Manning, B. D. (2009) *Biochemical Society transactions* **37**(Pt 1), 217-222

262. Zanchi, N. E., and Lancha, A. H., Jr. (2008) *European journal of applied physiology* **102**(3), 253-263

263. Cross, D. A., Alessi, D. R., Cohen, P., Andjelkovich, M., and Hemmings, B. A. (1995) *Nature* **378**(6559), 785-789

264. Huang, S., Shu, L., Dilling, M. B., Easton, J., Harwood, F. C., Ichijo, H., and Houghton, P. J. (2003) *Molecular cell* **11**(6), 1491-1501

265. Okoshi, R., Ozaki, T., Yamamoto, H., Ando, K., Koida, N., Ono, S., Koda, T., Kamijo, T., Nakagawara, A., and Kizaki, H. (2008) *J Biol Chem* **283**(7), 3979-3987

266. Lee, Y. G., Lee, S. W., Sin, H. S., Kim, E. J., and Um, S. J. (2009) *Oncogene* **28**(7), 1040-1052

267. Ogawa, E., Okuyama, R., Ikawa, S., Nagoshi, H., Egawa, T., Kurihara, A., Yabuki, M., Tagami, H., Obinata, M., and Aiba, S. (2008) *Oncogene* **27**(6), 848-856

268. Watcharasit, P., Bijur, G. N., Zmijewski, J. W., Song, L., Zmijewska, A., Chen, X., Johnson, G. V., and Jope, R. S. (2002) *Proc Natl Acad Sci U S A* **99**(12), 7951-7955

269. Turenne, G. A., and Price, B. D. (2001) *BMC cell biology* **2**, 12

270. Barbieri, C. E., and Pietenpol, J. A. (2005) *Cancer biology & therapy* **4**(4), 419-420

271. Greer, E. L., Oskoui, P. R., Banko, M. R., Maniar, J. M., Gygi, M. P., Gygi, S. P., and Brunet, A. (2007) *J Biol Chem* **282**(41), 30107-30119

272. Breuleux, M., Klopfenstein, M., Stephan, C., Doughty, C. A., Barys, L., Maira, S. M., Kwiatkowski, D., and Lane, H. A. (2009) *Molecular cancer therapeutics* **8**(4), 742-753

273. Aqeilan, R. I., Pekarsky, Y., Herrero, J. J., Palamarchuk, A., Letofsky, J., Druck, T., Trapasso, F., Han, S. Y., Melino, G., Huebner, K., and Croce, C. M. (2004) *Proc Natl Acad Sci U S A* **101**(13), 4401-4406

274. Bachmann, R. A., Kim, J. H., Wu, A. L., Park, I. H., and Chen, J. (2006) *J Biol Chem* **281**(11), 7357-7363

275. Zhang, X., Shu, L., Hosoi, H., Murti, K. G., and Houghton, P. J. (2002) *J Biol Chem* **277**(31), 28127-28134

276. Kim, J. E., and Chen, J. (2000) *Proc Natl Acad Sci U S A* **97**(26), 14340-14345

277. Sancak, Y., and Sabatini, D. M. (2009) *Biochemical Society transactions* **37**(Pt 1), 289-290

278. Dobbelstein, M., Strano, S., Roth, J., and Blandino, G. (2005) *Biochem Biophys Res Commun* **331**(3), 688-693

279. Ben-Yehoyada, M., Ben-Dor, I., and Shaul, Y. (2003) *J Biol Chem* **278**(36), 34475-34482

280. Mills, A. A., Qi, Y., and Bradley, A. (2002) *Genesis* **32**(2), 138-141

281. Mills, A. A., Zheng, B., Wang, X. J., Vogel, H., Roop, D. R., and Bradley, A. (1999) *Nature* **398**(6729), 708-713

282. Liu, P., Jenkins, N. A., and Copeland, N. G. (2003) *Genome research* **13**(3), 476-484

283. Deugnier, M. A., Teuliere, J., Faraldo, M. M., Thiery, J. P., and Glukhova, M. A. (2002) *Breast Cancer Res* **4**(6), 224-230

284. Lakhani, S. R., and O'Hare, M. J. (2001) *Breast Cancer Res* **3**(1), 1-4

285. Barbieri, C. E., and Pietenpol, J. A. (2006) *Experimental cell research*

286. Davison, T. S., Vagner, C., Kaghad, M., Ayed, A., Caput, D., and Arrowsmith, C. H. (1999) *J Biol Chem* **274**(26), 18709-18714

287. Kravchenko, J. E., Ilyinskaya, G. V., Komarov, P. G., Agapova, L. S., Kochetkov, D. V., Strom, E., Frolova, E. I., Kovriga, I., Gudkov, A. V., Feinstein, E., and Chumakov, P. M. (2008) *Proc Natl Acad Sci U S A* **105**(17), 6302-6307

288. Di Agostino, S., Cortese, G., Monti, O., Dell'Orso, S., Sacchi, A., Eisenstein, M., Citro, G., Strano, S., and Blandino, G. (2008) *Cell cycle (Georgetown, Tex* **7**(21), 3440-3447

289. Wang, J. Y., and Ki, S. W. (2001) *Biochemical Society transactions* **29**(Pt 6), 666-673

290. Welch, P. J., and Wang, J. Y. (1993) *Cell* **75**(4), 779-790

291. Welch, P. J., and Wang, J. Y. (1995) *Mol Cell Biol* **15**(10), 5542-5551

292. Rosenbluth, J. M., and Pietenpol, J. A. (2009) *Autophagy* **5**(1)

293. Cloughesy, T. F., Yoshimoto, K., Nghiemphu, P., Brown, K., Dang, J., Zhu, S., Hsueh, T., Chen, Y., Wang, W., Youngkin, D., Liau, L., Martin, N., Becker, D., Bergsneider, M., Lai, A., Green, R., Oglesby, T., Koleto, M., Trent, J., Horvath, S., Mischel, P. S., Mellinghoff, I. K., and Sawyers, C. L. (2008) *PLoS medicine* **5**(1), e8

294. Efeyan, A., Ortega-Molina, A., Velasco-Miguel, S., Herranz, D., Vassilev, L. T., and Serrano, M. (2007) *Cancer Res* **67**(15), 7350-7357

295. Tovar, C., Rosinski, J., Filipovic, Z., Higgins, B., Kolinsky, K., Hilton, H., Zhao, X., Vu, B. T., Qing, W., Packman, K., Myklebost, O., Heimbrook, D. C., and Vassilev, L. T. (2006) *Proc Natl Acad Sci U S A* **103**(6), 1888-1893

296. Bunz, F., Hwang, P. M., Torrance, C., Waldman, T., Zhang, Y., Dillehay, L., Williams, J., Lengauer, C., Kinzler, K. W., and Vogelstein, B. (1999) *The Journal of clinical investigation* **104**(3), 263-269

297. Espinosa, J. M. (2008) *Oncogene* **27**(29), 4013-4023

298. Ren, Y. X., Finckenstein, F. G., Abdueva, D. A., Shahbazian, V., Chung, B., Weinberg, K. I., Triche, T. J., Shimada, H., and Anderson, M. J. (2008) *Cancer Res* **68**(16), 6587-6597

299. Keller, C., Arenkiel, B. R., Coffin, C. M., El-Bardeesy, N., DePinho, R. A., and Capecchi, M. R. (2004) *Genes & development* **18**(21), 2614-2626

300. Blais, A., Tsikitis, M., Acosta-Alvear, D., Sharan, R., Kluger, Y., and Dynlacht, B. D. (2005) *Genes & development* **19**(5), 553-569

301. Hasty, P., Bradley, A., Morris, J. H., Edmondson, D. G., Venuti, J. M., Olson, E. N., and Klein, W. H. (1993) *Nature* **364**(6437), 501-506

302. Andarawewa, K. L., Erickson, A. C., Chou, W. S., Costes, S. V., Gascard, P., Mott, J. D., Bissell, M. J., and Barcellos-Hoff, M. H. (2007) *Cancer Res* **67**(18), 8662-8670

303. Zhang, J., Smolen, G. A., and Haber, D. A. (2008) *Cancer Res* **68**(8), 2789-2794

304. Adorno, M., Cordenonsi, M., Montagner, M., Dupont, S., Wong, C., Hann, B., Solari, A., Bobisse, S., Rondina, M. B., Guzzardo, V., Parenti, A. R., Rosato, A., Bicciato, S., Balmain, A., and Piccolo, S. (2009) *Cell* **137**(1), 87-98

305. Li, Y., and Prives, C. (2007) *Oncogene* **26**(15), 2220-2225

306. Masuda, N., Kato, H., Nakajima, T., Sano, T., Kashiwabara, K., Oyama, T., and Kuwano, H. (2003) *Cancer Sci* **94**(7), 612-617

307. Sarrio, D., Rodriguez-Pinilla, S. M., Hardisson, D., Cano, A., Moreno-Bueno, G., and Palacios, J. (2008) *Cancer Res* **68**(4), 989-997

308. Romualdi, C., De Pitta, C., Tombolan, L., Bortoluzzi, S., Sartori, F., Rosolen, A., and Lanfranchi, G. (2006) *BMC genomics* **7**, 287

309. Garcia, J. A., and Danielpour, D. (2008) *Molecular cancer therapeutics* **7**(6), 1347-1354

310. Bjornsti, M. A., and Houghton, P. J. (2004) *Cancer Cell* **5**(6), 519-523

311. Kozak, M. (2003) *Gene* **318**, 1-23

312. Stoneley, M., and Willis, A. E. (2004) *Oncogene* **23**(18), 3200-3207

313. Lau, L. M., Wolter, J. K., Lau, J. T., Cheng, L. S., Smith, K. M., Hansford, L. M., Zhang, L., Baruchel, S., Robinson, F., and Irwin, M. S. (2009) *Oncogene*

314. Kovalev, S., Marchenko, N., Swendeman, S., LaQuaglia, M., and Moll, U. M. (1998) *Cell Growth Differ* **9**(11), 897-903

315. Ueda, Y., Hijikata, M., Takagi, S., Chiba, T., and Shimotohno, K. (1999) *Oncogene* **18**(35), 4993-4998